

REGULATION OF CYTOKINE-MEDIATED VASCULAR PERMEABILITY
UNDER FLOW-INDUCED SHEAR STRESS

A DISSERTATION SUBMITTED TO THE GRADUATE DIVISION OF THE
UNIVERSITY OF HAWAI‘I AT MĀNOA IN PARTIAL FULFILLMENT
OF THE REQUIREMENTS FOR THE DEGREE OF

DOCTOR OF PHILOSOPHY

IN

MOLECULAR BIOSCIENCES AND BIOENGINEERING

DECEMBER 2015

By

Pavlos Anastasiadis

Dissertation Committee:

Michelle L. Matter, Chairperson

Charles R. Keese

Scott Lozanoff

Vivek Nerurkar

John S. Allen

Marcus A. Tius

Keywords: vascular endothelium, endothelial permeability, fluid shear stress,
sepsis, GTPases, cytokines

© Copyright by
Pavlos Anastasiadis
All Rights Reserved
September 2015

DEDICATION

This work is dedicated to all those who contributed to the advancement of science and technology and whose names history decided to keep hidden from us.

ACKNOWLEDGEMENTS

I thank my dissertation committee members for their time and valuable comments. In particular, I would like to express my warmest thanks to my supervisor and mentor, Dr. Michelle L. Matter at the University of Hawaii Cancer Center.

My parents and sisters have maintained my sanity during the very demanding and challenging years of the doctorate program. For their unquestionable loyalty and unconditional trust I will always remain grateful to them.

Mr. John V. Levas and his wonderful family have remained throughout this time at the very forefront of support. I thank them eternally.

My colleagues at the University of Hawaii Cancer Center deserve a great deal of appreciation. Due to their collegiality and support, the very long hours in the laboratory during the week, the weekends and holidays, appeared in brighter colors than would have been without their delightful presence.

ABSTRACT

Endothelial cells form the innermost lining of blood vessels throughout the circulatory system. They exhibit a remarkable ability to adapt rapidly to biomechanical and biochemical stimuli from their microenvironment. Vascular endothelial cells play an essential role during the onset of inflammatory conditions and sepsis. Sepsis accounts for the highest number of mortalities in non-cardiac intensive care units and is linked to numerous other underlying conditions including cancer, inflammatory conditions and diabetes. Cancer patients, in particular, are especially susceptible to infections that lead to sepsis and show significantly higher mortality rates due to the immunocompromised nature of the host defense system. Currently, there are no available treatments for sepsis. Furthermore, TNF α has been implicated as one of the major pro-inflammatory cytokines in sepsis. In the current work, we used physiologically relevant shear stress rates and translated them into a well-controlled *in vitro* system applying fluid shear stress onto primary endothelial microvascular endothelial cells. We identified a complex formed by the active form of the small GTPase R-Ras and the cytoskeletal scaffold protein filamin A (FLNa) that can regulate TNF α -mediated activation of endothelial cells under fluid shear stress conditions. R-Ras binds directly to repeat 3 of FLNa forming a complex that is necessary for endothelial barrier integrity. We show here that activated GTP-bound R-Ras blocks vascular permeability. Permeability is monitored using the electrical cell impedance spectroscopy (ECIS) method that acquires real-time transendothelial electrical resistance (TEER) values. From the electrical resistance, impedance and capacitance, endothelial permeability can be derived by employing the ECIS model and quantified at nanoscale precision levels concurrently with endothelial cells subjected to fluid shear stress. We also demonstrate a novel platform comprised

of ECIS and physiologically relevant fluid shear stress levels to test novel inhibitors or compounds that block TNF α -mediated vascular permeability. Thus, we show that the R-Ras/FLNa complex is important in regulating vascular endothelial permeability under fluid shear stress conditions. This work may offer insights into the regulation of endothelial permeability by providing novel targets to block vascular hyperpermeability or leakiness.

TABLE OF CONTENTS

ACKNOWLEDGEMENTS	IV
ABSTRACT.....	V
LIST OF TABLES	XII
LIST OF FIGURES	XIII
LIST OF ABBREVIATIONS	XV
CHAPTER 1 INTRODUCTION: VASCULAR ENDOTHELIUM AND SEPSIS	1
1.1 Endothelium	2
1.2 Physiology and anatomical geometric features of the vascular endothelium...	2
1.2.1 Arterioles	3
1.2.2 Capillaries.....	4
1.2.3 Venules	5
1.2.4 Plasticity and the dynamic nature of the endothelium.....	5
1.2.5 Hemostasis.....	7
1.3 Endothelial functional and structural heterogeneity.....	9
1.3.1 Heart endothelium	9
1.3.2 Endothelial cells in coronary arteries	9
1.3.3 Endothelial cells in myocardial microvessels.....	9
1.3.4 Pulmonary endothelial cells.....	10
1.3.5 Bronchial endothelial cells	10
1.3.6 Glomerular capillary endothelial cells.....	11
1.3.7 Hepatic sinusoidal endothelial cells	11
1.3.8 Brain endothelium	12
1.4 Vascular endothelial barrier function	12
1.4.1 Heterogeneity of endothelial permeability	14
1.4.2 Regulation of vascular endothelial permeability	15
1.4.3 Adherens junctions	16
1.4.4 Tight junctions.....	21
1.4.5 Gap junctions.....	23
1.4.6 Desmosomes.....	24

1.5	Electrical cell-impedance spectroscopy and endothelial barrier function	25
1.6	Sepsis	30
1.6.1	Pathophysiology of sepsis	31
1.6.2	Clinical manifestations of sepsis	31
1.6.3	Epidemiology of sepsis.....	32
1.6.4	Biomarkers of sepsis.....	33
1.6.5	Mitochondrial dysfunction in sepsis.....	34
1.6.6	Animal sepsis models	35
1.7	Fluid shear stress and the vascular endothelium	37
1.7.1	Adhesion proteins	40
1.7.2	Ion channel activation.....	41
1.7.3	Calcium.....	41
1.7.4	Caveolae	42
1.7.5	Primary cilia	42
1.7.6	Cytoskeleton	43
1.7.7	Glycocalyx.....	44
1.7.8	Integrins.....	47
1.7.9	Vesiculo-vacuolar organelles.....	49
1.7.10	Tyrosine kinase receptors	49
1.8	Small GTPases.....	51
1.8.1	Introduction	51
1.8.2	Small GTPases in sepsis.....	55
1.8.3	Small GTPases and vascular permeability	58
1.9	Figures	59
1.10	Tables.....	74

**CHAPTER 2 THE R-RAS AND FLNA COMPLEX REGULATES TUMOR NECROSIS
FACTOR ALPHA-MEDIATED VASCULAR PERMEABILITY UNDER FLUID
SHEAR STRESS..... 76**

Abstract.....	77
2.1 Introduction	79
2.1.1 Cytokines.....	79

2.1.2	The cytoskeletal scaffold protein filamin A and its role in mechanotransduction and mechanosensing.....	81
2.1.3	The small GTPase R-Ras.....	85
2.2	Materials and Methods.....	88
2.2.1	Cell Culture.....	88
2.2.2	Plasmids constructs.....	88
2.2.3	siRNA knockdown of R-Ras and FLNa.....	88
2.2.4	Permeability-inducing treatment.....	89
2.2.5	Fluid shear stress.....	89
2.2.6	Electrical Cell Impedance Spectroscopy.....	90
2.2.7	Immunohistochemistry.....	90
2.2.8	Immunoblotting.....	91
2.2.9	Src inhibition via PP2 inhibitor.....	92
2.2.10	Immunoprecipitation and kinase activation analysis.....	92
2.3	Results.....	94
2.3.1	Loss of direct interaction between R-Ras and FLNa promotes vascular permeability in endothelial cells subjected to fluid shear stress.....	94
2.3.2	Loss of the R-Ras binding site at FLNa repeat 3 promotes vascular permeability in endothelial cells under fluid shear stress.....	96
2.3.3	Constitutively active R-Ras rescues endothelial monolayer.....	97
2.3.4	Constitutively active R-Ras blocks TNF α -mediated vascular permeability.....	99
2.3.5	Constitutively active R-Ras exerts its barrier-protective properties only in the presence of FLNa repeat 3.....	101
2.3.6	R-Ras mutations lead to a phenotype associated with the RASopathy spectrum of vascular malfunctions and malignancies.....	101
2.3.7	The pharmacological Src inhibitor PP2 blocks vascular permeability.....	102
2.3.8	FLNaRP3 blocks barrier function recovery.....	103
2.4	Discussion.....	105
2.5	Figures.....	108

**CHAPTER 3 A REAL-TIME TEER-BASED SCREENING ASSAY UNDER
FLOW-INDUCED SHEAR STRESS FOR IDENTIFYING DRUG-SPECIFIC
INHIBITION OF CYTOKINE-MEDIATED VASCULAR PERMEABILITY** 149

3.1	Abstract.....	150
3.2	Introduction	151
3.3	Materials and Methods	153
3.3.1	Cell Culture.....	153
3.3.2	Permeability-inducing and antagonist treatment.....	153
3.3.3	Fluid shear stress	153
3.3.4	Electrical Cell Impedance Spectroscopy (ECIS).....	154
3.3.5	Immunoblotting.....	154
3.3.6	Immunohistochemistry	155
3.4	Results	157
3.4.1	TEER-based analysis of cytokine-induced endothelial permeability under flow-induced shear stress.....	157
3.4.2	Quantifying the inhibition of cytokine-induced endothelial permeability by specific antagonists under flow-induced shear-stress.....	157
3.4.3	Endothelial cells exhibit high levels of viability despite exposure to flow-induced shear stress conditions.....	158
3.4.4	Fluid shear stress does not induce morphological or topological variations on tight junction complexes of endothelial cells	159
3.4.5	Under shear stress conditions, the permeability-inducing agents (histamine, IL-1 β and thrombin) promote redistribution of the tight junction adapter protein ZO-1 and increase actin stress fiber formation	159
3.4.6	Treatment of endothelial monolayers with the selective antagonists clemastine and methylprednisolone inhibited cytokine-mediated rearrangement of ZO-1 and reduced stress fiber formation.....	160
3.4.7	Under fluid shear stress conditions treatment with the permeability-inducing agents histamine, IL-1 β and thrombin promotes phosphorylation of VE-cadherin at tyrosine residues 685 and 731	160

3.4.8	The histamine antagonist clemastine blocks permeability-inducing agent-mediated VE-cadherin phosphorylation	161
3.4.9	Under shear stress conditions, treatment with a permeability-inducing agent promotes phosphorylation of Src at Y416	162
3.4.10	Clemastine blocks permeability-inducing agent-mediated increase in Src phosphorylation at Y416.....	162
3.5	Discussion.....	164
3.6	Figures	167
APPENDIX A INFECTIOUS BIOFILMS AND SEPSIS		176
	Abstract.....	177
	Introduction	179
	Bacterial strains and cultivation of biofilms.....	181
	Lectins, antibodies and immunofluorescence.....	181
	Targeted ultrasound	183
	Lectin-staining for biofilms	184
	Epifluorescence Microscopy	184
	Ultrasonic investigation of biofilms	184
	Results	188
	Conclusions	192
	Figures	195
	Tables	203
	References.....	207

LIST OF TABLES

Table 1.1	75
Table A.1.....	204
Table A.2.....	205
Table A.3.....	206

LIST OF FIGURES

Figure 1.1	60
Figure 1.2	61
Figure 1.3	62
Figure 1.4	64
Figure 1.5	65
Figure 1.6	66
Figure 1.7	67
Figure 1.8	68
Figure 1.9	69
Figure 1.10	70
Figure 1.11	71
Figure 1.12	72
Figure 1.13	73
Figure 2.1	109
Figure 2.2	111
Figure 2.3	112
Figure 2.4	113
Figure 2.5	114
Figure 2.6	116
Figure 2.7	118
Figure 2.8	120
Figure 2.9	122
Figure 2.10	124
Figure 2.11	126
Figure 2.12	127
Figure 2.13	129
Figure 2.14	131
Figure 2.15	133
Figure 2.16	135

Figure 2.17	137
Figure 2.18	139
Figure 2.19	141
Figure 2.20	143
Figure 2.21	145
Figure 2.22	147
Figure 3.1	168
Figure 3.2	170
Figure 3.3	171
Figure 3.4	172
Figure 3.5	173
Figure 3.6	174
Figure 3.7	175
Figure A.1	196
Figure A.2	197
Figure A.3	199
Figure A.4	200
Figure A.5	201
Figure A.6	202

LIST OF ABBREVIATIONS

ABD	Actin-binding domain
AC	Alternating current
AKT	Protein kinase B (also known as PKB)
Ang-2	Angiopoietin-2
APA	Anti-Protein A
ATP	Adenosine triphosphate
CA R-Ras	Constitutively active R-Ras
cAMP	Cyclic adenosine monophosphate
Csk	C-terminal Src kinase
Cx32	Connexin 32
Cx37	Connexin 37
Cx43	Connexin 43
Cx45	Connexin 45
DAG	Diacylglycerol
DAPI	4',6-diamidino-2-phenylindole, dihydrochloride
DN R-Ras	Dominant negative R-Ras
E. coli	Escherichia coli
ECIS	Electrical cell impedance spectroscopy or sensing
ECM	Extracellular cell matrix
ECSM-2	Endothelial cell-specific molecule-2
EGF	Epithelial growth factor
EPC	Endothelial progenitor cell

EPCR	Endothelial protein C receptor
FAK	Focal adhesion kinase
FGFs	Fibroblast growth factor
FITC	Fluorescein isothiocyanate
FLNaRP3	FLNa repeat 3 only
FLNa Δ 3	FLNa deletion repeat 3
GAP	GTPase-activating protein
GDP	Guanosine-5'-diphosphate
GEF	Guanine nucleotide exchange factor
GST	Glutathione S-transferase
GTP	Guanosine-5'-triphosphate
HBSS	Hepes buffered saline solution
HCAECs	Human coronary artery endothelial cells
HDMVECs	Human dermal microvascular endothelial cells
hFN	Human fibronectin
HUVECs	Human umbilical vein endothelial cells
IBSC	Integrated backscatter coefficient
ICAM-1	Intercellular adhesion molecule-1
IFN γ	Interferon gamma
IFN- γ	Interferon gamma
IGF-1	Insulin-like growth factor-1
IgG	Immunoglobulin G
IL-1 β	Interleukin-1 β
IL-6	Interleukin-6
IL-8	Interleukin-8
IP3	1,4,5-trisphosphate (IP3)
JAM	Junctional adhesion molecule
LDL	Low-density lipoprotein
LPS	Lipopolysaccharide

MAPK	Mitogen-activated protein kinases
MCP-1	Monocyte chemoattractant protein-1
MLCK	myosin light chain kinase
mtDNA	Mitochondrial deoxyribonucleic acid
N-cadherin	Neural cadherin
NF- κ B	Nuclear factor kappa-light-chain-enhancer of activated B cells
NO	Nitric oxide
OD	Optical density
PAF	Platelet-activating factor
PAI	Plasminogen activator inhibitor
PAK	p21-activated kinases
PAMPs	Pathogen-associated molecular patterns
PAR	Protease-activated receptors
PBS	Phosphate buffered saline
PBS-T	Phosphate buffered saline plus Tween 20
PDGF-A	Platelet-derived growth factor-A
PDGF-B	Platelet-derived growth factor-B
PECAM-1	Platelet/endothelial cell adhesion molecule-1
PI3K	Phosphatidylinositol-4,5-bisphosphate 3-kinase
PKA	Protein kinase A
PKB	Protein kinase B
PKC	Protein kinase C
PKP-1	Plakophilin-1
PKP-2	Plakophilin-2
PKP-3	Plakophilin-3
PKP-4	Plakophilin-4
RF	Radio-frequency
ROI	Region of interest
RPM	Revolutions per minute

RT	Room temperature
RTK	Receptor tyrosine kinase
SHP2	SH2-containing phospho-tyrosine phosphatase
siRNA	Small interfering ribonucleic acid
StDev	Standard deviation
TCB	Targeson conjugation buffer
TEER	Transendothelial or transepithelial electrical resistance
TF	Tissue factor
TFPI	Tissue factor pathway inhibitor
TLRs	Toll-like receptors
TNF α	Tumor necrosis factor α
TRITC	Tetramethylrhodamine
TSB	Tryptic soy broth
VASP	Vasodilator-stimulated phosphoprotein
Vav2	Guanine nucleotide exchange factor Vav2
VE-cadherin	Vascular endothelial cadherin
VEGF	Vascular endothelial growth factor
VEGFR-1	Vascular endothelial growth factor receptor-1
VEGFR-2	Vascular endothelial growth factor receptor-2
vWF	von Willebrand factor
WBC	White blood cell
ZO-1	Zonula occluden-1
ZO-2	Zonula occluden-2
ZO-3	Zonula occluden-3

This page has been left blank intentionally.

CHAPTER 1

Introduction: Vascular Endothelium and Sepsis

1.1 Endothelium

The endothelium lines the innermost layer of all blood vessels in the human circulatory system separating blood from the underlying tissues (Figure 1.1). It actively participates in the innate and adaptive immune responses, metabolic events, the distribution of oxygen, nutrients and paracrine factors, blood coagulation, regulation of vascular tone, and the removal of metabolic products (Cines et al. 1998, Pober et al. 2009, Potente et al. 2011). In the last few decades, the endothelium has acquired a progressively increasing appreciation as it is now regarded a vastly complex organ with a broad spectrum of vitally significant functions.

Endothelial cells exhibit a vast transcriptional activity that distinguishes them from other cell types. This reflects their essential role in the pathophysiology of numerous diseases ranging from cardiovascular-related pathologies (e.g., atherosclerosis), inflammatory processes (e.g., sepsis, septic shock) to cancer (e.g., metastasis, tumor angiogenesis) (Adams et al. 1995).

In particular, the vascular endothelium has become the epicenter of intense research due to its key role in: (i) sepsis, severe sepsis and septic shock (highest mortality rates in non-cardiac intensive care units) (ii) cardiovascular-related diseases (highest single-cause mortality rates) and (iii) tumor metastasis (90% of cancer deaths are attributed to cancer metastasis).

1.2 Physiology and anatomical geometric features of the vascular endothelium

The circulatory system is composed of blood vessels conducting blood across the entire body as it is propelled by the rhythmic palpations of the heart throughout the vascular tree. The systemic circulation branches out of the left heart ventricle through the aorta, an artery that is characterized by both a wide diameter (approx. 2 – 3 cm) and high elasticity. The aorta is succeeded by progressively narrower arteries that arborize, ending in terminal arterioles at vascular beds across the entire circulatory system. The arterioles give rise to capillaries that perform the basic and life-sustaining functions of delivering nutrients and oxygen to the tissues while in return collecting metabolic end products that they convey to venules to which they convert. Venules coalesce into even wider veins that ultimately convert to the superior and

inferior vena cavae through which blood is returned to the heart via the right atrium. The arterioles, capillaries and venules constitute the microvasculature (Poher 2008, Iaizzo 2009, Poher et al. 2009, Granger et al. 2010, Klabunde 2011). The three building blocks of the microcirculatory system will be presented in more detail in the following sections.

1.2.1 Arterioles

As the blood is distributed from the heart and aorta through the major arteries to the progressively smaller and more numerous branches of the arterial system, a tree-type network of arterioles is formed. Arterioles exert control on the vascular resistance of organs and consequently the total blood volume and oxygen distribution within the various vascular beds (Ellis et al. 2005). The mean diameter of arterioles varies between 10 and 200 μm (Klabunde 2011). Arterioles, similar to their arterial parent vessels, are covered in their innermost lumen by a monolayer of endothelial cells while the periphery of the vessel may be circumferentially covered by fibroblasts and network of non-myelinated nerves (Johnson 2008, Iaizzo 2009, Granger et al. 2010). Arterioles are structurally very flexible and may dilate by up to 50% from normal resting conditions or conversely, may contract in particular at distal locations in the periphery (Schmid-Schonbein et al. 1985, Schmid-Schönbein et al. 1986). Arterioles constantly receive a variety of vasoconstrictor and vasodilator stimuli playing a vital role in responding to physical stimuli. They constrict and maintain a smaller diameter when intravascular pressure elevates (myogenic response). Conversely, when blood flow decreases, they experience flow-induced dilation. A typical sequence of events is prompted when a capillary bed initiates a dilatory signal that is transduced via the vascular endothelium to the arterioles supplying this capillary bed causing an increase in blood flow. The endothelial cells lining larger arterioles and arteries further upstream in the parent vessels, will respond to the increased flow-induced shear stress by dilating to the extent where regional shear stress in the capillary bed is restored to normal conditions (Ellis et al. 2005). In addition to physical stimuli, arterioles respond to variations in the immediate chemical environment by means of dilation and constriction (Johnson 1977, Johnson 1989, Christensen et al. 2001, Johnson 2008).

1.2.2 Capillaries

Capillaries extending from terminal arterioles are the smallest and most numerous among all blood vessels in the human circulatory system ranging from 5 – 10 μm in diameter. Their number is estimated at approximately 10 billion forming a network of 25,000 miles (~40,000 km); the estimated average length of individual capillary vessels is around 1 mm. Erythrocytes are highly deformable and have the ability to squeeze through the capillary network during their passage (Poher 2008, Iuzzo 2009, Klabunde 2011). Capillaries are surrounded circumferentially by a thin basement membrane and occasionally by pericytes while the innermost layer is formed by a single monolayer of endothelial cells (Rhodin 1968, Poher 2008). The primary function of capillaries in tissue perfusion and supplementation with nutrients and oxygen is achieved due to their thin inner diameter. Capillary networks exhibit a variation of barrier function or permeability owing to the vascular bed they are located at (Poher 2008). Capillaries are further subdivided into two families depending on the structure of their endothelial cells: (i) continuous, and (ii) fenestrated. In continuous capillaries, adjacent endothelial cells remain linked via interendothelial junctional complexes allowing the passage of substances with low molecular sizes (e.g., O_2 , CO_2 , steroid hormones), whereas they remain less permeable to water-soluble substances (e.g., Na^+ , K^+ , glucose and amino acids).

In fenestrated capillaries, the endothelial cells are characterized by the presence of wide pores allowing larger macromolecular compounds or even whole cells to pass through these structures. Fenestrated capillaries are primarily located in organs where rapid movement of materials is critical for their proper function (e.g., intestines, bone marrow, kidneys, liver). Certain substances are transported across individual endothelial cells by a molecular transportation mechanism termed transcytosis. In homeostatic conditions, endothelial cells contain increased numbers of endocytic and exocytic vesicles. Fusion of these structures leads to the formation of continuous vesicular channels across individual endothelial cells (Johnson 2008, Poher 2008, Iuzzo 2009).

1.2.3 Venules

Capillary networks coalesce into venules, which are slightly larger in diameter (post-capillary venules). They share a common feature with capillary vessels in that they are equally porous allowing phagocytic leukocytes to transmigrate from the lumen to the affected tissue areas (Iaizzo 2009). Post-capillary venules define the beginning of the venular network, structurally similar to the arteriolar network (Schmid-Schönbein et al. 1986). The mean diameter of venules ranges between 10 – 200 μm (Klabunde 2011). The venules are devoid of a smooth muscle circumferential coating. They are the most reactive to inflammation, among blood vessels, with their intercellular endothelial junctional proteins allowing for plasma proteins and circulating cells to diffuse from the bloodstream into the interstitial space (Johnson 2008).

Venules represent the major site of transvascular protein exchange and leukocyte trafficking and metastasizing tumor cells (Granger et al. 2010). The post-capillary venules are characterized by a structurally similar vessel wall compared to the one observed in capillaries. Venous vessels are devoid of vascular smooth muscle cells. Venous vascular resistance represents approximately 10% of the total resistance of the vascular tree. One of the major homeostatic features of the venular structures lies in stabilizing capillary hydrostatic pressure, a key determinant of fluid exchange between blood and the underlying tissues. Variations in venous resistance have a much greater impact on capillary pressure than similar fluctuations in arterial resistance would have (Johnson 2008).

1.2.4 Plasticity and the dynamic nature of the endothelium

The vascular endothelium exhibits extraordinary plasticity despite the genetic predetermination of individual endothelial cells. Physiological necessity and hemodynamic factors are capable of reversing phenotypic characteristics of single endothelial cells (Atkins et al. 2011). A very characteristic example of the plasticity of vascular endothelial cells is represented by cells in transplanted arterial and venous blood vessel grafts. They display a remarkable capacity to adjust their expression profile in an effort to correspond to the functional needs of the host vessel (Moyon et al. 2001, Othman-Hassan et al. 2001). Endothelial cells

located across straight segments of arteries align themselves in the direction of blood flow. This observation does not apply to endothelial cells at branching points in the arterial tree. These regions are characterized by turbulent flow patterns with Reynolds numbers typically above 2,000 (Passerini et al. 2004, Lupu et al. 2005, Chatzizisis et al. 2007). When segments of the thoracic aorta in a dog animal study were surgically excised and then re-implanted after a 90° rotation from the original vessel orientation, the nuclear pattern of the endothelial cells on the excised and subsequently re-implanted sections realigned in the direction of the blood flow within 10 days from surgery (Flaherty et al. 1972).

Other mechanisms in support of the tremendous potential of vascular endothelium to dynamically respond to injuries and pathogenic insults is the process of endothelial repair. Endothelial progenitor cells participate actively in vasculogenesis and re-endothelialization by undergoing differentiation toward endothelial cells (Asahara et al. 1997, Asahara et al. 1999, Krautkramer et al. 2014). Increased presence of cytokines in the systemic circulatory, as is the case with the invasion of pathogenic microorganisms or as a result of a sterile infection further enhance the release of endothelial progenitor cells (EPCs) from the bone marrow. The growth factors angiopoietin-1 (Ang-1) and angiopoietin-2 (Ang-2), vascular endothelial growth factor (VEGF), stroma-derived factor 1a, granulocyte colony-stimulating factor, and erythropoietin, have been associated directly with the mobilization and proliferation of circulating EPCs (Hattori et al. 2001, Moore et al. 2001, Bahlmann et al. 2003, Heeschen et al. 2003, Bahlmann et al. 2004, Kim et al. 2006, Shao et al. 2008, Shao et al. 2008, Pitchford et al. 2009, Krautkramer et al. 2014). The involvement of EPCs in endothelial repair mechanisms during the pathogenesis of infectious diseases and in particular sepsis and severe sepsis that is accompanied by organ failure has been the topic of several studies (Aird 2003, Rafat et al. 2007, Patschan et al. 2011, Krautkramer et al. 2014). The degree of circulating EPCs in septic patients correlates with survival rates and to a degree the severity of the clinical manifestation of the disease (Krautkramer et al. 2014).

1.2.5 Hemostasis

Another critical function that vascular endothelial cells perform through their anticoagulant properties is the maintenance of blood in a fluid state. Conversely, when blood vessel walls experience injurious insults, endothelial cells orchestrate the limited formation of blood clots to prevent life-threatening blood loss, support wound healing and consequently avert the entry of pathogenic microorganisms through the injured site. From an anticoagulant perspective, endothelial cells express tissue factor pathway inhibitor (TFPI), heparan, thrombomodulin, endothelial protein C receptor (EPCR), tissue-type plasminogen activator, ecto-ADPase, prostacyclin and nitric oxide. For its procoagulant function, vascular endothelial cells express tissue factor (TF), plasminogen activator inhibitor (PAI), vWF and thrombin receptor. Adding to the heterogeneity of the vascular endothelium, endothelial-derived procoagulant and anticoagulant factors exhibit increased distribution patterns between the different vascular beds (Aird 2001). While EPCR is predominantly present in arteries and veins, thrombomodulin is ubiquitously expressed in the entirety of the vascular endothelium (Ishii et al. 1986, Laszik et al. 2001). In rat and baboon animal models of sepsis, the subjects exhibited no detectable changes in thrombomodulin antigen levels after administration of *Escherichia coli* (*E. coli*) (Drake et al. 1993, Laszik et al. 2001). Mice challenged with lipopolysaccharide (LPS) appeared with increased EPCR mRNA expression in the large vessels of the heart and lung endothelium (Gu et al. 2000). In humans, both thrombomodulin and EPCR levels appeared downregulated in coronary arteries inflicted with atherosclerotic plaque (Laszik et al. 2001). Furthermore, thrombomodulin, the endothelial anticoagulant protein, is not expressed in the human brain at all (Ishii et al. 1986).

TFPI expression appears highest in human placenta and lung tissues as opposed to the brain exhibiting the lowest values (Osterud et al. 1995, Bajaj et al. 1999). In mouse models, TFPI mRNA expression is highest in the lung but undetectable in liver (Shimokawa et al. 2000). TFPI is expressed primarily by endothelial cells in the microvasculature. TF levels remain undetectable in normal unchallenged endothelium with markedly increased levels during the pathophysiology of an inflammatory condition. Endothelial cells in the marginal zone of splenic

follicles and in regions characterized by turbulent flow in the aortic branch of baboon sepsis models injected with *E. coli* revealed an upregulation of the TF gene (Drake et al. 1993, Lupu et al. 2005).

The most established approach in the study of vascular endothelial heterogeneity has been the isolation of endothelial cell populations harvested from a variety of vascular beds. This approach albeit physiologically estranged has offered valuable insights into comparative gene and protein expression, enzyme activity or cell signaling pathways in the endothelium. Nonetheless, despite the unquestionable merits these studies have offered in understanding functional and structural aspects of the endothelium they do exhibit a severe weakness. When endothelial cells are removed from their native microenvironment, they are functionally uncoupled from crucially important extracellular cues and manifest a phenotypic drift (Aird 2007, Aird 2007). Durr et al. demonstrated that 40% of native lung endothelial proteins expressed *in vivo* were undetectable under *in vitro* culture conditions (Durr et al. 2004). Fluid shear stress has been established as a crucial extrinsic factor capable of inducing variations in local endothelial permeability by modulating the expression and organization of interendothelial junction complex proteins. Due to the fact that the endothelium remains continuously exposed to fluid shear forces at its apical side, one approach for approximating *in vivo* conditions, while maintaining the advantages of a controlled environment that *in vitro* studies offer, is to emulate the native endothelial microenvironment *in vitro* by exposing endothelial monolayers to flow-induced shear stress. This approach offers the advantage that *in vivo* occurring hemodynamic parameters can be reproduced *in vitro* to approximate *in vivo* flow patterns both physiological and pathophysiological (Davies 1995, Davies et al. 1995, Ingber 2002, Shyy et al. 2002, Dai et al. 2004, Aird 2007, Aird 2007, Aird 2012).

1.3 Endothelial functional and structural heterogeneity

Endothelial cells exhibit functional and structural differences depending on the vascular bed where they reside. In the following sections, the attempt is made to describe in more detail some well-studied vascular beds and their respective endothelial functions.

1.3.1 Heart endothelium

The heart pumps with its rhythmic palpations the blood through the entire vascular system. It contains several compartments including the endothelial cells of the coronary arteries, the endocardium and the capillary endothelial cells. The endocardium forms the inner lining of the heart chambers and together with the cardiomyocytes forms the heart tube. Endocardial cells have larger dimensions compared to endothelial cells of other vascular beds in the circulatory system. They are characterized by an abundant presence of microvilli projecting into the heart cavity. The endocardium expresses connexin-43 (Cx43), connexin-40 (Cx40) and connexin-37 (Cx37) in contrast to the myocardial capillary endothelial cells, where these connexins are not present (Brutsaert et al. 1998). Similarly to the pulmonary circulatory system that allows for the perfusion of the lungs, the endocardium is perfused by the blood of both the systemic and the pulmonary system. The main roles of the endocardium are the modulation of cardiac contractility and rhythmicity (Paulus 1994, Brutsaert et al. 1998, Aird 2007).

1.3.2 Endothelial cells in coronary arteries

Coronary vessels arise from the ascending aorta. Epicardial arteries are succeeded by small muscular arteries that penetrate the myocardium. Endothelial cells of the coronary vessels derive from mesoderm-derived pro-epicardium. The coronary endothelial cells are primarily responsible for the regulation of coronary supply to the myocardium (Aird 2007).

1.3.3 Endothelial cells in myocardial microvessels

The capillary vessels of the heart possess continuous linings of endothelial cells. The capillary endothelium remains in intimate contact with the cardiomyocytes. Myocardial endothelial cells are more numerous than cardiomyocytes by a ratio of three to one (Hsieh et al. 2006). The distance between capillary endothelial cells and adjacent cardiomyocytes is

approximately 1 μm allowing for the optimal diffusion of oxygen and nutrients between the flowing blood and the underlying muscle tissues (Aird 2007).

1.3.4 Pulmonary endothelial cells

Capillary endothelial cells in the pulmonary system are arranged as a network of a densely interconnected mesh. Gas exchange is performed at the alveolocapillary membrane consisting of epithelial and endothelial cells that are separated by a thin basement membrane. Caveolae are abundantly expressed in the pulmonary endothelium (Gebb et al. 2004). One of the characteristic differences between endothelial cells in the lung and the systemic circulation lies in the expression of angiotensin. Angiotensin I-converting enzyme is expressed ubiquitously in all pulmonary endothelial cells but only 10% of systemic capillary endothelial cells express it (Balyasnikova et al. 2005). Alveolar capillary endothelial cells express platelet/endothelial cell adhesion molecule-1 (PECAM-1), whereas von Willebrand factor (vWF) is not expressed (Pusztaszeri et al. 2006). The transit time of neutrophils is particularly prolonged in pulmonary capillaries when compared with vascular beds across the circulatory system. This attribute has been assigned to the structural architecture of pulmonary capillary endothelial cells and the mechanoelastic properties of neutrophils. Perhaps indicative of the intricacy of lung endothelium, during inflammatory conditions, neutrophils become sequestered in the capillaries in a process mediated by mechanical deformability of neutrophils, rather than selectin-induced rolling and arrest, typical for endothelial capillaries across the systemic circulation (Doerschuk 2001, Aird 2007).

1.3.5 Bronchial endothelial cells

Endothelial cells in the bronchial blood vessels are characterized by increased leakiness, responsiveness to inflammatory mediators and exhibit a far greater angiogenic capacity when compared to pulmonary endothelial cells (Doerschuk 2001, Mitzner et al. 2004). Similarly to other vascular beds in the systemic circulation, leucocyte transmigration in the bronchial endothelium takes place in the postcapillary venules. One key difference is that bronchial

endothelial cells in contrast to endothelial cells in other vascular beds, constitutively express E-selectin, suggesting that they remain in a state of chronic activation (Feuerhake et al. 1998).

1.3.6 Glomerular capillary endothelial cells

The kidney is the recipient of approximately 20% of the cardiac output. Glomerular capillary endothelial cells are surrounded by the glomerular basement membrane and podocytes. Endothelial cells in this vascular bed form the initial barrier in the filtration process. These endothelial cells possess fenestrae with a diameter in the range between 60 and 80 nm covering nearly 20% of the endothelial surface (Deen et al. 2001). In contrast to fenestrated endothelium in the systemic vasculature, glomerular endothelial cells do not express the protein plasmalemmal vesicle-1 (Stan et al. 1999). However, they actively synthesize glycocalyx and basement membrane. The glycocalyx provides an additional filtration barrier with charge selectivity (Jeansson et al. 2006). Glomerular endothelial cells express constitutively PECAM-1. Conversely, they lack expression of vWF (Pusztaszeri et al. 2006). Capillary endothelial cells in the glomerulus contribute to the regulation of vasomotor tone by releasing endothelin-1, nitric oxide and prostaglandins (Aird 2007, Aird 2007).

1.3.7 Hepatic sinusoidal endothelial cells

Endothelial cells exhibit a wide spectrum of phenotypes across the liver vasculature. Venules in this vascular bed acquire a spindle-like shape, are non-fenestrated and are characterized by the presence of short microvilli. Endothelial cells at the transition region between terminal venules and hepatic sinusoid display a smooth and large shape and contain numerous actin fibers (Oda et al. 2003). Hepatic sinusoidal endothelial cells comprise roughly 50% of the non-parenchymal cells of the liver and appear discontinuous possessing membrane-associated, non-diaphragmed round cytoplasmic fenestrae 100 to 200 nm in length (Darling 2002). The sinusoidal endothelium acts as a dynamic filtration layer for solutes and plasma constituents. However, leucocyte transmigration and extravasation is not possible through their fenestrae. Instead, sinusoidal endothelial cells allow leucocytes to extend to the underlying matrix without having to extravasate completely. This attribute displays in the most

profound way the resourcefulness and dynamicity of the endothelium as well as its regional specialization to accommodate organ-specific functions (Aird 2007, Aird 2007).

1.3.8 Brain endothelium

The blood brain barrier is characterized by a wide spectrum of transporters. Since the paracellular permeability pathway in this vascular bed is occluded, nutrients and solutes cross the endothelial layers through the transcellular pathway. Hence, it is not surprising that brain endothelial cells express the glucose transporter GLUT-1 in abundance. They also express high levels of the neutral amino acid transporter LAT-1 facilitating the transport of nutrients and solutes from the blood to the underlying brain tissues (Boado et al. 1999, Stamatovic et al. 2008). Brain endothelial cells exhibit a low number of vesicles under quiescent conditions compared to endothelial cell types residing in other vascular beds. Inflammation-mediated activation of brain endothelial cells has an impact on increasing the number of these vesicles. These cells also possess a finely developed tubular system formed by membrane-associated tubules intruding deeply into the endothelial cells both from the luminal and abluminal surface (Castejon 1980, Coomber et al. 1986, Lossinsky et al. 2004). Furthermore, the cytoskeleton of brain endothelial cells plays an essential role in the formation of interendothelial junction integrity. It exhibits a uniform thickness with limited formation of pinocytotic vesicles and lacks fenestrations. The wall thickness in brain capillary endothelial cells is nearly 40% of the thickness compared to capillary endothelial cells in other regions of the vasculature (Coomber et al. 1986, Stamatovic et al. 2008).

1.4 Vascular endothelial barrier function

As stated in previous sections, the vascular endothelium represents an integral part of the circulatory system comprising the innermost lining of blood vessels by forming a continuous monolayer of endothelial cells. Although functional and anatomical characteristics exist among the several vascular beds, the entire vascular endothelium with exception of the lymphatic endothelium, acts as a selective barrier separating blood plasma from the interstitium (Mehta et

al. 2006). Endothelial cells in the vascular tree perform a wide array of vitally important functions spanning vascular smooth muscle tone, host response to invading microorganisms, angiogenesis and tissue fluid hemostasis. Maintaining a highly functional semipermeable barrier allows for the selective passage of macromolecular components inward and outward of the lumen. This endothelial function is of vital importance. Loss of endothelial barrier integrity is the hallmark of inflammatory conditions (e.g., sepsis) leading to chronic inflammation and ultimately morbidity or death.

The characteristic permeability of circulating macromolecules depends on their molecular radii and the barrier properties of the particular vascular bed and its residing endothelial cells. The transvascular flux of solutes and fluid provide evidence that protein transport across the endothelium is performed by the interaction of a vast number of endothelial components. In this regard, the traditional theory regarding the endothelium as a passive structure through which plasma proteins diffuse to the interstitium represents an obsolete model and has consequently been abandoned (Mehta et al. 2006). In homeostatic conditions, vascular endothelial monolayers present a cellular barrier to the permeation of liquids and solutes. Interendothelial discontinuities in the cleft region (Figure 1.2) between adjacent endothelial cells are in the order of 3 nm and account for the permeation of small molecules (e.g., glucose, mannitol, and fructose), amino acids, and urea (Michel et al. 1999). The passage of small molecules with molecular radii smaller than 3 nm is accomplished through the paracellular route (Pappenheimer et al. 1951, Mehta et al. 2006, Komarova et al. 2010). The transcytosis pathway accommodates the passage of larger molecules (e.g., plasma proteins, albumin and water). A significant amount of water (up to 40% of the hydraulic pathway) is ferried across the endothelium barrier via transcytosis by aquaporins, water-transporting membrane channels (Preston et al. 1991, Verkman 1998, Michel et al. 1999, Mehta et al. 2006). Interestingly, water represents an atypical example in that, unlike other larger macromolecules, water can be traversed across the vascular endothelium by paracellular means and also transcellularly by means of aquaporin (Mehta et al. 2006).

1.4.1 Heterogeneity of endothelial permeability

Endothelial cells throughout the entire circulatory system share a large number of common features. Independently of their location in the vascular tree, they share the same embryonic precursor cells, hemangioblasts. Despite the remarkable similarities that endothelial cells exhibit, differences have been reported with regard to permeability variations depending on the vascular bed where the respective endothelial cells reside (Suter et al. 1964, Bruns et al. 1968, Clementi et al. 1969, Simionescu et al. 1974, Grisham et al. 1975, Crone 1984, Gloor et al. 2001, Arap et al. 2002, Pasqualini et al. 2002, Aird 2003, Mehta et al. 2006). For example, endothelial cells follow typically a flat and cuboidal geometry in veins (Girard et al. 1995, Miyasaka et al. 2004). Thickness varies from less than 0.1 μm in capillaries and veins to 1 μm in the aorta (Florey 1966). *In vitro* studies under static conditions have revealed that endothelial cells in the pulmonary microcirculatory were 3-, to 4-fold more restrictive to albumin when compared to endothelial arterial or vein segments. Complementary transendothelial electrical resistance assays demonstrated a 10-fold increase in pulmonary microvessel endothelial monolayers when compared to larger endothelial vessels (Del Vecchio et al. 1992, Lum et al. 1994, Schnitzer et al. 1994, Schnitzer et al. 1994, Kelly et al. 1998).

Endothelial cells also exhibit a specific genetic fingerprint depending on the vascular bed where they reside. Differences in genes regulating expression of extracellular cell matrix (ECM) proteins, integrins, guanine nucleotide exchange factors (GEFs) and myosin light chain kinase (MLCK) in large versus small vessel endothelia have been reported. Differences in endothelial electrical resistance assays and hence, variations in their respective permeability are accompanied by differences in ultrastructural composition. Endothelial cells located in the lung microvasculature exhibit a more dense and organized mesh of interendothelial junction complex proteins when compared to endothelial cells from larger vessels. Caveolar density in the capillary endothelium is highest across the vascular beds in the circulatory system, possibly offering yet another explanation to the restrictiveness of lung microvascular endothelium to albumin. Furthermore, signal transduction patterns regulating endothelial barrier function differ from one vascular bed to another. Endothelial cells of microvascular origin exhibit distinct profiles with

regard to thrombin-induced intracellular Ca^{2+} , forskolin and cyclic nucleotide levels (Mehta et al. 2006, Aird 2007, Aird 2007, Bos et al. 2007).

1.4.2 Regulation of vascular endothelial permeability

Endothelial cells form a semipermeable monolayer in the lumen of the vasculature allowing selectively the passage of solutes and plasma proteins from the lumen to the interstitium, protecting the underlying tissue beds from toxic components in the bloodstream, removing metabolic waste products and CO_2 , delivering oxygen and actively participating in the immune host response against invading pathogens.

Vascular endothelial permeability is the primary and foremost attribute of the endothelium. Adjacent endothelial cells across the entire vascular tree form linkages to one another by junction protein complexes. At the sites of junction complexes, interendothelial cells engage in the formation of adherens junctions (or zonula adherens), tight junctions (or zonula occludens) and gap junctions.

Although epithelial cells follow a spatially well-defined distribution of both adherens and tight junctions, in the endothelium the junction architecture along the endothelial cleft is less structured and adherens junctions are intermingled with tight junctions (Simionescu 2000).

Interendothelial protein complexes participate in the regulation of two independent barrier pathways termed, paracellular and transcellular permeability. The paracellular permeability pathway is formed by interendothelial junctions comprised of transmembrane adhesion proteins that are anchored to the actin cytoskeleton. As a consequence, not only do they actively regulate the passage of plasma proteins, solutes, and fluid across the endothelial barrier but they also mechanically stabilize endothelial cells (Bazzoni et al. 2004, Komarova et al. 2010).

The loss of endothelial barrier function leads to a plethora of life-threatening complications. Chronically elevated permeability that cannot be restored through the re-absorptive function of the lymphatic system leads to the clinical manifestation of edema, a common complication

presented in patients with sepsis or severe sepsis. Cancer patients in particular face an increased risk as vascular leakage facilitates the dissemination of metastatic cancer cells that break away from the primary tumor, intra-, and extravasate through the blood lumen in order to form remote colonies in the body. Furthermore, vascular leakage contributes to the accumulation of fluid in the stroma and the elevated interstitial pressure commonly observed in patients with solid tumors (Weis et al. 2005).

1.4.3 Adherens junctions

Adherens junctions are protein complexes formed by members of the cadherin family of adhesion proteins. Endothelial cells express ubiquitously vascular endothelial cadherin (VE-cadherin) and neural cadherin (N-cadherin). While VE-cadherin is expressed by all endothelial types, N-cadherin is also present in neural and smooth muscle cells. T-cadherin and P-cadherin, also members of the cadherin family, are expressed in various degrees by endothelial cells across the vascular tree (Ivanov et al. 2001, Bazzoni et al. 2004, Dejana et al. 2008). VE-cadherin is expressed exclusively by endothelial cells independently of the vascular bed where they reside (Dejana et al. 1995, Venkiteswaran et al. 2002).

Cadherins are Ca^{2+} -dependent, homophilic, single-pass transmembrane proteins whose extracellular region interacts with other cadherin proteins in adjacent cells, whereas intracellularly their cytoplasmic tails are anchored to catenins that are ubiquitously present at sites of adherens junction complexes. Cadherins perform their cell-cell adhesion functions by forming a cadherin dimer (Leckband et al. 2000, Yagi et al. 2000, Gavard 2009).

Adherens junctions are among the key regulators of paracellular permeability. Adherens junctions are ubiquitously expressed in both the vascular and lymphatic endothelium. Transmembrane adhesion proteins from the cadherin family mediate homophilic adhesions to neighboring endothelial cells (Dejana et al. 1995, Aberle et al. 1996, Dejana et al. 1999, Gumbiner 2000, Yagi et al. 2000, Angst et al. 2001, Bazzoni et al. 2004, Dejana 2004, Bazzoni 2006).

The major structural component of endothelial adherens junctions is VE-cadherin mediating homophilic binding and adhesion of adjacent cells in a Ca^{2+} -dependent manner (Liaw et al. 1990, Lampugnani et al. 1995, Lampugnani et al. 1997, Anastasiadis et al. 2000, Dejana et al. 2001). VE-cadherin is comprised of an extracellular and a cytoplasmic component (Figure 1.3). The extracellular domain of VE-cadherin is comprised of five cadherin-like repeats. The cytoplasmic VE-cadherin tail contains two functional domains, the juxtamembrane domain and the COOH-terminal domain. Both these domains interact with members of the catenin family. The juxtamembrane domain of VE-cadherin binds p120-catenin. The COOH-terminal domain binds either β -catenin or plakoglobin in a mutually exclusive fashion. β -Catenin or plakoglobin is then associated to α -catenin which, in turn, binds to several actin-binding proteins, including α -actinin, ajuba, and ZO-1 (Dejana et al. 1999, Bazzoni et al. 2004, Bazzoni et al. 2004, Dejana 2004, Mehta et al. 2006, Weis et al. 2006). VE-cadherin plays a major role in the stable assembly of adherens junctions and the maintenance of barrier integrity. Ectopic expression of VE-cadherin mutant lacking the extracellular domain in human or mouse dermal microvascular endothelial cells resulted in the destabilization of the adherens complex with subsequent disturbances in the barrier function (Broman et al. 2002, Venkiteswaran et al. 2002).

The linkage between p120-catenin and VE-cadherin's juxtamembrane domain is an integral part in the stability of adherens junctions and consequently their contribution to endothelial barrier integrity in health and disease. Although VE-cadherin is the primary component of adherens junctions, catenins have been also attributed an important role in maintaining adherens junction functionality. The binding of α -catenin to α -actinin, vinculin or vasodilator-stimulated phosphoprotein (VASP) is of paramount importance in maintaining the association of E-cadherin with the actin cytoskeleton intact. Furthermore, α -catenin has a major role in promoting interactions among adherens junctions, tight junctions and gap junctions by binding with ZO-1. Hence, α -catenin, a member of the catenin protein family, has an intimate relationship in the complex regulation of interendothelial integrity and in extension endothelial permeability (Muller et al. 2005, Mehta et al. 2006).

Hu et al. investigated the role of endothelial p120-catenin in response to LPS. LPS-induced downregulation of p120-catenin was observed upon LPS challenge. The protein levels of p120-catenins are associated with the severity of sepsis. Depletion of p120-catenin resulted in LPS-induced intercellular adhesion molecule-1 (ICAM-1) expression, neutrophil recruitment into the lung microvasculature, production of the pro-inflammatory cytokines TNF α and IL-6 and the formation of lung edema. Hu et al. concluded that p120-catenin negatively regulates inflammatory host responses to LPS by inhibiting the activation of mitogen-activated protein kinases (MAPK) and NF- κ B (Hu et al. 2010).

In a study investigating the effects of shear stress on endothelial adherens junctions, it was shown that VE-cadherin expression was reduced after endothelial cell exposure to fluid shear stress at 15 dyn/cm² for 8.5 h. Interestingly, the cytoplasmic α - and β -catenin expression levels remained unaffected by shear stress (Noria et al. 1999). This finding suggests that some constituents of adherens junction complexes can be degraded by shear stress induced changes while others remain unaltered adding to the complexity of endothelial permeability regulation by hemodynamic forces. Likewise, this signifies the importance of studying endothelial barrier function in an environment that imitates their natural *in vivo* microenvironment as closely as technically possible.

Thrombin is a permeability-inducing agent that leads to endothelial permeability increases and the formation of interendothelial gaps (Garcia et al. 1986, Rabiet et al. 1996, Ellis et al. 1999). The endothelial barrier function is further destabilized by inhibitors targeting protein tyrosine phosphatases. Conversely, inhibiting protein tyrosine kinases promotes and stabilizes endothelial barrier function (Staddon et al. 1995, Gloor et al. 1997, Gilbert-McClain et al. 1998, Shi et al. 1998, van Nieuw Amerongen et al. 1998).

Thrombin-induced endothelial barrier dysfunction is accompanied by modifications at the intercellular cadherin-catenin complexes. In fact, endothelial monolayers challenged with thrombin resulted in the disappearance of VE-cadherin and catenin complexes (α -catenin, β -catenin, plakoglobin and p120-catenin) at interendothelial retraction sites. Moreover, lower

amounts of α -catenin, β -catenin, plakoglobin and p120-catenin remained associated with VE-cadherin (Rabiet et al. 1996).

It has been shown that protein tyrosine phosphatase SHP2 is associated with VE-cadherin complexes in confluent, quiescent human umbilical vein endothelial cells (HUVECs). More specifically, SHP2 selectively associated with β -catenin in the VE-cadherin complex. Challenging endothelial monolayers with thrombin, led to tyrosine phosphorylation of SHP2 by a Src family kinase and resulted in its dissociation from the VE-cadherin complex. Thrombin-induced SHP2 dissociation from VE-cadherin further initiated the phosphorylation of VE-cadherin associated with β -catenin, plakoglobin and p120-catenin (Ukropec et al. 2000).

Phosphorylation of VE-cadherin at tyrosine 658 (Y658) in its cytoplasmic tail acts restrictively to its association with p120-catenin, whereas phosphorylation of tyrosine 731 (Y731) in the cytoplasmic tail of VE-cadherin prevents β -catenin from interacting with VE-cadherin. In both cases, tyrosine phosphorylation at Y658 or Y731 in the cytoplasmic tail of VE-cadherin causes a disturbance in the adherens junction complex (Potter et al. 2005). p120-catenin, a cytoplasmic scaffold protein, has been established as one of the major substrates for the Src family kinases (Kanner et al. 1991). p120-Catenin binds to the juxtamembrane domain in the cytoplasmic tail of protein members of the cadherin family contributing to their stability (Reynolds et al. 2004, Alcaide et al. 2012).

β -Catenin or plakoglobin (γ -catenin) can potentially translocate into the nucleus modulating transcriptional activities (Hecht et al. 2000, Giles et al. 2003, Baumeister et al. 2005). For example, it has been shown that laminar fluid shear stress at 10 dyn/cm² caused β -catenin to translocate to the nucleus where it acted upon transcription factors. Furthermore, in the same study, fluid shear stress resulted in reduced expression levels of β -catenin. This suggests that under conditions of fluid shear stress, cadherins recruit less β -catenin to the site of adherens junction complexes (Norvell et al. 2004).

Src family kinases have been implicated in vascular endothelial growth factor receptor-2 (VEGFR-2) signaling and endothelial permeability, angiogenesis, cell motility and apoptosis (Eliceiri et al. 1999, Abu-Ghazaleh et al. 2001, Weis et al. 2004). Elevated Src expression and activity levels correlate with proliferative disorders and various cancer types (Frame 2002).

The ability of the protein tyrosine kinase Csk (C-terminal Src kinase) to negatively regulate Src family kinases has been attributed to its ability to render these kinases inactive by phosphorylating a negative regulatory tyrosine (Latour et al. 2001). Csk has been shown to interact directly with VE-cadherin through the SH2 domain of Csk (Baumeister et al. 2005).

VE-cadherin, a major constituent of adherens junction complexes along with its interacting partners at sites of adherens junctions are instrumental in maintaining endothelial barrier integrity by forming homophilic interactions between VE-cadherins of adjacent endothelial cells and via the association of VE-cadherin to actin through the cytoskeletal catenins. VEGFR-2 has been shown to associate with VE-cadherin. When VEGF binds to VEGFR-2, it activates it and causes its dimerization. VEGF-induced dimerization of VEGFR-2 triggers a sequential Src-mediated activation of Vav2, a Rho-specific GEF, Rac and p21-activated kinases (PAK). The activated PAK, in turn, leads to the phosphorylation of serine 665 (S665), serine 666 (S666) and serine 667 (S667) in the cytoplasmic tail of VE-cadherin. It is speculated that the serine-phosphorylation of VE-cadherin is coordinated with the tyrosine phosphorylation of the VE-cadherin and its associated cytoplasmic catenin partners by Src. Serine-phosphorylation of VE-cadherin causes the recruitment of β -arrestin2 that triggers the internalization of VE-cadherin into clathrin-coated pits and ultimately the disassembly of endothelial adherens junctions. The direct implication of this process is barrier dysfunction resulting in increased endothelial permeability. Internalized VE-cadherin in endosomes may be recycled back to the endothelial plasma membrane indicating the dynamic nature of disassembly and reorganization of endothelial adherens junctions during vessel remodeling (Esser et al. 1998, Xiao et al. 2003, Weis et al. 2004, Potter et al. 2005, Gavard et al. 2006).

1.4.4 Tight junctions

Tight junctions, similarly to adherens junctions, are located in the endothelial intracellular cleft compartment. Although, tight junctions in the endothelium are related to epithelial tight junctions, their topological organization is not as strictly defined as in epithelial cells and varies from one vascular bed to another across the circulatory system. Besides the organizational differences in tight junctions between endothelial and epithelial cells, proteins that are part of tight junction complexes in endothelial cells are not necessarily found in the epithelium. For example, symplekin is expressed in the tight junction complexes of epithelial cells but is absent in endothelial tight junctions (Keon et al. 1996).

Tight junctions mediate adhesion in the vascular endothelium forming tight seals between adjacent endothelial cells that participate instrumentally in the regulation of paracellular permeability. Tight junctions exhibit an outstanding variability among the different vascular beds in the endothelium (Franke et al. 1988). Perhaps the most prevalent sign of the importance of tight junctions in paracellular permeability is their pronounced and well-organized presence in brain microvessels regulating the blood brain barrier. Furthermore, the blood retinal barrier displays a rich presence of tight junctions. Tight junctions are also primarily expressed in endothelial arteries, whereas in veins and capillaries they are characterized by a looser organization. The general rule holds true in the majority of instances, that the higher the degree of fluid exchange in a specific organ the less organized the tight junctions in this organ's endothelium will be (Bazzoni et al. 2004).

In the endothelial microvasculature, tight junctions are less complex within capillaries compared to arterioles. Venules exhibit even less organized tight junction complexes. Conversely, large arteries exposed to higher fluid shear rates, exhibit highly organized structures of tight junctions (Franke et al. 1988, Bazzoni et al. 2004, Lai et al. 2005, Furuse et al. 2006, Kim et al. 2006, Aird 2007, Aird 2007).

The tight junction complexes are comprised by several proteins. The claudin family of proteins are the major tight junction transmembrane components (Furuse et al. 2006). Claudins

exhibit both homophilic and heterophilic adhesive properties via their extracellular domains. Endothelial tight junctions highly express claudin-5 (Morita et al. 2003). The prominent role of tight junctions in the regulation of blood brain barrier is best demonstrated in a study that used claudin-5 deficient mice showing that these mice suffered selective impairment in blood brain barrier function for molecules with a molecular weight less than 800 kDa (Nitta et al. 2003). Other claudins characterized in endothelial cells are claudin-3 and claudin-11 (Wolburg et al. 2003, Challier et al. 2005, Enerson et al. 2006, Lievano et al. 2006). Decreased claudin expression has been closely linked to pathological conditions associated with blood brain barrier dysfunction (Liebner et al. 2000, Davies 2002, Sawada et al. 2003, Wolburg et al. 2003, Harhaj et al. 2004, Hawkins et al. 2004, Bazzoni 2006).

Occludin is yet another transmembrane component of tight junctions. Occludin, historically the first integral membrane protein discovered to localize to tight junctions, is characterized by four extracellular transmembrane domains, whereas its cytosolic carboxyl-terminus interacts directly with F-actin and the scaffold proteins ZO-1, ZO-2 and ZO-3 (Furuse et al. 1993, Furuse et al. 1994, Haskins et al. 1998, Itoh et al. 1999, Wittchen et al. 1999).

In the vascular endothelium, occludin is exclusively expressed in the blood brain barrier and the blood retina barrier. Occludin has been linked to increased tight junction-related barrier function (Hirase et al. 1997). Downregulation of occludin, on the other hand, has been associated with pathological conditions in regard to blood brain barrier, blood retina barrier disruption, stroke, diabetes, hypoxia and aglycemia (Antonetti et al. 1998, Vajkoczy et al. 2000, Huber et al. 2001, Brown et al. 2002, Brown et al. 2005, Erickson et al. 2007).

In a different study, VEGF-treated retinal endothelial cells exhibited disrupted paracellular permeability accompanied by decreased levels of occludin. Occludin is phosphorylated on a multitude of serine and threonine residues via protein kinase C (PKC) activation upon VEGF treatment leading to increased permeability (Antonetti et al. 1999, Harhaj et al. 2006).

Both tight junction constituents, claudins and occludins, interact with numerous intracellular proteins, including ZO-1, ZO-2, ZO-3, AF-6, protease-activated receptor-3 (PAR-3), cingulin and 7H6 antigen. The linkage of these proteins leads to the formation of protein complexes located at the submembrane side of tight junctions (Bazzoni et al. 2004, Harhaj et al. 2004).

Occludin has also been implicated in the modulation of tight junction barrier integrity by fluid shear stress. Flow-induced shear stress leads to decreases in occludin expression contributing to accompanying increases of paracellular endothelial permeability. Shear stress at 10 and 20 dyn/cm² led to a reduction of occludin levels by approximately 50% after 3 h exposure to fluid shear stress indicating that occludin is insensitive to the magnitude of the applied shear stress at least between 10 and 20 dyn/cm². In contrast to the reduced expression levels of occludin in response to shear stress, ZO-1 expression levels remained the same despite exposure to fluid shear stress suggesting that ZO-1 and occludin are differentially regulated in response to shear stress. Endothelial cells exposed to fluid shear stress undergo morphological changes most likely with the involvement of transmembrane proteins (e.g., occludin) at cell-cell contacts of adjacent cells. ZO-1, a peripheral membrane-associated protein and one of the major constituents of tight junctions has been implicated in the disassembly and reassembly of endothelial tight junctions (Fanning et al. 1996, Fanning et al. 1998, DeMaio et al. 2001).

1.4.5 Gap junctions

In contrast to adherens and tight junctions that control cell-to-cell adhesion, gap junctions mediate cell-to-cell communication. They are formed by connexins. The vascular endothelium expresses Cx43, Cx40, Cx37 and connexin-32 (Cx32). Within gap junctions, connexins organize in connexons acting as channels for the intercellular passage of ions and molecules of smaller molecular weights (Galbraith et al. 2002, Mehta et al. 2006, Goodenough et al. 2009, Okamoto et al. 2009). Gap junction complexity and functionality varies across the vascular tree as does the relative abundance of connexins (Galbraith et al. 2002). Arterioles, for instance, exhibit an outstanding degree of complexity in their gap junctions. Smooth muscle cells express primarily Cx43. Although there is an overlap of connexin expression among smooth muscle cells that

surround the endothelial layer and endothelial connexin expression, only smooth muscle cells express connexin-45 (Cx45), whereas connexin-37 is uniquely expressed in the vascular endothelium (Little et al. 1995, Gabriels et al. 1998, van Kempen et al. 1999, Kruger et al. 2000, Goodenough et al. 2009).

Interestingly, gap junctions are formed between the smooth muscle and endothelial cells as a means of communication between these two cell types that stand in an intimate relationship across the vascular tree (Gabriels et al. 1998). The vascular endothelium adjusts expression levels of gap junction proteins in response to the changing conditions of the immediate microenvironment of endothelial cells. For example, in areas of turbulent flow (e.g., at vessel branch points or bifurcations), the Cx43 expression is noticeably upregulated (Gabriels et al. 1998). In many vitally important vascular processes, gap junctions function as rapid messengers within the proximity of the vascular bed where they reside. They have been implicated in the conducted spread of vasodilation. When endothelial cells are stimulated accordingly, they initiate a rapidly propagating bidirectional wave of relaxation along the vessel axis indicating the importance of gap junctions as communications network for the endothelium (Welsh et al. 1998, Figueroa et al. 2003, de Wit et al. 2006, Goodenough et al. 2009).

1.4.6 Desmosomes

Desmosomes are specialized and highly ordered complex molecular domains residing at membrane intercellular regions and mediating cell-cell adhesion and cytoskeletal linkages (Green et al. 2007, Kowalczyk et al. 2013). Desmosomes contribute to the integration of cellular components to tissue beds and stabilize them against mechanical forces (Delva et al. 2009, Thomason et al. 2010, Saito et al. 2012).

In contrast to epithelial cells, desmosomes are largely not present in the endothelium with the exception of lymphatic and venous endothelial cells that exhibit structural components similar to epithelial desmosomes and are called complexus adhaerentes (Schmelz et al. 1993). The complexus adhaerentes contain plakoglobin and desmoplakin that are tethered to

VE-cadherin (Schmelz et al. 1993, Ebata et al. 2001, Borrmann et al. 2006, Franke et al. 2006, Hammerling et al. 2006, Bass-Zubek et al. 2009).

Desmosomes are involved in the interaction of at least three distinct protein families: (i) the cadherins, (ii) the armadillo proteins and (iii) the plakins (Getsios et al. 2004). The desmosomal cadherins have been described to directly interact with a subset of armadillo protein family members including plakoglobin and the p120-catenin related proteins expressed in humans, plakophilin-1 (PKP1), plakophilin-2 (PKP2), plakophilin-3 (PKP3) or γ -catenin and p0071 or plakophilin-4 (PKP4) (Hatzfeld 1999, Chen et al. 2002, Bonne et al. 2003, Hatzfeld 2007).

Desmosomes are prominent sites of adhesion and have been reported in close association with the intermediate filament in the cytoplasm providing mechanical stability in epithelial and cardiac muscle cells and most notably in endothelial cells. They have been described as having a unique ultrastructural appearance while their molecular composition depends on the cell type. Impairment of their functionality leads to disturbances in the mechanical robustness of cells and tissues as has been reported previously (Holthofer et al. 2007).

PKP4 (or p0071) and p120-catenin subfamily members are closely related. They have been reported to localize in proximity to adherens junctions and desmosomes (Hatzfeld et al. 2003). Furthermore, there is evidence that in endothelial cells, p0071 competes with VE-cadherin by displacing it from the complex (Calkins et al. 2003, Hatzfeld et al. 2003).

1.5 Electrical cell-impedance spectroscopy and endothelial barrier function

Transendothelial electrical resistance is an attractive method that has been used widely for the evaluation of endothelial barrier function. Traditionally, microporous semi-permeable membrane chambers have been used to assess permeability properties of normal and treated cellular monolayers (DePaola et al. 2001).

Independently of endothelial cell type and location in vascular bed, endothelial cells share a common denominator in that they respond to mechanical and biochemical changes originating from their immediate microenvironment in a dynamic fashion. The way in which they converse mechanical forces into biochemical signaling is time-dependent and may range from milliseconds to seconds and even several minutes (Janmey et al. 2011). Traditionally, the available techniques to study changes in endothelial barrier function have been end-point assays without regard to the dynamic nature of the endothelium. Studying the endothelial barrier function under physiologically relevant fluid shear stress conditions requires a technique that allows for real-time monitoring. The ECIS model and instrumentation (Applied BioPhysics, Troy, NY) allows for real-time barrier function monitoring and quantification either under static or fluid shear stress conditions (Davies 1989, Geiger et al. 1992, Nollert et al. 1992, Davies et al. 1994, Sill et al. 1995, Tardy et al. 1997, DePaola et al. 2001).

During data acquisition, a constant current source applies an alternating current (AC) signal of 1 μA at a period duration of a pre-defined frequency (Figure 1.4). The current is applied between a disk-shaped electrode with a diameter of 0.25 mm (total surface area is 0.05 mm^2) and a larger counter-electrode with a diameter of 10 mm. The counter-electrode surrounds the small electrode.

Both the small and surrounding counter-electrode are connected to a phase-sensitive lock-in amplifier that monitors voltage changes between them while an AC signal is supplied through a resistor at 1 $\text{M}\Omega$. The source of the electric AC current is set at 1 V. A wide array of frequencies ranging from 40 Hz to 64 kHz are supported for probing endothelial monolayers or other cell types (Giaever et al. 1991).

The ECIS instrument monitors both the voltage across the small electrode and the larger surrounding electrode and the phase of the voltage relative to the applied current. The ECIS model assumes the cell and electrode system as a series RC circuit converting the data not only to impedance but extends it further to include electrical resistance and capacitance (Giaever et al. 1991, Keese et al. 2004).

In the case where no cells are seeded onto the gold-film ECIS electrode slides (Figure 1.5A) adding only the cell culture growth medium allows for it to act as the electrolyte (Figure 1.5B). The applied AC flows from the ECIS electrodes toward the electrolyte unobstructed and disperses eventually into the culture medium. When cells are seeded and start forming a monolayer, the current is constricted by the cell membranes (Figure 1.6). At this point, the current is forced to flow beneath and between adjacent endothelial cells, resulting in significant increases in impedance and resistance. The microampere current and the resulting voltage drop do not cause any disturbance to the cells rendering the ECIS method as non-invasive. However, the endothelial monolayer causes substantial changes in the measured values of electrical impedance, resistance and capacitance (Giaever et al. 1991, Keese et al. 2004). The ECIS model has attracted attention for a wide spectrum of cell and molecular assays including cell attachment and cell spreading, cell locomotion, cell morphological studies, toxicological studies, cellular signal transduction and tumor metastasis (Giaever et al. 1991, Tirupathi et al. 1992, Reddy et al. 1998, Wegener et al. 1999, Wegener et al. 2000, Keese et al. 2002, Keese et al. 2004).

The ECIS model treats the endothelial cells as a resistor and a capacitor in series. The individual cells are regarded as circular disks hovering above the gold-film electrode substrate (Giaever et al. 1986, Ghosh et al. 1993, DePaola et al. 2001). The three quantities that ECIS quantifies are electrical resistance (Figure 1.7), the alpha parameter (Figure 1.8) and cell membrane capacitance (Figure 1.9). The specific impedance for a cell-covered ECIS electrode is expressed by the following mathematical formula (Giaever et al. 1991):

$$\frac{1}{Z_c} = \frac{1}{Z_n} \left(\frac{Z_n}{Z_n + Z_m} + \frac{\frac{Z_m}{Z_n + Z_m}}{\frac{i\gamma r_c}{2} \frac{I_0(\gamma r_c)}{I_1(\gamma r_c)} + 2R_b \left(\frac{1}{Z_n} + \frac{1}{Z_m} \right)} \right) \quad (1.1)$$

where I_0 and I_1 are modified Bessel functions of the first kind, i is $\sqrt{-1}$, Z_c is the specific impedance of a cell-covered electrode, Z_n is the actual measured specific impedance of a cell-free electrode, Z_m is the actual measured specific impedance of the cell monolayer, R_b is the

specific resistance between adjacent cells in the monolayer, r_c is the cell radius, R is the resistivity of the cell culture medium, and h is the height of the space between the ventral side of the cell and the substratum (Giaever et al. 1986, Giaever et al. 1991, Wegener et al. 2000).

The solution is dependent on the resistance between adjacent cells (R_b) per unit area. The second parameter on which the solution of the above equation depends on is α defined as follows (Giaever et al. 1991):

$$\gamma r_c = r_c \sqrt{\frac{\rho}{h} \left(\frac{1}{Z_n} + \frac{1}{Z_m} \right)} \quad (1.2)$$

or

$$\gamma r_c = \alpha \sqrt{\frac{1}{Z_n} + \frac{1}{Z_m}} \quad (1.3)$$

where ρ is the resistivity of the cell culture medium acting as the electrolyte and h is the distance between the ventral side of the cells and the ECIS gold-film substrate (Giaever et al. 1986, Giaever et al. 1991, Wegener et al. 2000).

ECIS-based transendothelial or impedance studies have been performed primarily under static cell culture conditions with the exception of a limited number of studies conducted under fluid shear stress.

DePaola studied the behavior of bovine aortic endothelial cells under shear stress conditions at 10 dyn/cm² for either a duration of 5 h or for two consecutive 30 min cycles separated by a 2 h time window of paused shear stress. The study reported that TEER of the monolayer increased sharply by approximately 1.2-fold of the baseline values within the first 15 min from the onset of flow followed by a gradual decrease in resistance by 0.85 and 1.1 times the baseline values after 5 h and 30 min respectively. Bovine aortic endothelial cells revealed a reversibility of the flow-induced impedance changes when the flow component was removed (DePaola et al. 2001). Endothelial responses occur in a dynamic fashion as a function of the applied shear stress levels,

potential pre-treatments of endothelial cells with biochemical agents, exposure of cells to inhibitors or the silencing of signaling molecules. Changes in electrical impedance and resistance also reflect signaling events and morphological adaptation of endothelial cells to flow-induced shear stress.

Phelps et al. used the ECIS model to confirm the broadly accepted theory that shear stress gradients in regions of disturbed flow patterns induce structural and functional changes in intercellular junction protein complexes resulting in an increase of endothelial permeability and augmentation of transendothelial shuttling of macromolecules. In their study, Phelps et al. used bovine aortic endothelial cells and subjected them to disturbed fluid shear stress while monitoring changes in impedance and resistivity of the monolayer. Bovine aortic endothelial cells exposed to disturbed flow patterns exhibited significant increases of transendothelial transport of macromolecules in regions of pronounced shear stress gradients revealing that spatial variations in shear stress have a direct impact in the regulation of endothelial barrier function and transendothelial transport of macromolecular components (Phelps et al. 2000).

In another study, Breslin et al., subjected adult human dermal microlymphatic endothelial cells to laminar flow conditions at a baseline level of 0.5 dyn/cm^2 with subsequent increases in the shear stress level to 2.5, 5 and 9 dyn/cm^2 . Increases in endothelial permeability occurred as a function of shear stress levels but returned to the baseline permeability within 30 min when the fluid shear stress was adjusted back to 0.5 dyn/cm^2 . Interestingly, the magnitude-dependent response in barrier function was nullified when the cells were incubated with $10 \text{ }\mu\text{M}$ phalloidin that inhibited actin dynamics. Endothelial barrier function was further disturbed by inhibiting the activity of Rac1 with $50 \text{ }\mu\text{M}$ NSC23766 — an inhibitor of Rac1 activation — indicating that lymphatic endothelial cells respond dynamically to variations in flow shear stress. Furthermore, these changes occurred in a Rac1-mediated manner (Phelps et al. 2000, Levay et al. 2013).

Bevan et al., showed that the relationship between laminar shear stress and the endothelial nitric oxide is one of the key determinants of endothelial cell responses in the systemic circulation. They used glomerular endothelial cells in tissue sections and subjected them to

physiologically relevant levels of laminar shear stress at 10–20 dyn/cm². After exposure to laminar flow shear stress levels for a duration of 24 h the glomerular endothelial cells aligned to the flow orientation with their stress fibers parallel to the direction of flow. Fluid shear stress triggered Akt and endothelial nitric oxide phosphorylation. It also resulted in increased levels of nitric oxide production, whereas inhibition of the phosphatidylinositol 3-kinase/Akt (PI3K/Akt) pathway attenuated the phosphorylation of endothelial nitric oxide and the nitric oxide production levels. Expectedly, laminar shear stress also induced barrier function changes (Bevan et al. 2011).

1.6 Sepsis

Sepsis is defined as a complex systemic inflammatory response syndrome triggered by the invasion of pathogenic microorganisms. It manifests clinically as a dysregulated systemic response of the innate immune system (Bone et al. 1992, Galley 2011, Nduka et al. 2011, Aziz et al. 2013, Schulte et al. 2013).

Sepsis that is accompanied by single or multiple organ failure is termed severe sepsis or septic shock in the presence of arterial hypotension (Levy et al. 2003, Levy et al. 2010, Galley 2011, Nduka et al. 2011, Aziz et al. 2013, Schulte et al. 2013).

Historically, sepsis represents one of the first pathological conditions with reports dating back to the time of the Hippocrateans. Ever since sepsis has remained a primary medical challenge to modern-day biomedicine despite the tremendous advances in modern biomedical technology, clinical settings and ICUs and despite a coordinated effort to tackle and elucidate in a fundamentally profound way its molecular underlying mechanisms. Perhaps the most profound manifestation of the challenges that sepsis poses to clinicians and research scientist, remains the fact that currently there are no available treatments for this condition.

1.6.1 Pathophysiology of sepsis

The pathophysiology of sepsis is overly complex and its underlying molecular mechanisms are far from fully elucidated. There is a consensus about the onset of sepsis in that it is triggered when pathogenic microorganisms gain access to the bloodstream. LPS, flagellin, peptidoglycan, bacterial DNA and zymosan have an intricate ability to activate the innate immune system. Collectively, LPS, flagellin, peptidoglycan, bacterial DNA and zymosan are referred to as pathogen-associated molecular patterns (PAMPs) (Fink et al. 2014). PAMPs activate the innate immune system by engaging toll-like receptors (TLRs), monocytes, macrophages, polymorphonuclear leukocytes, pulmonary epithelial cells and most notably endothelial cells that are the primary focus in the current study. Besides the direct dissemination of invading pathogens, a host may develop sepsis due to secondary causes triggered by postsurgical interventions, traumata, burns, hemorrhages and gut ischemia (Pastores et al. 1996, Mokart et al. 2005, Lever et al. 2007, Bogner et al. 2010, Cai et al. 2010). Typical LPS levels in septic patients have been reported to range between 0.2 and 1 ng/mL (Marshall et al. 2002, Stief et al. 2007, Buttenschoen et al. 2008).

Endothelial microvascular endothelial cells respond to LPS by increasing their permeability and thus, facilitating the transmigration of leukocytes to the infected tissue regions. At the same time, LPS-induced barrier dysfunction leads to disruption of homeostasis, organ dysfunction and lung edema (Gong et al. 2008, Kolosova et al. 2008, Tiruppathi et al. 2008). LPS-induced endothelial microvascular hyperpermeability has been associated with the activation of Src family kinases. Moreover, it actively participates in the phosphorylation of adherens protein complex constituents (Gong et al. 2008).

1.6.2 Clinical manifestations of sepsis

The clinical manifestations of sepsis are characterized by a broad variability dependent on the nature of the causative pathogens, the underlying health status of the patient, the time interval between diagnosis and administration of treatment and the responsiveness of the patient to administered treatment. The cardiopulmonary system is in the majority of cases most vulnerable

to acute organ dysfunction (Angus et al. 2013). Damage to the respiratory system is clinically manifested as acute respiratory distress syndrome, defined as hypoxemia with bilateral infiltrates of non-cardiac origin (Ranieri et al. 2012). Cardiovascular complications are primarily manifested as hypotension or an elevated serum content of lactate requiring the use of vasopressors. At the same time, the possible presence of myocardial dysfunctions pose additional therapeutic challenges (Dellinger et al. 2008).

From a clinical standpoint, typically patients who present with sepsis, experience symptoms of fever, anorexia, tachycardia, systemic arterial hypotension, systemic vascular resistance, abnormal sensorium, leukocytosis, leukopenia, thrombocytopenia, impaired blood coagulation and elevated concentrations of blood lactate (Fink et al. 2014). Paradoxically, pro-inflammatory and anti-inflammatory host responses coexist during the clinical manifestation of sepsis. Although the systemic inflammatory response syndrome (SIRS) criteria as defined during the consensus definitions established in 1992 and slightly modified in 2004 offer clinical guidelines and allowed for patients to participate in clinical sepsis trials, this approach has been recently challenged (Vincent et al. 2013).

1.6.3 Epidemiology of sepsis

The number of septic patients in the United States exceeds 750,000 cases annually posing not only a public health threat but also a financial burden (Angus et al. 2001, Angus et al. 2006, Angus et al. 2013, Mayr et al. 2014). The financial expenses caused by sepsis have been estimated at \$16.7 billion annually in United States alone (Sands et al. 1997, Angus et al. 2001, Angus et al. 2006, Ernst et al. 2006). Angus et al. reported that one out of six patients diagnosed with severe sepsis has an underlying neoplastic disease placing them at a 30% higher risk of mortality compared to cancer-free patients suffering from severe sepsis (Angus et al. 2001, Williams et al. 2004, Angus et al. 2006, Angus et al. 2013). The evidently increased risk of death among cancer patients diagnosed with severe sepsis may be attributed to opportunistic or nosocomial infections, increased production of cytokines and chemokines and a distinctly compromised immune system. Patients with hematologic cancers appear to be more

immunocompromised than patients with solid organ malignancies while cancers associated with vital organs are more likely to cause organ impairment. The occurrence of sepsis and severe sepsis has been described as a significant cause of death among cancer patients and represents a major burden in the availability of treatment options (Williams et al. 2004). Besides cancer patients, diabetics are also associated with increased vulnerability to infectious pathogens that may develop and lead to sepsis (Shah et al. 2003, Muller et al. 2005, Koh et al. 2012). Beyond the civilian population undergoing sepsis caused either as a direct result or as a secondary cause triggered by an underlying disease (e.g., hematologic or solid cancers, diabetes mellitus), military personnel is in particular affected by sepsis. Combat-related casualties among military personnel leading to severe sepsis are leading causes of morbidity and mortality with mortality rates exceeding 50% (Surbatovic et al. 2007, Murray 2008).

1.6.4 Biomarkers of sepsis

It is evident that distinguishing between non-infectious related SIRS from sepsis is crucial especially considering that early diagnosis of sepsis is critical for a favorable outcome and has a direct impact on survival. Concerted efforts for the development of assays that will permit the timely and accurate diagnosis of sepsis in patients are multivariate and include not only pharmacological approaches but also biotechnological solutions with the development of electronic biochips. Currently, the only FDA-approved biomarker is procalcitonin. Procalcitonin is an 116-amino acid protein whose levels are less than 0.1 µg in healthy individuals as opposed to septic patients who present with increased levels of this protein in their systemic circulation. Pentraxin, soluble decoy receptor 3 (also known as TNFRSF6B), the high-affinity immunoglobulin Fcγ surface receptor I (also known as CD64) and the cytokine interleukin-27 are also biomarkers that are frequently used clinically for distinguishing non-infectious SIRS from sepsis (Cid et al. 2010, Huttunen et al. 2011, Kim et al. 2012, Uusitalo-Seppala et al. 2013, Wong et al. 2013, Fink et al. 2014, Wong et al. 2014).

Endotoxin triggers macrophages leading to an increase in the release of a plethora of early pro-inflammatory mediators, such as tumor necrosis factor alpha (TNFα), interleukin-1β (IL-1β),

interleukin-6 (IL-6), interleukin-8 (IL-8), Interferon gamma (IFN- γ) and monocyte chemoattractant protein-1 (MCP-1) and also result in augmented levels of secondary mediators for tissue injury, such as nitric oxide and reactive nitrogen species (Opal et al. 2002, Lakhani et al. 2003). During sepsis, neutrophils are activated and while initially they assist in neutralizing invading bacteria, they may contribute at later stages to tissue injury induced by respiratory burst, cytotoxicity, degranulation, organ damage and most importantly increased vascular permeability (Hoesel et al. 2005).

1.6.5 Mitochondrial dysfunction in sepsis

A sepsis-induced inflammatory response has direct consequences on mitochondrial function. Impaired tissue perfusion due to intrinsic and extrinsic fluid loss, myocardial depression, microcirculatory disturbances in blood flow and loss of vascular tone, have the potential to result in tissue hypoxia directly affecting the capacity of oxygen availability at the mitochondria level and hence severely compromising the ability of oxidative phosphorylation of adenosine diphosphate (ADP) to adenosine triphosphate (ATP) (Stidwill et al. 1998, Srinivasan et al. 2012). During sepsis and severe sepsis antioxidant host defenses are compromised resulting in substantial damage to lipids, proteins and nucleic acids in mitochondria. An example of how an overly compromised immune and antioxidant host system can further lead to complications is peroxidation of the mitochondrial lipid cardiolipin. Cardiolipin is located in the inner mitochondrial membrane (Figure 1.10) and contributes primarily to energy metabolism. Peroxidation of cardiolipin leads to the dissociation of cytochrome c, reduced ATP production and increased release of reactive oxygen species (Droge 2002, James et al. 2002, Turrens 2003, Kakkar et al. 2007). Due to the proximity of mtDNA to the electron transport system, mtDNA may contribute to mutations. Since mtDNA as opposed to genomic DNA does not contain any non-coding sequences, the probability of mutations leading to functional impairment are significantly higher (Ozawa 1999, Van Remmen et al. 2001).

Inflammatory-induced host responses that are further triggered by oxidative stress occur through the activation of redox pathways for transcription activation and an increased presence

of inflammatory mediators in the systemic circulation including cytokines and pentraxin-3 (Arnalich et al. 2000, Paterson et al. 2000, Hill et al. 2009).

Due to the overwhelming evidence linking sepsis and mitochondrial dysfunction, sepsis-induced mitochondrial impairment has remained the subject of intense research. It has further been hypothesized that mitochondrial dysfunction may partially contribute to organ failure that manifests clinically in the case of severe sepsis (Brealey et al. 2003, Brealey et al. 2004, Crouser 2004). In addition, mitochondrial dysfunction has been intensely studied in animal models of sepsis (Gellerich et al. 1999, Crouser et al. 2002, Gellerich et al. 2002, Brealey et al. 2003, Brealey et al. 2004, Crouser 2004).

Despite the fact that oxidative stress due to mitochondrial dysfunction has been linked to the pathophysiology of organ failure in severe sepsis, it would appear logical that antioxidant approaches could prove valuable (Galley 2011). Nonetheless, antioxidant treatment in critically ill patients suffering from sepsis and severe sepsis did not show promising results (Mishra 2007, Victor et al. 2009).

1.6.6 Animal sepsis models

Animal models are employed with the ultimate goal to generate translatable results with the potential to be extrapolated and applicable to human conditions (Warren et al. 2010). Due to the high mortality rates of septic patients there is a concerted ongoing research on multiple levels in an effort to understand and tackle the underlying molecular mechanisms of sepsis and offer treatment options. In this tireless effort, animal models are a substantial part and an indispensably valuable tool in the hands of researchers.

Sepsis animal models have come into scrutiny due to the existence of substantial differences in the way vertebrate species confront infection. This may cast acquired insights based on animal studies as futile (Warren et al. 2010). The differences in the protective mechanisms of species with regard to invading microorganisms are due to resistance and tolerance (Raberg et al. 2007, Schneider et al. 2008). Warren et al. suggested that the protein composition of blood sera among

different species accounts for the discrepancies in suppressing macrophage-mediated production of inflammatory cytokines. Their studies show that mouse serum suppressed significantly the production of LPS-mediated TNF α by peritoneal macrophages to a much greater extent when compared to human serum (Warren et al. 2010). Considering the wide discrepancies in the response of different animal species to LPS (Table 1.1) and in particular the striking difference between humans and mice, it stands to reason that in the effort to better elucidate sepsis, animal studies need to be put in perspective.

A commonly used technique to assess molecular signaling pathways in sepsis models is to challenge animal subjects with LPS, an antigen present on the cellular membrane of Gram-negative bacteria (Warren et al. 2010). The dose of LPS used to provoke immune responses in mice lies usually in the range between 1 – 25 mg/kg (Schaedler et al. 1961, Glode et al. 1976, McCuskey et al. 1984, Reynolds et al. 2002). Considering that the dose of LPS that is injected in single bolus IV injections into human volunteers to induce immune reactions lie in the range of 2 – 4 ng/kg, it is obvious that mice exhibit a significantly higher tolerance toward LPS (Sauter et al. 1980, Suffredini et al. 1989, van der Poll et al. 1990, Copeland et al. 2005). In a separate report, a patient was admitted to the ER with septic shock as a result of self-administration of 1 mg of Salmonella minnesota endotoxin intravenously 2.5 h before admission in an attempt to treat a previously diagnosed tumor. The patient's core temperature and heart rate returned to normal levels only after approximately 60 h (Taveira da Silva et al. 1993). Copeland et al. compared acute inflammatory responses to endotoxin in mice and humans and observed numerous alterations in hematologic and cytokine markers. Changes in peripheral white blood counts (WBCs) after endotoxin injection increased over a 24 h period in humans, but the mice showed no significant alterations. Differential cell counts revealed similar patterns for the peripheral neutrophils and lymphocytes in humans and mice despite the fact that the majority of the circulating WBCs in humans are neutrophils, whereas in mice the majority are lymphocytes. Cytokines demonstrated a time-dependent increase and returned to baseline levels during the 24 h time course (Copeland et al. 2005). TNF soluble receptor-1 (TNFR-1) appeared

increased in human serum reaching peak levels within the first 2 h after injection, but there were no noticeable differences in the mouse plasma.

Despite the fact that obvious differences in LPS tolerance between humans and mice exist, the role of endotoxin in sepsis and septic shock has been challenged (Taveira da Silva et al. 1993). Independent animal and clinical studies have shown that microorganisms devoid of endotoxin have the ability to induced septic shock and that products of Gram-negative bacteria other than endotoxin may cause sepsis and septic shock leading to mortality (Parker et al. 1987, Natanson et al. 1989, Danner et al. 1990). Although Gram-positive bacteria do not contain endotoxin on their cell walls they do express peptidoglycan and lipoteichoic acid that upon entry into the bloodstream can attach to cell surface receptors and act in a pro-inflammatory fashion (Majcherczyk et al. 1999, Wang et al. 2000, Morath et al. 2001). Gram-positive bacteria produce potent exotoxin with serious implications in septic shock (Cohen 2002). *Staphylococcus aureus* is a Gram-positive bacterial strain producing the toxic-shock syndrome toxin 1 that has been implicated in toxic shock (Adams et al. 2009). Toxic shock syndromes belong to the most severe forms of septic shock due to the fact that they may occur without prior warning symptoms in healthy individuals reaching mortality rates greater than 50% (Cohen 2002, Adams et al. 2009).

1.7 Fluid shear stress and the vascular endothelium

Application of fluid shear stress to endothelial cells activates signal transduction molecules triggering downstream signaling cascades that allow the endothelium to translate mechanical forces from the immediate microenvironment to biochemical signaling. Since endothelial cells remain constantly exposed to blood-induced hemodynamic forces, it stands to reason that they are equipped with a wide range of mechanosensitive components ranging from ion channels, heterotrimeric G proteins, small GTPases, protein kinases to adherens and tight junction complexes (Chien 2007, Wang et al. 2009).

Many of the cellular components are known to play pivotal roles in how endothelial cells respond to flow-induced shear stress. In the following sections, the effort is undertaken to describe briefly these cellular components and their role in the regulation of fluid shear stress response.

Endothelial cell responses to fluid shear stress vary and include changes in the electrophysiological membrane potential, gene regulation, protein synthesis and expression, transcription factor activation, morphological changes and activation of G proteins (Davies 1989, Davies et al. 1993, Davies et al. 1997, Tzima 2006).

During fluid shear stress-induced mechanotransduction, mechanical forces from the cellular microenvironment are converted to biochemical signaling and transmitted to the interior of endothelial cells. Endothelial cells, in turn, translate these signals and respond to them by initiating a series of cell signal transduction pathways, including gene and protein expression (Langille et al. 1986, Zhang et al. 2008).

The endothelium with the entirety of its mechanosensitive components is essential for homeostasis by maintaining anticoagulant properties, by actively participating in vasoregulation and most importantly by regulating vascular permeability. Endothelial cells mediate the responses to acute and chronic inflammatory conditions (e.g., sepsis and severe sepsis) (Langille et al. 1986, Zhang et al. 2008).

Fluid shear stress-mediated signaling to subcellular sites remotely located from the luminal surface underscores the importance of the cytoskeletal transmission of forces. Shear stress is a major regulator in phosphorylation events at sites of focal adhesion sites. Endothelial adherens and tight junction complexes have been implicated in rapid phosphorylation events from the onset of flow-induced shear stress (Fujiwara et al. 2001, Shyy et al. 2002, Tzima et al. 2005).

Intriguingly, the nuclear membrane of endothelial cells undergoes changes as cytoskeleton-mediated stress is transmitted having a potential effect on allowing transcription

factors to enter the nuclear space through nuclear pores and thereby influence gene expression (Maniotis et al. 1997, Dalby et al. 2007).

Laminar shear stress has been implicated in the regulation of several genes related to the vasculature. In endothelial cells, it suppresses the cell cycle transition from the G1- to the S-phase leading to increases of p21, a known inhibitor of cyclin-dependent kinases. The maintenance of physiological shear stress levels prevents endothelial cells to undergo apoptosis in response to several stimuli, including TNF α , oxidized LDL and angiotensins II (Dimmeler et al. 1996, Dimmeler et al. 1999, Akimoto et al. 2000, Lin et al. 2000).

Fluid shear stress-mediated activation of Rho is associated functionally to endothelial cell migration, MAPK signaling pathway and cytoskeletal reorganization, whereas inhibition of RhoA with C3 exoenzyme restricts endothelial migration (Hsu et al. 2001).

Several threonine/serine and tyrosine kinases are located near the plasma membrane of endothelial cells, focal adhesions and the cytoplasm. Focal adhesion kinase (FAK), c-Src, PI3K, MLCK and the Akt kinase are among these kinases (Li et al. 1997, Bhullar et al. 1998, Dimmeler et al. 1998, Go et al. 1998, Jalali et al. 1998, Watanabe et al. 1998, Chen et al. 1999). For example, PI3K, Akt and protein kinase A (PKA) pathways are involved in the synergistic regulation of endothelial nitric oxide synthase leading to increased levels of nitric oxide production (Dimmeler et al. 1999, Boo et al. 2002).

Fluid shear stress plays a pivotal role in the regulation of vascular remodeling, restructuring of blood vessels, blood pressure, atherogenesis, response to chronic and acute inflammatory conditions, cardiac embryogenesis and atherogenesis (Langille et al. 1986, Davies 1997, Takahashi et al. 1997, Chien et al. 1998, Hove et al. 2003).

More importantly, shear stress mediates the initiation of several cell signal cascades in endothelial cells including the regulation of potassium and calcium channels, activation of heterotrimeric and small G proteins, nitric oxide production, tyrosine phosphorylation of proteins

(e.g., c-Src, FAK), activation of mitogen-activated protein kinase, PKC, activation of transcriptional regulators (e.g., c-fos, c-jun, c-myc, NF- κ B) (Naruse et al. 1993, Khachigian et al. 1995, Tseng et al. 1995, Li et al. 1996, Li et al. 1997, Yoshikawa et al. 1997, Gudi et al. 1998, Traub et al. 1998).

The following sections list several other elements playing pivotal roles in vascular endothelial biology under conditions of fluid shear stress.

1.7.1 Adhesion proteins

Selectins are carbohydrate-binding molecules with a binding affinity to fucosylated and sialylated glycoprotein ligands. They are expressed on endothelial cells, leukocytes and platelets. L-selectin is expressed exclusively on leukocytes while E-selectin is restricted to endothelial cells. Selectins exhibit significant levels of homology among different species or within the same species with the exception of transmembrane and cytoplasmic domains. The lectin domain binding sugars exhibits high degrees of conservation, suggesting that L-, P-, and E-selectins bind similar sugar structures. Ironically, the transmembrane and cytoplasmic domains reveal a significant conservation across species but not among the selectin of the same species (Ley 2003). P-, and E-selectins are expressed at high-density levels on the luminal plasma membrane in the vascular endothelium (Ley 2008). These selectins are also present as soluble molecules in serum or plasma and their level in the blood may be considered as risk factors for vascular disease (Demerath et al. 2001).

The adhesion molecule E-selectin is exclusively confined to endothelial cells and is expressed in activated and not resting endothelial cells (Feuerhake et al. 1998). When vascular endothelial cells transition from resting to activated during the pathogenesis of an inflammatory response, expression of E-selectin is initiated and largely confined to postcapillary venules (Petzelbauer et al. 1993, Yano et al. 2006). P-selectin is expressed in endothelial cells and in megakaryocytes. When endothelial cells are in their resting state, P-selectin is stored intracellularly in Weibel-Palade bodies and similarly to E-selectin, its expression is confined to a great extent in postcapillary venules (McEver et al. 1989, Keelan et al. 1994). Upon activation,

P-selectin is translocated to the cell surface of endothelial cells and platelets. E-selectin is not expressed in resting endothelial cells with the sole exception of skin microvessels that do express E-selectin following the presence of cytokines (Keelan et al. 1994).

Eppihimer et al. attempted to characterize expression levels of E-, and P-selectins under *in vivo* conditions after LPS challenge. The study reported that maximal expression of P-selection occurred at 4 h after intraperitoneal administration of LPS. The levels of P-selectin retreated to a steady state level lasting for a duration of 24 h (Eppihimer et al. 1996). The time required to reach peak values for P-selectin expression under *in vivo* conditions agreed with previous *in vitro* observations (Weller et al. 1992, Hahne et al. 1993, Shen et al. 1995, Eppihimer et al. 1996). Unlike the time window to reach maximal expression, though, elevated values for P-selectin between 4 h and 24 h were not in agreement with *in vitro* studies. Cytokine-induced expression of P-selectin in endothelial cells under *in vitro* conditions revealed significantly lower expression values after the 4 h peak time (Hahne et al. 1993, Eppihimer et al. 1996). The differences were attributed to the possibility that *in vivo*, LPS may trigger other cell types to secrete cytokines in an effort to maintain expression levels of P-selectin in postcapillary venules (Eppihimer et al. 1996).

1.7.2 Ion channel activation

Ion channels respond in a rapid manner to flow-induced shear stress. K^+ ion channels activate inwardly in a time scale of milliseconds after initiation of shear stress. The K^+ is not only Ca^{2+} activated but also transcriptionally regulated by fluid shear stress (Olesen et al. 1988, Cooke et al. 1991, Jacobs et al. 1995, Forsyth et al. 1997, Ballermann et al. 1998). Endothelial cells in the vasculature respond by activating different ion channels depending on the vascular bed across the endothelium (Olesen et al. 1988, Ballermann et al. 1998).

1.7.3 Calcium

Endothelial cells express a variety of Ca^{2+} -permeable ion channels, including receptor-mediated ion channels (Adams et al. 1989). Exposure of endothelial cells to fluid shear stress is known to induce a rapid production of inositol 1,4,5-trisphosphate (IP3) and

diacylglycerol (DAG) from membrane phosphatidylinositol (Adams et al. 1989, Prasad et al. 1993). A decrease in calcium concentration in the culture medium resulted in the prompt disassembly of VE-cadherin and catenins at endothelial cell junctions (Dejana et al. 1995).

1.7.4 Caveolae

Caveolae mediate transcellular transfer of blood-borne molecules across the endothelium. Caveolae are 70 nm membrane-bound and flask-shaped vesicles that usually remain open to the luminal or abluminal side (Aird 2007). Some caveolae exhibit a non-membranous stomatal diaphragm containing the plasmalemma protein-1 (Stan et al. 1999, Aird 2007). The density of caveolae is estimated to be approximately 10,000 per individual cell in the capillary endothelium, a number far greater when compared with arteries, arterioles, veins or venules. Caveolae contain a smooth inner surface in contrast to the electron-dense coat of clathrin-coated pits. Endothelial cells across the vasculature contain a far greater number of caveolae than clathrin-coated pits with the exception of liver sinusoids (Aird 2007). Among the different continuous nonfenestrated endothelial beds, the number of caveolae is highest in the heart, the lungs, and the skeletal muscles (Bendayan 2002, Aird 2007). In contrast, caveolae are sparsely present in the brain endothelium (Simionescu et al. 2002). Despite the fact that caveolae also exist in non-endothelial cell types, caveolin-1, the major structural protein of caveolae is regulated by distinct transcriptional mechanism in endothelial cells (Kathuria et al. 2004, Aird 2007).

1.7.5 Primary cilia

Primary cilia project outwards from the plasma membrane toward the extracellular microenvironment (Davenport et al. 2005). They depend on intraflagellar transport to assist in providing them with ciliary receptors and channel proteins as they lack protein synthesis mechanisms (Kozminski et al. 1993, Rosenbaum et al. 2002, Kwon et al. 2006, Yoder 2007). Bystrevskaya et al. reported the presence of endothelial primary cilia in the vascular endothelium (Bystrevskaya et al. 1988, Kwon et al. 2006). It has been established that expression of endothelial primary cilia correlates with the level of fluid shear stress profile for the respective

vascular bed. Iomini et al. demonstrated that primary cilia of endothelial cells under *in vitro* conditions disassembled when exposed to laminar flow-induced shear stress (Iomini et al. 2004). Furthermore, it has been reported that absence of cilia desensitizes endothelial cells to fluid-induced shear stress (Kwon et al. 2006, Hierck et al. 2008).

1.7.6 Cytoskeleton

The endothelial cytoskeleton is essential in providing the mechanical mainframe for maintaining and performing basic cellular functions. The cytoskeletal functions in the vascular endothelium are of critical importance especially due to the fact that cells are constantly exposed to hemodynamic forces. Similarly to other cell types, the endothelial cytoskeleton consists of three basic components: (i) actin microfilaments, (ii) microtubules, and (iii) intermediate filaments. The cytoskeletal components are not independent from one another but form a communication network through which they coordinate in maintaining endothelial homeostasis (Dudek et al. 2001, Shimizu et al. 2013).

Endothelial cells remain in direct contact with circulating components in the blood, and the lymphatic fluid. Hence, the cytoskeleton is an integral part of a critically important endothelium in mechanotransduction, angiogenesis, apoptosis, motility, vasculogenesis, vascular response to inflammation by participating in the regulation of paracellular protein complexes with a direct impact on leukocyte diapedesis and ultimately endothelial barrier function (Majno et al. 1961, Garcia et al. 1986, Hirata et al. 1995, Dudek et al. 2001, Shimizu et al. 2013).

Cytoskeletal actin and myosin components comprise approximately 15–20% of endothelial cell protein content demonstrating the importance of actomyosin filaments in the performance of endothelial cell functions (Gottlieb et al. 1991). Actin filaments interact with proteins at the plasma membrane site in processes that involve cell-cell and cell-ECM interactions by stabilizing intercellular proteins. Their involvement in the regulation of intercellular protein complexes demonstrates their active participation in the regulation of endothelial barrier function and therefore, their active role in the exchange of oxygen, nutrients and waste products between the blood and the tissues (Dudek et al. 2004). The microtubules of endothelial cytoskeleton consist

of α -, and β -tubulins, compression-resistant hollow rods. Their main function is to support cell structure maintenance and the formation of spindles during mitosis (Klymkowsky 1999, Goode et al. 2000).

The endothelial cytoskeleton interacts with membrane-bound junction complex proteins in the regulation of: (i) cell shape and mechanical stability, (ii) motility and migration, and (iii) cell-cell and cell-ECM interactions (Dudek et al. 2004, Mehta et al. 2006). The actin microfilament system is focally linked to a multitude of protein members of the zona occludens, zona adherens, glycocalyx components, and focal adhesion complex proteins (Dudek et al. 2004).

Focal adhesions and cell-ECM complexes also interact in regulating the integrity of vascular endothelial cells and consequently maintain barrier function integrity. The focal adhesion complexes form linkages between the ECM and the actin cytoskeleton via integrins. Integrins in turn interact with a spectrum of actin-binding proteins, such as α -actinin, talin, filamin, vinculin, paxillin, zyxin, and tensin (Mehta et al. 2006). The transmembrane integrins are associated with FAK, a tyrosine kinase that is recruited to the complex by tyrosine phosphorylation orchestrated by permeability-inducing agonists (Burrige et al. 1987, Romer et al. 1992).

During pathophysiological edema formation in the pulmonary endothelium, paracellular gaps form at sites of inflammatory edema. This process compromises endothelial barrier integrity and results in prominent cell shape alterations implicating the direct engagement of endothelial structural components comprised of cytoskeletal microfilaments and microtubules (Majno et al. 1961, Shimizu et al. 2013).

1.7.7 Glycocalyx

The glycocalyx plays an essential role in microvascular physiology by actively regulating endothelial permeability (Woodcock et al. 2012). Hemodynamic forces originating from blood flow through the circulatory system results in the formation of a frictional process. The friction created as the blood flows over the endothelial structures remains low due to the endothelial

glycocalyx (Figure 1.11) — a proteoglycan layer lining the luminal surface of the endothelium (Pries et al. 2000, Van Teeffelen et al. 2007, Weinbaum et al. 2007, Fels et al. 2014).

The endothelial glycocalyx, comprised by a polymer structure rich in water and anionic charges (e.g., heparan sulfate), serves as a functional cushion between the erythrocytes and the endothelial membrane. The anionic properties of the endothelial glycocalyx exert negative electrostatic forces keeping the negatively charged erythrocytes at a safe distance from the plasma membrane of the endothelial layer. Consequently, erythrocytes exhibit a minimal adhesiveness to the endothelium allowing blood to flow in a virtually frictionless manner through the blood vessels (Liu et al. 2009). This indicates the essential role that endothelial glycocalyxes play in the regulation of blood flow (Vink et al. 1995, Secomb et al. 1998, Reitsma et al. 2007, Stevens et al. 2007, Liu et al. 2009). Computational models studying the interaction between fluidic shear stress and its effect on endothelial glycocalyxes have postulated that flow-induced shear stress is dissipated in the glycocalyx prior to reaching the plasma membrane of endothelial cells. The removal of heparan sulfate glycoaminoglycans by means of enzymatic digestion lead to a diminished production of vasodilatory factors in response to fluidic shear stress (Florian et al. 2003).

The thickness of the endothelial glycocalyx ranges from a few hundreds nanometers in capillary endothelial cells to a few micrometers in the arterial endothelium (Figure 1.12). Typically the thickness of the glycocalyx layer ranges from approximately 100 nm to 1000 nm. Volumetrically, it has been estimated that the glycocalyx comprises a volume of approximately 1.7 L (van den Berg et al. 2003, van Haaren et al. 2003, Nieuwdorp et al. 2006, Reitsma et al. 2007, Nieuwdorp et al. 2008). Since the glycocalyx is the very first endothelial cell component subjected to hemodynamic forces it stands to reason that its proper function is of essential significance in the conductance of biomechanical and biochemical signaling from the cellular microenvironment into the endothelial cells (Fels et al. 2014).

Furthermore, studies have reported that the endothelial glycocalyx serves as a barrier by allowing macromolecules (e.g., albumin) to stay embedded in its structure (Stevens et al. 2007).

Consequently, the endothelial glycocalyx is essential for the regulation of endothelial permeability (Becker et al. 2010, Dvorak 2010, Curry et al. 2012, Peters et al. 2012).

However, pathophysiological conditions (e.g., inflammation, sepsis) can cause damage to the endothelial glycocalyx resulting in its shedding that is manifested by a gradual degradation and loss of its negative charge (Devaraj et al. 2009, Lipowsky et al. 2011, Kolarova et al. 2014). A direct consequence of a deteriorated glycocalyx that does no longer exert a negative charge leads to an intimate contact with erythrocytes and endothelial cells with increased drag forces exercised by the blood flow (Liu et al. 2009).

During the pathophysiology of sepsis, exposure of endothelial cells to LPS or TNF α causes a reduction in thickness and stiffness of the glycocalyx that is clinically manifested in loss of vascular tone, loss of albumin, hypovolemia, edema formation and in the case of severe sepsis, organ dysfunction while persistence of these alternation has been linked to a poor clinical outcome (Wiesinger et al. 2013, Chelazzi et al. 2015).

In a rat experimental model of sepsis, increased levels of TNF α correlated with reduced expression of syndecan-1. Moreover, the interaction of syndecan-1 with TNF α initiates structural rearrangement of endothelial cells and disassembly of junction complexes that results in increased paracellular permeability (Christaki et al. 2008, Adembri et al. 2011).

TNF α -induced mast-cell degranulation results in the release of cytokines and mast-cell derived TNF α . TNF α -induced mast-cell degranulation has been implicated in the shedding of the glycocalyx (Gilles et al. 2003, Reil et al. 2007, Zhang 2008, Chappell et al. 2009). Furthermore, it leads to the liberation of proteases (e.g., tryptase and cathepsin B) allowing for the cleavage of which syndecans and hyaluronan from the endothelial membrane (Annecke et al. 2010).

Despite the insights that numerous studies have reported with regard to the endothelial glycocalyx, accumulating evidence points to the fact that some cultured endothelial cell types do not exhibit a glycocalyx layer as it occurs under *in vivo* conditions (Potter et al. 2008). The

observation that substantial structural and compositional differences exist between endothelial cells grown under static cell culture conditions and endothelial cells subjected to fluid shear stress raises concerns about *in vitro* glycocalyx models (Potter et al. 2008, Curry et al. 2012). The complication arising from these studies indicate the importance of imitating the endothelial microenvironment as closely as technically possible to *in vivo* conditions, in particular with regard to flow-induced shear stress.

1.7.8 Integrins

Integrins are heterodimeric adhesion receptor proteins formed by the non-covalent pairing of α and β subunits at the plasma membrane. Each subunit is a type I transmembrane glycoprotein composed of a relatively large extracellular domain, and a short cytoplasmic tail with the exception of the $\beta 4$ subunit (Hynes 1987, Ruoslahti et al. 1987, Hynes 1992, Giancotti et al. 1999, Hynes 2002). Mammalian cells contain 18 α - and 8 β -subunits leading to a combination of at least 24 different heterodimers that have been identified thus far. Cell-cell and cell-ECM adhesion is mediated by the binding interaction of the extracellular domain of integrins to diverse protein ligands and the subsequent conformational changes in the cytoplasmic tail leading to the initiation of cellular signaling events and ultimately the translation into dynamic cellular responses, such as cell spreading, migration and cell survival or apoptosis. The short cytoplasmic tails of heterodimeric integrins interact directly with intracellular ligands through which the receptors connect with signaling pathways and cytoskeletal networks (Ruoslahti et al. 1987, Gehlsen et al. 1988, Ruoslahti et al. 1994, Giancotti et al. 1999, Crichtley 2000, Geiger et al. 2000, Liu et al. 2000, Brakebusch et al. 2003, Calderwood 2004).

The majority of integrins recognize extracellular matrix proteins. Similarly, extracellular matrix proteins (e.g., fibronectin, laminins, collagen, vitronectin) have a binding affinity toward integrins (Hynes 1987). Integrins have the inherent ability to signal through the cell membrane in a bidirectional manner. The extracellular domain of integrins relays signals from within the cell and is termed inside-out-signaling, whereas the binding of extracellular matrix proteins elicits

signals from the cellular microenvironment that are further transmitted into the cell, designated as outside-in-signaling (Smyth et al. 1993, Williams et al. 1994, Giancotti et al. 1999).

The vascular endothelium expresses several members of the integrin family, including the receptors for fibronectin, laminin and collagen. In order for endothelial cells to be capable and recognize a wide array of extracellular matrix proteins under a variety of physiological and pathophysiological settings, they express several different integrins. For example, the fibronectin-specific receptors, $\alpha_v\beta_1$ and $\alpha_5\beta_1$ are abundantly expressed in quiescent endothelial cells, whereas the $\alpha_v\beta_3$ -vitronectin receptor is expressed exclusively during angiogenic events while the antagonist inhibiting the $\alpha_v\beta_3$ function results in apoptosis of proliferating endothelial cells (Brooks et al. 1994, Matter et al. 1998, Short et al. 1998, Matter et al. 2001, Liao et al. 2015). Other vitronectin-binding integrins expressed by the endothelium are $\alpha_v\beta_3$, $\alpha_v\beta_5$ and $\alpha_v\beta_6$ (Cheresh 1987, Klein et al. 1993, Friedlander et al. 1995, Christofidou-Solomidou et al. 1997). The angiogenic integrins $\alpha_v\beta_3$ and $\alpha_v\beta_5$ are expressed in endothelial cells and play a pivotal role in endothelial cell survival (Brooks et al. 1994, Brooks et al. 1995, Friedlander et al. 1995, Friedlander et al. 1996). Integrin $\alpha_v\beta_3$ is responsible for transmitting survival signals that result in the inhibition of p53 activity and suppression of the bax apoptosis pathway in endothelial cells (Stromblad et al. 1996).

Ample evidence exists implicating flow-induced shear stress in the activation of integrins. (Tzima et al. 2005, Tzima et al. 2006, Hahn et al. 2009, Collins et al. 2012, Conway et al. 2013). Fluid shear stress causes conformational changes of integrins triggering their activation. Once flow-induced integrin activation is in place, endothelial cells subjected to laminar flow align their orientation toward the direction of the flow. Furthermore, shear stress-induced integrin activation also mediates the activation of NF- κ B (Tzima et al. 2001, Tzima et al. 2002, Tzima et al. 2003). A mechanosensory complex comprised of PECAM-1 (activates Src), VE-cadherin and VEGFR-2 (activates PI3K) has been described. PI3K induces integrin activation via a conserved pathway (Hughes et al. 1998). The events leading to integrin activation occur within 15 s from the onset of fluid shear stress (Lu et al. 1997). The cytoplasmic domain of PECAM-1 binds Src

directly and activates it. Following, VE-cadherin transmits this signal to PI3K. Studies using PECAM-1^{-/-} mouse models revealed that these mice are impaired with regard to F-actin organization and activation of the NF-κB pathway. These findings suggest the importance of the complex comprised by PECAM-1, VEGFR-2 and PI3K in fluid shear stress-activated endothelial cells (Tzima et al. 2005).

1.7.9 Vesciculo-vacuolar organelles

Similarly to caveolae, vesciculo-vacuolar organelles (VVOs) mediate transcytosis in the vascular endothelium. VVOs represent focal collections of membrane-bound vesicles and vacuoles. They represent the major route of extravasation of macromolecular substances at sites of increased vascular permeability (Dvorak et al. 1996, Brown et al. 1997, Dvorak et al. 1999, Aird 2007). VVOs are abundant in the venular endothelium where they occupy a substantial portion (16–18%) in the cytoplasm (Dvorak et al. 1996, Feng et al. 1996, Feng et al. 1999). In normal endothelium, they permit only minimally the entry and passage of macromolecular tracers (Kohn et al. 1992, Feng et al. 1996).

1.7.10 Tyrosine kinase receptors

Tyrosine kinases represent a family of enzymes with the intrinsic ability to phosphorylate tyrosine residues, therefore providing a modality for signal transduction across the plasma membrane mediating diverse cell signaling events, including cell proliferation, migration, survival and apoptosis. The human genome expresses approximately 90 tyrosine kinases, including 58 receptor tyrosine kinases (RTKs). RTKs are transmembrane proteins comprised of an extracellular ligand-binding domain and cytoplasmic tyrosine kinase domains (Partanen et al. 1992, Manning et al. 2002, Drake et al. 2014). Once a ligand binds to the extracellular domain, RTKs are activated resulting in their dimerization or oligomerization (Ullrich et al. 1990, Drake et al. 2014). Selective activation of the RTKs, vascular endothelial growth factor receptor-1 (VEGFR-1) and vascular endothelial growth factor receptor-2 (VEGFR-2) in conjunction with gene silencing have revealed that VEGFR-2 is the major receptor in the vascular endothelium transducing VEGF signals (Holmes et al. 2007, Sawamiphak et al. 2010). Sawamiphak et al.

showed that ephrin-B2 controls VEGFR-2 internalization and signaling. Internalization of VEGFR-2 in turn, is crucial for activation and downstream signaling of the receptor (Sawamiphak et al. 2010). This interaction between the bi-directionally signaling Eph receptors and ephrin ligands and VEGFR-2 is yet another demonstration of the intricacy of endothelial mechanosensing combining a plethora of different intra-, and extracellular components that act in concert to converse biomechanical stimuli into biochemical signaling. Polypeptide growth factors and hormones, including epithelial growth factor (EGF), insulin, insulin growth factor-1 (IGF-1), platelet-derived growth factors (PDGF-A, PDGF-B), fibroblast growth factors (FGFs) are among the several ligands binding RTKs (Heldin et al. 1990, Ullrich et al. 1990). Tyrosine kinase with immunoglobulin and epidermal growth factor homology domain-2 is one of the major endothelial-specific receptor tyrosine kinases expressed primarily in endothelial cells (Partanen et al. 1992, Kontos et al. 2002). Clinical and animal studies have revealed that Tie-2 and its corresponding ligand angiopoietin-2 (Ang-2) participate in neovascularization at sites of vascular endothelium subjected to injury (Jones et al. 2001, Chong et al. 2004, Lee et al. 2004, Shyu et al. 2004, Kim et al. 2006). The same complex (Ang-2 and Tie-2) assists in enhancing endothelial tube formation, cell migration and survival of umbilical cord blood derived EPCs (Hildbrand et al. 2004, Gill et al. 2005, Brindle et al. 2006, Shyu 2006). Tie-2 has already been implicated in shear stress-mediated regulation of vascular endothelium via interactions in a complex comprised by PI3K, protein kinase B (PKB) and AKT (Lee et al. 2003, Yang et al. 2012). TNF α , a major cytokine implicated in endothelial inflammation and septic events has been shown to cleave the endothelial RTK Tie-1 resulting in the release of a soluble extracellular domain and an endodomain fragment (Yabkowitz et al. 1997, Yabkowitz et al. 1999, Kontos et al. 2002). Ang-2, the ligand of the RTK Tie-2, similarly to the adhesion protein P-selectin, is stored in endothelial Weibel-Palade bodies and upon stimulation rapidly released (Fiedler et al. 2004). Despite the fact that both Ang-2 and P-selectin are stored in endothelial Weibel-Palade bodies, which constitute the principal endothelial storage granules of the proagulant vWF, they are mutually exclusive and have been shown to be stored in separate granules (Wagner 1993, Hop et al. 2000, Fiedler et al. 2004).

1.8 Small GTPases

1.8.1 Introduction

The discovery of small GTPases can be traced back to 1982 when RAS genes encoding small G proteins that remained in their active state due to mutational defects, were discovered in human cancers (Cox et al. 2010). These mutations resulted in Ras proteins with compromised capability of hydrolyzing the bound guanosine-5'-triphosphate (GTP) nucleotide and thus, allowing the Ras proteins to remain in their active conformation for a prolonged time duration (Barbacid 1987, Bos 1989).

This discovery triggered a large-scale sequencing of cancer genomes leading to the identification of more than 500 cancer genes (Vogelstein et al. 2013). However, the three most frequently mutated oncogenes in human cancers remain the three RAS genes (HRAS, KRAS and NRAS). The frequency of RAS mutations in the lung, colon and pancreatic cancers, among the most lethal cancers, has spurred vivid research efforts in the development of RAS inhibitors. Despite an intense concerted effort focused on the development of inhibitory drug compounds, no effective RAS inhibitors have been approved thus far, further cultivating the perception that RAS oncoproteins are a non-druggable cancer target. On the other hand, therapeutic advances achieved by means of signal transduction in mutation-induced activated G proteins, offered a revived impetus toward realizing the grave importance of GTPases and their role in health and disease (Takai et al. 2001, Thompson 2013, Cox et al. 2014).

Small GTPases have been compared to molecular switches with major impact in the regulation of diverse cellular processes, including cell proliferation, differentiation, cytoskeletal organization, and intracellular membrane trafficking (Brummelkamp et al. 2002). The Ras superfamily is most commonly subdivided into five distinct subfamilies: (i) Ras, (ii) Rho, (iii) Rab, (iv) Arf and (v) Ran (Vetter 2014). The assignment of individual small GTPases to a specific subfamily is based on sequence similarity among the member proteins of the Ras superfamily. Despite the fact that different small GTPases exhibit variations in their intracellular localization and independently of the subfamily they belong to, they all share a common

structural feature, namely the G domain. The G domain is responsible for the association and the high affinity toward GTP and guanosine-5'-diphosphate GDP (Vetter et al. 2001).

The GTP-bound structural conformation is biologically active triggering the initiation of cellular functions by interaction and activation of their respective effectors. Small GTPases alternate between the inactive GDP- and active GTP-bound conformation (Figure 1.13). In their GTP-bound state, small GTPases are biologically active and trigger cellular function to be initiated by interacting and activating their associated effectors (Vetter et al. 2001, Li et al. 2004, Bos et al. 2007, Cox et al. 2010, Vetter 2014).

The majority of small G proteins exhibit a strong affinity toward either the GDP or GTP nucleotide. In fact, their affinity lies in the lower picomolar (10^{-12}) to the nanomolar (10^{-9}) range (Freymann et al. 1999, Bos et al. 2007). The high affinity between G proteins and GDP or GTP is inversely proportional to their respective dissociation rate, which is expectedly slow with a half-life on the order of one or more hours. Small G proteins acquire their activated status by exchanging the associated GDP with GTP. However, biochemical pathways in cellular processes, requiring the activation of small GTPases, occur within a few minutes or seconds. Hence, the naturally very slow occurring dissociation of GDP would not be supportive for the required timescale that many cellular processes depend on. Hence, the exchange of GDP for GTP depends on the activity of GEFs (Bos et al. 2007). The importance of GEFs in assisting small G proteins to acquire their active state becomes even more evident when considering that GEFs accelerate the exchange reaction by several orders of magnitude rendering them of inextricable importance (Vetter et al. 2001). This explains why GEFs play a major role in different aspects of biological signaling, interfering by induction, inhibition, or modulation of their catalytic activity (Bos et al. 2007).

The question arises as to the mechanisms that GEFs employ in order to induce successfully dissociation of the bound GTP nucleotide from the small G protein. Nucleotides (GDP and GTP) associate with small G proteins by binding covalently implying that there is a binding site on small G proteins that accommodates the binding of nucleotides. GEFs target the

nucleotide-binding sites of small G proteins. The conformational modifications result in conformational changes with significantly reduced affinity for either GDP or GTP. It is noteworthy to address that G proteins exhibit comparable affinities toward GDP and GTP without a clear preference for either one of them. The lack of preference by small G proteins or their respective GEFs toward either one of the available nucleotides (GDP or GTP) may cause some confusion as to why the ratio of small G proteins bound to GTP appears to be significantly higher than GDP-bound small G proteins at each given time in the cell. The explanation is provided by a study that investigated the interactions between the GEF of the small G protein Ran, RCC1 and the small G protein Ran itself. In general, the complexes that can be formed between a small G protein, either one of the two available guanosine nucleotides GDP or GTP and the respective GEF are termed binary and ternary. The affinities exhibited in the binary complex formed either between Ran and GDP/GTP or between Ran and the RCC1 are very high. Conversely, the affinities in binary complexes formed between a GDP- or GTP-bound Ran toward either GTP or GDP are very low. Similarly, in the ternary complex formed by a GDP-, or GTP-bound Ran and the RCC1, the affinity toward the GEF (RCC1) is very low. Consequently, the association of a GEF with its respective small G protein weakens its affinity for either GDP or GTP nucleotides and inversely, a GDP- or GTP-bound small G protein exhibits a weaker affinity toward its respective GEF protein (Bos et al. 2007). Another important insight into the function of small G proteins affects the cellular and tissue content in GDP and GTP. In fact, mammalian cells and tissues contain GTP at an approximately tenfold higher concentration compared to GDP. Typical values range from 0.3 to 0.5 mM for GTP, whereas the concentration of GDP lies between 0.03 and 0.06 mM (Traut 1994, Vetter et al. 2001). This explains why the cellular content of GTP-bound G proteins is significantly higher than GDP-bound small GTPases (Bos et al. 2007). Although G-binding proteins alternate between their active GTP-, and GDP-bound conformations, they can also remain in an unbound state with no GTP-, and GDP-bound nucleotides. However, the latter has been reported to be rarely the case (Li et al. 2004).

The canonical features of small GTPases, members of the Ras superfamily, require small GTPases to cycle between a GTP-bound active state and a GDP-bound inactive state. The exchange of GDP for GTP is facilitated by guanosine nucleotide exchange factors (GEFs) while the transition to the inactive GDP-bound state is achieved by GTP hydrolysis, facilitated by GTPase-activating proteins (GAPs) (Trahey et al. 1987, Gibbs et al. 1988, Chardin et al. 1993, Egan et al. 1993, Boriack-Sjodin et al. 1998, Donovan et al. 2002).

GTP hydrolysis causes for the GTPases to transition from the active to their inactive conformation resulting in the exchange of GTP for GDP. A GDP-bound small GTPase exhibits low affinity for its effectors that it would typically associate and interact with in its active GTP-bound state (Gilman 1987, Rybin et al. 1996, Antonny et al. 2001, Li et al. 2002). The duration of the GTP-bound active conformation allows under normal conditions for the cellular processes to be initiated so that the cellular functions are performed properly. The biological significance of GTP hydrolysis lies in the deactivation of G proteins (Goody 2003).

In pathophysiological cases where small GTPases are mutationally activated, the impairment of the catalyzing capabilities of GAPs that assist in the GTP hydrolysis and ultimately dissociation from GTP, leads to persistently active small GTPases (Bos et al. 2007). In an effort to replicate the successful employment of ATP inhibitors as effective antagonists of protein kinases, the quest for GTP inhibitors rendering GTPases inactive was undertaken. Although the parallel appears at first sight intriguing, a better understanding of the binding affinities in the case of ATP and GTP provides clarity as to why inhibitors competing with GTP have not brought the expected results. ATP molecules bind protein kinases at affinity levels in the millimolar range (10^{-3}). On the other hand, GTP binds GTPases at nanomolar to picomolar affinities rendering the discovery of effective inhibitors a highly complex task (Freyman et al. 1999, Bos et al. 2007, Cox et al. 2014). In a different approach, the effort to synthesize or discover small molecules imitating the function of GAPs was undertaken without any promising results (Stephen et al. 2014).

1.8.2 Small GTPases in sepsis

Eukaryotic GTPases have been identified as substrates for a number of distinct bacterial toxins with ADP-ribosyltransferase capabilities. Diphtheria toxin, cholera toxin and pertussis toxin have been among the first bacterial toxins recognized for their notorious ability to disrupt GTPase activity in cellular function. Diphtheria toxin was reported to act upon the heterotrimeric GTPase elongation factor-2 by ADP-ribosylation (Honjo et al. 1968).

Intriguingly, the inherent capability of bacterial toxins to posttranslationally modify proteins is not limited to heterotrimeric GTPases but extends to include small GTPases as well. Small GTPases belonging to the Ras and Rho subfamilies have also been implicated as targets of ADP-ribosyltransferase activity by bacterial toxins (Aktories et al. 1989, Aktories et al. 1989, Aktories et al. 1992).

C3-like transferases constitute a family of enzymes with the ability to ADP-ribosylate all three isoforms of the Rho subfamily (RhoA, RhoB, and RhoC). RhoA, RhoB, and RhoC have been reported to offer excellent substrate targets for ADP-ribosylation while other members of the Rho subfamily have been shown to be poor substrates (Just et al. 1992). C3-like transferases ADP-ribosylate the three Rho isoforms at their asparagine 41 residue, which is located in close vicinity of the effector region for RhoA, RhoB and RhoC, rendering them biologically inactive (Aktories et al. 1987, Kjoller et al. 1999, Just et al. 2001, Aktories et al. 2004). The underlying molecular mechanisms of inactivation remain enigmatic. Nonetheless, even when the Rho isoforms are targeted by C3-like transferases and after undergoing ADP-ribosylation, they still exhibit a partial potency to interact with some of their effectors. One such effector protein of the Rho isoforms is protein kinase N (Sehr et al. 1998).

Interestingly, ADP-ribosylation of Rho GTPases does not seem to have a major impact on their ability to bind to GDP or GTP nucleotides. In addition, RhoA, RhoB and RhoC maintain their intrinsic or GAP-induced GTPase activity.

C3-like transferases acting upon mammalian cells have been reported to induce dramatic actin cytoskeletal rearrangements (Chardin et al. 1989, Paterson et al. 1990, Wieggers et al. 1991). Even more dramatically, the primary effect of C3-like transferases leads to the loss of both actin stress fibers and integrin adhesion plaques. Since actin stress fibers and integrin adhesion plaques have been implicated in the regulation of endothelial permeability, it becomes evident, that C3-like transferases indirectly exert permeability-regulating features via small GTPases.

LPS, the component on the outer membrane of Gram-negative bacterial walls has been implicated as one of the major molecules involved in the initiation of sepsis and severe sepsis (Medzhitov 2001). C3-transferase has been shown to participate in the blockage of tyrosine phosphorylation and contractile mechanisms in response to LPS (Essler et al. 2000, Hippenstiel et al. 2000). However, *in vivo* evidence thus far with regard to the role of Rho kinase inhibition remains controversial (Lundblad et al. 2004, Tasaka et al. 2005). Inactivation of Rac1 has been shown to correlate with the onset of LPS-induced barrier dysfunction. The activation of RhoA as a result of LPS occurs delayed compared to Rac1 (Schlegel et al. 2009).

Sphingosine-1-phosphate (S1P), a barrier function protective agent and known activator of Rac1 prevented the formation of lung edema in a different study, suggesting that Rac1 inactivation is involved in LPS-induced endothelial barrier dysfunction (Coimbra et al. 2006, Bogatcheva et al. 2009, Schlegel et al. 2009).

LPS-induced inactivation of Rac1 and RhoA correlated with barrier dysfunction, although RhoA appeared activated at a later time point than Rac1 (Schlegel et al. 2009). A different study reported that S1P blocked lung edema. Since it has been established that S1P activates Rac1 it can be concluded that inactivation of Rac1 in response to LPS is one of the primary actors in LPS-induced endothelial barrier dysfunction (Peng et al. 2004). Furthermore, LPS-induced inactivation of Rac1 has been shown to be cAMP-dependent (Coimbra et al. 2006, Bogatcheva et al. 2009, Schlegel et al. 2009).

The cytokine TNF α that is intimately related to the onset and progression of sepsis and severe sepsis. RhoA and Rho kinase-dependent barrier dysfunction have been reported previously. However, this study was challenged by other reports stating that Rho kinase inhibition did not effectively attenuate TNF α mediated increases in endothelial permeability. Independently of the contradictory results, the main point lies in the fact that all these studies were conducted under static cell culture conditions pointing to the importance of imitating as closely as possible physiologically relevant fluid shear stress conditions especially when studying small GTPases and the endothelium (McKenzie et al. 2007, Schlegel et al. 2009).

TNF α has been reported to decrease significantly activity of the small GTPase Rac1 (Schlegel et al. 2009). Inactivity of Rac1 induced by TNF α resulted in reduced endothelial cAMP levels attributed to activation of phosphodiesterases (Koga et al. 1995, Seybold et al. 2005, Schlegel et al. 2009). Furthermore, it has been reported that CNF-1 induced activation of Rho GTPases blocks TNF α mediated endothelial barrier dysfunction (Schlegel et al. 2009). Hence, a decrease in endothelial cAMP levels resulting in Rac1 inactivation rather than RhoA activation have an additive effect in TNF α and LPS mediated endothelial barrier dysfunction.

Thrombin, a coagulant factor, has also been implicated in endothelial barrier function modulation. The G-protein coupled thrombin receptor protease-activated receptor-1 (PAR-1) results in a rapid increase in cytosolic Ca²⁺ levels. RhoA, in its turn, is activated upon PAR-1 receptor ligation, confirming the hypothesis that RhoA and Rho kinase are directly implicated in endothelial barrier dysfunction (Mehta et al. 2001, Mehta et al. 2006, Vandenbroucke et al. 2008, Beckers et al. 2010).

VEGF, platelet-activating factor (PAF), histamine and bradykinin have been reported to be directly implicated in intracellular Ca²⁺ level increases that, in turn, lead to increased endothelial permeability (Sun et al. 2006). VEGF has been associated to both RhoA and Rac1 signaling. RhoA, for example, mediated endothelial permeability increases in coronary venules both *in vitro* and *in vivo* (Waschke et al. 2004). However, other studies reported that RhoA activation

was not required for augmenting permeability in endothelial venules (Gavard et al. 2006, Gavard et al. 2008).

1.8.3 Small GTPases and vascular permeability

Due to their vast implication in cell signaling pathways it comes as no surprise that small G proteins are involved in the regulation of endothelial permeability. Rho GTPases have been implicated in the modification of endothelial barrier function by directly acting upon constituents of junction complexes (Kim et al. 2009). It is well-established that endothelial barrier-destabilizing mediators, such as VEGF, thrombin, or TNF α induce tyrosine-phosphorylation of VE-cadherin, β -catenin, or p120-catenin (Garcia et al. 1986, Lampugnani et al. 1992, Lum et al. 1996, Dejana et al. 2008). Studies in cultured endothelial cells have revealed that, in response to VEGF, Rac1 induces phosphorylation of VE-cadherin. Phosphorylation of VE-cadherin leads to recruitment of β -arrestin, which in turn, results in endocytosis of junction complex components leading ultimately to increased permeability (Gavard et al. 2006). Besides adherens junctions, small GTPases act upon tight junction components. The adaptor protein ZO-1, one of the major components of tight junction complexes, has been shown to undergo changes in its localization induced by constitutively active or inactive Rac1 mutants (Baumer et al. 2009). Furthermore, immunofluorescent assays revealed that ZO-1 and claudin-5 expression in endothelial monolayers were reduced following treatment with thrombin, histamine, or LPS (Wojciak-Stothard et al. 2001, Schlegel et al. 2009).

1.9 Figures

This page has been left blank intentionally.

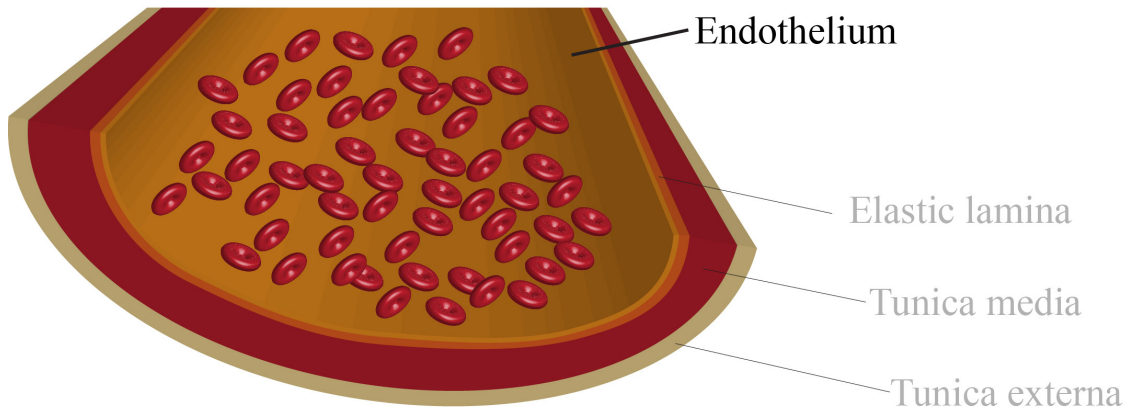


Figure 1.1

Structural components of blood vessels

Blood vessels are comprised of several structural components. The tunica externa is present on the outermost layer. Following further toward the lumen site, the tunica media and subsequently the tunica intima are formed. Endothelial cells form a thin monolayer lining the innermost of blood vessels.

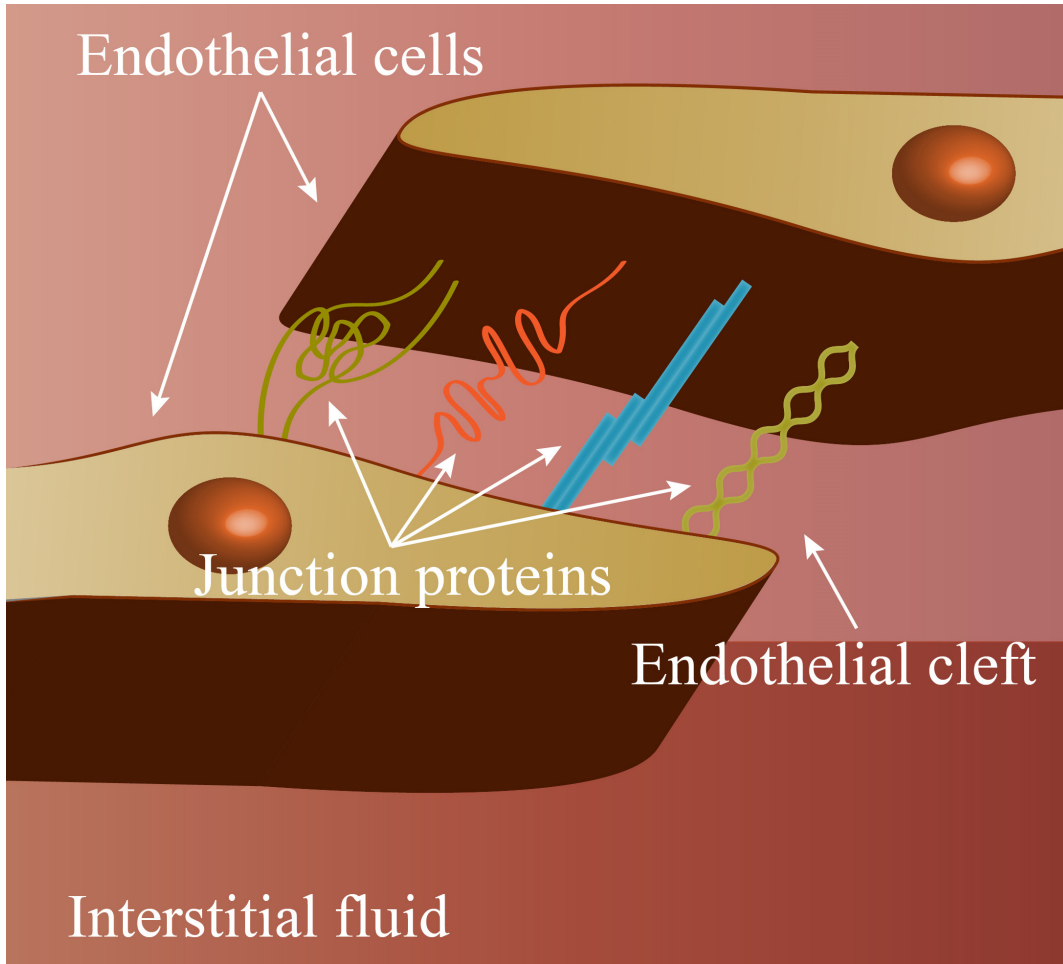


Figure 1.2

Endothelial cleft is the major site regulating permeability

The endothelial cleft is where adherens and tight junction complex constituents are located. Paracellular permeability is primarily regulated in this compartment of endothelial cells.

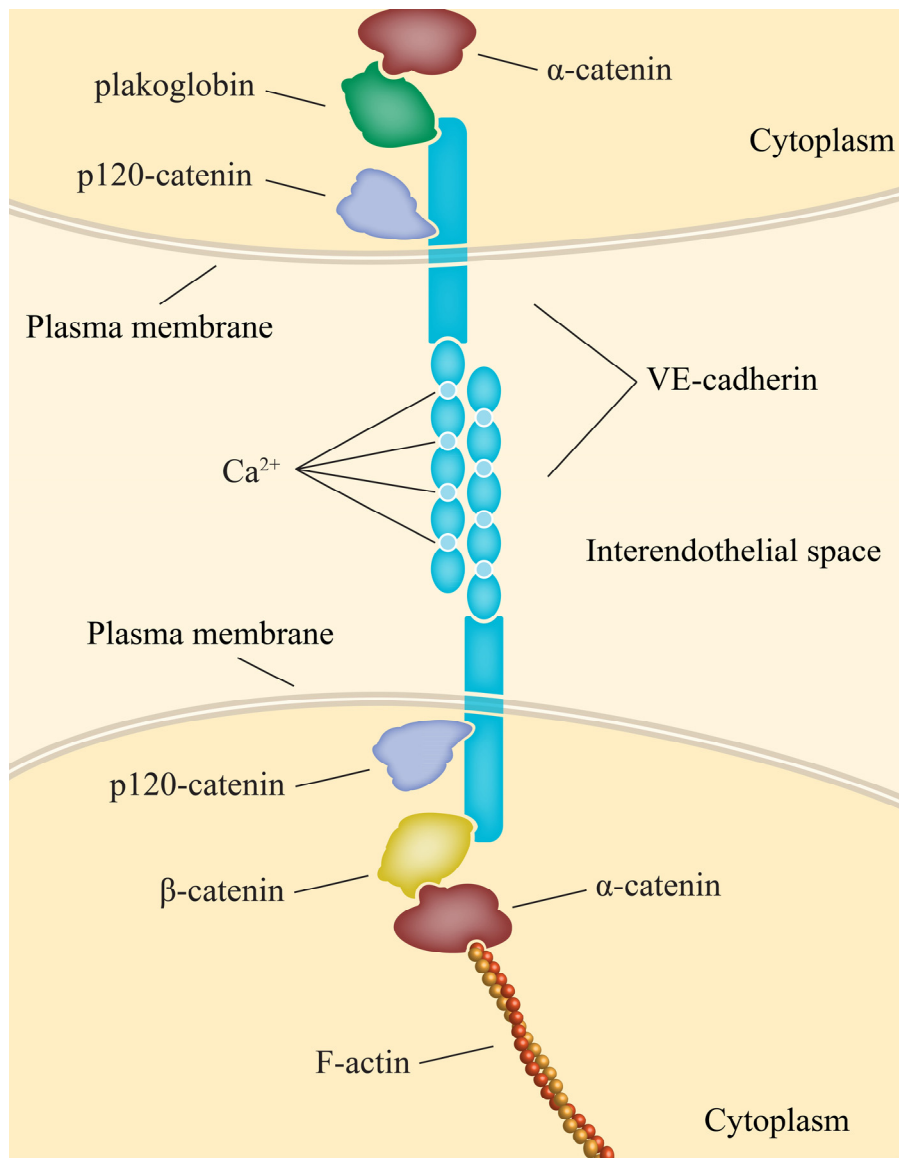


Figure 1.3

VE-cadherin structure

VE-cadherin is located at sites of adherens junction complexes. It binds on its extracellular domain with VE-cadherins of adjacent endothelial cells. At its cytoplasmic tail, it binds p120-catenin (juxtamembrane) and β-catenin or plakoglobin. β-Catenin and plakoglobin are

mutually exclusive meaning that if VE-cadherin binds to β -cadherin, then plakoglobin is excluded from this site. β -Catenin, in turn, binds to α -catenin that associates the VE-cadherin complex to the actin filaments.

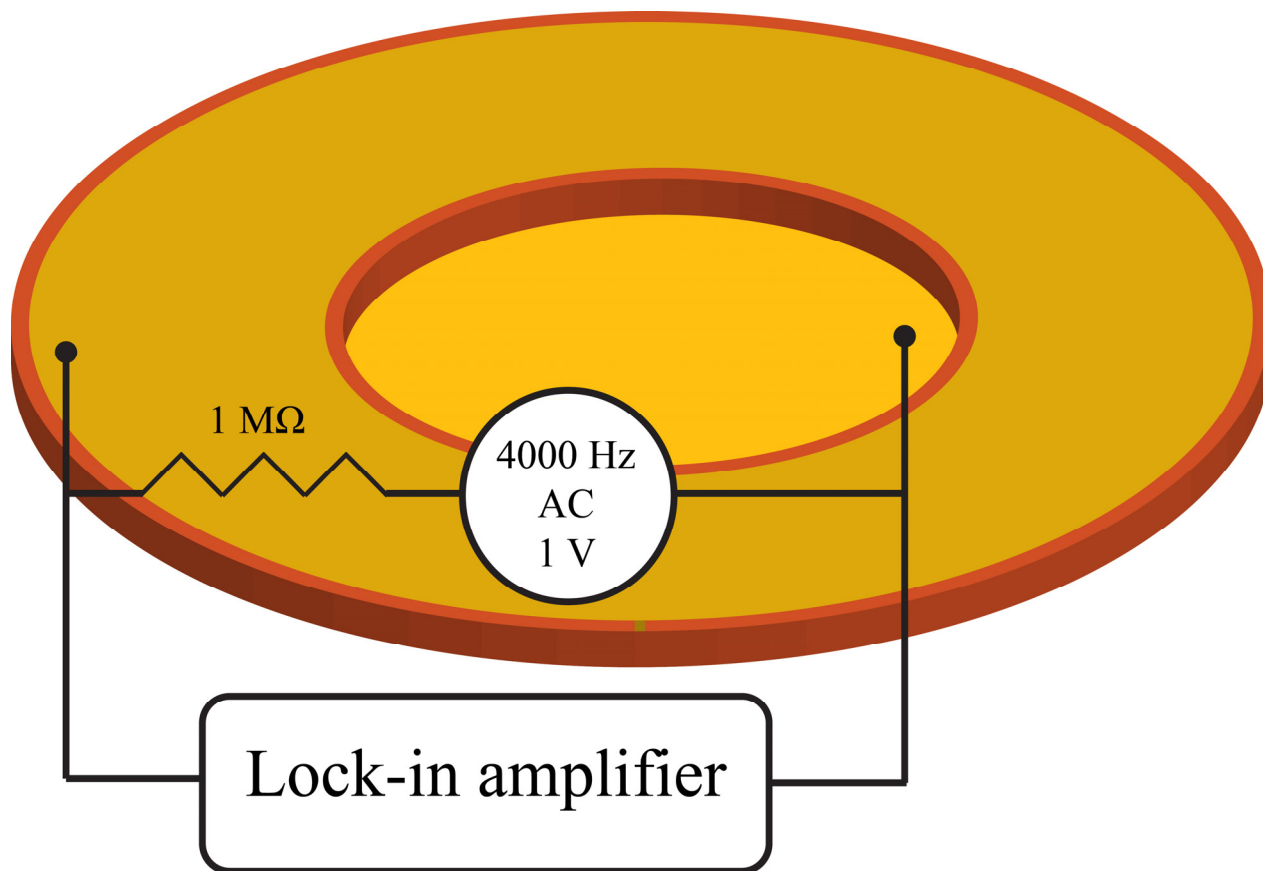


Figure 1.4

ECIS principle of function

A small electrode surrounded by a larger counter-electrode form an RC circuit in series. The ECIS measurement takes place within the surface area of the small electrode.

ECIS gold-film electrode

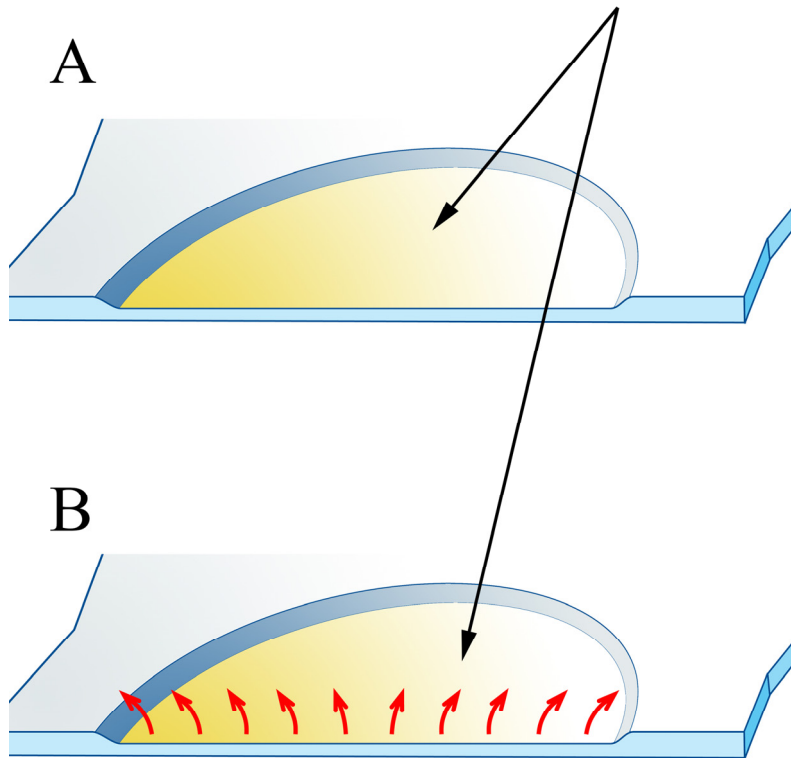


Figure 1.5

Basic functional principle of ECIS

The electrical current flows unobstructed in the absence of cells. The cell culture growth medium functions as the electrolyte.

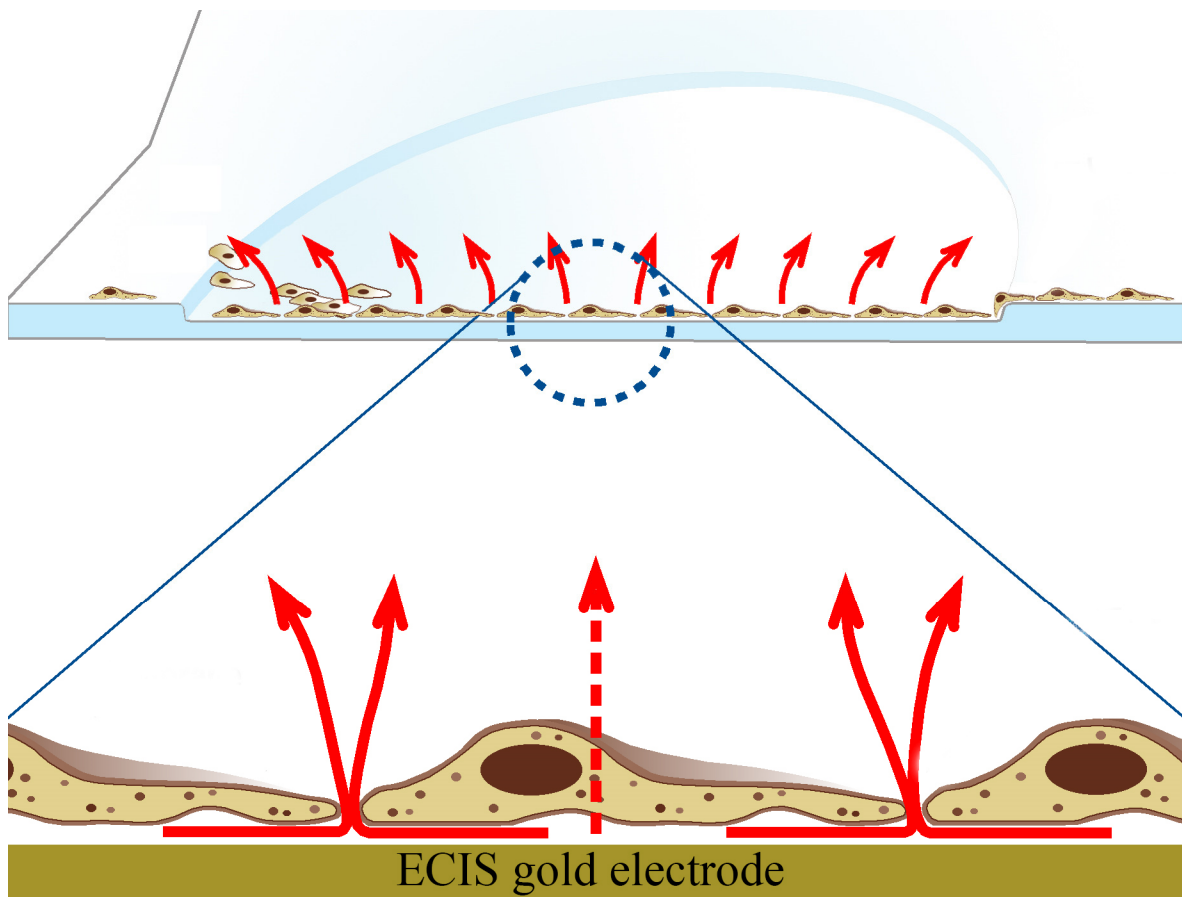


Figure 1.6

Electrical current flowing through a cell monolayer

Endothelial cells are seeded onto the ECIS slide and start adhering and spreading. As endothelial cells form a monolayer, the electrical current flowing beneath the substrate is restricted and must flow through the spacing formed by adjacent endothelial cells (interendothelial spacing) or at higher probing frequencies, through individual endothelial cells.

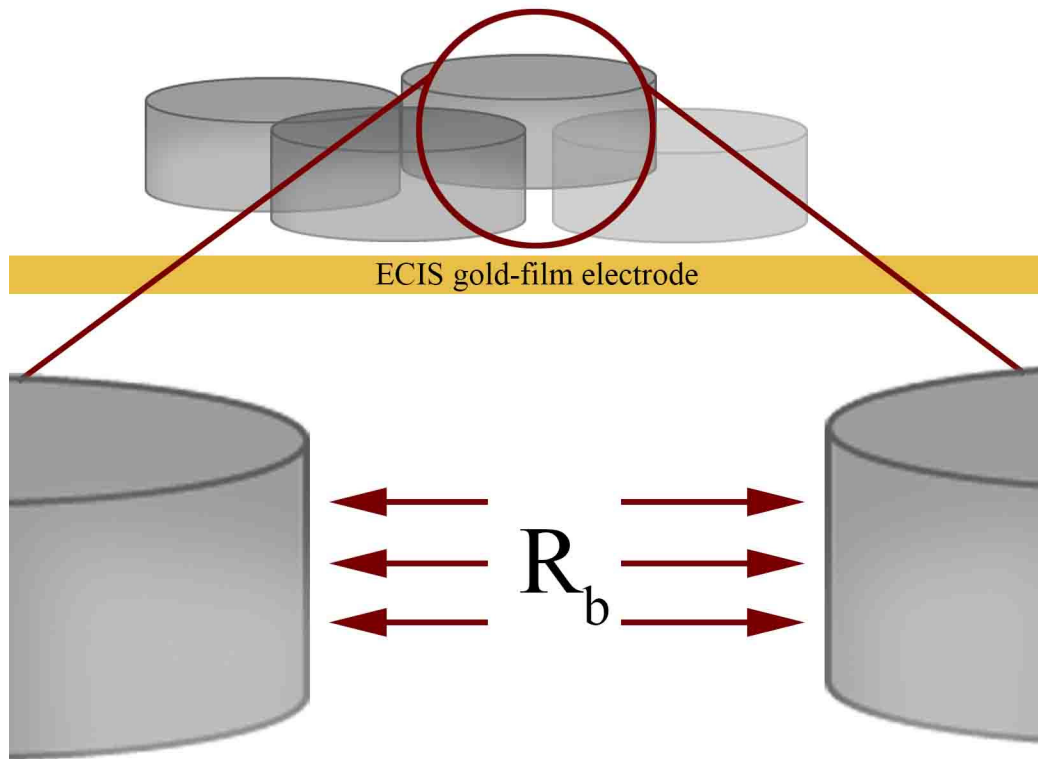


Figure 1.7

Transendothelial electrical resistance

ECIS monitors in real-time electrical resistivity of endothelial cells, known as transendothelial electrical resistance that is used to describe endothelial permeability. Transendothelial electrical resistance is inversely proportional to permeability.

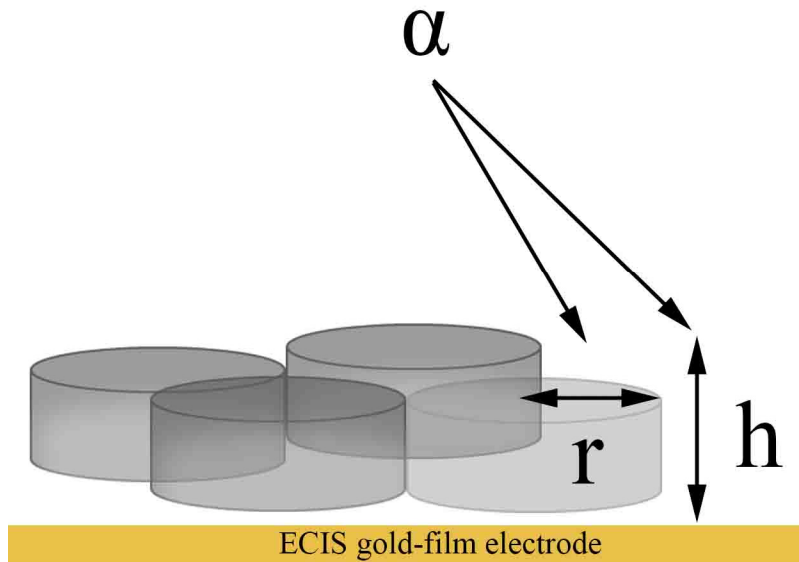


Figure 1.8

The ECIS parameter alpha

Alpha (α) is associated with the mean radius (r) of endothelial cells and their height (h) from the underlying substrate. This quantity is derived based on the ECIS model using electrical resistivity, impedance and capacitance values as have been determined experimentally.

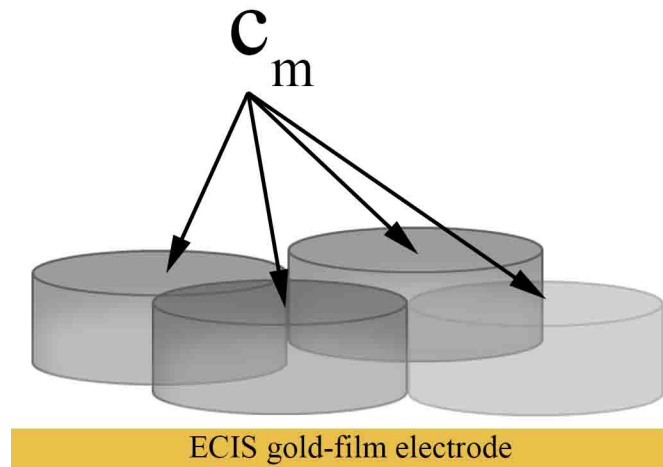


Figure 1.9

Membrane capacitance

ECIS monitors capacitance values of endothelial membranes in real-time during acquisition. The capacitance values offer an indication of the tightness of the monolayer.

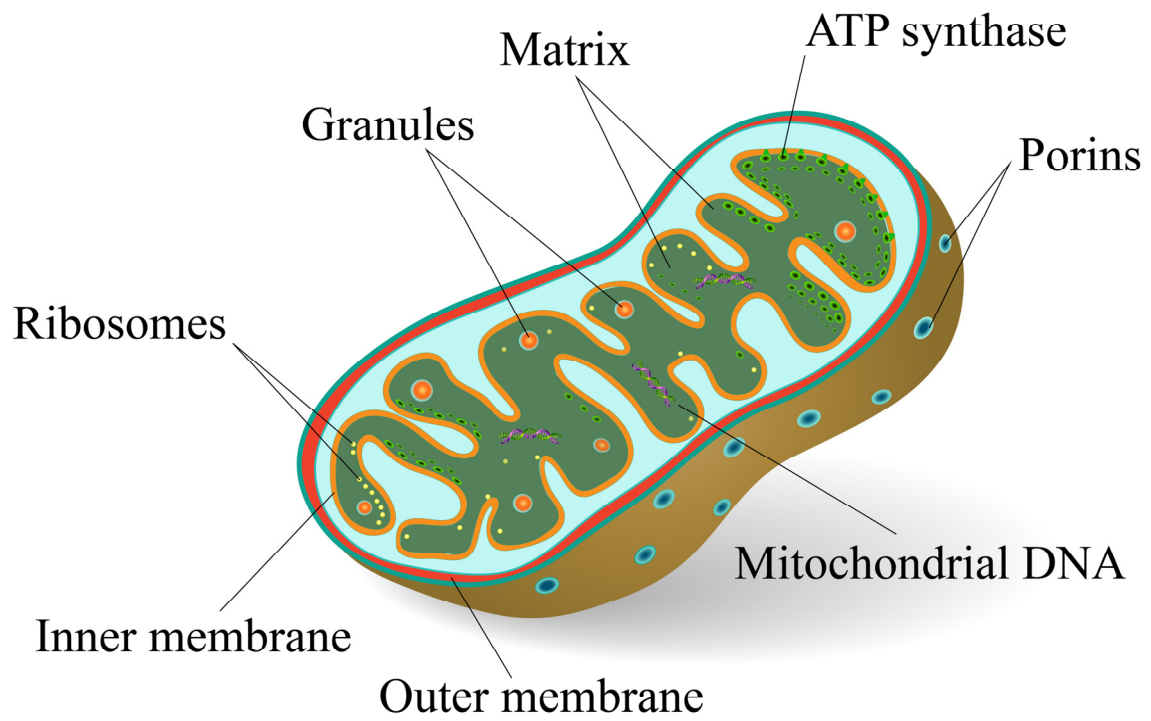


Figure 1.10
Structure of mitochondria

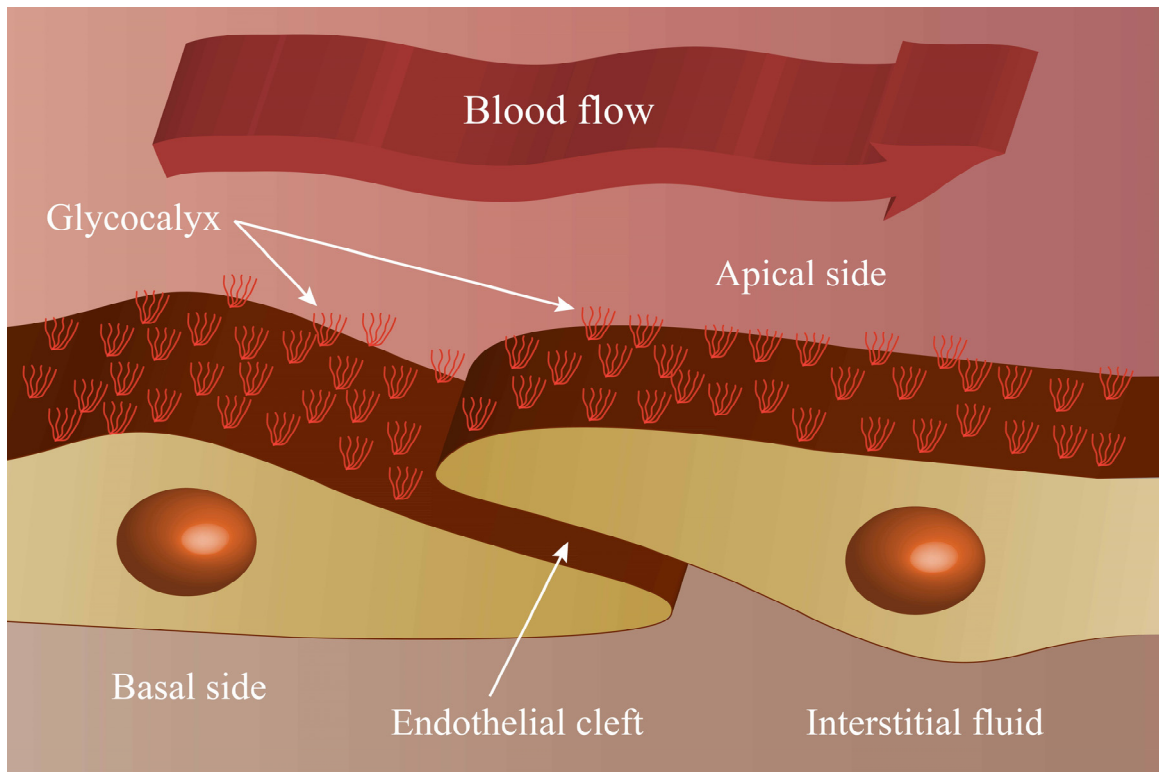


Figure 1.11

Endothelial glycocalyx

Adjacent endothelial cells form a monolayer lining the innermost of blood vessels, where they regulate vascular permeability. Blood flows on the apical side of the endothelium. The endothelial monolayer separates blood from the underlying tissues and interstitial space on the basal side of endothelial cells. Interstitial fluid is located on the basal side. On the apical side, the endothelial glycocalyx layer can be distinguished.

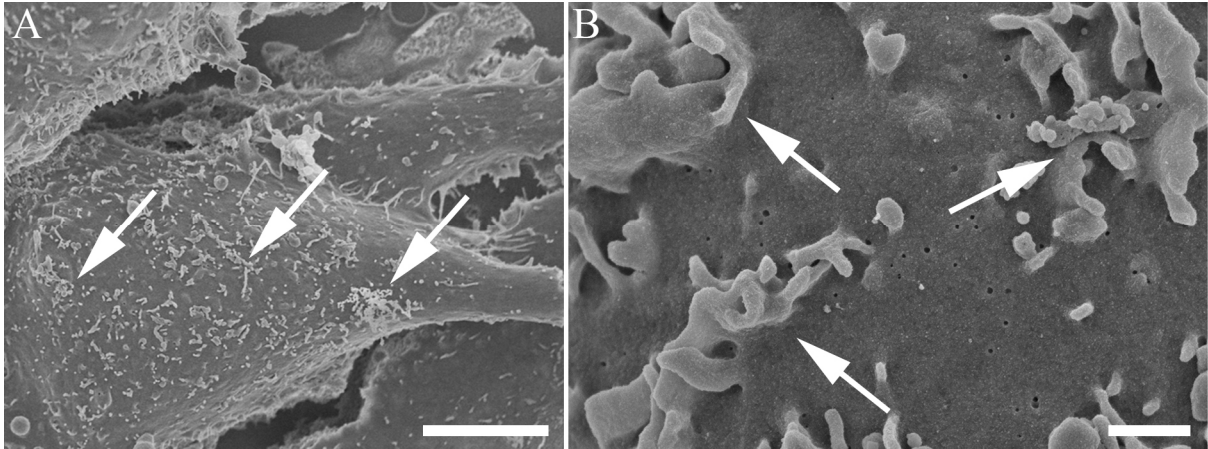


Figure 1.12

Endothelial glycocalyx in human coronary endothelial cells

SEM micrographs of human coronary endothelial cells. **(A)** Endothelial cells forming a monolayer. Their surface is covered by the endothelial glycocalyx. The scale bar corresponds to 1 μm . **(B)** The endothelial glycocalyx on the surface of human coronary endothelial cells (HCAECs) can be clearly distinguished. The scale bar corresponds to 500 nm.

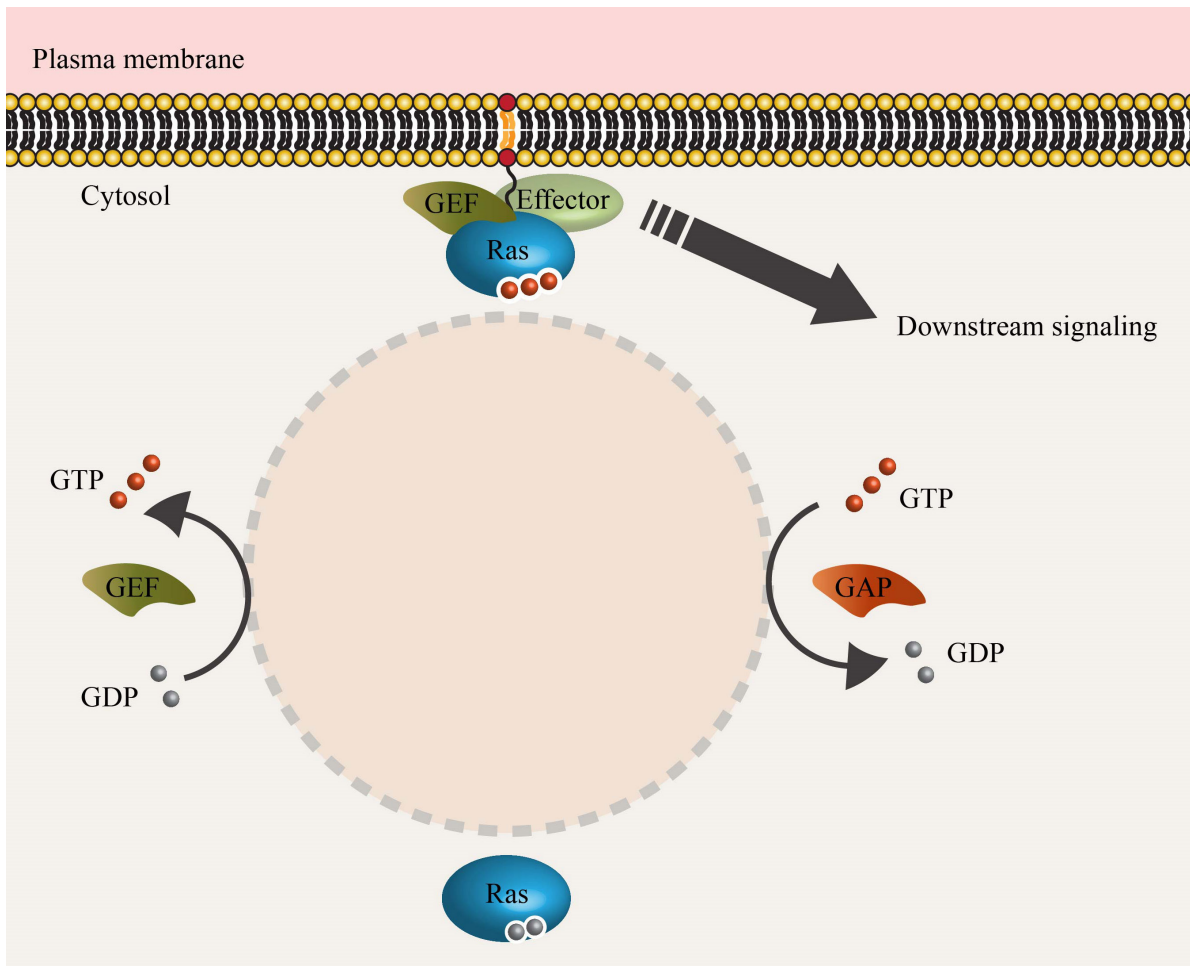


Figure 1.13

Small GTPase cycling between active GTP-bound and inactive GDP-bound state

Small GTPases function as molecular switches and transition between an active GTP-bound state to an inactive GDP-bound state stimulated by GEFs and GAPs. Small GTPase members of the RAS superfamily of small GTPases are stimulated by different GEFs and GAPs. Here, GEFs and GAPs that have been implicated to interact with R-Ras are shown.

1.10 Tables

This page has been left blank intentionally.

Species	LPS [$\mu\text{g}/\text{kg}$]	Reaction	References
Humans	0.004	Severe immunoreaction	(Suffredini et al. 1989, Suffredini et al. 1989, van Deventer et al. 1990, Martich et al. 1991)
	15	Septic shock	(Sauter et al. 1980, Taveira da Silva et al. 1993)
Rhesus monkeys	125 - 1250	Slight immunoreaction	(Sheagren et al. 1967)
Rabbits	10 - 15	Slight fever (short duration)	(Wolff et al. 1965, Sheagren et al. 1967, Mathison et al. 1988)
Rats	10000 - 20000	LD ₅₀	(Berczi et al. 1966, Kim et al. 1966, Clark 1982)
	25000 - 60000	LD ₁₀₀	
Sheep	20	LD ₅₀	(Golenbock et al. 1987, Schiffer et al. 2002)
Mice	5000	LD ₅₀	(Schaedler et al. 1961, Glode et al. 1976, McCuskey et al. 1984)
Hamsters	2000	LD ₅₀	(McCuskey et al. 1984)
Chickens	50000	No deaths	(Berczi et al. 1966, Adler et al. 1979, Clark 1982)
Dogs	125 - 500	LD ₅₀	(Reddin et al. 1966, Goldfarb et al. 1983, Cobb et al. 1995)
Lizards	200000	No harm	(Goodwin et al. 1952, Clark 1982)

Table 1.1
Sepsis animal models

Animal models used for studying sepsis and severe sepsis. Discrepancies in the tolerance levels between human and other animal species toward pathogenic factors pose an additional degree of complexity in the quest for novel therapeutic compounds against sepsis.

CHAPTER 2

The R-Ras and FLNa complex regulates tumor necrosis factor alpha-mediated vascular permeability under fluid shear stress

Abstract

Tumor necrosis factor alpha (TNF α) is an essential regulator of inflammatory processes in immune-related conditions including sepsis, septic shock and cancer. Following the invasion of pathogenic microorganisms, the host immune system responds by releasing TNF α in an effort to contain and eradicate the infection. In sepsis and septic shock, an overproduction of TNF α and other cytokines leads to the creation of an immune overreaction, a condition termed cytokine storm. During the onset of infection in sepsis, TNF α has been implicated as one of the major regulators of the host immune response. Overproduction of TNF α leads to tissue injury and in the case of septic shock to multiple organ failures.

Currently, there are no established treatments for sepsis or septic shock and despite a concerted effort to use TNF α as a pharmaceutical target, the drug compounds available induce severe side-effects in terms of immune responses and tumorigenesis. This stands to reason considering the key role that TNF α plays in the host immune system. In previously published work, our laboratory identified a complex formed by the small GTPase R-Ras and the cytoskeletal protein FLNa. The R-Ras/FLNa complex was shown to be essential in the maintenance of endothelial barrier integrity under static *in vitro* cell culture conditions.

Various attempts thus far have been undertaken to study endothelial cells as their crucial role in the regulation of immune responses and tumor metastasis has been recognized and established. The overwhelming majority of the published work has studied endothelial cells under static cell culture conditions. However, it is well-established that endothelial cells forming the innermost lining of blood vessels are constantly exposed to hemodynamic forces. Fluid shear stress acting upon endothelial cells across the entire circulatory system modify endothelial function.

In an effort to imitate and approximate physiologically relevant conditions under *in vitro* controlled parameters we investigated the effects of TNF α on primary microvascular endothelial cells under fluid shear stress conditions. Our results show that the complex formed by a

constitutively active GTP-bound state of the small GTPase R-Ras and the cytoskeletal protein FLNa reverses TNF α -mediated increases in endothelial permeability. A constitutively active form of R-Ras acts in a protective manner against the permeability-inducing potential of TNF α . Primary human dermal endothelial cells maintain the integrity of their barrier function in fluid shear stress conditions while being challenged with the TNF α cytokine.

2.1 Introduction

2.1.1 Cytokines

Cytokines are secreted by several cell types and are involved in a plethora of cellular processes, such as cell survival, proliferation, and differentiation. They are also an integral part of the immune system and are pivotal in the host response. Cytokines are a family of small signaling proteins secreted by a variety of cells including macrophages, lymphocytes and endothelial cells. They are integral in the maintenance of homeostasis. Nonetheless, excessive production of cytokines initiates tissue injury that may lead to organ dysfunction. During sepsis, excessive release of cytokines into the circulation triggers a systemic inflammatory process that very often is accompanied by single or multiple organ failures. $\text{TNF}\alpha$, $\text{IL-1}\beta$, IL-6 , and IL-8 are the four cytokines that have been associated with the sepsis syndrome. During the pathogenesis of sepsis, cytokines are released leading to a cytokine cascade. The cytokine cascade is initiated when a pathogenic invasion challenges the immune system. Gram-negative cell wall bacterial endotoxin induces the production and secretion of proximal cytokines, including $\text{TNF}\alpha$ and IL-1 . Proximal cytokines, stimulate the production of distal cytokines, such as IL-6 and IL-8 . This vicious cycle of an excessive production and release of cytokines leads to a disturbance and perpetuation of the inflammatory response (Blackwell et al. 1996).

$\text{TNF}\alpha$ is a pleiotropic cytokine essential in acute and chronic inflammation, anti-tumor responses, sepsis and septic shock (Palladino et al. 2003, Schulte et al. 2013). It is primarily secreted by leukocytes, in particular, mononuclear phagocytes, T-lymphocytes and mast cells (Tracey et al. 1994). Mononuclear phagocytes synthesize $\text{TNF}\alpha$ largely in response to invading pathogens (e.g., LPS). T-cells secrete $\text{TNF}\alpha$ following antigen recognition. Mast cells constitutively synthesize $\text{TNF}\alpha$ storing it for rapid release in response to an infection. Although, under physiological conditions, circulating $\text{TNF}\alpha$ levels exhibit values less than 1 pg/mL, during the onset of gram-negative sepsis these levels can rapidly rise beyond 100 pg/mL (Debets et al. 1989).

Human TNF α is synthesized as a 26-kDa protein and expressed on the plasma membrane. Following expression of newly synthesized TNF α on the plasma membrane, it is subsequently cleaved in the extracellular domain by matrix metalloproteinases. TNF α cleavage leads to the release of a mature soluble 17 kDa protein. Both the cell-associated and secreted forms of TNF α require trimerization in order to acquire biological activity (Kriegler et al. 1988).

TNF α exerts its biological activity through binding to either one of two structurally distinct membrane-associated receptors, TNF α receptor-1 (TNFR-1) and TNF α receptor-2 (TNFR-2). Both TNFR-1 and TNFR-2 are transmembrane glycoproteins. The extracellular domains of the two TNF α receptors share structural and functional homology. Conversely, TNFR-1 and TNFR-2 exhibit significant differences in their intracellular domains. TNFR-1 and TNFR-2 transduce their signals through both overlapping and distinct signaling pathways. One of the major differences distinguishing the intracellular domains of the two receptors is the presence of a death domain in TNFR-1, whereas TNFR-2 lacks this domain. TNFR-1 has been implicated in the pro-inflammatory and shock-inducing properties of TNF α . TNFR-1 deficient mice exhibit an extraordinary resistance to endotoxin-induced lethality, whereas mice deficient of TNFR-2 continue to respond to endotoxin (Evans et al. 1994, Josephs et al. 2000).

The TNF α signaling cascade with regard to TNFR-1 is initiated by its binding to the extracellular domain of the receptor. Binding of TNF α to TNFR-1 results in conformational changes that lead to the recruitment of TNFR-associated via death domain protein (TRADD) to the cytoplasmic domain of TNFR-1. TRADD, in its turn, recruits the receptor interacting protein-1 (RIP-1), a serine/threonine kinase, to the complex formed by the cytoplasmic domain of TNFR-1 and TRADD. The newly formed complex consisting of TNFR-1, TRADD and RIP-1 (also termed signalosome), triggers various kinase cascades leading to the activation of NF- κ B, a transcription factor and activator protein-1 (AP-1) (Martin et al. 2002, Pober et al. 2007).

The TNF α -mediated sequence of pro-inflammatory events results in the leakage of plasma proteins from the blood into the interstitial space. More importantly, it induces the reorganization

of actin and tubulin destabilizing tight and adherens junctions formed by adjacent endothelial cells (Poerber et al. 1987, Petrache et al. 2003). Although, loss of endothelial barrier integrity in response to TNF α is mediated partly due to NF- κ B, the precise mechanisms, and involved protein complexes are elusive (Clark et al. 2007).

Due to the implication of TNF α in the inflammatory host response, there has been a directed effort in developing pharmacological compounds capable of inhibiting TNF α and thereby inactivating its downstream signaling events.

Monoclonal TNF α antibodies (e.g., adalimumab, certolizumab, pegol, golimumab and infliximab) associate to membrane-bound TNF α . On the other hand, fusion proteins (e.g., etanercept) target soluble circulating TNF α (Gottlieb 2007, Tracey et al. 2008).

In both cases, whether targeting membrane-associated TNF α or free circulating TNF α , the ultimate target is to suppress downstream inflammatory mediators and contain the inflammatory process. Although TNF α inhibitors appear to contain selectively downstream signaling that may compromise host defense mechanisms, they have been implicated in adverse side-effects expressed in the form of a worsening inflammatory reaction or tumorigenesis. These undesirable side-effects could be possibly due to the essential role that TNF α plays in host defense and as a tumor suppressor (Raza 2000, Kirman et al. 2004, Gottlieb 2007).

2.1.2 The cytoskeletal scaffold protein filamin A and its role in mechanotransduction and mechanosensing

FLNa is a large cytoplasmic protein with important functions in cross-linking cortical actin filaments to form three-dimensional structures rendering mechanical stability to cells. FLNa null and point mutations are involved in a broad range of developmental malformations in the brain, bones, limbs and other organs suggesting that FLNa is a versatile signaling scaffold protein. It interacts with a vast array of more than 90 signaling proteins that have been reported thus far, indicating its importance and diversity (Ehrlicher et al. 2011, Nakamura et al. 2011).

The FLNa polypeptide chain (Figure 2.1) has a molecular mass of 280 kDa consisting of an amino-terminal actin-binding domain (ABD) followed by a rod-like domain of 24 immunoglobulin repeats (Nakamura et al. 2011). Structurally, the immunoglobulin repeats form anti-parallel β -sheets, interrupted by two flexible loops forming hinge structures (Hartwig et al. 1975, Wang et al. 1975, Gorlin et al. 1990, Feng et al. 2006). The FLNa protein is an extended homodimer comprising two identical subunits. It dimerizes via the last carboxyl-terminal repeat allowing it to acquire a V-shaped three-dimensional structure essential to its diverse multifunction (Weihsing 1988, Gorlin et al. 1990, Feng et al. 2006). The actin-binding domains and FLNa repeats 1-15 are designated 'rod domain 1', whereas FLNa repeats 16-23 are designated 'rod domain 2'. FLNa rod domain 1 along with the actin-binding domains form a linear structure that allows binding to actin filaments. FLNa rod domain 2 on the other hand does not interact with actin filaments and contains the binding sites for FLNa interacting protein partners (Ehrlicher et al. 2011).

Actin filaments (F-actin) are concentrated at the cell periphery. Its dynamic remodeling is attributed with cellular functions as crucially important as cell translocation, morphological changes and more importantly resistance to mechanical forces from the immediate microenvironment (Matsudaira 1994, Discher et al. 2005). F-actin performs these tasks in conjunction with its interacting partners of which FLNa is the most potent. Cellular FLNa expression is essential for normal development; a fact that is supported by the observations that FLNa deletions or point mutations lead to congenital anomalies and death (Robertson et al. 2003, Robertson 2005, Feng et al. 2006, Ferland et al. 2006, Hart et al. 2006, Kyndt et al. 2007). Cells lacking FLNa expression exhibit impaired locomotion and resistance against mechanical stress (Flanagan et al. 2001, Kainulainen et al. 2002).

Moreover, FLNa is involved in integrin signaling indicating its essential role in cell signaling and mechanotransduction. By bridging integrins, submembrane actin filaments and signal transduction molecules, FLNa has an enormous ability to regulate cellular activities including actin polymerization (Stossel et al. 2001). Furthermore, FLNa has been reported to be

phosphorylated affecting the way it interacts with its partnering proteins but most importantly influencing its association with GTPases (Yada et al. 1990, Ueda et al. 1992). Numerous serine/threonine protein kinases have been shown to induce phosphorylation of filamins, including protein kinase A, PKC, Ca²⁺/calmodulin-dependent protein kinase II and p90 ribosomal S6 kinase (Wallach et al. 1978, Kawamoto et al. 1984, Chen et al. 1989, Ohta et al. 1996, Jay et al. 2000, Stossel et al. 2001). FLNa has been reported to associate with several of the Rho family small GTPases, whereas Ral binds FLNa in a GTP-dependent manner (Marti et al. 1997, Ohta et al. 1999, Bishop et al. 2000). Cdc42, RhoA and Rac1 have been reported to bind FLNa constitutively. Intriguingly, trio, a guanine nucleotide exchange factor for Rho family GTPases, binds FLNa directly. The direct interaction of GEFs with FLNa suggests that Rho GTPases can bind to FLNa through their GEFs leading to their activation. In addition, this interaction may regulate the spatial organization of actin assembly (Bellanger et al. 2000, Stossel et al. 2001).

FLNa is involved in the regulation of various pathologies either directly or indirectly through its interacting signaling proteins. Hemizygous males exhibiting FLNa mutations die in utero. The ones who survive after birth, suffer from cardiac malformations and often die postnatally due to rupture of blood vessels (Eksioglu et al. 1996, Fox et al. 1998, Guerrini et al. 2004). Furthermore, mutations in FLNa are associated with cardiac valvular anomalies and are vulnerable to premature strokes or vascular disorders (Moro et al. 2002).

Feng et al. showed that FLNa-null mice die at midgestation due to hemorrhage originating from abnormal vessels. More importantly, it has been shown that FLNa-null vascular endothelial cells exhibit decreased function at cell-cell contacts and in particular adherens junctions, suggesting the importance of FLNa in the maintenance of endothelial barrier integrity (Feng et al. 2006).

The essential role of FLNa in the vascular endothelium is also demonstrated by the endothelial cell-specific molecule-2 (ECSM-2), a surface protein exclusively expressed by

endothelial cells. ECSM-2 interacts directly with FLNa. The complex formed by ECSM-2 and FLNa has been implicated in the regulation of endothelial chemotaxis and tube formation by actin cytoskeleton modulation (Armstrong et al. 2008).

Vascular endothelium is the primary target of metastasizing cells. Hence, the finding that FLNa is involved in the pathogenesis of cancer metastasis is not surprising. Caveolin-1, yet another interacting protein partner of FLNa, promotes PI3K/AKT-mediated phosphorylation of FLNa at serine 2152 (S2152) in human breast cancer cells (Ravid et al. 2008).

The role of FLNa in mechanotransduction events under fluid shear stress is evident through its direct binding to β 1-integrin resulting in a stiffening of cell monolayers and hence, allowing them to exhibit an improved resistance to fluid shear stress. FLNa-null cells subjected to fluid shear stress do not exhibit changes in their mechanoelastic composition with regard to stiffness and thus show an impaired resistance toward fluid shear stress (Glogauer et al. 1998, Stossel et al. 2001). Understandably, the mechanoprotective function of FLNa is essential in vascular endothelium that remains constantly exposed to fluid shear stress due to hemodynamic forces in the blood vessels. Mechanical factors from the immediate cellular microenvironment exerting force on FLNa may result in a stretching conformation of FLNa with the direct implication of allowing binding interfaces of FLNa to become available for interaction with binding partners. Consequently, FLNa interacting proteins are recruited to the site of FLNa leading to spatial rearrangements (Kainulainen et al. 2002, Nakamura et al. 2007).

FLNa translocation from the plasma membrane proximity to submembrane or cytoplasmic regions leads to actin redistribution and the formation of gaps in endothelial monolayers, indicating the essential role of this protein in the regulation of endothelial barrier function (Hastie et al. 1997, Wang et al. 1997). More importantly, FLNa has been shown to associate with the small GTPase R-Ras via FLNa repeat 3 (Gawecka et al. 2010). The interaction of this R-Ras/FLNa complex is essential in the maintenance of endothelial barrier function under static cell culture conditions (Griffiths et al. 2011). The ability of FLNa to recruit

membrane-associated proteins (e.g., p190RhoGAP) and render them inactive indicates that FLNa plays a pivotal role in the regulation of vascular endothelial permeability. The multifaceted nature of FLNa becomes even more evident when considering its capabilities to move cleaved fragments to the cell nucleus where it targets nuclear receptors (Mammoto et al. 2007, Bedolla et al. 2009).

In the current study, we examined the R-Ras/FLNa complex under fluid shear stress conditions at physiologically relevant levels in the microvasculature. We have determined that maintaining the linkage between the small GTPase R-Ras and the cytoskeletal FLNa intact, maintains barrier integrity. Furthermore, TNF α -induced loss of barrier function led to an increased endothelial permeability that could be reversed by a constitutively active form of R-Ras. Conversely, dominant negative R-Ras was not capable of rescuing TNF α -induced barrier dysfunction. We performed a sequence of experimental permutations by employing a constitutively active R-Ras, a dominant negative R-Ras, a FLNa construct lacking the repeat 3 (e.g., R-Ras binds to FLNa repeat 3) and R-Ras constructs with patient mutations. Endothelial cells were challenged with TNF α while simultaneously subjected to fluid shear stress. Our results point to the identification of the TNF α inhibitory properties of active GTP-bound R-Ras.

2.1.3 The small GTPase R-Ras

The GTPase R-Ras is a member of the Ras family acting as a molecular switch by cycling between an inactive GDP- and an active GTP-bound state (Figure 2.2) (Lowe et al. 1987, Lowe et al. 1987, Wittinghofer et al. 1996). Together with TC21 and M-Ras they form the Ras subfamily including TC21 (R-Ras2) and M-Ras (R-Ras3) (Reuther et al. 2000). R-Ras exhibits close structural similarity to other members of the Ras family. However, its function is distinct from the prototypic Ras proteins (K-, H-, N-Ras) (Sawada et al. 2012). Furthermore, while point mutations in K-, H- and R-Ras have been reported to occur in human cancers, R-Ras mutations do not exhibit a similar transformative effect suggesting that R-Ras is weakly oncogenic (Lowe et al. 1987, Marte et al. 1997, Bos 1998, Vojtek et al. 1998, Pylayeva-Gupta et al. 2011).

Nonetheless, the forced expression of constitutively active R-Ras led to substantial increases in growth and invasiveness of a specific cervical cancer cell line (Rincon-Arano et al. 2003, Mora et al. 2007). Overwhelming evidence shows that R-Ras has a negative inhibitory effect on cancer cells including proliferation, migration and cell cycle progression in *in vitro* cell culture conditions (Song et al. 2014). Distinct from K- and H-Ras, R-Ras lacks the ability to activate Raf-1 (a serine/threonine-protein kinase) and RalGDS (a Ras-specific GEF) (Ehrhardt et al. 2002, Linnemann et al. 2002, Kim et al. 2012).

Despite the significant homology between R-Ras and H-Ras, the two G proteins exhibit opposite effects with regard to cell-extracellular matrix adhesion (Sethi et al. 1999, Cole et al. 2003). They also show significant divergent C-terminal sequences (Saez et al. 1994).

Furthermore, the N-terminus of R-Ras is a region of great sequence diversity. In particular, R-Ras contains a unique 26 amino acid sequence at the N-terminus rich in glycine and proline (Holly et al. 2005). R-Ras enhances the affinity and avidity of integrins and thus, induces a stronger integrin-mediated cell adhesion, whereas H-Ras has an inhibitory effect on integrin activity (Zhang et al. 1996, Hughes et al. 1997). The ability of R-Ras to exert control over integrin activation is regulated in part by phosphorylation. The Eph receptor, EphB2, phosphorylates R-Ras primarily on its tyrosine residue 66 (Y66), located in the effector binding domain of R-Ras (Zou et al. 1999). The primary if not single Src phosphorylation site for R-Ras is Y66. Nonetheless, binding of Src to R-Ras is not dependent on phosphorylation at Y66 (Zou et al. 2002). This phosphorylation event results in the R-Ras impairment to activate integrins. In addition, cell-extracellular matrix adhesion is impaired when EphB2 is activated (Zou et al. 1999). EphA2 is also one of the Eph receptors reported to downregulated integrin-mediated cell adhesion (Miao et al. 2000). R-Ras and H-Ras also have a differential effect on cell differentiation. R-Ras contains a Src homology-3 (SH3) domain binding proline motif site required for its integrin-activating function, an attribute that constitutes this small G protein different from other members of the Ras family of GTPases (Zou et al. 1999, Wang et al. 2000,

Zou et al. 2002, Sawada et al. 2015). Furthermore, Eph receptors and Src have the ability to phosphorylate R-Ras (Zou et al. 1999, Wang et al. 2000, Zou et al. 2002).

In vivo R-Ras is expressed in primary endothelial cells, mural cells (smooth muscle cells and pericytes) of small arterioles and arteries. It can also be expressed in cancers of epithelial origin, such as in breast, cervical and gastric cancer (Komatsu et al. 2005, Nishigaki et al. 2005, Sawada et al. 2012, Gao et al. 2014, Song et al. 2014).

Deletion of R-Ras expression enhances angiogenesis in tumor implants, whereas this enhancement rendered tumor vessels incapable of maturation as characterized by severe deformation and functional vessel impairment (Komatsu et al. 2005, Sawada et al. 2012).

The Matter group has previously shown that R-Ras associates with the cytoskeletal protein FLNa by a yeast-two-hybrid screening. GST-filamin fusion proteins that corresponded to three different regions of FLNa confirmed that R-Ras binds to FLNa through the GST fusion protein corresponding to FLNa repeat 1-10 but not the other remaining two regions. These finding supports that R-Ras forms a complex with FLNa (Figure 2.1) by binding directly to its repeat 3 (Gawecka et al. 2010).

The Matter group went on to show that the interaction of R-Ras with the cytoplasmic protein FLNa is essential for the maintenance of endothelial barrier integrity, whereas loss of the interaction between R-Ras and FLNa leads to barrier dysfunction by increasing VE-cadherin phosphorylation at Y731 and Src phosphorylation at Y416. Furthermore, R-Ras and FLNa associate at the endothelial plasma membrane in quiescent arterial cells (Griffiths et al. 2011).

Inhibition of Src by its chemical inhibitor, PP2, restored endothelial permeability by blocking dominant negative R-Ras mediated barrier dysfunctions. GTP loading of R-Ras is a requirement for the small GTPases to exert its stabilizing function on endothelial barrier function, whereas loss of R-Ras activity promotes vascular permeability through increased Src activity (Griffiths et al. 2011).

2.2 Materials and Methods

2.2.1 Cell Culture

Primary human dermal microvascular endothelial cells (HDMVECs; Cell Applications, San Diego, CA) were cultured in MCDB 131 basal medium (Sigma Aldrich, St. Louis, MO). The basal medium was supplemented with 0.5 ng/mL human recombinant vascular endothelial growth factor₁₆₅ (hVEGF₁₆₅), 20 ng/mL human recombinant insulin growth factor (hIGF-R³; SAFC, Lenexa, KS), 10 ng/mL human fibroblast growth factor (hFGF; Peprotech, Rocky Hill, NJ), 5 ng/mL human recombinant epithelial growth factor (hEGF; Peprotech, Rocky Hill, NJ), 1 µg/mL ascorbic acid (Sigma Aldrich, St. Louis, MO), 0.2 µg/mL hydrocortisone (Sigma Aldrich, St. Louis, MO), 0.125 µg/mL amphotericin (Sigma Aldrich, St. Louis, MO), 5 µg/mL gentamicin (Life Technologies, Waltham, MA), and 5% fetal bovine serum (FBS; Life Technologies, Waltham, MA). HDMVECs were kept in tissue culture-treated petri dishes that were previously coated with a solution of 0.25% porcine gelatin (Sigma Aldrich, St. Louis, MO) at 37 °C in a humidified cell incubator atmosphere (5% CO₂, 95% air).

2.2.2 Plasmids constructs

Human R-Ras (R-Ras), human FLNa (FLNa), human wild type R-Ras (WT R-Ras) and their mutants, constitutively active R-Ras (CA R-Ras), dominant negative R-Ras (DN R-Ras), hFLNa 3rd repeat deletion (FLNaΔ3) and hFLNa repeat 3 alone (FLNaRP3) have been described previously (Zhang et al. 1996, Wang et al. 2000, Zou et al. 2002, Komatsu et al. 2005).

2.2.3 siRNA knockdown of R-Ras and FLNa

siRNA-mediated gene knockdown in HDMVECs was performed using the Amaxa nucleofector II device and the Dharmacon smartpool siRNAs targeting R-Ras, FLNa or the combination of both R-Ras and FLNa. For electroporation purposes only HDMVECs at a confluency level of approximately 70% and subjected to ten or fewer passages were used. Cells were washed with 30 mM HBSS and removed enzymatically from the culture dishes by applying 0.025% Trypsin and 0.1 mM EDTA. Following trypsinization, the reaction was neutralized with

TNS, the cell solution centrifuged for a duration of 7 min at 180×g and the cell number determined. Cell pellets were suspended in 100 μL of a nucleofector solution (Lonza) and mixed with 100 nM of R-Ras siRNA, FLNa siRNA or both R-Ras siRNA and FLNa siRNA. HDMVECs transfected with siGENOME non-targeting siRNAs at a final concentration of 100 nM were used as controls. The solution was transferred to an electroporation cuvette and subjected to electroporation using the Amaxa nucleofection program S-005. Immediately after electroporation, 500 μL of pre-equilibrated complete culture medium was added to the electroporation cuvette and the cells allowed to incubate for 15 min within a cell incubator. For immunostaining assays, the transfected cells were seeded onto ibidi flow chambers; for immunoblotting assays we used glass slides pre-coated with human fibronectin; and finally, for TEER assays, HDMVECs were seeded onto the ECIS flow chamber arrays.

2.2.4 Permeability-inducing treatment

HDMVECs were activated by subjecting cell monolayers to the cytokine and known permeability-inducing factor TNFα at a final concentration of 50 ng/mL. TNFα was added at the specified concentration to the complete HDMVECs medium and the solution was allowed to equilibrate in the flow apparatus setting for 5-10 min prior to immunoblotting, immunohistochemical or transendothelial electrical resistance (TEER) assays. Following, endothelial cell monolayers were subjected to fluid shear stress at 2 dyn/cm² for 15 min at 37 °C in a humidified cell incubator atmosphere (5% CO₂, 95% air).

2.2.5 Fluid shear stress

Fluid shear stress levels applied to the endothelial cells were controlled using a peristaltic pump (Masterflex, Vernon Hill, IL). The wall shear stress, τ_w (dyn/cm²) exerted onto the endothelial monolayer as a function of the measured volumetric flow rate, Q (mL/min) was calculated by applying Poiseuille's formula (Poiseuille 1830):

$$\tau_w = \frac{6Q\mu}{ah^2} \quad (2.1)$$

where τ_w is the wall shear stress in dyn/cm², Q , the volumetric flow rate in mL/min, μ , is the dynamic viscosity in Pa·s, α , is the channel width and h , is the channel height.

2.2.6 Electrical Cell Impedance Spectroscopy

Endothelial permeability was determined using the electrical cell-impedance sensing (ECIS; Applied BioPhysics, Troy, NY) methodology as has been described previously (Keese et al. 1990, Giaever et al. 1991, Giaever et al. 1993, Wegener et al. 2000). ECIS flow chamber slides (Figure 2.3A) (F8×10E PC; Applied Biophysics, Troy, NY) were pre-coated with a 10 mM L-cysteine solution for 15 min at RT to stabilize the gold electrodes and subsequently washed three times with molecular grade distilled water. Following, the L-cysteine pre-treated gold-electrode slides were coated with a human fibronectin solution at 75 µg/mL concentration (BD Biosciences, San Jose, CA) for 1 h at RT. HDMVECs were seeded onto the slides at a concentration of 1.2×10^6 cells/mL and allowed to grow to confluency for 48 h at 37 °C in a humidified cell incubator atmosphere (5% CO₂, 95% air). ECIS allows for the data acquisition to be conducted in a wide spectrum of frequencies (Wegener et al. 2000). In the current study, we probed among other frequencies for 4,000 Hz (TEER) and 64,000 Hz (capacitance). For the duration of the fluidic exposure of the HDMVECs monolayers, impedance (measured in Ohms; Ω), resistance (measured in Ohms; Ω) and capacitance (measured in nF) were recorded in real-time at the specified frequencies. The statistical evaluation of the ECIS data was performed using one-way ANOVA in conjunction with the Tukey correction of confidence intervals and significance algorithm for a set of at least three data samples. The statistical data evaluation was performed using Prism version 6.04 (GraphPad Software, La Jolla, CA).

2.2.7 Immunohistochemistry

HDMVECs plated on ibidi flow μ -Slide VI^{0.4} channels (Figure 2.3B) (Ibidi, Munich, Germany) were subjected to flow-induced shear stress as described above. Immediately after completion of the flow assays, cells were fixated in 4% paraformaldehyde and 0.3% sucrose for 10 min at 37 °C, washed 3× in PBS (10 mM; pH 7.4), permeabilized (0.3% TritonX-100, 5 min at RT), and blocked for 30 min at 37 °C in 10 mM PBS (pH 7.4) with 10% normal goat serum,

0.25% Triton X-100, 0.1% Tween 20, 2% glycine and 0.02% NaN₃. Following blocking, HDMVECs were incubated with a primary antibody targeted against the tight junction protein ZO-1 for 1 h at 37°C. After three washing steps with 0.1% BSA and 0.1% Tween 20 in PBS, cells were incubated for 1 h at 37 °C in Alexa Fluor® anti-rabbit 488 goat anti-rabbit IgG (H+L) secondary antibody (Life Technologies, Waltham, MA). Following secondary incubation and after three washing steps in PBS for 5 min each, cells were incubated with rhodamine phalloidin (Life Technologies, Waltham, MA) for 1 h at 37°C, washed 3× with PBS, incubated with DAPI (4',6-diamidino-2-phenylindole; Life Technologies, Waltham, MA) for 5 min at RT and mounted with mounting media (Ibidi, Munich, Germany). Images were collected on a Leica TCS SP5 confocal scanning laser microscope (Leica, Wetzlar, Germany) at a magnification of 200×.

2.2.8 Immunoblotting

Positively charged rectangular glass slides (Thermo Fisher, Waltham, MA) were rinsed with ethanol and air-dried, sterilized in a steam-autoclave, placed in a 100 mm sterile petri dish and coated with a 15 µg/ml human fibronectin solution (hFN; BD Biosciences, San Jose, CA) overnight at 4 °C. The hFN solution was removed, and HDMVEC suspensions were seeded onto the slides at a concentration of 1.2×10^6 cells/ml. Cells were grown to confluency for 48 h at 37 °C (5% CO₂, 95% air). For immunoblotting assays, endothelial cells were subjected to fluidic shear stress at a shear stress of 2 dyn/cm² (Figure 2.4A and B) with a parallel flow chamber apparatus (GlycoTech, Gaithersburg, MD). Immediately after fluid exposure, HDMVEC whole cell lysates were prepared using a kinase lysis buffer consisting of 20 mM HEPES (pH 7.4), 150 mM NaCl, 50 mM KF, 50 mM β-glycerolphosphate, 2 mM EGTA (pH 8.0), 1 mM Na₃VO₄, 10% glycerol, 1% Triton X-100, a protease inhibitor cocktail (Roche Diagnostics, Basel, Switzerland) and a phosphatase inhibitor cocktail (Pierce Scientific, Rockford, IL). Clearing of cell lysates was achieved by centrifugation at 16,000 rpm for 10 min at 4 °C. Samples of cell lysates were subjected to the Bradford protein assay (Bio-Rad Laboratories, Hercules, CA) to determine total protein concentration. Equal protein concentrations of HDMVEC lysates were subjected to run on a 12% SDS–PAGE gel and transferred to nitrocellulose membranes (Bio-Rad

Laboratories, Hercules, CA) and immunoblotted. Membranes were blocked for 1 h at RT with blocking buffer (3% BSA in 0.1% PBS-T) and incubated with antibodies directed against either VE-Cadherin (AbCam, Cambridge, United Kingdom), phospho-VE cadherin Y685 (ECM Biosciences, Versailles, KY), phospho-VE cadherin Y731 (Life Technologies, Waltham, MA), Src (AbCam, Cambridge, United Kingdom), phospho-Src Y416 (Cell Signaling Technology, Danvers, MA), SHPT2 (Santa Cruz Biotechnology, Dallas, TX), tubulin (AbCam, Cambridge, United Kingdom) or β -actin (Sigma-Aldrich, St. Louis, MO). Membranes were washed and incubated with horseradish peroxidase-conjugated secondary antibodies (Bio-Rad, Hercules, CA) for 1 hr at RT. Immunoblots were developed by ECL Plus (Pierce Scientific, Rockford, IL) and the Konica Minolta SRX-101A processor (Konica Minolta, Wayne, NJ). Densitometry of Western blots was performed using ImageJ (Schneider et al. 2012).

2.2.9 Src inhibition via PP2 inhibitor

Endothelial cell monolayers were pretreated with the pharmacological inhibitor of Src, PP2 at a concentration of 1 μ M or the carrier diluent DMSO for 1 h prior to fluid-induced shear stress assays.

2.2.10 Immunoprecipitation and kinase activation analysis

Glutathione *S*-transferase (GST) fusion proteins containing the R-Ras binding domain (RBD) were used to precipitate GTP-loaded R-Ras as described previously (Smith et al. 2001, Harper et al. 2008, Harper et al. 2011). To examine R-Ras activation following fluid shear stress exposure, HDMVECs were transfected with 3 \times Flag-tagged WT R-Ras (3 μ g), allowed to grow to confluency for 48 h and finally subjected to flow-induced shear stress. To examine the activation of endogenous R-Ras, HDMVECs were seeded onto the flow chamber glass slides and allowed to grow to confluency for 48 h. Following, the glass slides were mounted onto the flow apparatus, and the HDMVEC monolayers were subjected to shear stress at 2 dyn/cm² with normal culture media or stimulated with 50 ng/mL TNF α . Subsequently, the cells were harvested and whole cell lysates prepared. Cell lysates were subjected to GST-R-Ras-RBD agarose pulldown with end-to-end rotation at 4 $^{\circ}$ C for 2 h. The GST-R-Ras-RBD agarose pellets were

recovered after extensive washing, and levels of GTP-bound R-Ras were determined by immunoblotting with anti-R-Ras monoclonal antibody.

2.3 Results

2.3.1 Loss of direct interaction between R-Ras and FLNa promotes vascular permeability in endothelial cells subjected to fluid shear stress

The observation that FLNa null mice suffer from severe vascular deficits, such as dilated vasculature, hemorrhage, and edema suggested to us that FLNa is an important regulator in the vascular barrier function. Human coronary artery endothelial cells (HCAECs) show a prominent loss of barrier function when the linkage between R-Ras and FLNa is not intact. In static *in vitro* conditions the interaction between R-Ras and FLNa is crucial for maintaining barrier function and loss of this interaction leads to significant increases in endothelial permeability (Griffiths et al. 2011). Since vascular endothelial cells remain constantly exposed to fluid shear stress under *in vivo* conditions, we were interested in investigating whether the direct interaction between the small GTPase R-Ras and the cytoskeletal protein FLNa would be altered under flow-induced shear stress condition. HDMVEC monolayers where expression of R-Ras, FLNa or both R-Ras and FLNa was reduced by siRNA knockdown prior to exposure to flow shear stress, demonstrated a remarkable decrease in TEER (Figure 2.5; TEER and endothelial permeability are inversely related) compared to the scrambled siRNA ($p < 0.0001$). HDMVECs, where R-Ras expression was knocked down via siRNA exhibited barrier dysregulation ($1981 \pm 9.46 \Omega$) when exposed to fluid shear stress (2 dyn/cm^2), endothelial monolayers with reduced FLNa expression ($2169 \pm 99.46 \Omega$), HDMVECs with siRNA-induced knockdown of both R-Ras and FLNa demonstrated a disruption in barrier integrity comparable to HDMVECs with reduced R-Ras expression ($1986 \pm 25.45 \Omega$). HDMVECs that were challenged with the cytokine TNF α showed clear signs of barrier dysfunction, whereas permeability was the highest among all studied cases ($1973 \pm 24.24 \Omega$). The baseline for control cells was determined by exposing normal HDMVECs to fluid shear stress (2 dyn/cm^2). The respective control TEER baseline values were at $2683 \pm 19.24 \Omega$ after 15 min from the onset of fluid shear stress. As hypothesized, the interactive relationship between R-Ras and FLNa continues to be of pivotal importance when approximating *in vivo* conditions by exposing primary endothelial monolayers to fluid shear stress. HDMVECs are capillary endothelial cells exposed to laminar flow shear stress less than 6 dyn/cm^2 under *in*

in vivo conditions. Therefore, in all experimental settings, HDMVECs were exposed to laminar fluid shear stress at 2 dyn/cm² for 15 min in physiological conditions at 37 °C and a humidified cell culture incubator (95% relative humidity, 5% CO₂).

After confirming the importance of R-Ras and FLNa interaction in the maintenance of barrier function integrity under fluid shear stress conditions, we sought to examine whether flow-induced shear stress within the physiological regime of shear stress levels observed under *in vivo* conditions would induce any disturbances to endothelial adherens junctions. For this reason, HDMVECs exposed to fluid shear stress were subsequently immunostained for VE-cadherin, a prominent constituent protein in adherens junction complexes. Induction of fluid shear stress at 2 dyn/cm² did not induce any disturbances to the expression pattern of VE-cadherin for normal HDMVECs (Figure 2.6) as can be seen in endothelial monolayers transfected with control scrambled siRNA.

Formation of actin stress fibers was expected and confirmed (F-actin staining) as fluid shear stress causes actin rearrangement and the formation of stress fibers even under physiological conditions. The stress fibers form rather at the cellular periphery compared to pathophysiological cases where R-Ras, FLNa or both R-Ras and FLNa protein expression was knocked down using siRNA. In the latter case, stress fiber formation appears increased. The stress fibers are thick and diffusely distributed across the entire surface of endothelial cells. Similarly, in the case of HDMVECs activated through TNF α -mediated inflammation, the formation of stress fibers is evident. VE-cadherin appears undisturbed and continuous at the cell periphery in the case of HDMVECs transfected with scrambled siRNA. Endothelial cells where the linkage between R-Ras and FLNa was interrupted via transfection with R-Ras siRNA, FLNa siRNA or both R-Ras and FLNa siRNA exhibited obvious interruptions in the staining pattern of VE-cadherin (Figure 2.6). VE-cadherin appeared in thick stripes, discontinuous and with an evident zipper-formation suggesting that the endothelial monolayer was compromised.

The immunostaining confirms the previously obtained TEER results about the compromised barrier function of endothelial monolayers where R-Ras and FLNa interaction is disrupted. These cells exhibited increased permeability as indicated by the inversely proportionate TEER values (Figure 2.6).

2.3.2 Loss of the R-Ras binding site at FLNa repeat 3 promotes vascular permeability in endothelial cells under fluid shear stress

It has been shown previously that R-Ras binds to the FLNa repeat 3 (Griffiths et al. 2011). Therefore, lack of FLNa 3 repeat would block R-Ras from binding to FLNa leading to barrier dysfunction and cause increased permeability similar to HDMVECs when R-Ras or FLNa or both R-Ras and FLNa expression was knocked down.

We tested this hypothesis with a FLNa construct that had its repeat 3 deleted (FLNa Δ 3). HDMVECs were transfected by electroporation with p3xFlag FLNa Δ 3 or the control p3xFlag empty vector (EV). FLNa knockdown promoted endothelial permeability ($2086 \pm 125.9 \Omega$) indicating a compromised barrier integrity. Endothelial monolayers where endogenous FLNa was knocked down by means of siRNA and FLNa Δ 3 re-expressed, exhibited a vastly compromised barrier function with increased permeability ($1831 \pm 70.51 \Omega$) as compared to the FLNa knockdown case (Figure 2.7; $p < 0.05$).

Furthermore, we wanted to study the effects of a compromised R-Ras/FLNa complex when HDMVECs were not only subjected to fluid shear stress but also treated with TNF α (50 ng/mL) simultaneously. HDMVECs were transfected with the FLNa Δ 3 construct allowing for the expression of FLNa lacking its repeat 3, the binding site of R-Ras. Endothelial monolayers exhibited increased permeability greater than permeability values received for HDMVECs transfected with EV, or HDMVECs challenged with TNF α (50 ng/mL) under fluid shear stress conditions (Figure 2.7; $p < 0.01$).

Further, we were interested in any possible cytoskeletal reorganizations as a result of the missing interaction between R-Ras and FLNa using FLNa Δ 3. HDMVECs transfected with the

same constructs that were used for the TEER/ECIS assays were immunostained targeting VE-cadherin. Similarly to the previous assay (Figure 2.8), flow-induced shear stress alone did not influence expression of VE-cadherin in control cells with the formation of some minimal stress fibers at the cell periphery (Figure 2.8). As seen in the previous TEER/ECIS assays (FLNa knockdown) HDMVECs with transfection-induced expression of FLNa Δ 3 did not rescue endothelial barrier integrity due to the lack of FLNa repeat 3 and hence, due to the lack of R-Ras/FLNa association. Compatible with the permeability-induced phenotype, endothelial monolayers (FLNa siRNA + FLNa Δ 3) exhibited discontinuous patterns of VE-cadherin with zipper-like structures (Figure 2.8). Thick stress fibers diffusely expressed on the entire cell surface suggesting that endothelial permeability was vastly compromised. Similar patterns for VE-cadherin and the stress fibers were observed for HDMVECs transfected with FLNa Δ 3 and then exposed to TNF α or HDMVECs exposed to TNF α at 50 ng/mL for 15 min simultaneously with exposure to fluid shear stress at 2 dyn/cm². VE-cadherin appeared discontinuous with thick and zipper-like formations typical for loss of barrier integrity. The actin (stained with phalloidin) exhibited thick stress fibers that covered the entire cell surface.

2.3.3 Constitutively active R-Ras rescues endothelial monolayer

R-Ras is a small GTPase acting as a molecular switch through its binding affinity to GDP or GTP. The Matter group has previously reported the significance of the interaction between R-Ras and FLNa in regulating vascular endothelial permeability (Griffiths et al. 2011).

In the current study, we aimed at approximating *in vivo* physiological flow conditions in well-defined *in vitro* assays by exposing endothelial monolayers to fluid shear stress. As has been demonstrated thus far the interaction between R-Ras and FLNa plays a pivotal role in the regulation of endothelial permeability under physiologically relevant fluid shear stress conditions. The question that arises is whether it is the active or inactive state of R-Ras that through the binding to FLNa constitutes this interaction so vitally important for the maintenance of barrier integrity. In order to answer this question we proceeded with two different R-Ras

constructs, a constitutively active R-Ras (CA R-Ras) and a dominant negative R-Ras (DN R-Ras).

Both the CA R-Ras and DN R-Ras have been described previously (Spaargaren et al. 1994, Zhang et al. 1996, Keely et al. 1999). The constitutively active R-Ras remains in its active GTP-bound state and stays continuously active while the dominant negative R-Ras is constantly bound to GDP and remains in an inactive state.

HDMVECs were transfected with R-Ras siRNA causing a reduction of endogenous levels of R-Ras. Re-expression of active or inactive GTP-, or GDP-bound R-Ras respectively was performed by transfecting either construct into HDMVECs. HDMVECs transfected with the CA R-Ras exhibited a remarkable recovery. Indeed, CA R-Ras is capable of rescuing barrier function in endothelial monolayers (Figure 2.9). CA R-Ras transfected HDMVECs exhibited TEER values at similar levels as seen in the control cells transfected with the EV. HDMVECs transfected with DN R-Ras showed an increase in endothelial permeability comparable to HDMVECs treated with the cytokine TNF α for 15 min at a concentration of 50 ng/mL (Figure 2.9).

We sought to confirm changes in barrier integrity by immunostaining (Figure 2.10). HDMVEC monolayers previously transfected with R-Ras siRNA combined with either CA R-Ras or DN R-Ras respectively were stained for VE-cadherin via an anti-VE-cadherin antibody and actin using phalloidin. HDMVECs where CA R-Ras was expressed, exhibited a pattern compatible with a compromised permeability phenotype due to the zipper formation of VE-cadherin (Figure 2.10). Nonetheless, VE-cadherin appeared continuous with minimal disturbances (Figure 2.10). Similarly, actin stress fibers although thicker than in control cells, appeared mostly at the cell periphery. Endothelial monolayers transfected with DN R-Ras showed all signs of a permeability-compromised phenotype. VE-cadherin was clearly discontinuous, and thick stress fibers appeared covering the entire cell surface (Figure 2.10).

These results suggest that it is the GTP-bound active state of R-Ras that plays a prominent role in maintaining barrier integrity. Next, we sought to confirm this via GTPase activation assays. HDMVECs under static conditions and endothelial monolayers exposed to fluid shear stress at 2 dyn/cm² were harvested and subjected to the activity assay (Figure 2.11A). While HDMVECs maintained some levels of GTP-bound R-Ras, endothelial monolayers exposed to fluid shear stress exhibited a marked increase in activity levels of R-Ras.

The same tendency was confirmed by means of TEER/ECIS when comparing HDMVECs under static and flow-induced shear stress conditions (Figure 2.11B). Endothelial monolayers exposed to fluid shear stress exhibited higher TEER values than statically cultured HDMVECs at statistically significant levels ($p < 0.001$). This is in agreement with previously published work showing that flow-induced shear stress causes a transient increase in TEER and therefore a reduction in permeability as TEER and permeability are inversely proportionate (DePaola et al. 2001). This stands to reason considering the hemodynamic forces endothelial cells are exposed to in their native microenvironment *in vivo* and the fact that junction complexes are activated when cells move from a quiescent into an activated state.

2.3.4 Constitutively active R-Ras blocks TNF α -mediated vascular permeability

The comparison between static HDMVECs and cell monolayers exposed to flow-induced shear stress revealed that R-Ras exhibits significantly higher GTP-bound levels when monolayers are exposed to fluid shear stress. Pro-inflammatory cytokines of which TNF α is one of the most prominent, activate endothelial cells under static or fluid shear stress conditions. The effect of TNF α on endothelial barrier integrity under flow-induced shear stress seemed at this point a very intriguing question to ask.

Consequently, we were interested in determining the activity levels of R-Ras in quiescent versus cytokine-activated endothelial cells when monolayers were exposed to fluid shear stress conditions. Flow-induced shear stress induced a dramatic increase of GTP-bound R-Ras compared to HDMVEC monolayers exposed to the same levels of shear stress and challenged

with TNF α (Figure 2.12A). A subsequent densitometric quantification of the R-Ras activation assay revealed a clear discrepancy between quiescent and TNF α activated endothelial monolayers (Figure 2.12B).

Higher GTP-bound R-Ras levels translated into higher TEER values and thus, stronger barrier function (Figure 2.12C). Indeed, when endothelial monolayers were exposed to fluid shear stress at physiologically relevant levels of what is observed in capillary vascular endothelial cells *in vivo*, monolayers that were in a rather quiescent state exhibited much higher TEER values at statistically significant levels when compared to endothelial monolayers exposed simultaneously to fluid shear stress and TNF α . This suggests that not only does R-Ras play a prominent role in stabilizing endothelial barrier function under fluid induced shear stress conditions but it is its active GTP-bound state that acts protectively and maintains barrier function and integrity. The real-time TEER values acquired by means of ECIS were highly supportive of this observation.

We further explored the role of active GTP-bound or inactive GDP-bound R-Ras in cell populations where endogenous R-Ras was knocked down by siRNA. In addition we challenged endothelial cells with TNF α and subjected them to fluid shear stress. HDMVECs, where endogenous R-Ras levels were reduced by R-Ras siRNA transfection, showed a recovery in their barrier function when CA R-Ras was expressed compared to controls (R-Ras siRNA + EV). In fact, their TEER is slightly higher than the respective baseline control values (Figure 2.13). These very promising results indicated to us that indeed, CA R-Ras was capable of rescuing TNF α challenged endothelial cells even without the presence of endogenous R-Ras. Expression of DN R-Ras was not able to rescue endothelial barrier function and stayed at comparable levels with HDMVECs exposed to TNF α (Figure 2.13).

Confocal imaging confirmed the findings that were observed by TEER/ECIS. HDMVEC monolayers were transfected with R-Ras siRNA and either CA R-Ras or DN R-Ras. VE-cadherin patterns were compatible with control cells. The staining appeared continuous with

a slight zipper-like structure (Figure 2.14). Stress fiber formation after fluid shear stress exposure was observed at slightly higher levels than in control cells. Conversely, DN R-Ras transfected endothelial cells exhibited discontinuous VE-cadherin patterns and prominent formation of thick actin stress fibers diffused across the entire cell surface (Figure 2.14).

2.3.5 Constitutively active R-Ras exerts its barrier-protective properties only in the presence of FLNa repeat 3

HDMVECs were transfected with constitutively active R-Ras (CA R-Ras) and dominant negative R-Ras (DN R-Ras). CA R-Ras expressed in TNF α -treated endothelial cells restored their vascular barrier function. FLNaRP3 that was re-expressed in endothelial cells treated with TNF α failed to restore barrier integrity despite the presence of endogenous FLNa. This may indicate that the presence of FLNa repeat 3 alone (FLNaRP3) binds up endogenous R-Ras in an inhibitory manner preventing the complex formed between R-Ras and FLNa to perform its protective role in the maintenance of endothelial barrier integrity (Figure 2.15).

2.3.6 R-Ras mutations lead to a phenotype associated with the RASopathy spectrum of vascular malfunctions and malignancies

The role of R-Ras mutations associated with disease is attributed to a constitutively active GTP-bound state. Aberrant R-Ras function has been demonstrated to cause disturbances in signal transduction via the RAF/MEK/ERK signaling cascade and the PI3K/AKT pathway (Flex et al. 2014). We prepared two previously characterized R-Ras mutants, the R-Ras G39Dup and R-Ras V55M and investigated their effect on endothelial barrier integrity. In all cases endogenous levels of R-Ras and FLNa were intact and HDMVECs were transfected with the R-Ras mutants. Subsequently, 48 h later endothelial monolayers were exposed to fluid shear stress with real-time TEER/ECIS data acquisition. HDMVECs transfected with the mutant R-Ras constructs, G39Dup and V55M respectively, showed significantly lower values for TEER compared to the control cells ($p < 0.0001$) although they maintained some level of barrier integrity as permeability was markedly less than cells treated with TNF α (Figure 2.16).

Since mutants induce their deleterious effects through maintaining GTPases in a constitutively active state, we compared the TEER values of the mutants in endothelial cells transfected with the constitutively active R-Ras (CA R-Ras). HDMVECs transfected with CA R-Ras manifested TEER values at similar levels to control cells (transfected with the EV) and remained at statistically higher levels than the R-Ras mutants. This suggests that although mutant R-Ras implicated in a variety of RASopathies cannot be maintained in an active state at all times, it may remain primarily active.

Confocal imaging of HDMVECs monolayers of cells previously transfected with the R-Ras mutants and subsequently exposed to fluid shear stress manifested signs of a permeability phenotype (Figure 2.17). VE-cadherin was discontinuous in both cases and exhibited the zipper-like formation around the cell periphery. Similarly, actin stress fiber appeared thick and presented themselves across the entire cell surface.

2.3.7 The pharmacological Src inhibitor PP2 blocks vascular permeability

The pharmacological Src inhibitor PP2 was used to block TNF α -mediated endothelial permeability. HDMVECs transfected with CA R-Ras and treated for 1 h with PP2 at 1 μ M not only maintained baseline barrier function but exhibited TEER values higher than control cells despite the fact that the monolayers was challenged with TNF α (Figure 2.18). Hence, CA R-Ras, as shown here in previous assays, acts protectively in favor of barrier function but when combined with the Src inhibitor that prevents VE-cadherin phosphorylation especially under fluid shear stress then this combination seems to have an additive effect on the stabilization of endothelial barrier function. Endothelial cells transfected with DN R-Ras (and treated with PP2) exhibited a barrier dysregulation at slightly higher levels than control cells that were not treated with PP2 but were exposed to TNF α at the same concentration (50 ng/mL) (Figure 2.18). This indicated that activity of R-Ras is a key determinant of endothelial barrier maintenance. Loss of R-Ras function promotes endothelial permeability most likely by increased Src activity that has been previously reported to phosphorylate VE-cadherin, a prominent member of endothelial adherens junctions with a crucial role in the regulation of paracellular permeability.

HDMVECs transfected with the mutant FLNa Δ 3, treated with PP2 for 1 h at 1 μ M and challenged with TNF α for 15 min while under flow-induced shear stress, showed a markedly increase in permeability significantly higher than control cells transfected with EV or cells transfected with only the mutant FLNa Δ 3 (Figure 2.19). Conversely, HDMVECs transfected with FLNaRP3 and then treated with PP2 appeared to maintain a stable barrier function contrary to the mutant FLNa Δ 3 that did not (Figure 2.20).

2.3.8 FLNaRP3 blocks barrier function recovery

Adherent to previous findings by the Matter group that R-Ras binds to FLNa repeat 3 we wanted to elaborate further on this and prepared a FLNa construct comprised by only repeat 3 (FLNaRP3). FLNaRP3, the binding site between FLNa and R-Ras induced similar anomalies as were observed in endothelial cells with FLNa siRNA knockdowns shown previously under static conditions or in the current study under physiologically relevant flow-induced shear stress levels. Conversely, since R-Ras interacts with FLNa via its repeat 3 (deletion of repeat 3 compromises barrier integrity), would re-expression of FLNaRP3 maintain barrier integrity? In order to examine this question, a mutant FLNa was developed that expressed solely FLNa repeat 3 (FLNaRP3). HDMVECs were transfected with the control (EV), FLNaRP3 and both FLNaRP3 and FLNa siRNA simultaneously. When endogenous FLNa was knocked down by siRNA, expression of FLNaRP3 did not rescue endothelial permeability with TEER at similar levels compared to endothelial cells transfected with FLNaRP3 and subsequently exposed to TNF α or HDMVECs treated with TNF α alone (Figure 2.21).

Immunostaining of endothelial monolayers after exposure to fluid induced shear stress confirmed the observations acquired through our TEER/ECIS assays. HDMVECs with endogenous levels of FLNa reduced via FLNa siRNA and expression of FLNaRP3 exhibited clear signs of the leaky endothelial phenotype. VE-cadherin staining appeared with discontinuities and exhibited zipper-like structures with thick stress fibers diffusely distributed along the endothelial cell surface (Figure 2.22). Considering that VE-cadherin is expressed at sites of adherens junction complexes and that it is one of the primary regulators of paracellular

permeability in endothelial cells, the phenotype of a compromised VE-cadherin expression pattern confirms the trend that had been previously observed in the TEER/ECIS assays (Figure 2.21). These results suggest that FLNaRP3 does not rescue endothelial barrier function. On the contrary, expression of FLNaRP3 in HDMVECs induces permeability. This could be due to the fact that the cytoskeletal FLNa interacts with more than 80 reported proteins and that loss of endogenous levels of FLNa compromise signaling cascades involving other permeability-related factors (Nakamura et al. 2011). Furthermore, FLNaRP3 was abundantly expressed and, therefore, had to bind up endogenous R-Ras. Binding of R-Ras to FLNaRP3 alone does not transduce any intracellular signaling further downstream since these binding events happen in close proximity to the plasma membrane where the small GTPase R-Ras is located after activation. FLNaRP3 does not contain its actin binding domain (ABD) and, therefore, is incapable of providing any mechanical stabilization to the cellular framework further contributing to a compromised endothelial barrier function.

2.4 Discussion

We showed that TNF α -mediated endothelial dysfunction accompanied by increased permeability could be inhibited by constitutively active R-Ras. Intriguingly, even in the case where microvascular endothelial cells are subjected to TNF α treatment under fluid induced shear stress conditions, constitutively active R-Ras is capable of rescuing barrier integrity within a few minutes from the onset of fluid shear stress. Independently of the GTP-, or GDP-bound R-Ras, the presence of intact FLNa including its repeat 3 (the binding site of R-Ras) is crucial for the formation of the R-Ras/FLNa complex. Only then, active GTP-bound R-Ras can exert its protective mechanism on endothelial barrier integrity.

The underlying molecular mechanisms remain still elusive. It has been shown previously that loss of the interaction between the R-Ras and FLNa leads to VE-cadherin phosphorylation, a prominent constituent protein of adherens junctions (Griffiths et al. 2011). VE-cadherin phosphorylation by Src may trigger internalization of VE-cadherin in a manner similar to VEGF-mediated internalization of VE-cadherin (Wallez et al. 2008). Perhaps active GTP-bound R-Ras pulls FLNa in close proximity to the plasma membrane. Considering that FLNa repeat 3 lies closely to the actin-binding domain of FLNa, R-Ras could potentially cause cytoskeletal rearrangements across the plasma membrane favoring the maintenance of barrier integrity. By pulling FLNa toward the membrane, R-Ras indirectly causes F-actin to translocate closer to the membrane compensating for internalized VE-cadherin.

Furthermore, it has been shown that R-Ras inhibits the internalization of VEGFR-2 in cultured endothelial cells allowing for the VEGFR-2 signaling cascade to proceed in a VEGF-dependent manner. Constitutively active R-Ras causes a decrease in VEGFR-2 tyrosine phosphorylation triggered by the binding of its ligand, whereas dominant negative R-Ras results in increased VEGFR-2 tyrosine phosphorylation upon binding of the receptor ligand (Sawada et al. 2015). The major VEGFR-2 tyrosine phosphorylation residues that trigger endothelial cells to respond to VEGF stimulation are Y951 (kinases insert domain), Y1054 and Y1059 (kinase

domain), Y1175 and Y1214 (C-terminal tail of receptor) (Takahashi et al. 2001, Matsumoto et al. 2005, Holmes et al. 2007).

Hughes et al. described a mechanosensory complex comprised of PECAM-1 (a known Src activator), VE-cadherin and VEGFR-2 (an activator of PI3K) (Hughes et al. 1998). Under fluid shear stress, the PECAM-1/VE-cadherin/VEGFR-2/PI3K complex could get activated allowing for Src to phosphorylate VE-cadherin, an observation previously confirmed for human coronary artery endothelial cells (Griffiths et al. 2011). It has also been demonstrated that PI3K is an effector that R-Ras shares with other members of the Ras family suggesting that PI3K interacts with R-Ras during the PECAM-1/VE-cadherin/VEGFR-2/PI3K signaling cascade.

Here we show that the complex formed between R-Ras and FLNa is essential for the maintenance of endothelial barrier integrity under fluid shear stress conditions. HDMVECs with knocked down R-Ras, FLNa or the combination of R-Ras and FLNa exhibited a barrier dysregulation with increased endothelial permeability at comparable levels with activated TNF α -treated endothelial cells.

In particular, constitutively active R-Ras is capable not only to maintain endothelial barrier integrity but in an intriguing way to rescue barrier function of TNF α -treated endothelial cells. Dominant negative R-Ras promoted vascular permeability in the presence and absence of TNF α in endothelial monolayers subjected to fluid shear stress.

In order for constitutively active R-Ras to exert its positive function on barrier integrity, it is necessary for the FLNa repeat 3 to be present. In the case of the FLNa construct missing its repeat 3, we demonstrated that constitutively active R-Ras fails to bind to FLNa and thereby lacks the ability to block vascular permeability.

Moreover, fluid shear stress results in the activation of R-Ras. Normal HDMVECs subjected to fluid shear stress at physiologically relevant levels exhibited increased activity of R-Ras compared to quiescent HDMVECs under static cell culture conditions. Similarly, when

TNF α -treated endothelial monolayers were subjected to fluid shear stress, it caused a significant reduction of R-Ras activity levels suggesting that R-Ras and TNF α act upon overlapping signaling pathways.

Our work indicates that R-Ras and active R-Ras, in particular, have the potential to offer new insights into the regulation of vascular permeability. TNF α -mediated vascular dysfunction plays an adverse role in the pathogenesis of sepsis and the onset of inflammation with very limited success in understanding the underlying molecular processes. Our work attempts to contribute to a better understanding of the R-Ras and FLNa regulation of vascular permeability under physiologically relevant fluid shear stress conditions.

2.5 Figures

This page has been left blank intentionally.

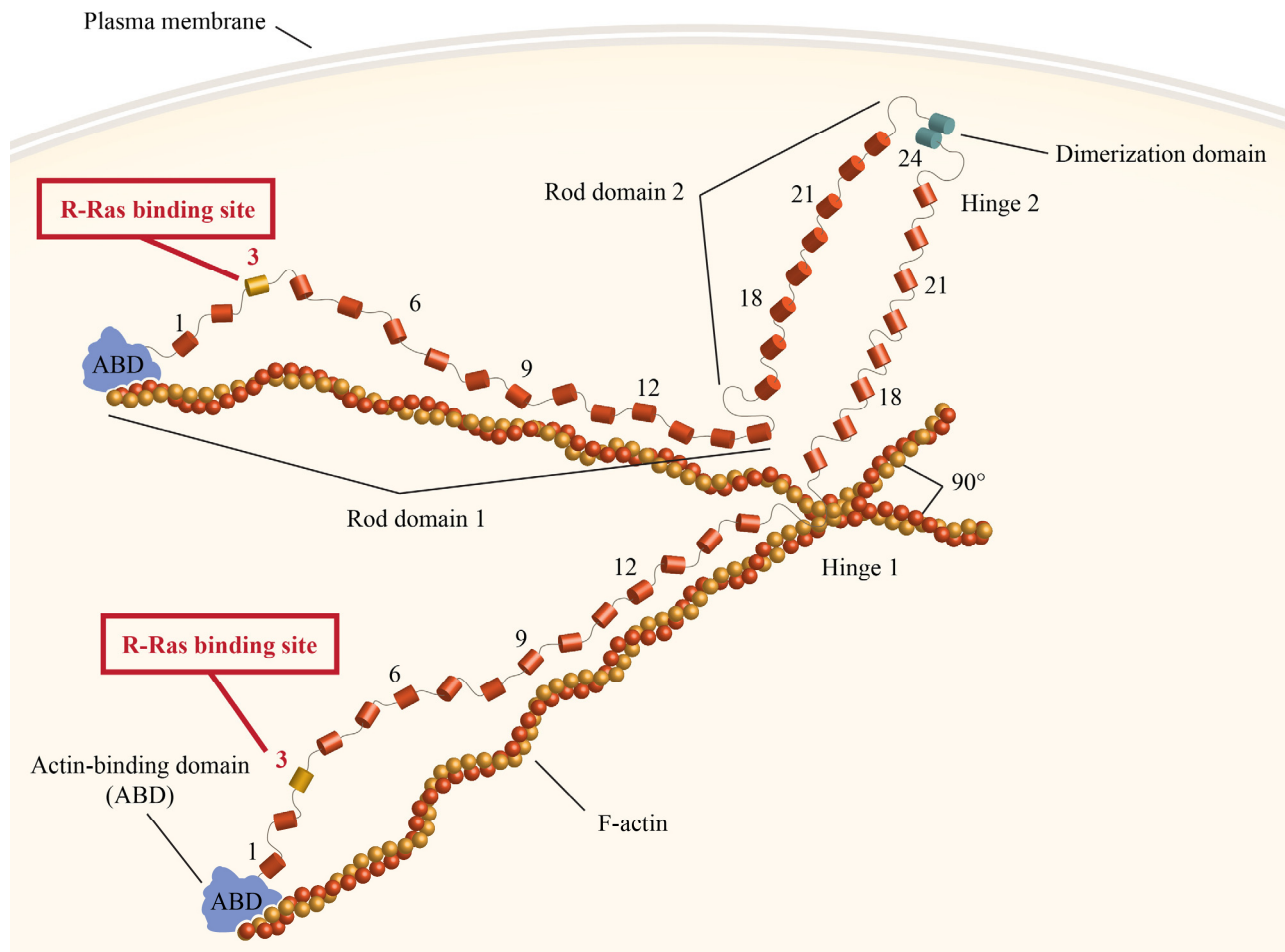


Figure 2.1

R-Ras associates with FLN1 at repeat 3

R-Ras associates directly with the cytoskeletal protein FLN1 at its repeat 3 (Gawecka et al. 2010). Loss of this interaction has been implicated in barrier dysfunction and increased

endothelial permeability (Griffiths et al. 2011). The FLNa polypeptide chain has a molecular mass of 280 kDa. It consists of an amino-terminal actin-binding domain (ABD) followed by a rod-like domain of 24 immunoglobulin repeats. The actin-binding domain and FLNa repeats 1-15 are designated 'rod domain 1', whereas FLNa repeats 16-23 are designated 'rod domain 2'. FLNa rod domain 2 does not interact with actin filaments and contains the binding sites for the majority of the FLNa interacting protein partners. There are two hinge regions between FLNa repeat 15 and 16 and between FLNa repeat 23 and 24. The dimeric structure of FLNa rearranges actin filaments in orthogonal structures.

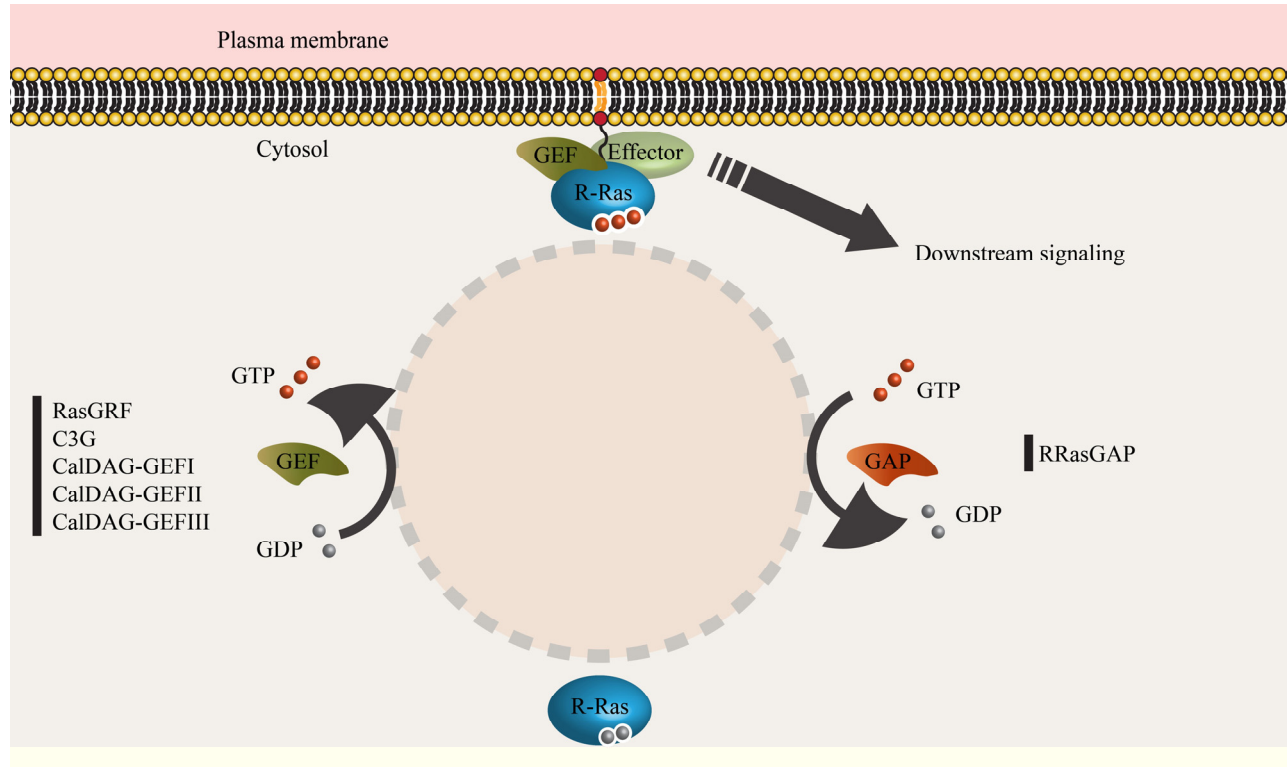
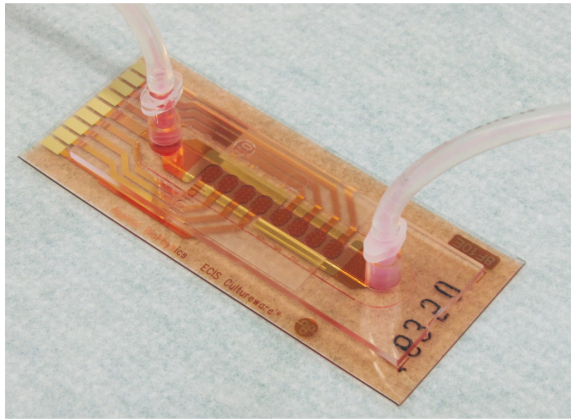


Figure 2.2

R-Ras is a small GTPase cycling between GTP and GDP

The small GTPase R-Ras is activated by exchange of GDP for GTP stimulated by guanine exchange factors (GEFs; green) and inactivated by exchanging GTP for GDP via hydrolysis stimulated by GTPases activating proteins (GAPs; red). R-Ras is regulated by specific GEFs and GAPs. The GEFs that have been implicated to associate with R-Ras are RasGRF, C3G, CalDAG-GEFI, CalDAG-GEFII and CalDAG-GEFIII. RRasGAP is the only GAP that has been linked to R-Ras thus far (Yamashita et al. 2000, Takaya et al. 2007).

A**B****Figure 2.3****ECIS and Ibidi flow chamber slides**

(A) ECIS gold-film flow chamber slide. The flow channel has a height of 0.4 mm and a length of 25 mm. The array connectors in the front of the slide are attached to the ECIS instrument. The slide is equipped with eight small electrodes along the axial length of the flow channel. Each electrode acquires real-time electrical resistivity, impedance and capacitance. Tubing going in and out of the chamber reservoirs are connected to a peristaltic pump and allow for the cell culture medium to circulate continuously for the duration of the flow assays. **(B)** The Ibidi flow chamber slide consists of six independent channels. The height of each channel comprises 0.4 mm. Tubing connected to the slide runs through a peristaltic pump propelling the cell culture medium through the flow channels and thereby subjecting endothelial monolayers to fluid shear stress.

A



B

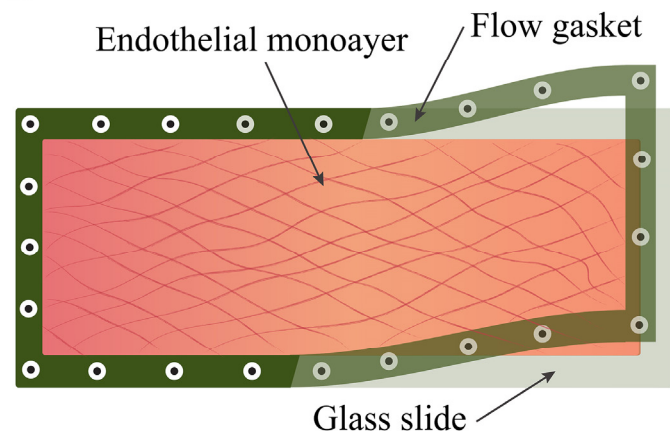


Figure 2.4

Ibidi flow chamber slide

(A) Endothelial cells are seeded onto fibronectin-coated glass slides. The silicon gasket (green) is placed between the glass slide with the endothelial monolayer and a vacuum lid. The vacuum lid is equipped with four inlets. Two of them serve as the flow inlet and outlet respectively, and the remaining two are connected to a vacuum source allowing for the setup to remain in place during fluid shear stress assays. **(B)** A schematic representation of the setup as described previously. The glass slide accommodates the endothelial monolayers, and the gasket is placed on top of the glass slides allowing for the vacuum lid to be mounted to the setup.

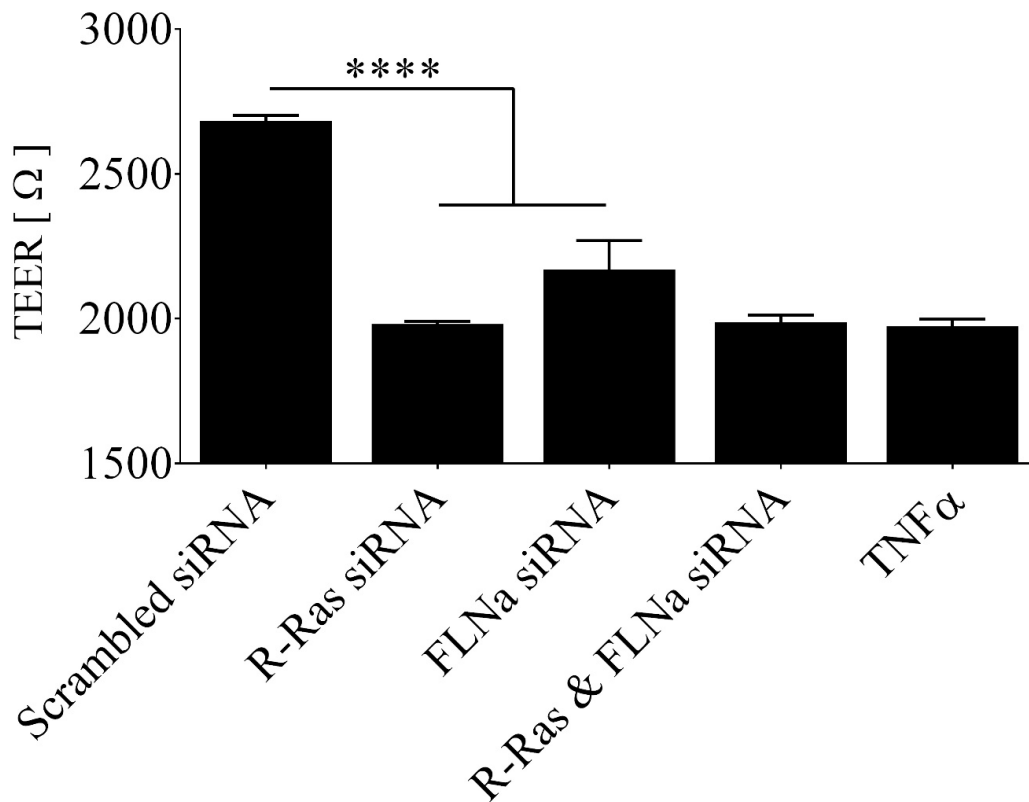


Figure 2.5

Loss of R-Ras and FLNa protein expression promotes vascular permeability under fluid shear stress conditions

The small GTPase R-Ras is expressed at various degrees across the vascular endothelium (Komatsu et al. 2005). Endogenous R-Ras and FLNa associate in arterial and microvascular endothelial cells forming a complex that protects vascular permeability (Griffiths et al. 2011). HDMVECs were transfected with R-Ras or FLNa siRNA individually or with R-Ras and FLNa

siRNAs combined. Transendothelial electrical resistance (TEER; measured in Ohms at a frequency of 4 kHz) of HDMVECs with scrambled siRNA or siRNA(s) directed against R-Ras, FLNa or R-Ras/FLNa or treated with the pro-inflammatory cytokine TNF α . Loss of R-Ras or FLNa or R-Ras/FLNa promotes vascular permeability under fluid shear stress conditions. Endothelial monolayers were subjected to fluid shear stress at 2 dyn/cm² for 15 min. HDMVECs with R-Ras or FLNa knockdowns exhibited increased permeability as indicated by the decreased TEER values (**** p < 0.0001). TNF α -mediated vascular permeability on HDMVECs was also assessed (**** p < 0.0001; relative to scrambled siRNA). Note that vascular permeability and TEER are inversely proportional. Real-time measurements of electrical resistance were conducted at a frequency of 4,000 Hz. The respective data points of electrical resistance at 15 min are depicted.

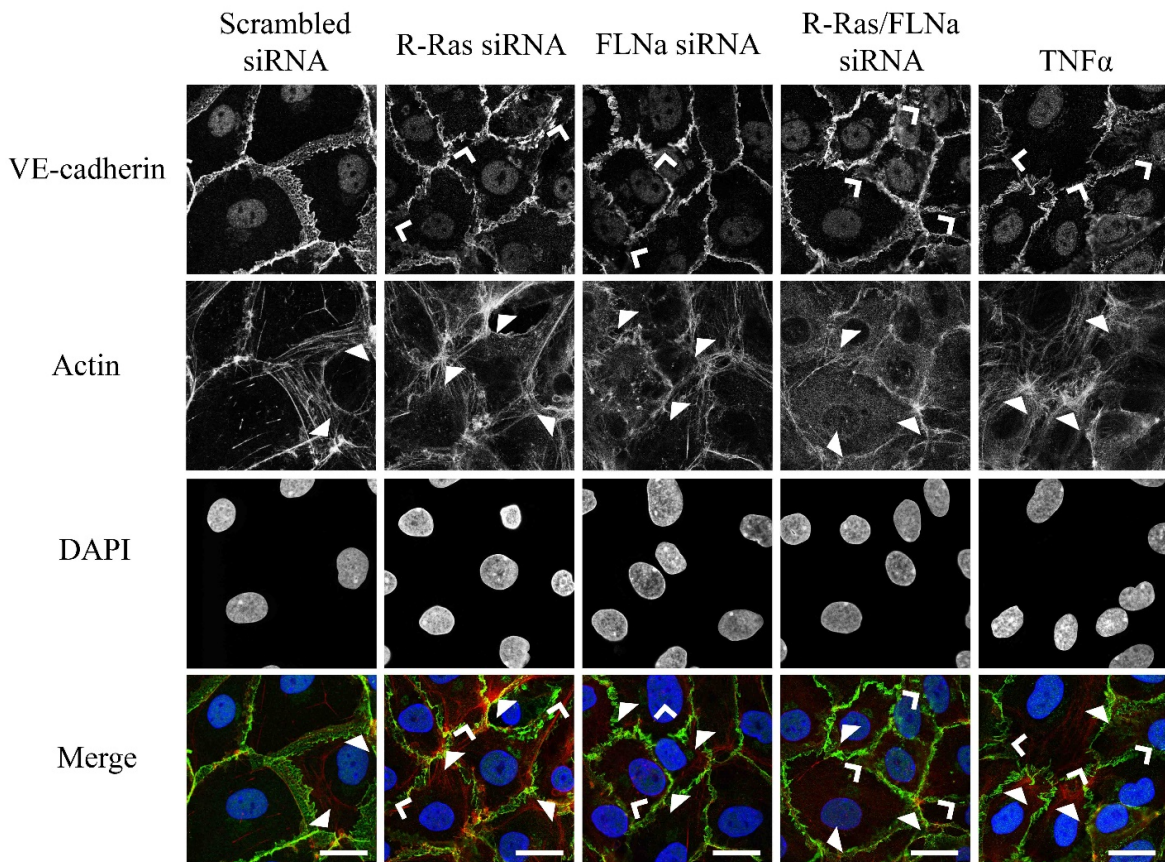


Figure 2.6

Loss of the R-Ras and FLNa complex alter cytoskeletal rearrangements in HDMVECs subjected to fluid shear stress

HDMVECs with knocked down R-Ras, FLNa or R-Ras/FLNa or treated with the pro-inflammatory cytokine TNF α were allowed to grow into monolayers on fibronectin-coated Ibidi flow chamber slides and subjected to fluid shear stress at 2 dyn/cm² for 15 min. Subsequently cells were fixated and immunostained with Alexa 594-phalloidin (red), anti-VE-cadherin antibody (green) and counterstained with DAPI (blue). Open arrowheads point

to VE-cadherin gaps formed in monolayers with knocked down R-Ras, FLNa or R-Ras/FLNa or treated with TNF α . Scale bars correspond to 20 μ m. Results are representative of at least three independent experiments. The confocal images were acquired at a magnification of 200 \times .

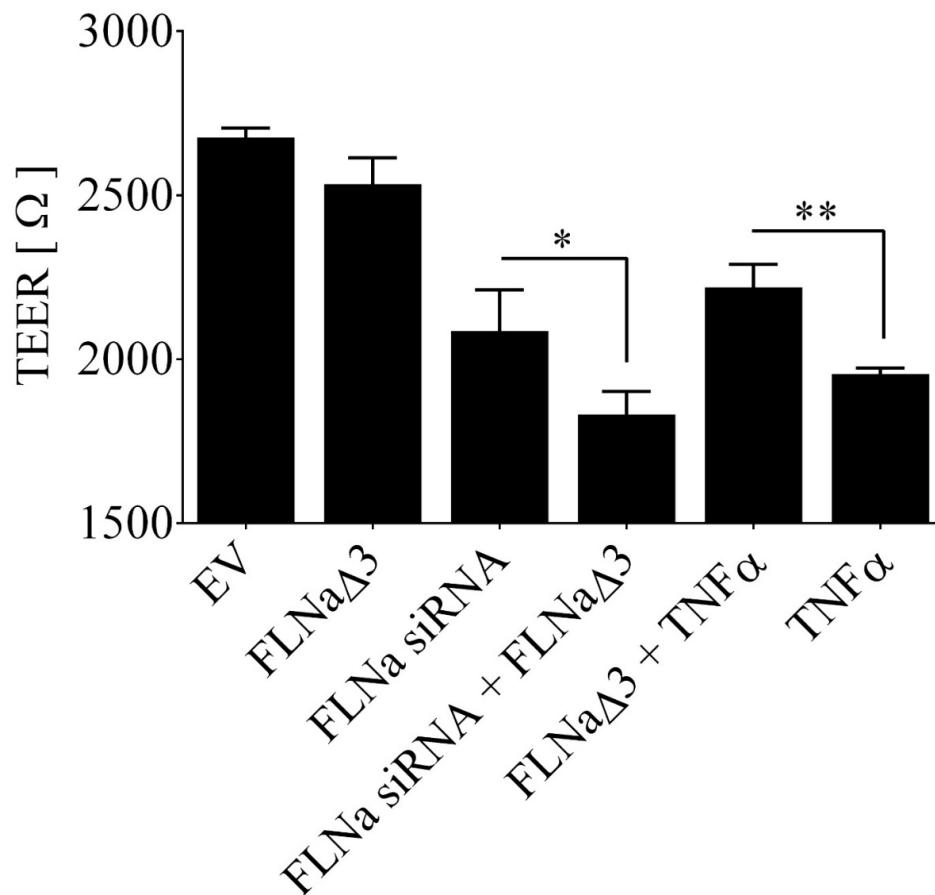


Figure 2.7

R-Ras interacts with FLNa via direct binding to its repeat 3

R-Ras forms a complex with FLNa by directly associating with FLNa repeat 3 (Griffiths et al. 2011). Transendothelial resistance (TEER) values for HDMVECs with endogenous FLNa and re-expressed FLNa lacking repeat 3 (FLNaΔ3), knocked down FLNa (FLNa siRNA), knocked down FLNa with re-expressed FLNaΔ3 (FLNa siRNA + FLNaΔ3), endogenous FLNa with

re-expressed FLNa Δ 3 and treated with TNF α (FLNa Δ 3 + TNF α) or HDMVECs treated with TNF α only. TEER values are compared to quiescent endothelial cells expressing scrambled siRNA. Cell monolayers were exposed to flow-induced shear stress and the respective TEER values acquired. In the case of the mutant FLNa Δ 3, R-Ras was incapable of binding to FLNa and hence, TEER values appeared decreased. In the case of HDMVECs with knocked down FLNa, re-expression of FLNa Δ 3 does not rescue vascular permeability (* $p < 0.05$). TNF α -treated endothelial cells with endogenous FLNa protein expression and re-expression of FLNa Δ 3 exhibit higher TEER than HDMVECs treated with TNF α alone (** $p < 0.01$). Real-time measurements of electrical resistance were conducted at a frequency of 4,000 Hz. The respective data points of electrical resistance at 15 min are depicted.

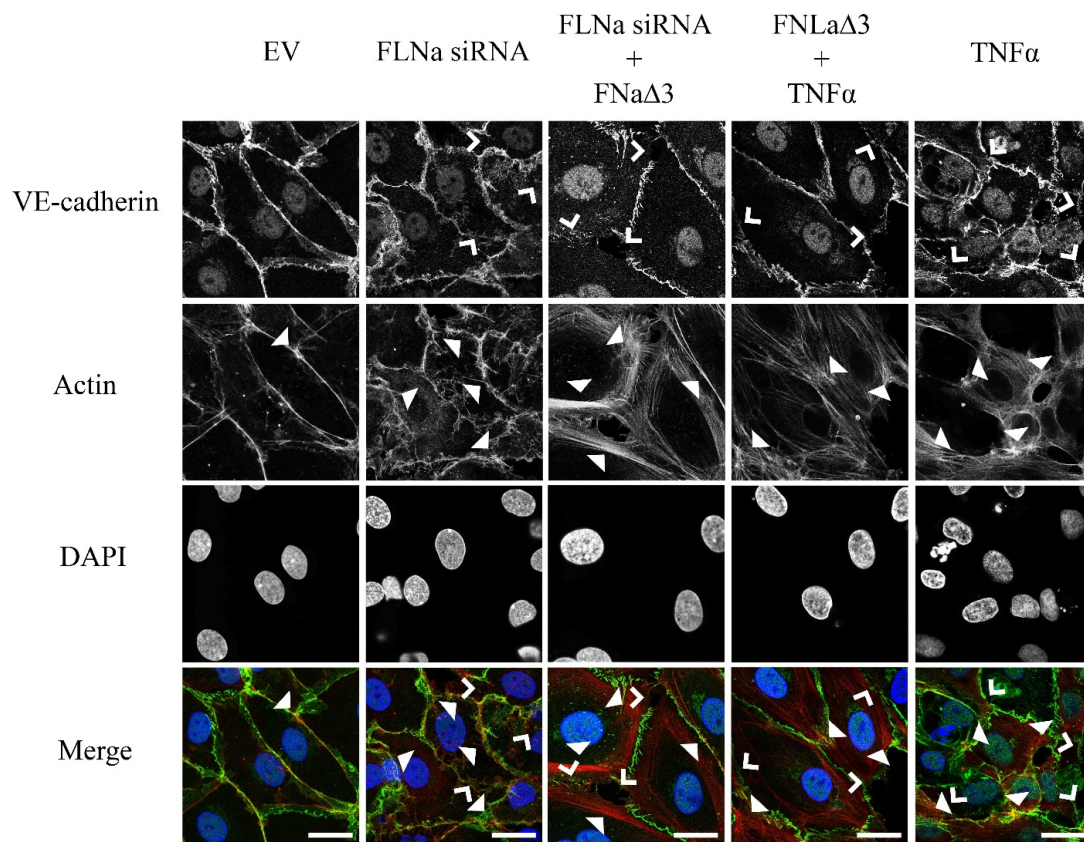


Figure 2.8

The association of R-Ras with FLNa maintains endothelial barrier integrity in HDMVECs under fluid shear stress

Confocal imaging of HDMVEC monolayers with knocked down FLNa, knocked down FLNa and re-expressed FLNaΔ3 (FLNa siRNA + FLNaΔ3), endogenous FLNa and re-expressed FLNaΔ3 treated with TNFα (FLNaΔ3 + TNFα) or HDMVECs treated with TNFα only. Cells were grown on fibronectin-coated Ibidi flow chamber slides and subjected to fluid shear stress at

2 dyn/cm² for 15 min prior to fixation. HDMVECs were immunostained with Alexa 594-phalloidin (red), anti-VE-cadherin antibody (green) and counterstained with DAPI (blue). Open arrowheads point to VE-cadherin gaps due to lack of association of R-Ras to FLNa. Closed arrowheads indicate the formation of stress fibers. The scale bars correspond to 20 μm. Results are representative of at least three independent experiments. Confocal micrographs were acquired at a magnification of 200×

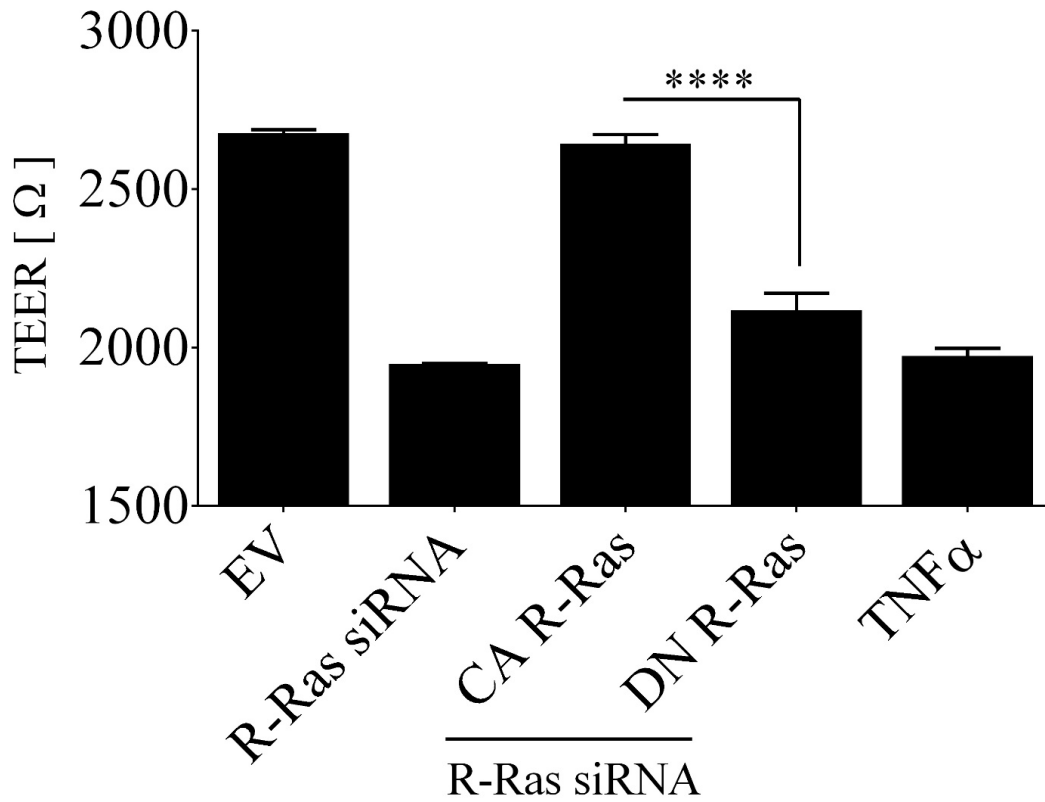


Figure 2.9

Constitutively active R-Ras restores endothelial barrier function under fluid shear stress

Transendothelial electrical resistance (TEER) of HDMVECs with knocked down R-Ras (R-Ras siRNA), knocked down R-Ras and re-expressed constitutively active R-Ras (CA R-Ras + R-Ras siRNA), knocked down R-Ras and re-expressed dominant negative R-Ras (DN R-Ras + R-Ras siRNA), and HDMVECs treated with TNF α alone (TNF α). Endothelial monolayers were grown

to confluency on fibronectin coated ECIS flow chamber slides and subjected to fluid shear stress at 2 dyn/cm² for 15 min. Control cells were transfected with the empty vector (EV) or were challenged with TNF α at 50 ng/mL. Barrier integrity in HDMVECs with knocked down R-Ras is lost in the case where DN R-Ras is re-expressed but restored when CA R-Ras is re-expressed (**** p < 0.0001). Real-time measurements of electrical resistance were conducted at a frequency of 4,000 Hz. The respective data points of electrical resistance at 15 min are depicted.

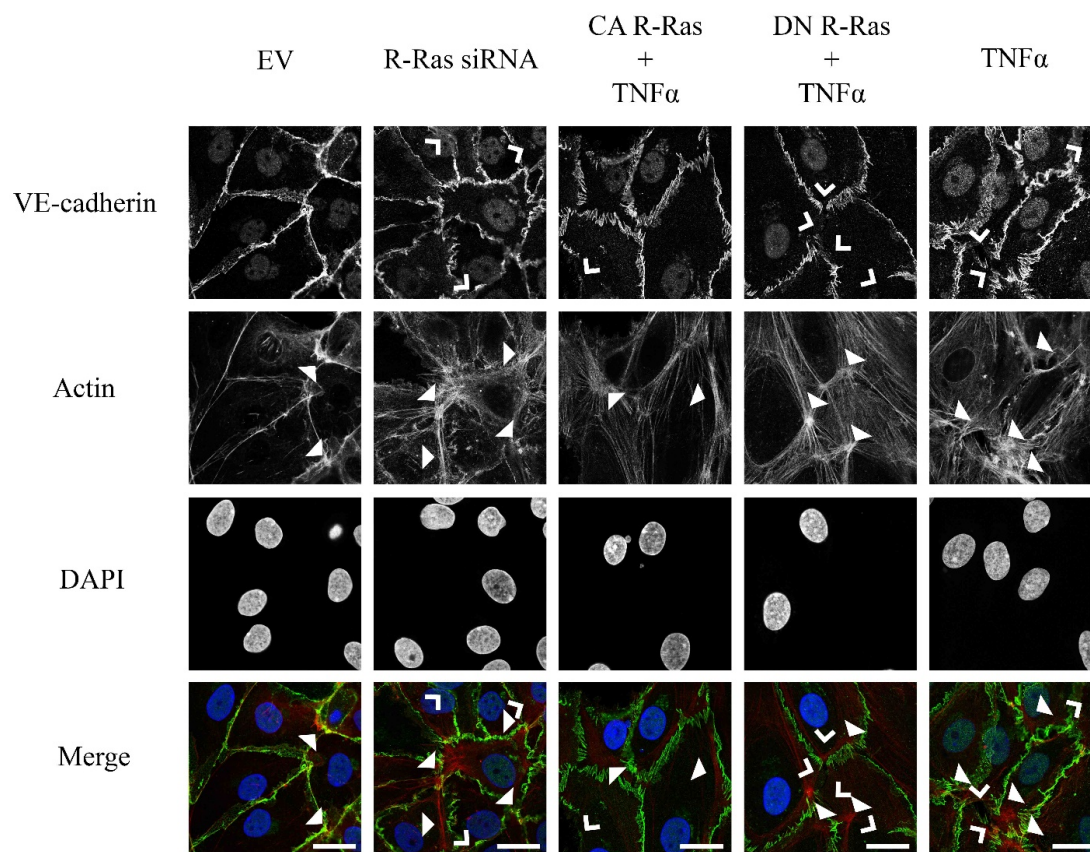


Figure 2.10

Constitutively active R-Ras restores endothelial barrier integrity under fluid shear stress conditions

Confocal imaging of HDMVEC monolayers after a 15 min exposure to fluid shear stress at 2 dyn/cm². Cells were grown on Ibidi flow chamber slides, exposed to flow-induced shear stress and subsequently fixated and stained with Alexa 594-phalloidin (red), anti-VE-cadherin antibody (green) and counterstained with DAPI (blue). HDMVECs transfected with constitutively active R-Ras (CA R-Ras) were able to restore permeability back to baseline values despite reduced endogenous R-Ras protein levels. VE-cadherin in these cells appears continuous with some

minimal formation of stress fibers. Open arrowheads point to VE-cadherin gaps, and closed arrowheads indicate stress fiber formation. The scale bars correspond to 20 μm . Results are representative of at least three independent experiments. Confocal micrographs were acquired at a magnification of 200 \times .

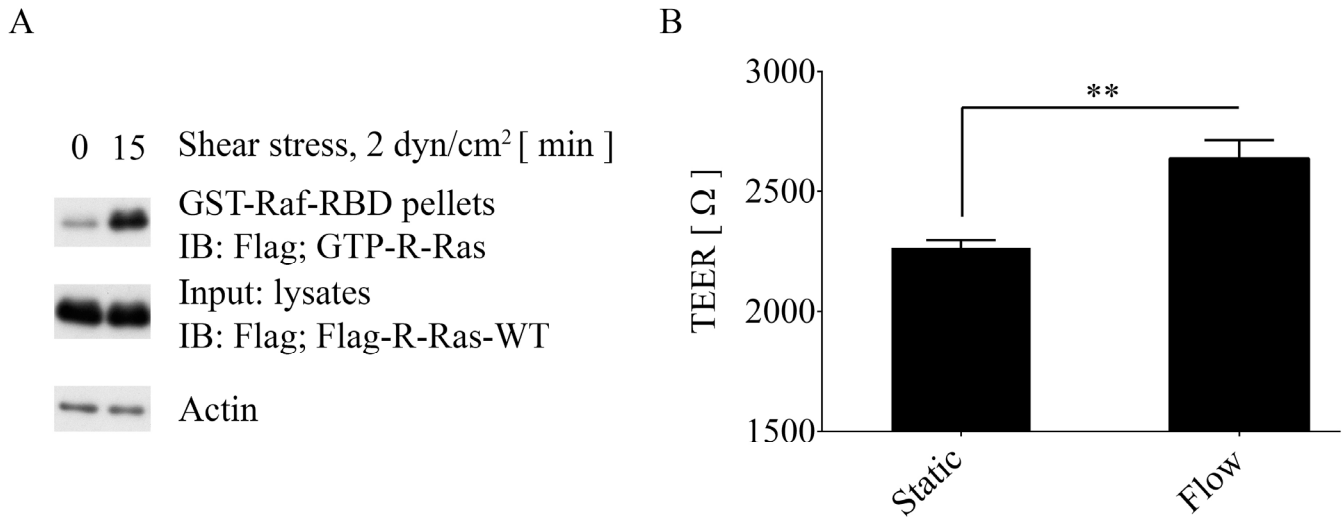


Figure 2.11

Fluid shear stress activates the small GTPase R-Ras

(A) R-Ras activation assay comparing activity levels of the small GTPase R-Ras under static cell culture and fluid shear stress conditions. When HDMVECs are subjected to fluid shear stress, R-Ras activity is significantly augmented. (B) Transendothelial electrical resistance (TEER) assays for HDMVECs under static culture conditions compared to endothelial monolayers subjected to flow-induced shear stress at 2 dyn/cm² for 15 min. Fluid shear stress results in increased TEER values indicating that shear stress blocks vascular permeability. Note that TEER and vascular permeability are inversely proportional. Real-time measurements of electrical resistance were conducted at a frequency of 4,000 Hz. The respective data points of electrical resistance at 15 min are depicted.

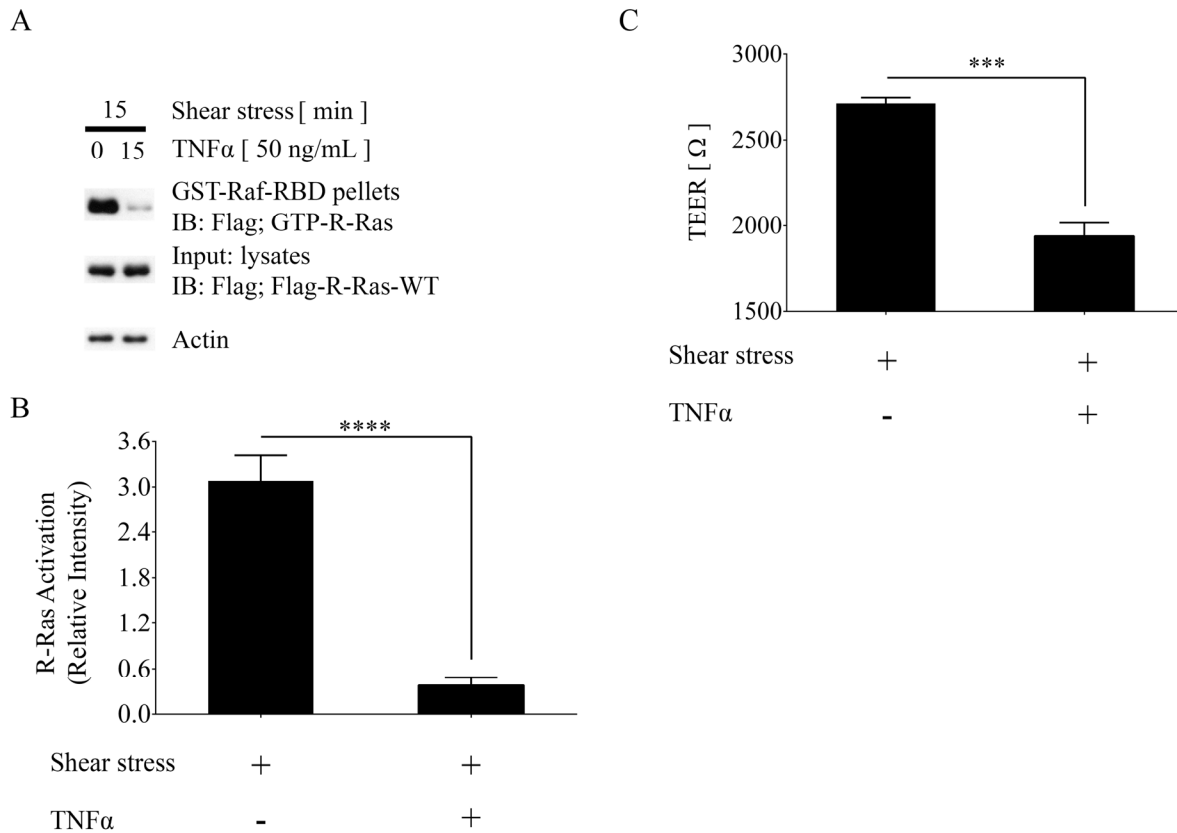


Figure 2.12

TNF α results in decreased R-Ras activity under fluid shear stress conditions

(A) R-Ras activity assay revealing that when endothelial monolayers are exposed to fluid shear stress, activity levels of R-Ras are increased in the absence of the pro-inflammatory cytokine TNF α . HDMVECs subjected to fluid shear stress in the presence of TNF α exhibit decreased R-Ras activity. (B) Densitometric analysis of R-Ras activity assay. (C) Transendothelial electrical resistance (TEER) assays for HDMVECs exposed to flow-induced shear stress. Quiescent endothelial cells (non-activated) are compared to TNF α -treated (activated) HDMVECs. TNF α leads to barrier dysfunction indicated by increased vascular permeability (low TEER values). Note that vascular permeability and TEER are inversely

proportionate. Real-time measurements of electrical resistance were conducted at a frequency of 4,000 Hz. The respective data points of electrical resistance at 15 min are depicted.

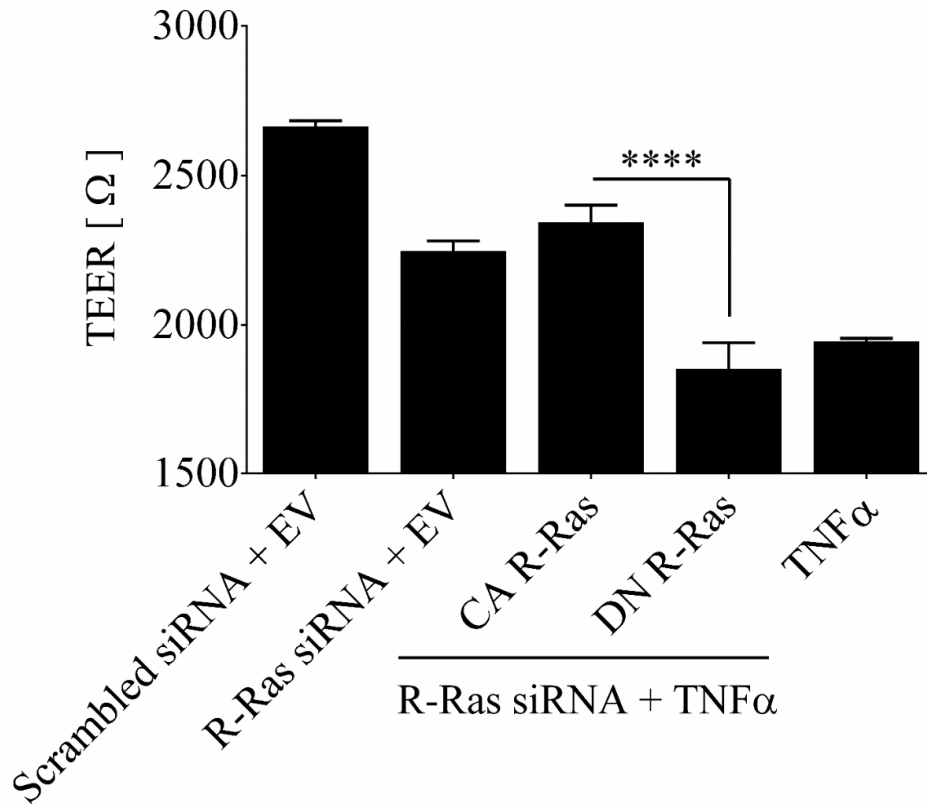


Figure 2.13

Constitutively active R-Ras restores TNF α -mediated endothelial dysfunction under fluid shear stress conditions

HDMVECs were transfected with constitutively active R-Ras (CA R-Ras) and dominant negative R-Ras (DN R-Ras). Subsequently endogenous R-Ras expression levels were reduced by means of siRNA. CA R-Ras restores barrier integrity when R-Ras expression levels are reduced by siRNA and endothelial cells are challenged with TNF α . HDMVEC monolayers were exposed

to fluid shear stress at 2 dyn/cm². Control cells were transfected with the empty vector (EV) or were treated with TNF α at 50 ng/mL. Real-time measurements of electrical resistance were conducted at a frequency of 4,000 Hz. The respective data points of electrical resistance at 15 min are depicted.

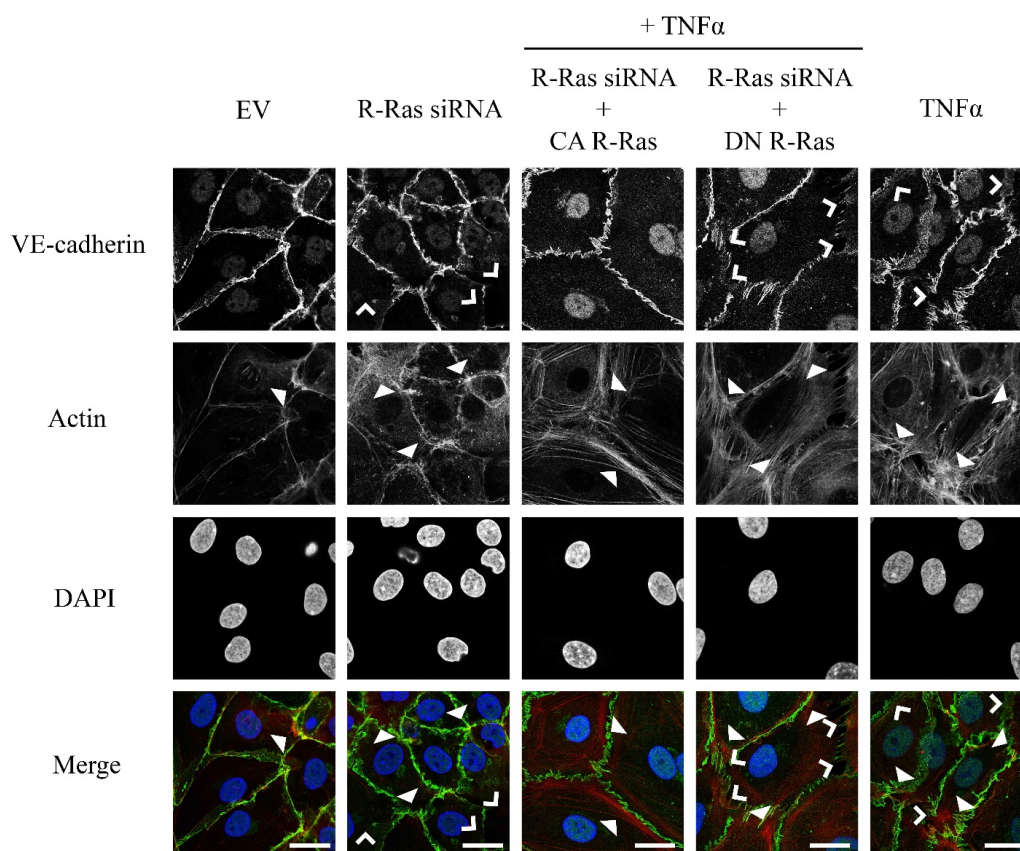


Figure 2.14

Active R-Ras rescues endothelial barrier integrity under fluid shear stress conditions

Confocal imaging of HDMVEC monolayers. Cells were grown on fibronectin-coated Ibidi flow chamber slides, exposed to flow-induced shear stress at 2 dyn/cm² and subsequently fixated and immunostained with Alexa 594-phalloidin (red), anti-VE-cadherin antibody (green) and counterstained with DAPI (blue). HDMVECs transfected with constitutively active R-Ras (CA R-Ras) and reduced levels of endogenous R-Ras were able to restore permeability back to baseline values even when cells were stimulated with TNF α . VE-cadherin in these cells appears

continuous with some minimal formation of stress fibers. Open arrowheads point to VE-cadherin gaps, and closed arrowheads indicate stress fiber formation. The scale bars correspond to 20 μm . Results are representative of at least three independent experiments. Confocal micrographs were acquired at a magnification of 200 \times .

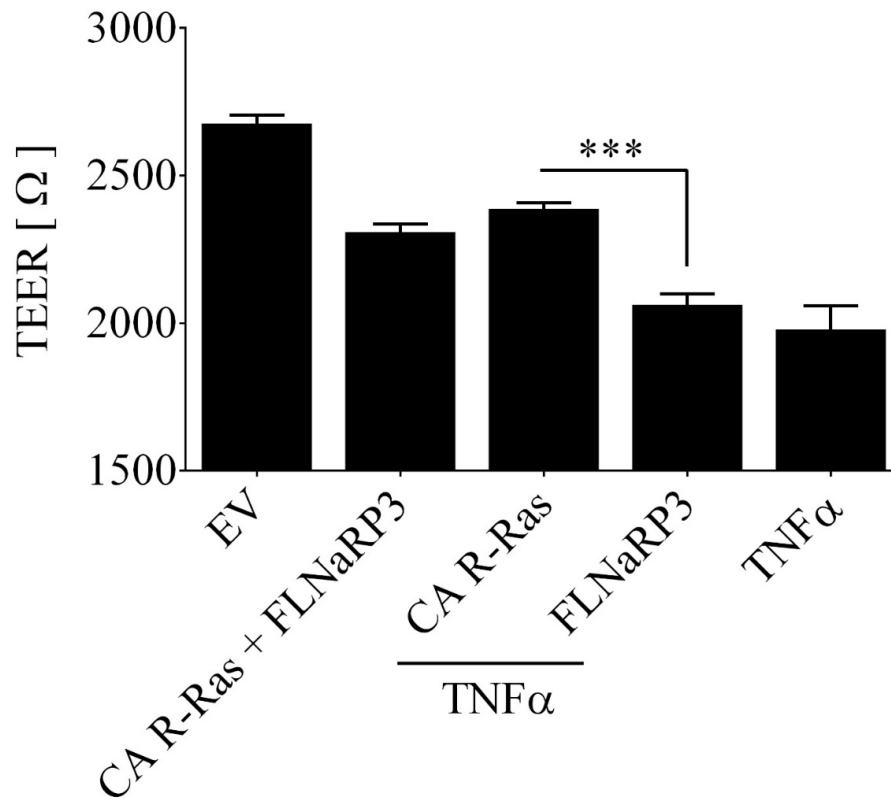


Figure 2.15

Constitutively active R-Ras depends on the presence of FLNa repeat 3 under fluid shear stress conditions

HDMVECs transfected with constitutively active R-Ras (CA R-Ras) and dominant negative R-Ras (DN R-Ras) in the presence of reduced R-Ras by siRNA. CA R-Ras rescues HDMVECs despite reduced endogenous R-Ras protein expression levels and re-expressed FLNa with repeat 3 only (FLNaRP3). CA R-Ras expressed in TNF α -treated endothelial cells restores their vascular

permeability. FLNaRP3 re-expressed in endothelial cells treated with TNF α fails to maintain barrier integrity. Monolayers were exposed to fluid shear stress at 2 dyn/cm² for 15 min. Control cells were transfected with the empty vector (EV) or treated with TNF α at 50 ng/mL. Real-time measurements of electrical resistance were conducted at a frequency of 4,000 Hz. The respective data points of electrical resistance at 15 min are depicted.

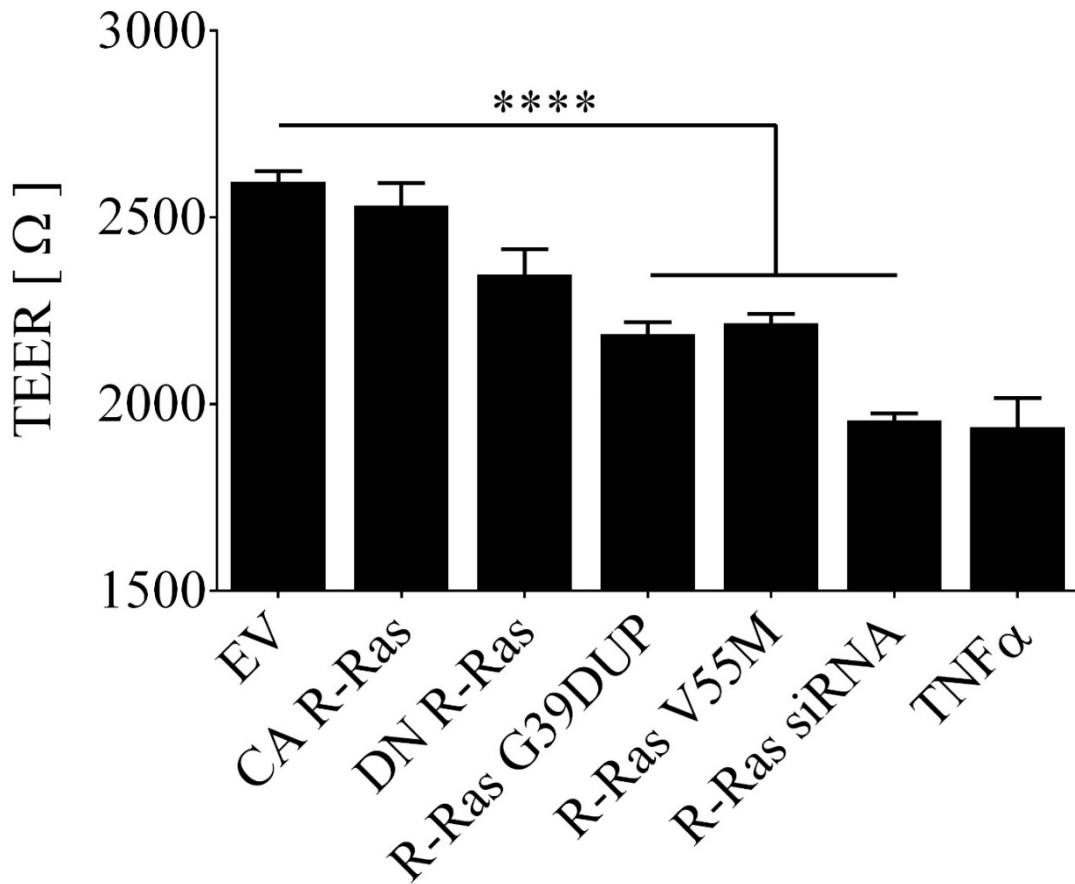


Figure 2.16

R-Ras with patient mutations fails to maintain vascular permeability under fluid shear stress conditions

HDMVECs transfected with R-Ras constructs with patient mutations in the presence of reduced R-Ras are compared with regard to vascular permeability. Constitutively active R-Ras rescues inflamed (activated) endothelial monolayers in cells with knocked down endogenous R-Ras.

Monolayers were exposed to fluid shear stress at 2 dyn/cm². Control cells were transfected with the empty vector (EV) or were stimulated with TNF α at 50 ng/mL. Real-time measurements of electrical resistance were conducted at a frequency of 4,000 Hz. The respective data points of electrical resistance at 15 min are depicted.

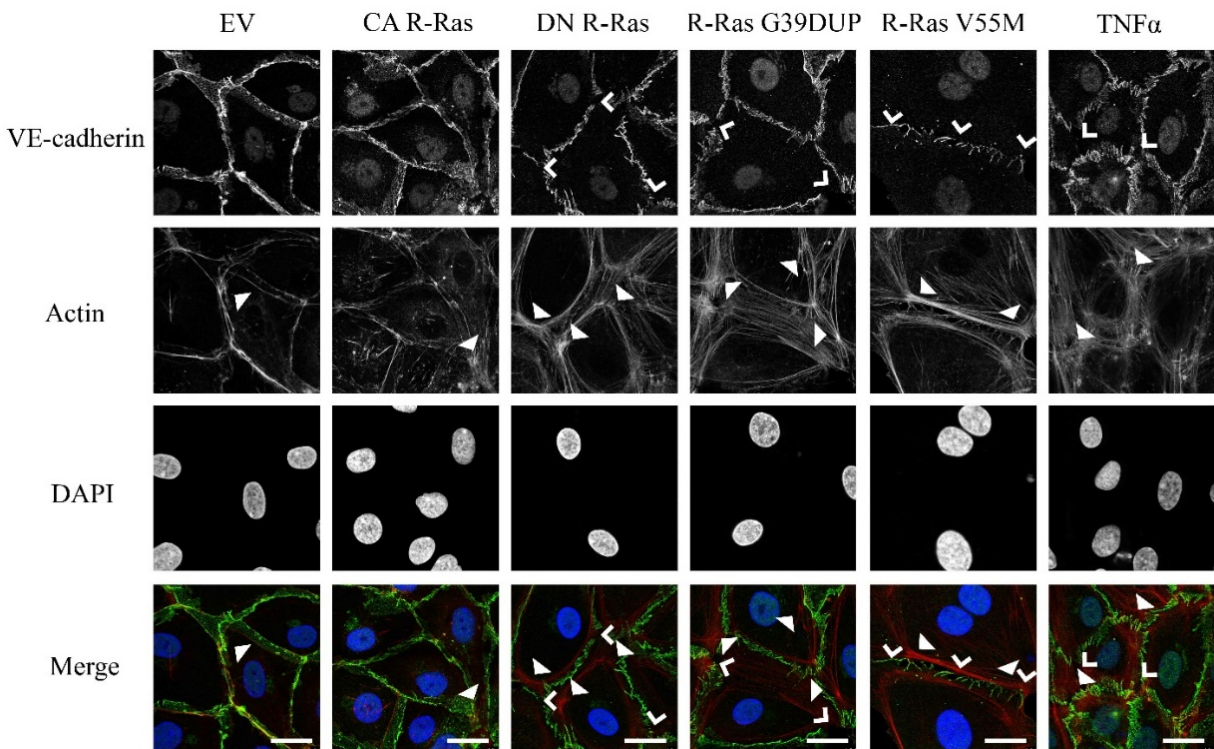


Figure 2.17

R-Ras with patient mutations leads to endothelial dysfunction under fluid shear stress

Confocal imaging of HDMVEC monolayers after a 15 min exposure to fluid shear stress at 2 dyn/cm². Cells were grown on Ibidi flow chamber slides, exposed to flow-induced shear stress and subsequently fixated and stained with Alexa 594-phalloidin (red) and anti-VE-cadherin antibody (green). Endothelial cell monolayers were counterstained with DAPI (blue).

HDMVECs were transfected with R-Ras (patient mutations) constructs G39DUP and V55M. VE-cadherin in these cells appears continuous with some minimal formation of stress fibers.

Open arrowheads point to VE-cadherin gaps, whereas closed arrowheads indicate stress fibers. The scale bars correspond to 20 μm . Results are representative of at least three independent experiments. Confocal micrographs were acquired at a magnification of 200 \times .

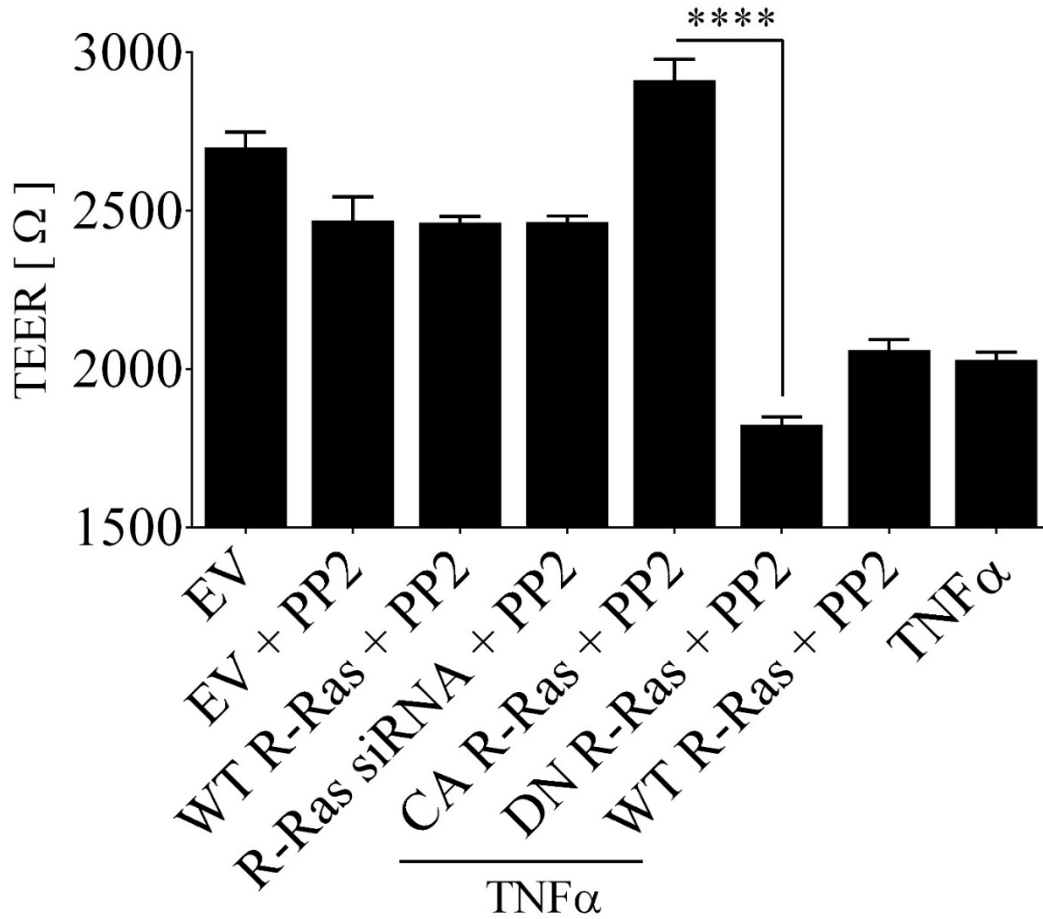


Figure 2.18

The pharmacological Src inhibitor PP2 blocks vascular permeability under fluid shear stress conditions

Src was blocked by its pharmacological inhibitor PP2 in confluent HDMVEC monolayers. Endothelial cells transfected with the empty vector (EV) and treated with PP2 (EV + PP2), with re-expressed wild type R-Ras (WT R-Ras) and treated with PP2 (WT R-Ras + PP2) and with R-Ras knockdown (R-Ras siRNA) and treated with PP2 (R-Ras siRNA + PP2) were able to

maintain vascular permeability at similar levels with no significant difference to the control HDMVECs transfected with the EV alone. Cells with re-expressed constitutively active R-Ras (CA R-Ras) treated with PP2 and subjected to TNF α (CA R-Ras + PP2 + TNF α) under fluid shear stress at 2 dyn/cm² for 15 min blocked vascular permeability. HDMVECs with re-expressed dominant negative R-Ras (DN R-Ras) treated with PP2 and TNF α (DN R-Ras + PP2 + TNF α) exhibited increased permeability when compared with the TNF α control (TNF α) and significantly higher when compared to CA R-Ras (**** p < 0.0001). Endothelial cells with re-expressed WT R-Ras treated with PP2 and TNF α (WT R-Ras + PP2 + TNF α) showed elevated vascular permeability at similar levels with the TNF α control (TNF α). Real-time measurements of electrical resistance were conducted at a frequency of 4,000 Hz. The respective data points of electrical resistance at 15 min are depicted.

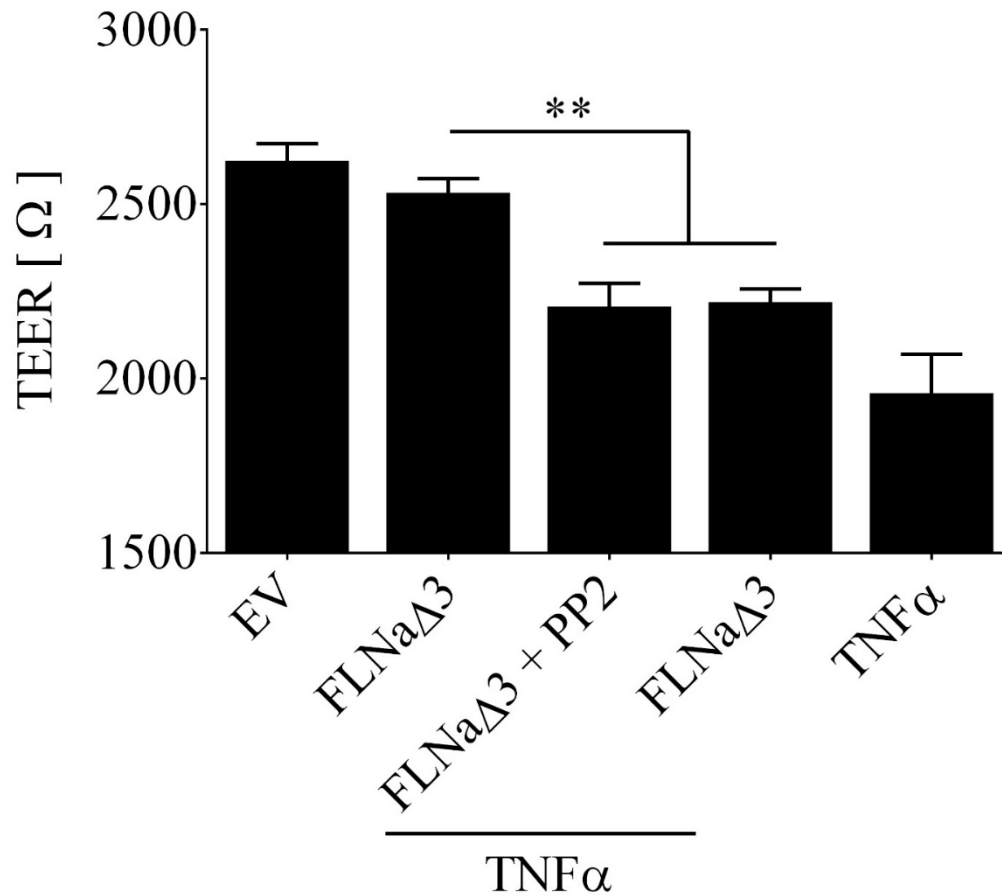


Figure 2.19

The pharmacological inhibitor PP2 is not sufficient to rescue TNF α -treated HDMVECs under fluid shear stress

HDMVECs with re-expressed FLNa with repeat 3 lacking (FLNa Δ 3), with re-expressed FLNa Δ 3 treated with PP2 and the pro-inflammatory cytokine TNF α (FLNa Δ 3 + PP2 + TNF α) and with re-expressed FLNa Δ 3 and treated with TNF α (FLNa Δ 3 + TNF α) were subjected to fluid shear stress at 2 dyn/cm² for 15 min. Endothelial cells with re-expressed FLNa Δ 3 maintained their barrier integrity due to the presence of endogenous FLNa. Note that endogenous FLNa protein

expression was unaltered. HDMVECs with re-expressed FLNa Δ 3 challenged with TNF α at 50 ng/mL under fluid shear stress exhibited increased permeability independently of the pharmacological Src inhibitor PP2. Endothelial cells with re-expressed empty vector (EV) were used as a control. All experiments were performed at a minimum of three experiments. Real-time measurements of electrical resistance were conducted at a frequency of 4,000 Hz. The respective data points of electrical resistance at 15 min are depicted.

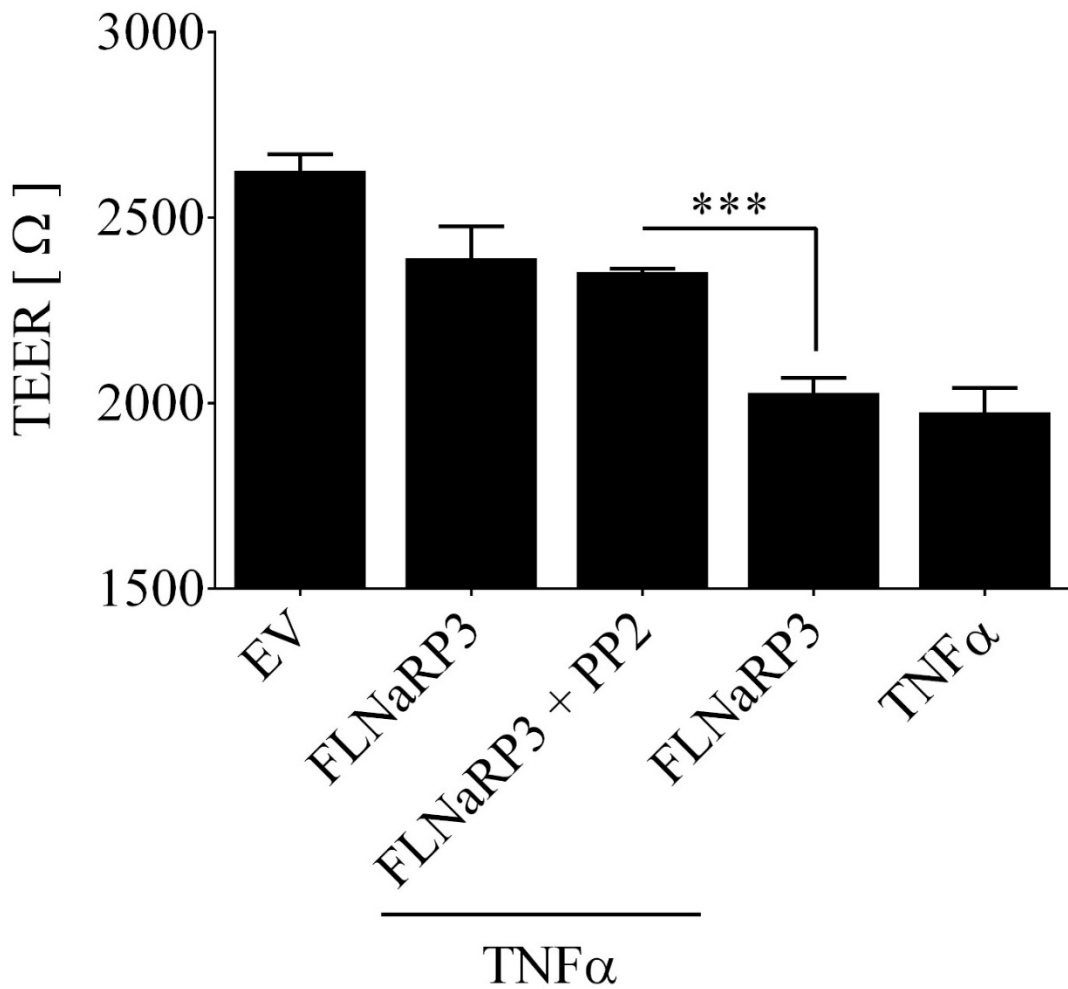


Figure 2.20

The pharmacological Src inhibitor PP2 is not sufficient to rescue endothelial barrier function under fluid shear stress

HDMVECs with re-expressed FLNa repeat 3 alone (FLNaRP3), with re-expressed FLNaRP3 treated with PP2 and the pro-inflammatory cytokine TNFα (FLNaRP3 + PP2 + TNFα) and with

re-expressed FLNaRP3 and treated with TNF α (FLNaRP3 + TNF α) were subjected to fluid shear stress at 2 dyn/cm² for 15 min. The pharmacological Src inhibitor (FLNaRP3 + PP2 + TNF α) protects barrier integrity compared to the control case in the absence of PP2 (FLNaRP3 + TNF α) at statistically significant levels (***) p < 0.001). Endothelial cells with re-expressed empty vector (EV) were used as a control. All experiments were performed at a minimum of three experiments. Real-time measurements of electrical resistance were conducted at a frequency of 4,000 Hz. The respective data points of electrical resistance at 15 min are depicted.

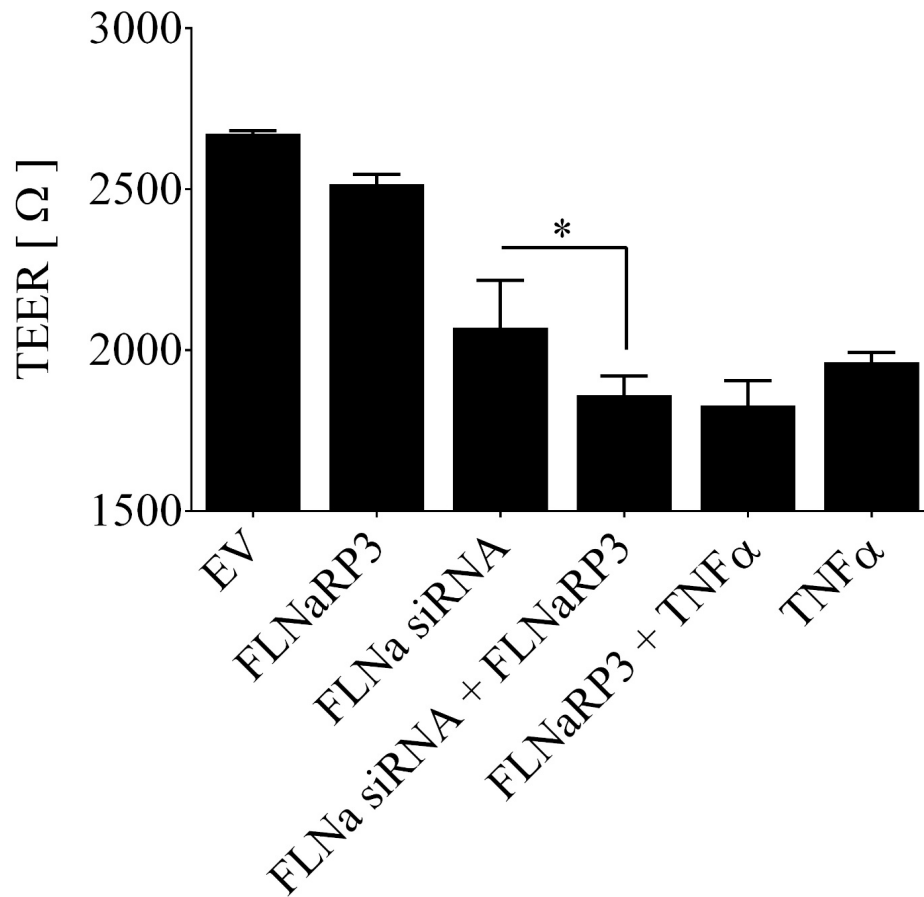


Figure 2.21

FLNaRP3 does not rescue HDMVEC barrier function under fluid shear stress

HDMVECs with re-expressed FLNa repeat 3 alone (FLNaRP3), with knocked down FLNa by siRNA (FLNa siRNA), with reduced endogenous FLNa protein expression by siRNA and with re-expressed FLNaRP3 (FLNa siRNA + FLNaRP3) and with re-expressed FLNaRP3 and treated with the pro-inflammatory cytokine TNF α (FLNaRP3 + TNF α) were subjected to fluid shear stress at 2 dyn/cm² for 15 min. HDMVECs with knocked down FLNa and re-expressed

FLNaRP3 exhibit increased vascular permeability. Note that TEER and vascular permeability are inversely proportional. Endothelial cells with re-expressed empty vector (EV) were used as control. All experiments were performed at a minimum of three experiments. Real-time measurements of electrical resistance were conducted at a frequency of 4,000 Hz. The respective data points of electrical resistance at 15 min are depicted.

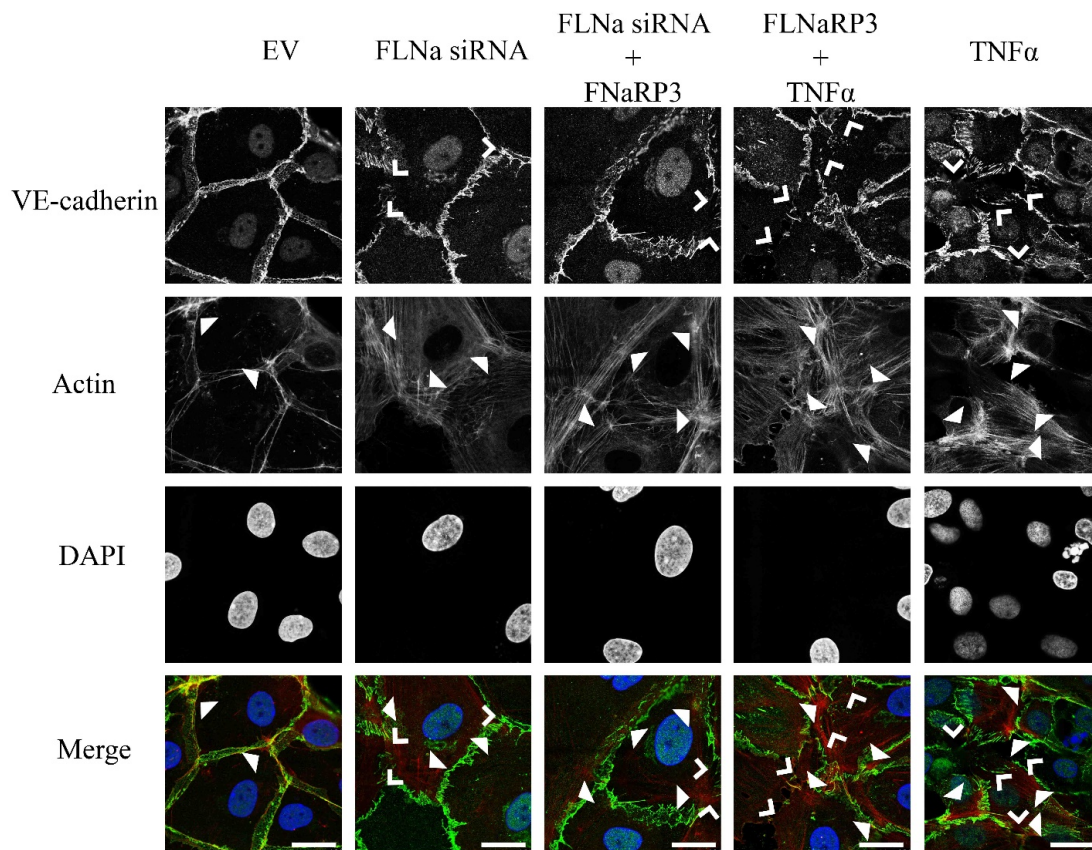


Figure 2.22

FLNaRP3 does not prevent cytoskeletal rearrangements in HDMVECs under fluid shear stress

HDMVECs with knocked down FLNa by siRNA (FLNa siRNA), with knocked down FLNa by siRNA (FLNa siRNA) and re-expressed FLNa repeat 3 alone (FLNa siRNA + FLNaRP3) and with re-expressed FLNaRP3 and treated with the pro-inflammatory cytokine TNF α (FLNaRP3 + TNF α) were subjected to fluid shear stress at 2 dyn/cm² for 15 min. HDMVECs with knocked down FLNa and re-expressed FLNaRP3 exhibit increased vascular permeability. Cells were

grown on Ibidi flow chamber slides, exposed to flow-induced shear stress and subsequently fixated and stained with Alexa 594-phalloidin (red) and anti-VE-cadherin antibody (green). Endothelial cell monolayers were counterstained with DAPI (blue). HDMVECs with re-expressed empty vector (EV) were used as a control. All experiments were performed at a minimum of three experiments. VE-cadherin in these cells appears continuous with some minimal formation of stress fibers. Open arrowheads point to VE-cadherin gaps, whereas closed arrowheads indicate stress fibers. The scale bars correspond to 20 μm . Results are representative of at least three independent experiments. Confocal micrographs were acquired at a magnification of 200 \times .

CHAPTER 3

A real-time TEER-based screening assay under flow-induced shear stress for identifying drug-specific inhibition of cytokine-mediated vascular permeability

3.1 Abstract

Vascular leakiness is a hallmark of inflammation, cancer, diabetes, and sepsis. It is also a key complication of cytokine and monoclonal antibody therapies. Increased vascular leak promotes fluid accumulation in tissues, causes an enhanced inflammatory response and induces fibrosis. Over time, this may lead to multiple organ failure and death. No therapies are available for blocking vascular leak in sepsis or other diseases. Currently, there are few methods to assess the vascular permeability effects of known drugs and novel therapeutic leads in a physiologically relevant yet rapid and low-cost manner. We report here a real-time transendothelial electrical (TEER)-based screening assay under flow-induced shear stress to identify drug-induced inhibition of cytokine-mediated vascular leak. Primary human dermal microvascular endothelial cell (HDMVEC) monolayers were subjected to flow-induced shear stress, treated with vascular permeability-inducing agents and assessed for permeability changes using electrical-cell impedance sensing. We report that the vasoactive agent histamine, the cytokine interleukin-1 β and thrombin promote endothelial leakiness in endothelial monolayers exposed to flow-induced shear stress. Selective antagonists, clemastine and methylprednisolone, blocked histamine-, cytokine- or thrombin-mediated endothelial permeability in endothelial monolayers exposed to physiological shear stress. Our findings demonstrate the utility of a physiologically relevant platform that measures rapid changes in endothelial permeability in response to therapeutic leads under flow-induced shear stress in real-time.

3.2 Introduction

The regulation of endothelial cell-cell junctions is crucial in maintaining barrier integrity and loss of these junctions promotes dysregulated permeability, which is a major contributing factor to morbidity and mortality in a number of diseases including sepsis (Blum et al. 1997, Dejana et al. 1999, Bazzoni et al. 2004, Dejana et al. 2009, Zhang et al. 2010). Endothelial tight junctions and adherens junctions are regulators of endothelial barrier function because they modulate paracellular diffusion. Tight junctions are composed of transmembrane proteins including the claudin and junctional adhesion molecule (JAM) family that link the membrane to the cytoskeleton to control endothelial barrier function (Lampugnani 2012). ZO-1 is an adaptor protein that binds components of tight junctions and the actin cytoskeleton (Tornavaca et al. 2015). Vascular endothelial cadherin (VE-cadherin) is a major structural component of adherens junctions that controls endothelial permeability.

Vascular permeability occurs upon loss of endothelial cell adherens junction integrity thereby inducing the formation of small gaps between endothelial cells. Phosphorylation of VE-cadherin at Tyr 685 and Tyr 731 promotes vascular leakiness *in vivo* and *in vitro* (Lampugnani et al. 2007, Dejana et al. 2009, Gavard 2009). A number of signaling pathways induce VE-cadherin phosphorylation including cytokines (Potter et al. 2005) and Src (Daniel et al. 1997, Esser et al. 1998, Wright et al. 2002, Lin et al. 2003). We reported previously that loss of a direct interaction between the cytoskeletal protein filamin A with the small GTPase R-Ras induces VE-cadherin phosphorylation at Tyr 658 promoting vascular permeability of endothelial monolayers under static conditions (Griffiths et al. 2011). Permeability-inducing agents including thrombin and histamine also promote endothelial leakiness by activating signaling pathways that regulate tight junctions, adherens junctions and the cytoskeleton (Aghajanian et al. 2008).

In vivo, the endothelium is continually exposed to blood flow that imparts hemodynamic forces among which the most prominent is fluid-induced shear stress. The endothelium responds to shear stress by converting the effect of shear stress into intracellular signals that regulate

endothelial barrier function and vascular leak (Davies et al. 1984, Levesque et al. 1985, Davies et al. 1993, Davies 1995, Pries et al. 1996, Galbraith et al. 1998, Resnick et al. 2003, Bacabac et al. 2005, Li et al. 2005, McCann et al. 2005, Fry et al. 2012, Conway et al. 2013, Uzarski et al. 2013). Recently it was reported that shear stress-induced activation of Src regulates VE-cadherin phosphorylation *in vivo* (Orsenigo et al. 2012). The effects of shear stress on modulating endothelial permeability are not yet completely understood.

Drug-induced changes in vascular leak are mainly assessed by measuring passive diffusion rates of probes conjugated with fluorochromes such as fluorescein isothiocyanate (FITC) when it moves through an endothelial monolayer or by using an electrical cell-impedance sensing (ECIS) based approach; both of which are performed primarily under static state conditions. We have developed a physiologically relevant *in vitro* TEER-based approach whereby HDMVEC monolayers are subjected to flow-induced shear stress in conjunction with real-time TEER measurements acquired by ECIS. In this manner *in vivo* hemodynamic shear stress that exists within the vasculature are taken into account in measuring drug effects on barrier function and subsequent changes in vascular permeability.

We demonstrate that physiological flow-induced shear stress linked to real-time TEER based analysis provides a rapid assessment of endothelial barrier integrity and subsequent changes in permeability. We assessed changes in endothelial leakiness under flow-induced shear stress in response to the permeability-inducing histamine, IL-1 β and thrombin. We then tested whether specific permeability antagonists (clemastine or methylprednisolone) blocked permeability-inducing agents that mediate endothelial permeability when exposed to shear stress. Our data points to a physiologically relevant platform that rapidly measures endothelial barrier function and changes in endothelial permeability under flow-induced shear stress in real-time.

3.3 Materials and Methods

3.3.1 Cell Culture

Primary HDMVECs (Cell Applications, San Diego, CA) were cultured in MCDB 131 basal medium (Sigma Aldrich, St. Louis, MO) supplemented with 0.5 ng/mL human recombinant vascular endothelial growth factor (hVEGF₁₆₅), 20 ng/mL human recombinant insulin growth factor (hIGF-R³; SAFC, Lenexa, KS), 10 ng/mL human fibroblast growth factor (hFGF; Peptotech, Rocky Hill, NJ), 5 ng/mL human recombinant epithelial growth factor (Peptotech, Rocky Hill, NJ), 1 µg/mL ascorbic acid (Sigma Aldrich, St. Louis, MO), 0.2 µg/mL hydrocortisone (Sigma Aldrich, St. Louis, MO), 0.125 µg/mL amphotericin (Sigma Aldrich, St. Louis, MO), 5 µg/mL gentamicin (Life Technologies, Waltham, MA) and 5% fetal bovine serum (FBS; Life Technologies, Waltham, MA). HDMVEC s were cultivated in tissue culture-treated dishes that were previously coated with 0.25% porcine gelatin (Sigma Aldrich, St. Louis, MO). Cells were kept at 37 °C in a humidified cell incubator atmosphere (5% CO₂, 95% air).

3.3.2 Permeability-inducing and antagonist treatment

Control HDMVECs were treated with the drug carrier DMSO (Sigma-Aldrich, St. Louis, MO), CLE (Santa Cruz Biotechnology, Dallas, TX) or MPS (Santa Cruz Biotechnology, Dallas, TX) alone for 16 h at a final concentration of 5 µM. Following the pretreatment with either DMSO, CLE or MPS, endothelial cells were stimulated with either 5 µM histamine, 20 ng/mL IL-1β or 20 U/mL thrombin for 15 min while exposed to fluidic shear stress at 2 dyn/cm².

3.3.3 Fluid shear stress

Fluid shear stress levels applied to the endothelial cells were controlled using a peristaltic pump (Masterflex, Vernon Hill, IL). The wall shear stress, τ_w (dyn/cm²) exerted onto the endothelial monolayer as a function of the measured volumetric flow rate, Q (mL/min) was calculated by applying Poiseuille's formula (Poiseuille 1830, Orsenigo et al. 2012):

$$\tau_w = \frac{6Q\mu}{ah^2} \quad (3.1)$$

where τ_w is the wall shear stress in dyn/cm², Q , the volumetric flow rate in mL/min, μ , is the dynamic viscosity in Pa·s, α , is the channel width and h , is the channel height.

3.3.4 Electrical Cell Impedance Spectroscopy (ECIS)

Endothelial permeability was determined using the electrical cell-impedance sensing (ECIS; Applied BioPhysics, Troy, NY) methodology as has been described previously (Keese et al. 1990, Giaever et al. 1991, Giaever et al. 1993, Wegener et al. 2000). ECIS flow chamber slides (F8×10E PC; Applied Biophysics, Troy, NY) were pre-coated with a 10 mM L-cysteine solution for 15 min at RT allowing for the gold electrodes to be stabilized. After the cysteine treatment, the ECIS flow chamber slides were washed three times with molecular grade distilled water. Following, the L-cysteine pre-treated gold-electrode slides were coated with a human fibronectin solution at 75 µg/mL concentration (BD Biosciences, San Jose, CA) for 1 h at RT. HDMVECs were seeded onto the slides at a concentration of 1.2×10^6 cells/mL and allowed to grow to confluency for 48 h at 37 °C in a humidified cell incubator atmosphere (5% CO₂, 95% air). ECIS allows for the data acquisition to be conducted in a wide spectrum of frequencies (Wegener et al. 2000). For the duration of the fluidic exposure of the HDMVEC monolayers, impedance (Ω), resistance (Ω) and capacitance (nF) were recorded in real-time at defined frequencies.

3.3.5 Immunoblotting

Positively charged rectangular glass slides (Thermo Fisher, Waltham, MA) were rinsed in ethanol and air-dried, sterilized in a steam-autoclave, placed in a 100 mm sterile petri dish and coated with a 15 µg/ml human fibronectin solution (hFN; BD Biosciences, San Jose, CA) overnight at 4 °C. hFN solution was removed, and HDMVEC suspensions were seeded onto the slides at a concentration of 1.2×10^6 cells/ml. Cells were grown to confluency for 48 h at 37 °C (5% CO₂, 95% air). For immunoblotting assays, endothelial cells were subjected to fluidic shear stress at 2 dyn/cm² with a parallel flow chamber apparatus (GlycoTech, Gaithersburg, MD).

Immediately after fluid exposure, HDMVEC whole cell lysates were prepared using a kinase lysis buffer consisting of 20 mM HEPES (pH 7.4), 150 mM NaCl, 50 mM KF, 50 mM

β -glycerolphosphate, 2 mM EGTA (pH 8.0), 1 mM Na_3VO_4 , 10% glycerol, 1% Triton X-100, a protease inhibitor cocktail (Roche Diagnostics, Basel, Switzerland) and a phosphatase inhibitor cocktail (Pierce Scientific, Rockford, IL). Clearing of cell lysates was achieved by centrifugation at 16,000 rpm for 10 min at 4 °C. Samples of cell lysates were subjected to the Bradford protein assay (Bio-Rad Laboratories, Hercules, CA) to determine total protein concentration. Equal protein concentrations of HDMVEC lysates were subjected to run on a 12% SDS–PAGE gel, transferred to nitrocellulose membranes (Bio-Rad Laboratories, Hercules, CA) and immunoblotted.

Membranes were blocked for 1 h at RT with blocking buffer (3% BSA in 0.1% PBS-T) and incubated with antibodies directed against either VE-cadherin (AbCam, Cambridge, United Kingdom), phospho-VE cadherin Y685 (ECM Biosciences, Versailles, KY), phospho-VE cadherin Y731 (Life Technologies, Waltham, MA), Src (AbCam, Cambridge, United Kingdom), phospho-Src Y416 (Cell Signaling Technology, Danvers, MA), SHPT2 (Santa Cruz Biotechnology, Dallas, TX), tubulin (AbCam, Cambridge, United Kingdom) or β -actin (Sigma-Aldrich, St. Louis, MO). Membranes were washed and incubated with horseradish peroxidase-conjugated secondary antibodies (Bio-Rad, Hercules, CA) for 1 hr at RT. Immunoblots were developed by ECL Plus (Pierce Scientific, Rockford, IL) and the Konica Minolta SRX-101A processor (Konica Minolta, Wayne, NJ). Densitometry of Western blots was performed using ImageJ (Schneider et al. 2012).

3.3.6 Immunohistochemistry

HDMVECs plated on ibidi flow μ -Slide VI^{0.4} channels (Ibidi, Munich, Germany) were subjected to flow-induced shear stress as described above. Immediately after completion of the flow assays, cells were fixated in 4% paraformaldehyde and 0.3% sucrose for 10 min at 37 °C, washed 3 \times in PBS (10 mM; pH 7.4), permeabilized (0.3% TritonX-100, 5 min at RT), and blocked for 30 min at 37 °C in 10 mM PBS (pH 7.4) with 10% normal goat serum, 0.25% Triton X-100, 0.1% Tween 20, 2% glycine and 0.02% NaN_3 . Following blocking, HDMVECs were incubated with a primary antibody targeted against the tight junction protein ZO-1 for 1 h at

37 °C, after three washing steps with 0.1% BSA and 0.1% Tween 20 in PBS, cells were incubated for 1 h at 37 °C in Alexa Fluor® anti-rabbit 488 goat-anti-rabbit IgG (H+L) secondary antibody (Life Technologies, Waltham, MA). Following secondary incubation and after three washing steps in PBS for 5 min each, cells were incubated with rhodamine phalloidin (Life Technologies, Waltham, MA) for 1 h at 37°C, washed 3x with PBS, incubated with DAPI (4',6-diamidino-2-phenylindole; Life Technologies, Waltham, MA) for 5 min at RT and mounted with mounting media (Ibidi, Munich, Germany). Images were collected on a Leica TCS SP5 confocal scanning laser microscope (Leica, Wetzlar, Germany) at a magnification of 200×.

3.4 Results

3.4.1 TEER-based analysis of cytokine-induced endothelial permeability under flow-induced shear stress

To confirm that transendothelial electrical resistance (TEER)-based analysis is a reliable method to rapidly monitor changes in endothelial permeability under shear stress and to validate the experimental system, we assessed barrier function via TEER with simultaneous shear stress exposure. TEER and permeability are inversely proportional. A decrease in TEER values indicates an increase in endothelial permeability. Human dermal microvascular endothelial cell (HDMVEC) monolayers exposed to shear stress and treated with the vascular permeability-inducing cytokine IL-1 β demonstrated a 2-fold increase in permeability compared to non-treated control monolayers also exposed to shear stress (Figure 3.1A; **** $p < 0.0001$). Histamine (Figure 3.1B; **** $p < 0.0001$) and thrombin (Figure 3.1C; **** $p < 0.0001$) also significantly induced permeability in HDMVEC monolayers exposed to shear stress compared to controls. Comparing impedance measurements between different sets of HDMVECs demonstrated that the qualitative analysis of TEER was consistent and comparable between separate experiments. These findings point to the utility of TEER-based analysis under shear stress to monitor permeability changes within an endothelial monolayer.

3.4.2 Quantifying the inhibition of cytokine-induced endothelial permeability by specific antagonists under flow-induced shear-stress

TEER-based analysis is primarily used to measure changes in endothelial permeability under static conditions where an endothelial monolayer is not exposed to shear stress (Kustermann et al. 2014). The utility of TEER-based quantitation to measure the efficacy of a drug or novel compound to block cytokine-induced permeability in an endothelial monolayer exposed to flow-induced shear stress has not been evaluated. Therefore, we next assessed whether TEER-based analysis under shear stress conditions may be a viable detection method to measure inhibition of vascular leak by selective antagonists. We tested whether cytokine-mediated endothelial permeability under shear stress might be inhibited with anti-permeability antagonists

as measured by TEER. Both IL-1 β and thrombin-mediated leakage were completely abrogated by treatment of HDMVEC monolayers with either clemastine (CLE) or methylprednisolone (MPS; Figure 3.1A, C, D and F; **** $p < 0.0001$) under shear stress. Treatment of HDMVEC monolayers with the histamine-antagonist CLE, which acts on the histamine H1 receptor, significantly blocked histamine-mediated permeability in endothelial monolayers exposed to flow-induced shear stress compared to vehicle control endothelial monolayers also exposed to shear stress (Figure 3.1B; **** $p < 0.0001$).

Treatment of confluent HDMVEC monolayers with MPS inhibited histamine-induced permeability as measured by TEER analysis in endothelial monolayers exposed to shear stress (Figure 3.1E; **** $p < 0.0001$). Moreover, barrier integrity as a function of TEER was significantly increased in HDMVEC monolayers treated with either drug alone (Figure 3.1A - F). Our data suggests that TEER may rapidly evaluate changes in endothelial barrier integrity and endothelial permeability in endothelial monolayers exposed to flow-induced shear stress. These measurements suggest rapid analysis of endothelial monolayer permeability with TEER monitoring when monolayers are also exposed to flow-induced shear stress.

3.4.3 Endothelial cells exhibit high levels of viability despite exposure to flow-induced shear stress conditions

Endothelial cell death may negatively impact barrier function and increase endothelial permeability. Therefore, we tested if HDMVEC monolayers exposed to either vasoactive agents or antagonists exhibited changes in viability under shear stress. Cell viability was not altered by treatment, and cell viability remained at approximately 95% for all HDMVEC monolayers tested under shear stress conditions (Figure 3.1G). We found that HDMVEC monolayers remain viable when exposed to shear stress in the presence of histamine, IL-1 β or thrombin (Figure 3.1G); similarly, HDMVECs exhibit high degrees of viability when treated with either vehicle control (DMSO), CLE or MPS (Figure 3.1G). These findings suggest that the observed changes in endothelial monolayer permeability measured by TEER were due specifically to the treatments applied to the monolayer and not to a loss of endothelial cell viability.

3.4.4 Fluid shear stress does not induce morphological or topological variations on tight junction complexes of endothelial cells

Physiological flow-induced shear stress acts on constituents of endothelial tight junction complexes (Colgan et al. 2007). We, therefore, investigated the role of physiological flow-induced shear stress (2 dynes/cm²) on HDMVEC tight junctions and cytoskeletal rearrangement. In agreement with Colgan et al. we found that tight junctions did not exhibit morphological changes in HDMVEC monolayers under flow-induced shear stress conditions as determined by the staining pattern of the tight junction adapter protein ZO-1 (Fig 2A control row) (Colgan et al. 2007). ZO-1 links tight junctions to the actin cytoskeleton (Yamazaki et al. 2008, Fanning et al. 2009, Van Itallie et al. 2009). We demonstrate that under physiological flow-induced shear stress ZO-1 is localized to endothelial cell membranes between adjacent cells (Figure 3.2A; control row). Moreover, moderate actin stress fibers developed under physiological shear stress (Figure 3.2 and Figure 3.4; control rows), confirming previous reports that in endothelial monolayers, flow-induced shear stress promotes actin rearrangement as detected by actin stress fiber formation (Malek et al. 1996, Noria et al. 2004).

3.4.5 Under shear stress conditions, the permeability-inducing agents (histamine, IL-1 β and thrombin) promote redistribution of the tight junction adapter protein ZO-1 and increase actin stress fiber formation

Because addition of permeability-inducing agents such as histamine, IL-1 β and thrombin alter the staining pattern of tight junction proteins and promote cytoskeletal rearrangement under static conditions, we next examined whether the staining pattern of ZO-1 might be affected and if cytoskeletal reorganization occurred upon treatment with these classical permeability-inducing agents when endothelial monolayers were exposed to shear stress (Galbraith et al. 1998).

Treatment of HDMVEC monolayers with histamine, IL-1 β or thrombin altered ZO-1 localization at cellular borders showing a disruption in ZO-1 continuity and induction of gap-like areas at points of endothelial cell-cell contacts (Figure 3.2, Figure 3.3 and Figure 3.4). These changes are indicative of increased endothelial permeability. Untreated HDMVEC monolayer

controls displayed ZO-1 staining as a strong cell border signal with a continuous line of varied thickness (Figure 3.2, Figure 3.3 and Figure 3.4; control row). Note that in endothelial monolayers flow itself induces minimal stress fiber formation (Figure 3.2, Figure 3.3 and Figure 3.4) as previously described (Malek et al. 1996, Noria et al. 2004); however shear stress-induced actin rearrangement does not promote endothelial permeability as determined by TEER analysis (Figure 3.1). We found that increased stress fiber formation occurred in HDMVEC monolayers treated with histamine, IL-1 β or thrombin and exposed to shear stress compared to controls (Figure 3.2, Figure 3.3 and Figure 3.4).

3.4.6 Treatment of endothelial monolayers with the selective antagonists clemastine and methylprednisolone inhibited cytokine-mediated rearrangement of ZO-1 and reduced stress fiber formation

We next assessed whether treatment of endothelial monolayers with the antagonists CLE or MPS would block permeability-inducing agent-mediated changes in ZO-1 localization and stress fiber formation. Indeed, in endothelial monolayers exposed to shear stress and treated with CLE or MPS, prior to inducing permeability, ZO-1 localization remained at cellular borders with a line of ZO-1 continuity similar to controls (Figure 3.2, Figure 3.3 and Figure 3.4). Gap-like areas in ZO-1 staining were reduced in the drug treated monolayers exposed to both a permeability-inducing agent and shear stress. These findings confirm our ECIS-based TEER data (Figure 3.1) suggesting that the antagonists CLE and MPS block endothelial monolayer permeability under shear stress conditions by inhibiting ZO-1 redistribution and actin rearrangement that occur upon treating the monolayer with a permeability-inducing agent.

3.4.7 Under fluid shear stress conditions treatment with the permeability-inducing agents histamine, IL-1 β and thrombin promotes phosphorylation of VE-cadherin at tyrosine residues 685 and 731

VE-cadherin is an adhesion junction protein that regulates endothelial cell permeability *in vitro* and *in vivo* (Lampugnani et al. 1995, Ali et al. 1997, Wright et al. 2002). *In vitro* studies under static conditions have demonstrated that tyrosine phosphorylation of VE-cadherin occurs

in endothelial monolayers treated with classical permeability-inducing agents (histamine, IL-1 β and thrombin) (Lum et al. 1996, Andriopoulou et al. 1999, Baldwin et al. 2001, Keller et al. 2003, Vandenbroucke et al. 2008, Gabay et al. 2010, Griffiths et al. 2011). It is this increase in phosphorylation at Y685 and Y731 that promotes endothelial cell permeability *in vitro* and *in vivo* (Turowski et al. 2008). Therefore, we next examined whether histamine, IL-1 β or thrombin treatment altered VE-cadherin phosphorylation when HDMVEC monolayers were exposed to shear stress. We found that phosphorylation at both Y685 and Y731 was significantly increased in HDMVECs treated with IL-1 β (Figure 3.5B and D), histamine (Figure 3.5A and D), or thrombin (Figure 3.5C and F) exposed to shear stress compared to untreated cells also exposed to shear stress (Figures 5A - F). These results suggest that upon physiological shear stress the endothelium responds to histamine, IL-1 β and thrombin-mediated endothelial permeability by increasing VE-cadherin phosphorylation. Thus, phosphorylation of VE-cadherin at Y685 and Y731 contributes to endothelial cell permeability under shear stress conditions.

3.4.8 The histamine antagonist clemastine blocks permeability-inducing agent-mediated VE-cadherin phosphorylation

We demonstrated by TEER analysis under shear stress conditions that treatment of HDMVECs with the histamine antagonist, CLE, significantly blocked histamine-mediated endothelial permeability compared to the vehicle control (Figure 3.1D). Therefore, we next assessed whether CLE inhibited vascular permeability under shear stress conditions via classical VE-cadherin permeability-signaling. Pre-incubation of endothelial monolayers with CLE, 10 h before histamine was added, fully inhibited VE-cadherin phosphorylation at Y685 and Y731 (Figure 3.5 A). Moreover, CLE also blocked VE-cadherin phosphorylation at these sites mediated by IL-1 β or thrombin (Figure 5B - C) suggesting that CLE blocks endothelial permeability by inhibiting VE-cadherin phosphorylation.

3.4.9 Under shear stress conditions, treatment with a permeability-inducing agent promotes phosphorylation of Src at Y416

The non-receptor tyrosine kinases of the Src family are mediators of vascular leak. Src signaling is required for VE-cadherin phosphorylation in response to permeability-inducing agents *in vitro* (Andriopoulou et al. 1999, Baumeister et al. 2005, Weis et al. 2005, Wallez et al. 2007, Gong et al. 2008, Gavard 2009). Recently, Orsenigo et al. reported that Src activation is required for shear-induced phosphorylation of VE-cadherin *in vivo* (Orsenigo et al. 2012). We found that Src phosphorylation at Y416 increased upon treatment with histamine, IL-1 β or thrombin under shear stress (Fig 6A-C). The levels of the SH2-containing phosphotyrosine phosphatase (SHP2) that regulates c-Src activation by controlling CSK access to Src kinases (Vaidyanathan et al. 2007) did not change in response to shear stress or when treated with a permeability-inducing agent. These findings demonstrate that endothelial monolayers treated with a permeability-inducing factor and exposed to shear stress increase vascular permeability by activation of VE-cadherin and Src.

3.4.10 Clemastine blocks permeability-inducing agent-mediated increase in Src phosphorylation at Y416

Finally, we assessed whether CLE, an antagonist of vascular leak, could block histamine, IL-1 β or thrombin-mediated Src phosphorylation in endothelial monolayers exposed to shear stress. Incubation of endothelial monolayers with CLE 10 hours before addition of histamine significantly inhibited Src phosphorylation at Y416 (Figure 3.6A), suggesting that CLE effectively blocks histamine-induced vascular leak, which we also detected by TEER analysis (Figure 3.1), by inhibiting Src and consequently VE-cadherin phosphorylation (Figure 3.5A and D). Moreover, CLE blocked downstream phosphorylation signaling events mediated by IL-1 β (Figure 3.6B) or thrombin (Figure 3.6C) suggesting that its inhibitory mode of action is at least, in part, through blocking the classical vascular permeability pathway of VE-cadherin and Src signaling. SHP2 expression levels did not change in response to exposure to shear stress or permeability-inducing agents (Figure 3.6D - F). Taken together, the findings of our study provide

validation of the utility of impedance analysis under physiological flow-induced shear stress as a novel platform for screening potential permeability inhibitors.

3.5 Discussion

We demonstrate the utility of a TEER-based in vitro platform that takes into account physiological shear stress on endothelial monolayers within a rapid, efficient and real time assay (Figure 3.7).

We show in this study that TEER measurements of endothelial monolayers exposed to shear stress can rapidly detect permeability-inducing agent-mediated leakiness as well as compounds that block permeability. Our model system may be applied to speedily and accurately measure the effects of known or novel compounds on cytokine-mediated endothelial permeability.

Our data indicate the permeability-inducing agents histamine, IL-1 β and thrombin promoted permeability of endothelial monolayers exposed to physiological shear stress. The histamine specific antagonist, CLE, significantly blocked histamine-mediated permeability in endothelial monolayers within our flow-induced shear stress model system (Gschwandtner et al. 2008, Johansen et al. 2008, Johansen et al. 2011, Apolloni et al. 2014). Histamine-induced endothelial permeability was also abrogated by the non-specific antagonist MPS. This small anti-inflammatory steroid molecule acts by blocking the biosynthesis of inflammatory mediators including prostaglandins and leukotrienes. Recently, Kustermann et al. reported that histamine-mediated permeability is abrogated by both CLE and MPS under static conditions (Kustermann et al. 2014). Our data confirms the ability of these antagonists to block endothelial monolayer permeability and adds the novel finding that exposure to physiological shear stress did not alter their efficacy. Histamine, IL-1 β and thrombin-mediated permeability were blocked by these antagonists as well suggesting that induction of permeability may activate a specific permeability signal transduction pathway in endothelial cells.

Endothelial cell tight junctions are key components of barrier function and regulate permeability. Tight junctions consist of several types of transmembrane proteins and cytosolic proteins that link the membrane to the actin cytoskeleton (Lampugnani 2012). Dysregulation of tight junctions leads to a decrease in barrier function and increases vascular leak. To determine

the effects of shear stress and the ability of antagonists to inhibit leakiness mediated by permeability-inducing agents we examined the localization of the tight junction adapter protein ZO-1. ZO-1 forms a complex with tight junction proteins including JAM and claudin family members and also binds to F-actin (Nitta et al. 2003, Lamagna et al. 2005, Cooke et al. 2006, Severson et al. 2009, Peddibhotla et al. 2013). Our data demonstrated that in endothelial monolayers exposed to shear stress ZO-1 remained at the cell borders whereas upon treatment with a permeability-inducing agent ZO-1 became punctate with gap-like regions. We also found that endothelial cell exposure to physiological shear stress initiated minimal actin stress fibers, which is in agreement with Tojkander et al. (Tojkander et al. 2012). It is important to note that initiation of shear stress did not alter barrier function or increased vascular permeability in the endothelial monolayers as determined by TEER/ECIS analysis. Treatment of endothelial monolayers with the permeability-inducing agents, histamine, IL-1 β and thrombin, promoted increased actin stress fiber formation that correlated with increased endothelial permeability.

Phosphorylation of VE-cadherin at Y685 and Y731 increases endothelial permeability under static conditions (Griffiths et al. 2011). In endothelial monolayers exposed to shear stress VE-cadherin phosphorylation at these two sites was not increased; however phosphorylation of VE-cadherin at Y685 and Y731 occurred upon treatment with a permeability-inducing agent such as histamine, IL-1 β and thrombin. We have previously reported that cytokine-induced endothelial permeability under static conditions increased phosphorylation of VE-cadherin at Y731 (Griffiths et al. 2011). We report here that under shear stress conditions, cytokine-induced permeability increases VE-cadherin phosphorylation at both Y731 and Y685 suggesting that physiological shear stress may affect endothelial response to permeability-inducing agents. Recently, Orsenigo et al. found that *in vivo* phosphorylation of VE-cadherin is modulated by hemodynamic forces and that phosphorylation of VE-cadherin at Y685 occurs in veins but not in arteries (Orsenigo et al. 2012). Such specific changes in VE-cadherin phosphorylation may be due to endothelial responses to shear stress exposure, suggesting that testing compounds that block cytokine-mediated vascular leak in endothelial monolayers under shear stress conditions

may be a more physiologically relevant method than testing endothelial monolayers under static conditions.

Src activity plays a role in VE-cadherin mediated vascular permeability. Indeed, Src deficient mice demonstrate a significant decrease in vascular leak and VE-cadherin phosphorylation upon treatment with a permeability-inducing agent (Eliceiri et al. 2002, Ha et al. 2008). Recently, an *in vivo* analysis of Src activation determined that Src phosphorylation is required for shear stress-induced VE-cadherin phosphorylation in mice (Orsenigo et al. 2012). Our data indicates that permeability-inducing agents activate Src in endothelial monolayers exposed to physiological shear stress. Phosphorylation of Src at Y416 was increased upon treatment with permeability-inducing agents (histamine, IL-1 β and thrombin) and could be blocked with the permeability inhibiting compounds CLE and MPS. PECAM-1 binds directly to Src and this complex is required for Src activation in endothelial monolayers exposed to shear stress conditions, suggesting a shear stress-sensing mechanism that regulates vascular leak in endothelial cells (Tzima et al. 2005). Taken together, our data supports the recent *in vivo* reports that a shear-sensing mechanism may regulate VE-cadherin phosphorylation and subsequent endothelial permeability (Tzima et al. 2005). Thus, our novel platform in which endothelial cells exposed to shear stress and TEER/ECIS measurements in real-time may provide a more physiologically and ultimately clinically relevant method to identify lead compounds that block vascular permeability.

3.6 Figures

This page has been left blank intentionally.

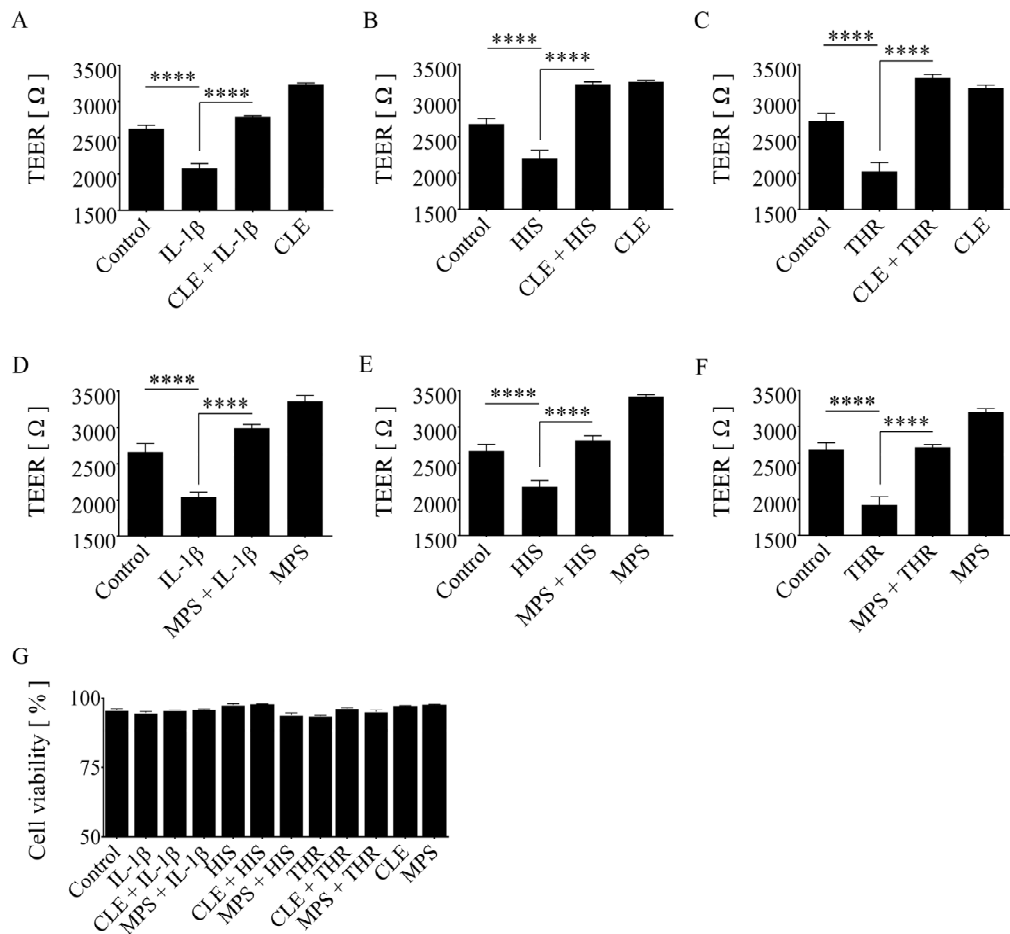


Figure 3.1

Impedance-based measurements of vascular leakage under flow-induced shear stress conditions

Impedance based analysis for vascular leakage in endothelial monolayers induced by IL-1β, histamine and thrombin exposed to flow-induced shear stress at 2 dyn/cm². (A-F) Treatment with IL-1β, histamine or thrombin promotes vascular permeability and the antagonists, clemastine (CLE) or methylprednisolone MPS (MPS) block it. TEER measurements on HDMVEC

monolayers treated with IL-1 β , histamine (HIS), thrombin (THR) or control (DMSO) or pre-treated with the antagonists CLE or MPS. TEER levels (y-axis) are the mean electrical resistance in $\Omega \pm$ SD corrected for the resistance of a naked well. **** $p < 0.0001$ by the student's t-test. **(G)** Cell viability analysis (%) of permeability-inducing agents, antagonists and controls after flow-induced shear stress. Treatments and flow-induced shear stress did not affect cell viability compared with untreated controls. Each bar represents the mean \pm SD (n=3 for each case). Real-time measurements of electrical resistance were conducted at a frequency of 4,000 Hz. The respective data points of electrical resistance at 15 min are depicted.

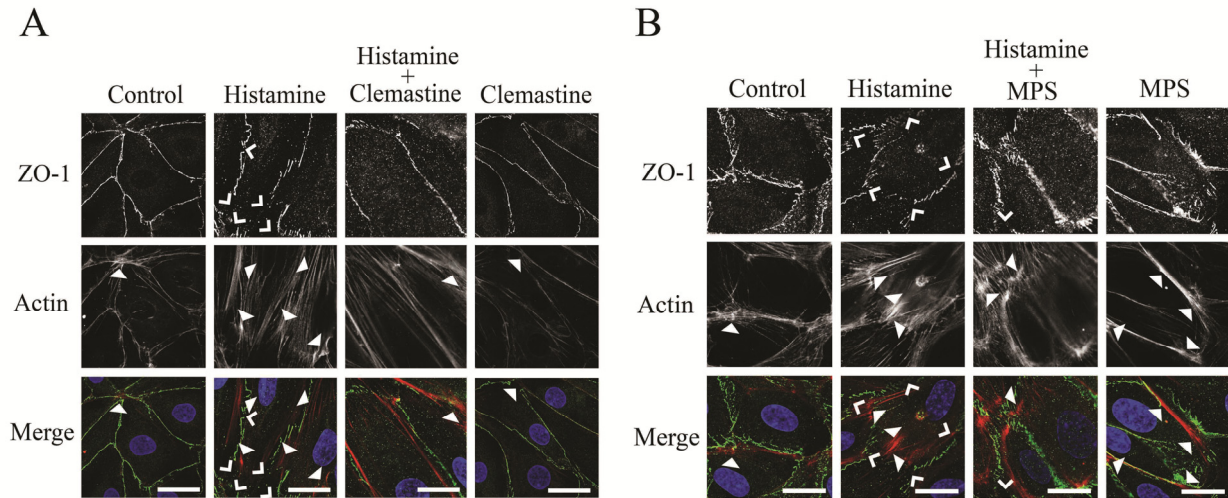


Figure 3.2

The antagonists CLE and MPS block histamine-induced cytoskeletal protein rearrangement in HDMVEC monolayers exposed to shear stress

Cells were grown on fibronectin-coated glass coverslips, exposed to flow-induced shear stress conditions (2 dyn/cm^2), fixed and stained with Alexa Fluor 555 phalloidin (red color) and an Alexa Fluor 488 anti-ZO-1 antibody (green color). Closed arrowheads indicate moderate stress fiber formation. Open arrowheads point to the gaps in ZO-1 staining that occur upon treatment with the permeability-inducing agent histamine. Treatment with antagonists **(A)** CLE or **(B)** MPS reduced histamine-mediated stress fiber formation and ZO-1 staining gaps between cells. DAPI was used to counterstain nuclei (blue color). Scale bars correspond to $20 \mu\text{m}$. Results are representative of three or more independent experiments.

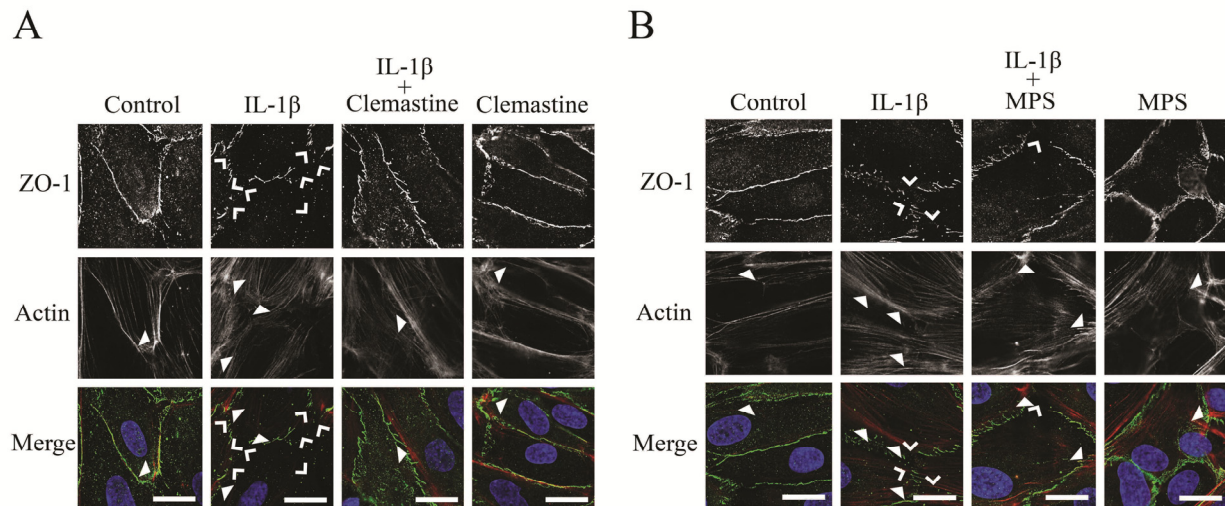


Figure 3.3

The antagonists CLE and MPS block IL-1 β -induced cytoskeletal protein rearrangement in HDMVEC monolayers exposed to shear stress

Cells were grown on fibronectin-coated glass coverslips, exposed to flow-induced shear stress conditions (2 dyn/cm²), fixed and stained with Alexa Fluor 555 phalloidin (red color) and an Alexa Fluor 488 anti-ZO-1 antibody (green color). Closed arrowheads indicate moderate stress fiber formation. Open arrowheads point to the gaps in ZO-1 staining that occur upon treatment with the permeability-inducing agent IL-1 β . Treatment with antagonists (A) CLE or (B) MPS reduced IL-1 β -mediated stress fiber formation and ZO-1 staining gaps between cells. DAPI was used to counterstain nuclei (blue color). Scale bars correspond to 20 μ m. Results are representative of three or more independent experiments.

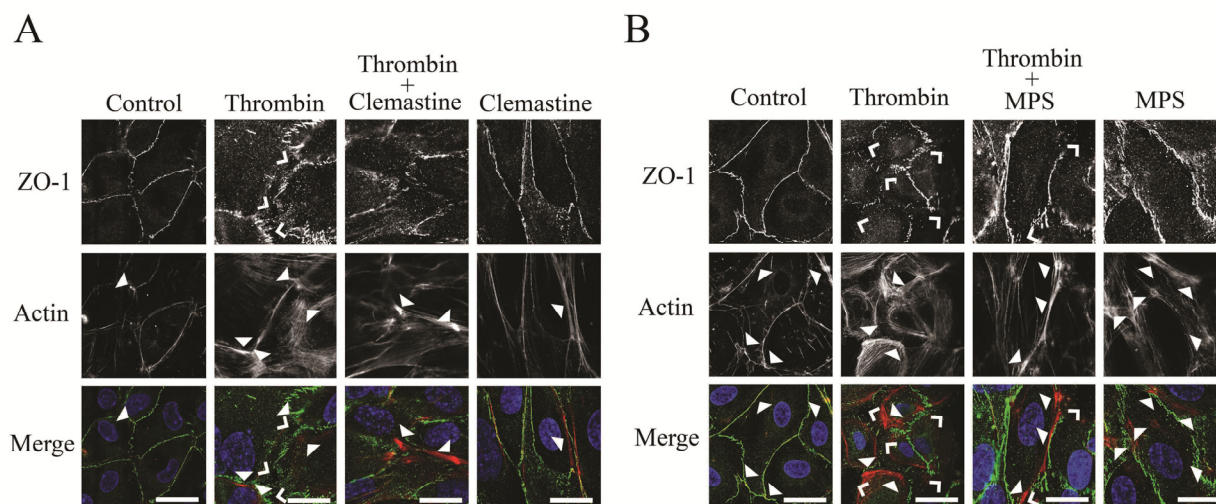


Figure 3.4

The permeability-inducing agents IL-1 β , histamine or thrombin promote VE-cadherin phosphorylation at Y731 and Y685 in HDMVEC monolayers exposed to shear stress and pre-treatment with the antagonists CLE and MPS block it.

Cells were grown on fibronectin-coated glass coverslips, exposed to flow-induced shear stress conditions (2 dyn/cm²), fixed and stained with Alexa Fluor 555 phalloidin (red color) and an Alexa Fluor 488 anti-ZO-1 antibody (green color). Closed arrowheads indicate moderate stress fiber formation. Open arrowheads point to the gaps in ZO-1 staining that occur upon treatment with the permeability-inducing agent IL-1 β . Treatment with antagonists **(A)** CLE or **(B)** MPS reduced thrombin-mediated stress fiber formation and ZO-1 staining gaps between cells. DAPI was used to counterstain nuclei (blue color). Scale bars correspond to 20 μ m. Results are representative of three or more independent experiments.

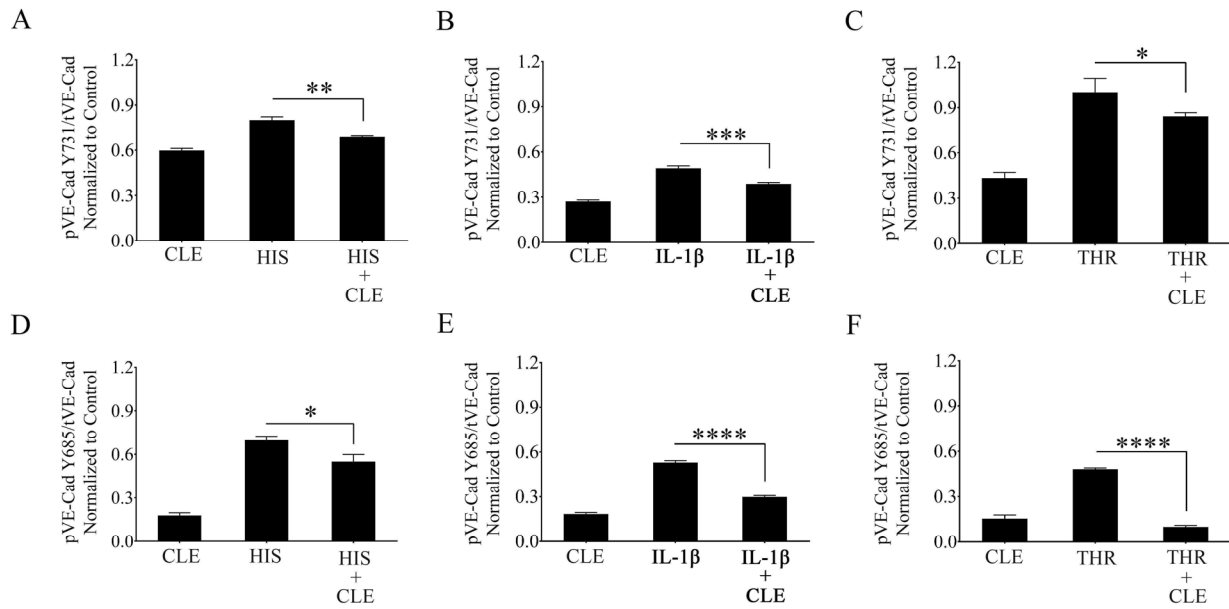


Figure 3.5

The permeability-inducing agents IL-1 β , histamine or thrombin promote VE-cadherin phosphorylation at Y731 and Y685 in HDMVEC monolayers exposed to shear stress and pre-treatment with the antagonist CLE blocks it.

Quantitative analysis of Western blots of HDMVEC monolayers treated with the permeability-inducing agents IL-1 β , histamine or thrombin, or pre-treated with the antagonist clemastine (CLE) alone or pre-treated with CLE prior to addition of IL-1 β , histamine or thrombin. (A-C) VE-cadherin Y731 and total VE-cadherin were quantitated from Western blots. Relative intensity of pVE-cadherin (Y731)/tVE-cadherin was determined. * $p < 0.05$; ** $p < 0.01$; *** $p < 0.001$ (Student's t test). The values represent the average of three independent experiments. (D-F) VE-cadherin Y685 and total VE-cadherin were quantitated from Western blots. Relative intensity of pVE-cadherin (Y685)/tVE-cadherin was determined. * $p < 0.05$; **** $p < 0.0001$ (Student's t test). The values represent the average of three independent experiments.

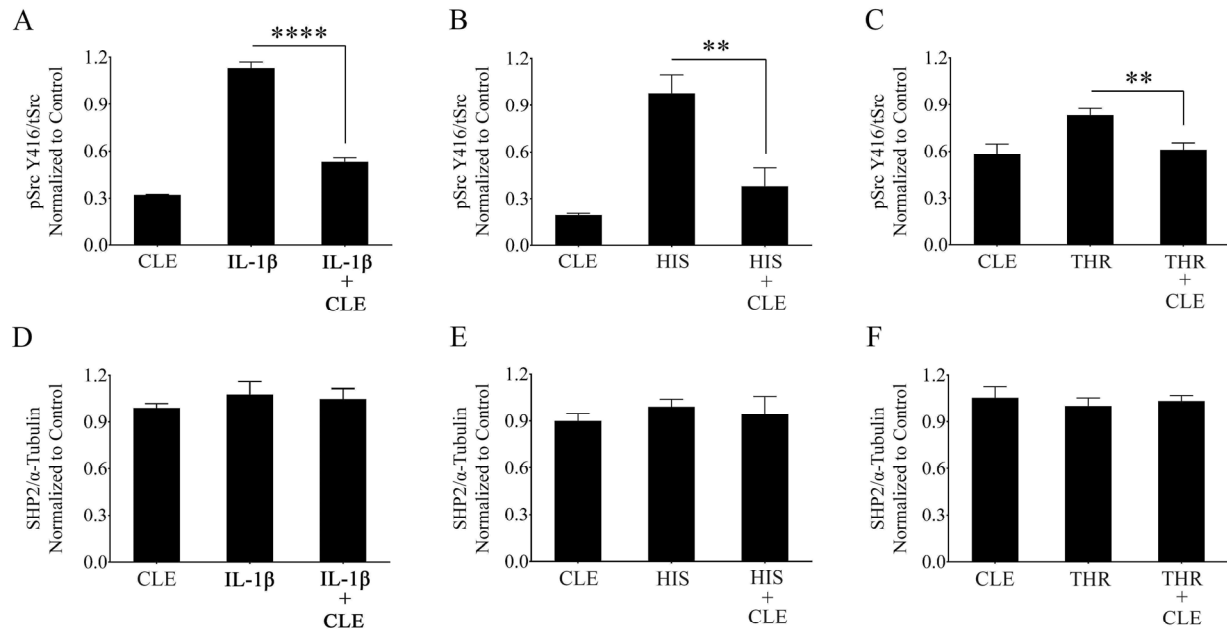


Figure 3.6

Permeability-inducing agents IL-1β, histamine or thrombin increase Src phosphorylation at Y416 and pre-treatment with the antagonist CLE blocks it.

Quantitative analysis of Western blots of HDMVEC monolayers treated with permeability-inducing agents IL-1β, histamine or thrombin, the antagonist CLE alone or pre-treated with CLE prior to addition of IL-1β, histamine or thrombin. (A-C) Quantitation of Western blots detecting phosphorylated Src (Y416) and total Src. Relative intensity of pSrc(Y416)/tSrc was determined. * $p < 0.05$ (Student's *t* test). The values represent the average of three independent experiments. (D-F) SHP2 protein levels were quantitated by Western blot analysis. Tubulin was used as a loading control. Relative intensity of SHP2/Tubulin were measured. ** $p < 0.01$; **** $p < 0.0001$ (Student's *t* test). The values represent the average of three independent experiments.

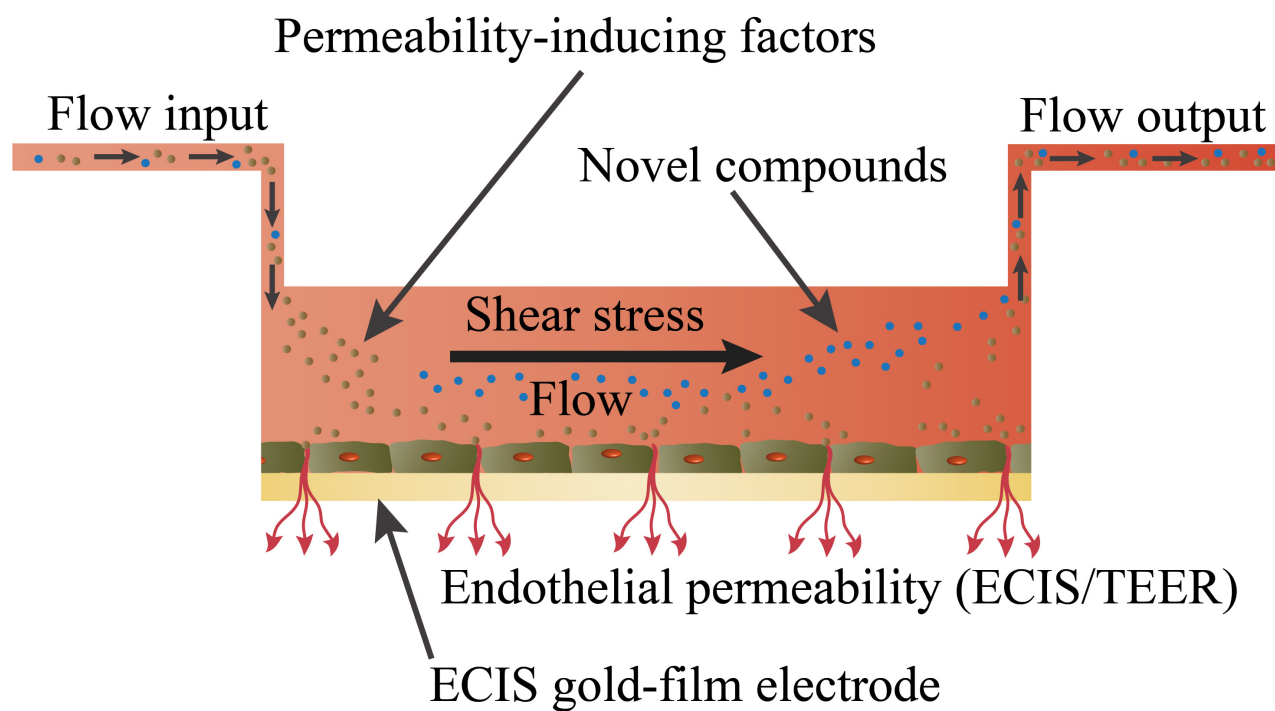


Figure 3.7

A flow-induced shear stress impedance TEER-based *in vitro* platform to identify inhibitors of vascular permeability in real time.

APPENDIX A

Infectious Biofilms and Sepsis

Abstract

Immuno-compromised patients (e.g., cancer, sepsis) such as those undergoing cancer chemotherapy are highly susceptible to bacterial infections leading to biofilm matrix formation. This surrounding biofilm matrix acts as a diffusion barrier that actively binds up antibiotics and antibodies, thereby promoting resistance to treatment. Developing non-invasive imaging methods that detect the presence of a biofilm matrix in the clinic are needed. The use of ultrasound in conjunction with targeted contrast agents may provide detection of early stage biofilm matrix formation and facilitate optimal treatment options prior to the development of an established biofilm matrix.

Ligand-targeted ultrasound contrast agents were investigated as a novel method for pre-clinical non-invasive molecular imaging of early and late stage biofilms. These agents were used to target, image and detect *Staphylococcus aureus* biofilm matrix formation *in vitro*. Binding efficacy was assessed on early to late stage biofilm matrices with respect to their increasing biomass ranging from $3.126 \times 10^3 \pm 427$ ultrasound contrast agents per mm^2 of biofilm surface area within the first 12 h to $21.985 \times 10^3 \pm 855$ at 96 h per mm^2 of biofilm matrix surface area. High-frequency acoustic microscopy was used to ultrasonically detect targeted contrast agents bound to a biofilm matrix and to assess biofilm matrix mechanoelastic physical properties. Acoustic impedance data demonstrated that biofilm matrices exhibit impedance values (1.9 MRayl) close to human tissue (ranging from 1.35 MRayl to 1.85 MRayl for soft tissues). Moreover, the acoustic signature of mature biofilm matrices were evaluated in terms of integrated backscatter ($0.0278 \text{ mm}^{-1} \times \text{sr}^{-1}$ to $0.0848 \text{ mm}^{-1} \times \text{sr}^{-1}$) and acoustic attenuation profiling (3.9 Np/mm for bound agents; 6.58 Np/mm for biofilm alone).

Early diagnosis of biofilm matrix formation is a key challenge in treating cancer patients with infection-associated biofilms. In this study, we report for the first time a combined optical and acoustic evaluation of infectious biofilm matrices. We demonstrate that the acoustic impedance of biofilms is similar to the impedance of human tissues, making *in vivo* imaging and detection of biofilm matrices difficult. We report that the combination of ultrasound and targeted

contrast agents can be used as a way to enhance biofilm imaging and early detection. Our findings suggest that the combination of targeted ultrasound contrast agents (UCAs) and ultrasound can be used as a novel molecular imaging technique for the timely detection of early to late biofilm formation. Finally, we show that high-frequency acoustic microscopy provides sufficient spatial resolution for quantification of biofilm mechanical and elastic properties.

Introduction

Biofilm-related sepsis has been linked to medical implants (Kennedy et al. 2010). Bacterial biofilms are three-dimensional extracellular matrices composed of carbohydrates, proteins and exopolysaccharides (Liu et al. 1994, Allison et al. 1998, Costerton et al. 1999, Wingender et al. 1999, Strathmann et al. 2002, Hall-Stoodley et al. 2004) that develop on solid-liquid or solid-air interfaces in the body (Costerton et al. 1999, Davey et al. 2000). Biofilms consist of bacterial cells and matrix proteins. The majority of biofilms contain 10% or less of bacterial cells and over 90% matrix (Flemming et al. 2010). Biofilm matrices are highly conserved dynamic structures. Initiation of a biofilm matrix occurs by a transient interaction of bacteria with a surface followed by an adhesive stage that allows for microcolony formation and a subsequent growth and maturation stage. The complexity of biofilms allows bacteria cells to survive a multitude of environments and promotes cell dispersion to colonize new areas. These matrices may form on medical devices or fragments of dead tissue (Lambe et al. 1991, Costerton et al. 1999, Kaplan 2005, Harris et al. 2006, Baldassarri et al. 2007). Clinically, biofilms may occur during chemotherapy and infectious diseases such as endocarditis (Sullam et al. 1985, Caldwell et al. 2002, Donlan et al. 2002, Petti et al. 2003, Hall-Stoodley et al. 2004).

Biofilm-associated infections are resistant to treatment and recur even after repeated antibiotic therapy. One primary issue is that established biofilm matrices act as diffusion barriers and actively bind up antibiotics and antibodies thereby providing increased resistance. Overall killing bacteria that are surrounded by a microbial biofilm require up to 1000 times higher concentrations of antibiotics than those without a surrounding biofilm (Nickel et al. 1985, Allison et al. 1995, Stewart et al. 2001, Parsek et al. 2003). Thus, detecting, treating and inhibiting biofilm formation inside the body is a key medical challenge.

Moreover, in the clinical setting antibiotic therapy efficacy is decreased in the presence of an established biofilm making early detection critical. For example, infective endocarditis may occur due to chronic infection, has a poor prognosis and is associated with high mortality rates (Caldwell et al. 2002, Donlan et al. 2002, Furuya et al. 2003, Petti et al. 2003). Indeed, there are

significant diagnostic challenges for endocarditis that are attributed to the inaccessibility of intra-cardiac biofilms and the non-specific nature of the clinical symptoms (Durack et al. 1994). Although echocardiography permits non-invasive detection of biofilms (Baddour et al. 2005) it has significant limitations in the detection of early biofilm matrix formation. In addition, clinical diagnosis primarily occurs after biofilm matrices are fully established, thereby significantly decreasing available treatment options. Therefore, early detection is a crucial component of diagnosis; however no current diagnostic methodology is available that clearly delineates early and late stage matrices.

Ultrasound is an effective method for imaging biofilms *in vitro* (Good et al. 2006, Holmes et al. 2006, Kujundzic et al. 2007, Shemesh et al. 2007, Vaidya et al. 2014). One method used to enhance biofilm detection is the addition of UCAs (encapsulated gas bubbles), which provide a unique acoustic scattering signature thereby significantly enhancing imaging capabilities (Sbeity et al. 2013). Furthermore, linking a ligand to a contrast agent's outer membrane aids in UCAs binding to tissue and is crucial in delineating disease specific regions from surrounding healthy tissue (Klibanov et al. 1999, Klibanov 2006, Klibanov 2007, Klibanov 2009, Anderson et al. 2011, Unnikrishnan et al. 2012).

In this study, ligand-targeted UCAs were used as a novel method for pre-clinical non-invasive molecular imaging of early and late stage biofilms. These agents were used to target and detect *Staphylococcus aureus* (*S. aureus*) biofilm formation. Binding efficacy was assessed on established biofilms as a function of surface area. A combination of acoustic and optical microscopy was used to quantify the mechanical and structural properties of a three-dimensional biofilm matrix. We show that high-frequency scanning acoustic microscopy (SAM) provides sufficient high spatial resolution for imaging and quantification of biofilm thickness and mechanoelastic properties.

Materials and Methods

Bacterial strains and cultivation of biofilms

We used a penicillin-resistant mutant of *S. aureus*. *S. aureus* and coagulase-negative staphylococci account for the majority of device-related infections (Baddour et al. 2003).

S. aureus cultures were stored frozen at -80 °C in 10% glycerol and 90% tryptic soy broth (TSB, T8907, Sigma-Aldrich, St. Louis, USA) solution dissolved in sterile ultrapure water (Alfa Aesar, Ward Hill, MA, USA).

A vial of frozen bacterial culture was thawed at room temperature (RT) and added to 250 mL of TSB. The inoculum was propagated and incubated overnight on an incubator shaker at 37 °C and 160 rotations per minute (RPMs). The bacterial cultures were harvested after standardization to an optical density at 600 nm (OD₆₀₀) of 0.05 relative to the TSB culture medium (Beckman Coulter, Inc., Fullerton, CA, USA).

Biofilm assays were conducted by adding three milliliters of the standardized bacterial culture solution to the pre-treated 35 mm glass (World Precision Instruments, Inc., Sarasota, FL, USA) and polystyrene petri dishes (Greiner Bio-One, Monroe, NC, USA). Glass and polystyrene petri dishes were treated in a previous step with Collagen IV (BD Biosciences, San Jose, CA, USA) for twenty minutes and rinsed in three washing steps with sterile distilled water. Prior to the addition of the inoculum, a 22 × 22 mm sterile micro cover glass (VWR International, LLC, West Chester, PA, USA) was placed into each of the polystyrene petri dishes. The glass and polystyrene petri dishes were then kept inside an incubator shaker at 37 °C and 120 RPMs for up to 96 hours without replacement and addition of fresh culture medium in the interim.

Lectins, antibodies and immunofluorescence

Fluorescently-labeled lectins, concanavalin A (conA; binds to α -Man, α -Glc) (Goldstein et al. 1978, Strathmann et al. 2002) and wheat germ agglutinin (WGA; binds to $(\beta$ -GlcNAc)₂ and NeuNAc; Sigma-Aldrich Corp., St. Louis, MO, USA) (Goldstein et al. 1978, Strathmann et al.

2002) conjugated with FITC were used for the visualization of carbohydrate-containing extracellular polymeric substances in biofilms of *S. aureus* (Table A.1) (Goldstein et al. 1978, Strathmann et al. 2002). Stock solution of ConA at a concentration of 1 mg/mL in 0.1 M sodium bicarbonate (pH 8.3) and WGA at a concentration of 1 mg/mL in phosphate buffered saline (PBS; pH 7.4) were prepared, aliquoted and stored at -20 °C. Prior to use, thawed portions of ConA and WGA aliquots were diluted with 0.1 M sodium bicarbonate (pH 8.3) and PBS (pH 7.4) respectively to a lectin final concentration of 10 µg/mL.

The blue-fluorescent nucleic acid stain 4',6-diamidino-2-phenylindole, dihydrochloride (DAPI, Sigma-Aldrich Corp., St. Louis, MO, USA) was used to visualize bacterial cell distribution in the biofilms. A DAPI stock solution at a concentration of 5 mg/mL and 14.3 mM in ultrapure water was prepared, aliquoted and stored at -20 °C. An aliquot was diluted to 300 nM in PBS immediately before use.

The monoclonal immunoglobulin antibody to protein A of *S. aureus* was used as a conjugation agent for the UCA particles. Anti-Protein A (APA) was developed in rabbit using protein A purified from *S. aureus* (Sigma-Aldrich Corp., St. Louis, MO, USA). Protein A localizes on the surface of staphylococcal bacterial strains and its distribution is inhomogeneous (Schneewind et al. 1995, DeDent et al. 2007). The lyophilized content of the vial was reconstituted in 2 mL PBS (pH 7.4) yielding a solution with a protein concentration of 23.7 mg/mL. The lectin from *P. aeruginosa* (PA-IL, Sigma-Aldrich Corp., St. Louis, MO, USA) was used, similarly to APA, to conjugate the surface of the UCA particles. The lyophilized content was diluted in 1 mL PBS (pH 7.4) yielding a protein concentration of 1 mg/mL. Following the reconstitution of APA and PA-IL, the proteins were biotinylated and conjugated onto the surface of the UCAs according to the method that will be described in more detail.

Sulfo-NHS-LC-Biotin (Thermo Scientific, Rockford, IL, USA) was applied to label APA and PA-IL with biotin. The vial of Sulfo-NHS-LC-Biotin was stored at -20 °C and equilibrated to RT before opening to avoid condensation. For the biotin labeling reaction 2.2 mg of Sulfo-NHS-LC-Biotin were dissolved in 400 µL ultrapure water immediately before use yielding

a 10 mM solution. A 20-fold molar excess of biotin reagent to label APA and PA-IL, resulting in 4-6 biotin groups per antibody molecule, was found to be suitable. For APA with a concentration of 23.7 mg/mL, a volume of 320 μ L Sulfo-NHS-LC-Biotin was used for the biotinylation reaction while 13.5 μ L Sulfo-NHS-LC-Biotin were used to label PA-IL with a concentration of 1 mg/mL. Following the incubation on ice for two hours at RT a Zeba[®] desalt spin column (Thermo Scientific, Rockford, IL, USA) was applied to remove the excess non-reacted and hydrolyzed Sulfo-NHS-LC-Biotin reagent from the APA and PA-IL solutions. The column was placed into a sterile 15 mL falcon tube and centrifuged at 1000 \times G for two minutes. After centrifugation the storage buffer collected at the bottom of the falcon tube was discarded, the column placed back into the same falcon tube and equilibrated by adding 2.5 mL of PBS (Thermo Scientific, Rockford, IL, USA) to the top of the resin bed and centrifuging at 1000 \times G for two minutes. Next, the flow-through was discarded, and the same step was repeated a total of three times. Subsequently the column was placed into a new sterile 15 mL falcon tube, and the antibody solution was applied onto the center of the resin bed. Finally, the column was centrifuged at 1000 \times G for two minutes. The collected purified flow-through antibody solutions were aliquoted and stored appropriately.

Targeted ultrasound

Biotin-conjugated lipid-encapsulated perfluorocarbon UCAs with a mean diameter of 3.02 μ m \pm 0.05 μ m (Targeson, Inc, San Diego, CA, USA) were removed from a sealed vial using a four-way stopcock-syringe combination with a 22 G needle while simultaneously venting the vial with an additional needle. Using a 22 G needle, targestar conjugation buffer (TCB, Targeson, Inc, San Diego, CA, USA) was withdrawn into the syringe containing the UCA particles to a total volume of 3.5 mL and centrifuged at 400 \times G for three minutes to remove excess free unincorporated lipids from the UCA particle solution. After centrifugation, the infranatant was drained drop-wise, and the UCAs were re-suspended in 1.0 mL TCB. Afterward, UCAs were incubated with 150 μ L FITC-streptavidin (Invitrogen, Carlsbad, CA, USA) at a concentration of 1 mg/mL for twenty minutes at RT with occasional gentle shaking of the vial. The unreacted FITC-streptavidin was removed in a centrifugal washing at 400 \times G for three

minutes similarly to the previous step and re-suspended in 1.0 mL TCB. Finally, the UCA particles were incubated on ice with either APA or PA-IL for 30 minutes while the unconjugated targeting antibody and ligand molecules were removed by a final centrifugal washing as was described in the previous steps.

Lectin-staining for biofilms

For the *S. aureus* biofilm matrix, a double staining approach with ConA and WGA was chosen (Goldstein et al. 1978, Strathmann et al. 2002). After incubation for twenty minutes in the dark at RT, excess staining solution was removed by rinsing three times with sterile distilled water.

Epifluorescence Microscopy

Epifluorescence microscopy was carried out with a Zeiss Axioskop 2 microscope equipped with an AxioCam MRc Rev 3. Negative and positive controls were conducted using epifluorescence microscopy. For each case, four biofilm samples were used to image five random positions on every sample. Each position was imaged by applying the respective filter for FITC, TRITC and DAPI. The negative control did not use any dyes to control for any possible autofluorescence effects.

Ultrasonic investigation of biofilms

Ultrasonic imaging and RF data acquisition was performed with a high-frequency scanning acoustic microscope (Fraunhofer IBMT, St. Ingbert, Germany). A detailed description of the acoustic lens used is shown in Table A.2.

The recorded RF data were stored for further processing. The post-processing was conducted using custom-written scripts in MATLAB (The Math-Works, Natick, MA, USA). The scripts were applied for the visual reconstruction in 2D and 3D of the raw RF data for the selected ROIs. RF raw signals were gated by applying a rectangular window function. The window length at 100 MHz excitation center frequency was set such as it corresponded to 10 wavelengths. The wavelength estimation is based on the center frequency of the lens (100 MHz).

The gating of RF raw time-signals allows estimations of scattering properties to be related to distinct ROIs in the volume under interrogation (Oelze et al. 2004). However, the gating process also allows unwanted frequency content to be added to the backscattered power spectrum that subsequently, leads to inaccurate estimates of scatterer properties. In order to minimize such unwanted effects, a Hamming window was applied (Oelze et al. 2004). The tapered windows reduced the high-frequency content added to the gated RF time-signals by smoothing the edges.

When the acoustic lens is moved over a ROI where the substrate is covered by an EPS layer under investigation, two echoes are received. One echo originates from the top surface of the layer, $S_0(t)$, and the second, $S(t)$, from the interface between the layer and the substrate. These signals can be written as follows (Briggs et al. 1993, Briggs 1995, Briggs et al. 2010):

$$S_0(t) = A_0 s(t - t_0) \times g(t, z_0) \quad (4.1)$$

$$S(t) = A_1 s(t - t_1) \times g(t, z_1) + A_2 s(t - t_2) \times g(t, z_2) \quad (4.2)$$

$S(t)$ is the reflected signal from the top and the sample-substrate interface of the EPS matrix. Provided that the defocus is positive meaning that the acoustic lens is elevated above the maximum focus position, it is adequate to constrain the function g to be independent of t and to be a real function of z only. The optimum value of z was found experimentally, by scanning along the z -axis and finding the minimum positive value at which the shape of the waveform remained approximately constant as a function of z . The z value was experimentally determined to be 900 μm . Within the approximation of the independence of the waveform shape on z , the signals can be written respectively as (Briggs et al. 1993):

$$S_0(t) = A_0 s(t - t_0) \times g(z_0) \quad (4.3)$$

$$S(t) = A_1 s(t - t_1) \times g(z_1) + A_2 s(t - t_2) \times g(z_2) \quad (4.4)$$

From the height of amplitude and position on the time axis of each maximum, the following parameters were measured:

$$\Delta T_{0/1} = t_0 - t_1 \quad (4.5)$$

$$\Delta T_{0/2} = t_0 - t_2 \quad (4.6)$$

where t_1 and t_2 are the arrival times of the sample and the interface echo respectively and t_0 is the time arrival of the reference signal (not shown) when no sample is placed in between the acoustic lens and the substrate. The velocity of the coupling medium, which in this case was degassed biofilm medium at 25 °C, was approximated to the velocity of distilled water and set to be 1497 m/s (Greenspan et al. 1959, Martin et al. 1959) while the attenuation of the same medium was set equal to the attenuation of distilled water at 25 °C, 2 dB/mm (Akashi et al. 1997). The density of the medium was calculated with a microbalance and a micropipette at 25 °C. From the density of the coupling medium, denoted as ρ_{cm} , and the respective ultrasonic velocity, denoted as v_{cm} , the acoustic impedance, Z_{cm} , of the coupling medium was deduced:

$$Z_{cm} = \rho_{cm} V_{cm} \quad (4.7)$$

From the difference in time between the reference signal, t_0 , and the reflection from the sample surface, t_1 , and by applying the velocity, v_0 , of the coupling medium, the thickness of the layer is:

$$d = \frac{1}{2}(t_0 - t_1)v_0 \quad (4.8)$$

From the ratio of magnitude of the reflection A_1 from the surface of the layer to the magnitude of the reference signal A_0 , and by applying the impedance Z_0 of the coupling medium as has been calculated in and the acoustic impedance of the substrate Z_s , the acoustic impedance of the biofilm sample is:

$$Z_{bf} = Z_0 \frac{A_0 + A_1}{A_0 - A_1} \quad (4.9)$$

Finally, from the amplitude A_2 of the echo from the interface between the layer and the substrate, the amplitude of the substrate echo A_0 , the attenuation in the cell, in units of Nepers per unit length, can be calculated as follows:

$$\alpha = \alpha_0 + \frac{1}{2d} \log_e \left(\frac{A_0}{A_2} \frac{Z_s - Z_{bf}}{Z_s + Z_{bf}} \frac{4(Z_c - Z_0)}{(Z_c - Z_0)^2} \frac{Z_s + Z_0}{Z_s - Z_0} \right) \quad (4.10)$$

Results

Biofilm formation occurs when bacterial cells enter the body and attach to the underlying endothelium or tissues. Over time, biofilms form a protective three-dimensional matrix that results in lower antibody efficacy *in vivo* (Figure A.1). Biofilm surface areas were assessed by epifluorescence microscopy images of stained *S. aureus* biofilms at various time points (Figure A.2A). Biofilm matrix surface area doubled during the first 12 hours after inoculation (growing from $26.85 \text{ mm}^2 \pm 6.72 \text{ mm}^2$ to $51.7 \text{ mm}^2 \pm 2.12 \text{ mm}^2$ at 12h and 24 h respectively; $p < 0.05$). Similar growth patterns were observed through 96 hours ($68.95 \text{ mm}^2 \pm 4.6 \text{ mm}^2$, $122.2 \text{ mm}^2 \pm 8.56 \text{ mm}^2$ and $179.2 \text{ mm}^2 \pm 2.97 \text{ mm}^2$ for 48 h, 72 h and 96 h respectively; $p < 0.05$). These data suggest that biofilm matrices are produced over time in our *in vitro* culture system.

To determine whether targeted UCAs bind to a biofilm matrix *in vitro*, we next examined whether targeted ultrasound contrast agents (UCAs) bound to the biofilm matrix over time. We observed an increase in the binding rate of targeted UCAs to the biofilm matrix (Figure A.2B). We tested whether labeled targeted UCAs were detectable upon a labeled biofilm matrix. Tetramethylrhodamine isothiocyanate (TRITC)-streptavidin conjugated UCAs (red staining) were detectable from fluorescein isothiocyanate (FITC) anti-WGA labeled matrix (green staining). At the 12 h time point $1.109 \times 10^3 \pm 142$ UCAs were bound to the biofilm. The number of bound bubbles significantly increased to $3.126 \times 10^3 \pm 427$ over the following 12 h. Between 24 h and 72 h labeled UCAs binding increased ($5.042 \times 10^3 \pm 285$ UCAs at 48 h, $7.563 \times 10^3 \pm 142$ at 72 h; $p < 0.05$). Between 72 h and 96 h a significant increase in targeted UCAs was observed ($7.563 \times 10^3 \pm 142$ to 21.985 ± 855 at 96 h; $p < 0.05$) suggesting that binding increases in correlation with biofilm matrix surface area. Fluorescence images stained for *S. aureus* biofilm matrix at various time points (Figure A.2A-D) confirms that targeted UCAs bound more as the biofilm matrix increased over 96 hours.

Developing a non-invasive diagnostic method to detect biofilm matrices early (or at initial stages) would be a valuable clinical tool if the targeted agents could be detected acoustically. Because we determined that targeted UCAs bind proportionately to biofilm matrix mass we next

assessed whether ultrasound could be used to detect targeted UCAs *in vitro*. The center frequency of the ultrasonic evaluation was 100 MHz (Good et al. 2006) allowing for a rigorous quantification of biofilm matrix mechanoelastic properties in our *in vitro* biofilm culture system (Table A.3).

For the physical evaluation of biofilm matrix properties (density, acoustic attenuation, ultrasound velocity, acoustic impedance and bulk modulus) a time-resolved high-frequency scanning acoustic microscope was used (Fraunhofer IBMT, St. Ingbert, Germany; Table A.2 and A.3). For imaging an acoustic lens is triggered by a piezoelectric transducer that emits and receives highly focused sound waves and resolved along the time axis (Figure A.3A). The echoes reflected from the sample surface, the substrate and the interface between the sample and the substrate were taken into consideration for mechanoelastic quantification. The acoustic lens is mounted on top of the stage of a Zeiss Axiovert M200, inverted light microscope (Figure A.3B). This custom arrangement (Weiss et al. 2007, Weiss et al. 2007), where the optical microscope objective and the acoustic lens are confocally aligned allows for corresponding optical (or fluorescence) imaging and therefore facilitating novel simultaneous acoustical and optical evaluation of specimen.

S. aureus mature biofilms at day five were ultrasonically and fluorescently evaluated (Figure A.4). UCAs were conjugated with TRITC-labeled streptavidin that allowed for the detection of the corresponding fluorescent signal. Because the acoustic lens is confocally aligned, we were able to overlay the corresponding acoustic and fluorescent signals. In each case, three or more different regions were scanned covering a total surface of 1 mm² for each independent acquisition. For the same time point, fluorescence and optical images were acquired from the identical regions (Figure A.4). The gray colored area corresponds to the acquired acoustic dataset of the biofilm matrix while the inset depicts a fluorescent image of a partial area within that ultrasonically acquired region. The epifluorescent images were comparable in terms of specimen location and provided different complementary information on the biofilm structure and

mechanical properties (Figure A.4). Microbubbles (Targeson, San Diego, USA) were 2 - 3 μm in diameter and were detected based on fluorescence and acoustic signals (Figure A.4).

We next examined whether regions of biofilm matrices can be delineated based on targeted and bound or non-targeted, non-bound UCAs. When no biofilm mass was present, the targeted UCAs remain unbound as there is no ligand for them to bind to (Figure A.5A). As biofilm matrix formation progresses, targeted UCAs bind to the ligand present in the biofilm matrix (Figure A.5B). Targeted UCAs bound to the biofilm matrix scattered sound and produced a detectable acoustic signature (Zinin et al. 2005, Zinin et al. 2009), which correlates with a biofilm matrix. The images shown in Figure A.4 depict both the corresponding optical and acoustic images of the UCAs. The acoustic image in Figure A.6A depicts UCAs reflectivity in backscatter intensity, and their spatial location is depicted as red signals in the fluorescent image. Furthermore, Figure A.6A demonstrates that bound UCAs provide a stronger backscatter intensity as compared to the regions of biofilm matrix alone.

Based on linear acoustics (Moran et al. 2002) the integrated backscatter coefficient and acoustic attenuation were calculated for regions of bound and unbound UCAs. The mean integrated backscatter coefficient (IBSC; Figure A.6) was determined for frequencies ranging from 97 MHz to 104 MHz from the measured biofilm regions in which targeted UCAs were bound versus biofilm matrix alone. This frequency range corresponded to 36 points at a sampling frequency of 400 MHz while the scanning of the region of interests (ROIs) was performed with step sizes in the order of 10 μm in the x- and y-direction respectively. The acquired mean values of the IBSCs for the ROIs that remained bound to targeted UCAs range from $0.0278 \text{ mm}^{-1} \times \text{sr}^{-1}$ to $0.0848 \text{ mm}^{-1} \times \text{sr}^{-1}$ while the values for the standard deviation (StDev) vary from $0.0016 \text{ mm}^{-1} \times \text{sr}^{-1}$ to $0.0043 \text{ mm}^{-1} \times \text{sr}^{-1}$. The evaluation of the ROIs corresponding to the matrix without UCA yielded for the IBSCs mean values in the range from $0.0167 \text{ mm}^{-1} \times \text{sr}^{-1}$ to $0.0694 \text{ mm}^{-1} \times \text{sr}^{-1}$ with StDev values ranging from $0.0012 \text{ mm}^{-1} \times \text{sr}^{-1}$ to $0.0024 \text{ mm}^{-1} \times \text{sr}^{-1}$ respectively.

The same ROIs used for the quantification of the IBSC were further evaluated with regard to sound attenuation (Figure A.6B). ROIs were analyzed in which UCAs were either bound to the

matrix or not bound. Each of the fifteen ROIs per condition consisted of nine pixels corresponding to 135 raw radio-frequency (RF) time-signals for the UCA ROIs and similarly fifteen ROIs for the matrix ROIs corresponding to another 135 raw RF time-signals. The frequency-dependent attenuation was calculated over the frequency range from 97 MHz to 104 MHz. Equivalent to our IBSC findings this frequency range consisted of 36 points at a sampling frequency of 400 MHz. The attenuation graphs for the ROIs with bound targeted UCAs and the ROIs with plain matrix over the selected frequency range are shown in Figure A.6B. Taken together, detection of targeted bound UCAs is significant compared with unbound UCAs. Our data highlight the potential of targeted UCAs as a means of molecular imaging to detect the early stages of biofilm matrix formation.

Conclusions

In this study, we report for the first time a combined optical and acoustic imaging method of infectious biofilm matrices. Ligand-targeted UCAs were used as a novel method for pre-clinical non-invasive molecular imaging of early to late stage biofilms. These agents were used to target *S. aureus* biofilm formation and assess the binding efficacy on early to late stage biofilm matrices with respect to their surface area. A combination of acoustic and optical microscopy was used to quantify *S. aureus* biofilm mechanoelastic properties. We show that time-resolved high-frequency SAM is a viable method for ultrasonic imaging in addition to quantifying mechanical and elastic properties of soft materials (e.g., tissues, cells, biofilm matrices) in a non-invasive setting. Moreover, the use of targeted UCAs with high-frequency SAM allow for UCAs detection at higher frequencies other than their resonance frequency. The mechanoelastic properties of the *S. aureus* biofilm matrix are summarized in Table A.3.

Biofilms occurring from infections pose a challenge to current medicine because of the difficulty of early detection and diagnosis. Biofilms protect bacteria and promote resistance to antibiotics and chemotherapeutic agents. Moreover, detecting early and late biofilm formation may be problematic due to their dynamic profile. Individual bacterial cells may detach from the biofilm to colonize other niches, or an entire biofilm colony may move as a whole across a region (Hall-Stoodley et al. 2004). Thus, biofilm-mediated rippling effects that occur during detachment and transmigration pose biomedical challenges. One example is ventilator-associated pneumonia in immunologically compromised patients that may occur due to biofilm rippling (e.g., cancer patients) (Inglis 1993). Our data indicates that the binding efficiency of UCAs correlates with matrix biomass. Thus, we propose that the rolling and rippling effects observed during biofilm maturation may reduce biomass and, therefore, decrease imaging capabilities at the late stages of biofilm matrix formation. It may be that there is a critical timeframe where UCAs bind well and imaging is enhanced and that as the biofilm grows, detaches and ripples binding is decreased. Developing better detection methodologies and hence diagnostic clinical imaging methods are needed to assess biofilm formation early. By detection of biofilm infections at their earlier stages, this method will potentially offer more treatment.

Due to the complex structure of biofilm matrices, we focused on the lectins concanavalin A and WGA (binds to β -GlcNAc₂ (Goldstein et al. 1978, Strathmann et al. 2002) because biofilms may switch between these two polysaccharides during growth (Table A.1). Targeting carbohydrate epitopes that are present in early biofilm matrices may provide novel biofilm markers that will enhance a more optimal molecular imaging, particularly at early-stage formation.

Ultrasound imaging devices are readily available in clinical settings and the application of ultrasound techniques for biofilm-relevant infections is familiar to hospital personnel for diseases such as infective endocarditis (Archibald et al. 1997, Baddour et al. 2005, Kaplan 2005) and cancer (Azzopardi et al. 2013). Targeted UCAs have the potential to recognize and bind to early stage biofilm matrix and thus, facilitate an early diagnosis. Our study demonstrated that while more targeted UCAs bound to larger biofilm matrix mass, a significant number of targeted UCAs also bound to less developed biofilm matrices. Targeted UCAs with ultrasound imaging may provide a means for early detection of biofilm formation within a non-invasive setting. This would include detecting endocarditis and biofilm matrix formation at the site of medical implants such as prosthetic devices, and catheters. Moreover, cancer patients rely on *catheterization* for chemotherapy treatment and biofilms are prevalent at the catheter interface. In immunologically compromised patients, rippling effects of the late stage biofilms have been reported to promote biofilm transmigration to the lungs causing additional complications in treatment (Inglis et al. 1995, Al Akhrass et al. 2012). Thus, the use of targeted UCAs may provide a rapid method to facilitate early diagnosis of pathological conditions.

High-frequency ultrasound may be used to assess biofilm development *in vitro*. Currently clinical biomicroscopy uses frequencies in the range of 15-50 MHz including intravascular ultrasound spectroscopy (IVUS), cardiovascular and ocular applications (Liang et al. 2003, Goertz et al. 2006, Silverman et al. 2006, Goertz et al. 2007, Silverman 2009, Phillips et al. 2012). In particular, clinical imaging applications, such as detecting metastases in the eye, are in the range of 15-50 MHz, although research has been performed to measure at the higher

frequency of 75 MHz (Silverman et al. 2006). The use of higher frequencies in the range of 100 MHz has been used for the imaging of choroidal metastasis (Witkin et al. 2012). Clinical ultrasound applications have focused on higher frequencies in the range of 100-200 MHz (Knsplik et al. 2000). Low resonance frequencies are used clinically for drug delivery applications in conjunction with UCAs and targeted drug delivery as these low frequencies induce microbubble rupture (Liu et al. 2006). Thus, in terms of imaging the higher frequencies provide enhanced imaging capabilities whereas lower resonant frequencies allow for more efficient targeted drug delivery. We report for the first time a method to quantify backscatter intensity and mechanoelastic properties of biofilms (Saijo et al. 1998, Saijo et al. 2000, Saijo et al. 2004, Saijo et al. 2007, Brand et al. 2008, Strohm et al. 2010). With regard to the integrated backscatter and the acoustic attenuation, considering differences in the frequency domain, similar values have been previously reported for cancer cells and tissues (Saijo et al. 1997, Saijo et al. 1998, Saijo et al. 2004, Baddour et al. 2005, Brand et al. 2008, Strohm et al. 2010). A more in-depth understanding of the three-dimensional biofilm matrix structural and mechanoelastic parameters will enhance biofilm imaging and subsequent treatment. Targeted UCAs potentially provide a novel means of imaging for the diagnosis of biofilm infections *in vivo*.

Figures

This page has been left blank intentionally.

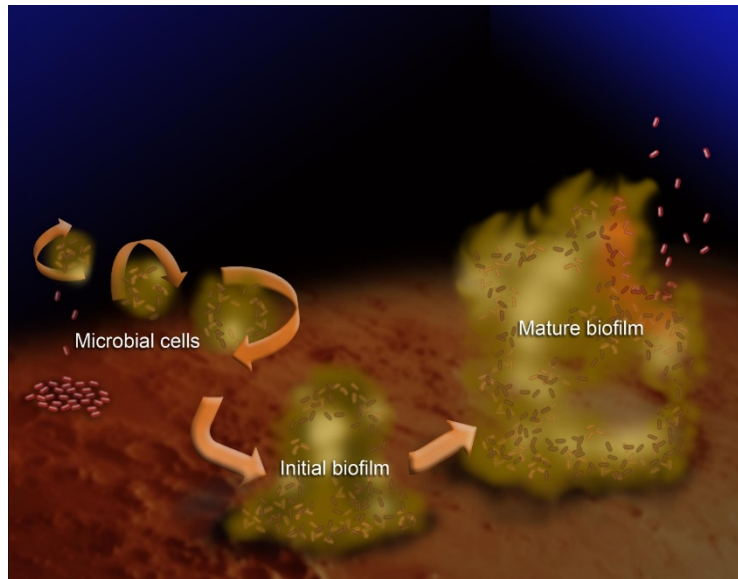


Figure A.1

Biofilm matrix formation

Individual bacterial cells gain entrance into the bloodstream and attach at favorable sites. As they continue growing, they form a protective biofilm matrix around them to withstand against hostile agents, the immune system or fluid turbulences caused by the bloodstream. As the biofilm mass matures, individual cells are dispersed into the bloodstream where they travel to distant sites in the body to form colonies.

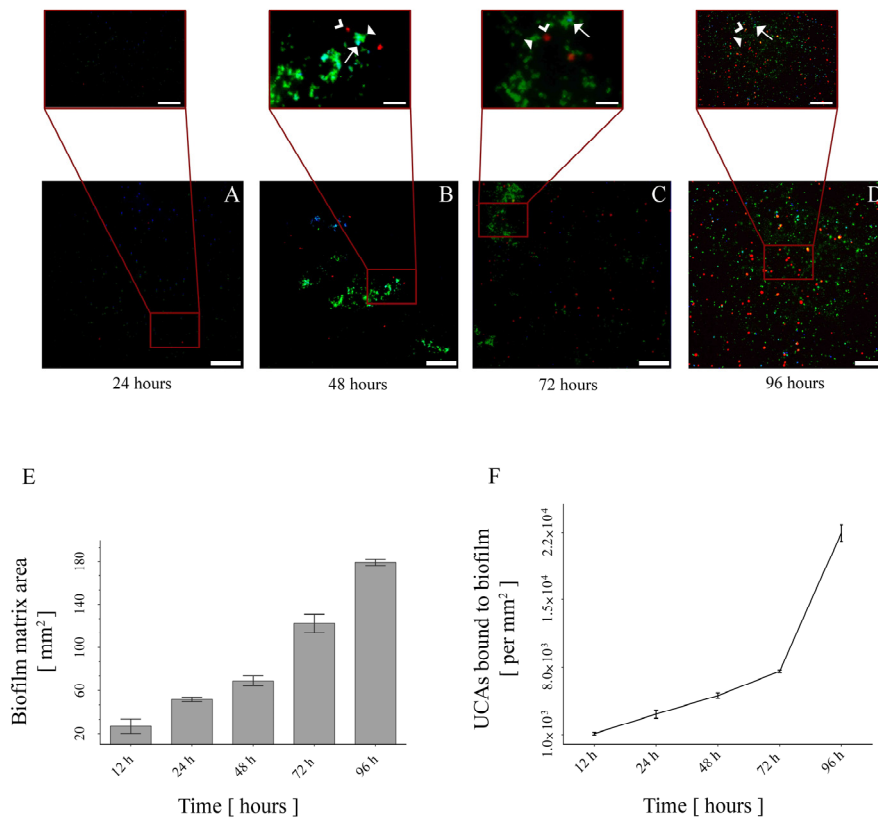


Figure A.2

Targeted ultrasound contrast agents as a function of biofilm matrix mass.

Targeted ultrasound contrast agents bind to the biofilm mass. As the biofilm matrix continues growing, the increased surface area is accompanied by a larger number of bound agents. (A) Biofilm mass over a time course of 96 hours at 12 h, 24 h, 48 h, 72 h and 96 h in terms of surface as the biofilm grows. (B) Number of targeted UCAs bound to the biofilm matrix over the same time course as in A at 12 h, 24 h, 48 h, 72 h and 96 h. (C) Confocal scanning laser microscopy imaging of the biofilm structure for 12 h, 24 h, 48 and 96 respectively. Bacterial cells are shown

in blue due to the nucleic staining, tUCAs are shown in red due to the conjugated streptavidin, and the biofilm matrix is shown in green due to the FITC-conjugated WGA.

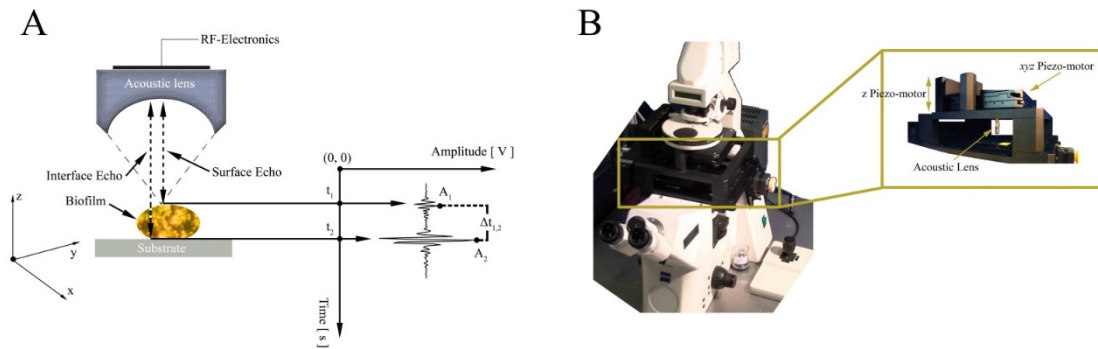


Figure A.3

High-frequency scanning acoustic microscopy at a center frequency of 100 MHz was used for the imaging and quantification of the biofilm structure

(A) A piezoelectric transducer transmits highly focused ultrasound beams directed against the sample under investigation. As the ultrasound waves travel through the sample and the medium, echoes are returned and recorded by the same acoustic lens. The echoes are resolved on the time axis and allow for a rigorous quantification. (B) The scanning acoustic microscopy unit is mounted on top of an inverted light microscope and thus allowing a correlation of the same regions in terms of optical or fluorescence and acoustical information retrieved in independent stages.

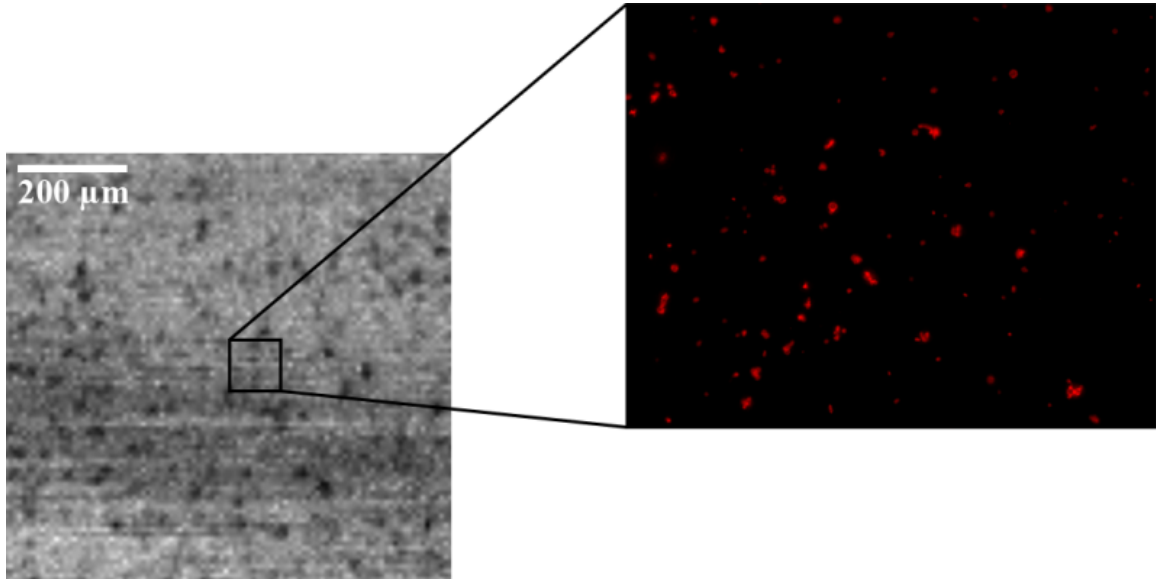


Figure A.4

Ultrasound and optical/fluorescent images

A 1×1 mm area of the biofilm sample was scanned at a center frequency of 100 MHz using the high-frequency scanning acoustic microscope. Darker spots indicate bound UCAs on the biofilm mass. The inset shows a smaller region imaged by fluorescence microscopy on the same sample.

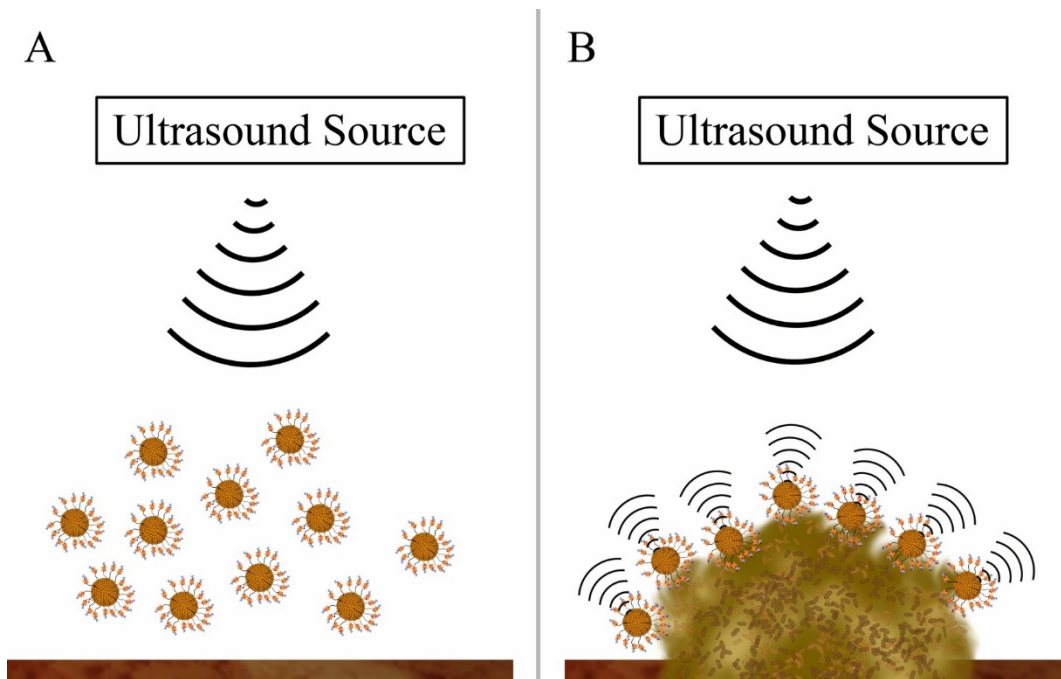


Figure A.5

Targeted UCAs bind the biofilm matrix and are detected by ultrasound

(A) Ultrasound is emitted by an ultrasound source against a region of interest where no biofilm mass is present. Consequently, targeted UCAs will float in the liquid unbound remaining unresponsive to ultrasound. (B) Biofilm formation shown with bound targeted ultrasound contrast agents. The agents will bind to the exopolysaccharide matrix of the biofilm due to the interaction of the interaction between the conjugated antibody and its counterpart based on Emil Fisher's key and lock principle.

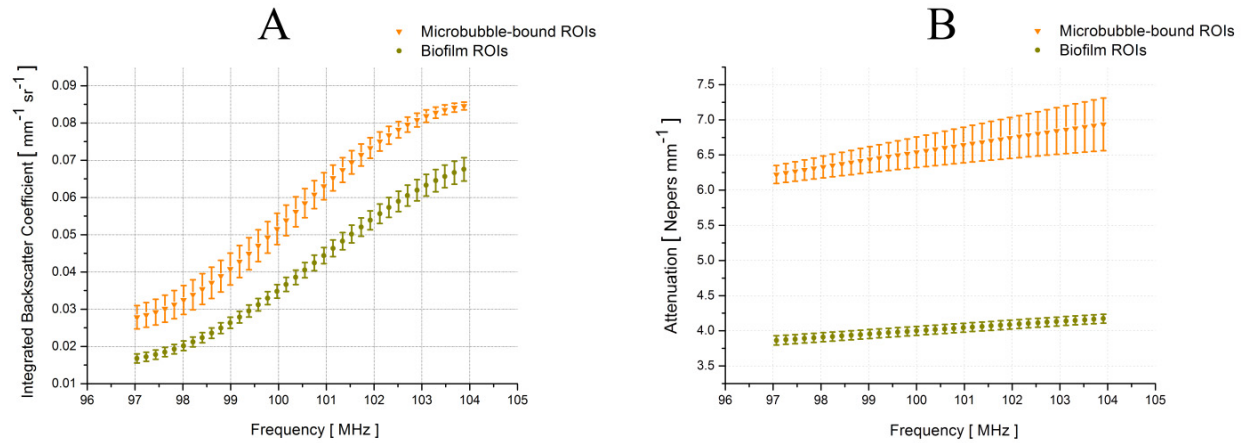


Figure A.6

Ultrasound quantification of biofilm structure using targeted UCAs

Biofilm structure quantified with scanning acoustic microscopy. (A) Integrated backscatter shown for a range of different frequencies from 97 MHz to 104 MHz. Regions where targeted UCAs are bound to the biofilm exhibit stronger backscatter and thus allowing for a detection of biofilm infection. (B) Attenuation of sound for the same frequency range as in A. Regions with bound targeted agents show a significantly higher sound attenuation than regions with no bound agents. The different sound signature of bound vs. non-bound regions could potentiate an easier diagnosis of infected regions.

Tables

This page has been left blank intentionally.

Lectin	Abbreviation	Conjugate	Main specificity	Reference
Concanavalin A (<i>Canavalia ensiformis</i>)	ConA	FITC, TRITC	α -Man, α -Glc	(Goldstein et al. 1978)
Wheat germ agglutinin (<i>Triticum vulgare</i>)	WGA	FITC, TRITC	(β -GlcNAc) ₂ , NeuNAc	

Table A.1

Carbohydrate-binding specificity of lectins employed for staining of *S. aureus* biofilms.

Acoustic Lens Properties	
Excitation Center Frequency [MHz]	100
Max PRF [kHz]	100
Gain [dB]	40
Sampling Rate [MSamples/s]	400
Focal Resolution [μm]	10
Aperture [μm]	950
Aperture Angle [$^\circ$]	55
Working Distance [μm]	900

Table A.2

Physical properties of high-frequency ultrasound lens for the scanning acoustic microscope used in the current study.

Physical property [unit]	Numerical value
Thickness [μm]	127.23 ± 2.87
Ultrasound velocity [m/s]	1523.14 ± 12.01
Attenuation [Neper/mm]	4.8 ± 0.92
Acoustic impedance [MRayl]	1.9 ± 0.01
Density [g/mm^3]	1.24658 ± 0.11
Young's modulus [GPa]	$0.0028 \pm 2.9 \times 10^{-5}$

Table A.3

Mechanical and elastic parameters of a mature *S. aureus* biofilm at 96 hours of growth under static culture conditions.

References

Aberle, H., H. Schwartz and R. Kemler (1996). "Cadherin-catenin complex: Protein interactions and their implications for cadherin function." Journal of Cellular Biochemistry **61**(4): 514-523.

Abu-Ghazaleh, R., J. Kabir, H. Jia, M. Lobo and I. Zachary (2001). "Src mediates stimulation by vascular endothelial growth factor of the phosphorylation of focal adhesion kinase at tyrosine 861, and migration and anti-apoptosis in endothelial cells." Biochem J **360**(1): 255-264.

Adams, D. J., J. Barakeh, R. Laskey and C. Van Breemen (1989). "Ion channels and regulation of intracellular calcium in vascular endothelial cells." FASEB J **3**(12): 2389-2400.

Adams, H., W. Brummelhuis, B. Maassen, N. van Egmond, M. El Khattabi, F. Detmers, P. Hermans, B. Braam, J. Stam and T. Verrips (2009). "Specific immuno capturing of the staphylococcal superantigen toxic-shock syndrome toxin-1 in plasma." Biotechnol Bioeng **104**(1): 143-151.

Adams, M. D., A. R. Kerlavage, R. D. Fleischmann, R. A. Fuldner, C. J. Bult, N. H. Lee, E. F. Kirkness, K. G. Weinstock, J. D. Gocayne, O. White and et al. (1995). "Initial assessment of human gene diversity and expression patterns based upon 83 million nucleotides of cDNA sequence." Nature **377**(6547): 3-174.

Adembri, C., E. Sgambati, L. Vitali, V. Selmi, M. Margheri, A. Tani, L. Bonaccini, D. Nosi, A. L. Caldini, L. Formigli and A. R. De Gaudio (2011). "Sepsis induces albuminuria and alterations in the glomerular filtration barrier: a morphofunctional study in the rat." Crit Care **15**(6): R277.

Adler, H. E. and A. J. DaMassa (1979). "Toxicity of endotoxin to chicks." Avian Dis **23**(1): 174-178.

Aghajanian, A., E. S. Wittchen, M. J. Allingham, T. A. Garrett and K. Burrige (2008). "Endothelial cell junctions and the regulation of vascular permeability and leukocyte transmigration." J Thromb Haemost **6**(9): 1453-1460.

Aird, W. C. (2001). "Vascular bed-specific hemostasis: role of endothelium in sepsis pathogenesis." Crit Care Med **29**(7): S28-34; discussion S34-25.

Aird, W. C. (2003). "Endothelial cell heterogeneity." Crit Care Med **31**(4 Suppl): S221-230.

Aird, W. C. (2003). "The role of the endothelium in severe sepsis and multiple organ dysfunction syndrome." Blood **101**(10): 3765-3777.

Aird, W. C. (2007). "Phenotypic heterogeneity of the endothelium: I. Structure, function, and mechanisms." Circ Res **100**(2): 158-173.

Aird, W. C. (2007). "Phenotypic heterogeneity of the endothelium: II. Representative vascular beds." Circ Res **100**(2): 174-190.

Aird, W. C. (2012). "Endothelial cell heterogeneity." Cold Spring Harb Perspect Med **2**(1): 6429.

Akashi, N., J. Kushibiki and F. Dunn (1997). "Acoustic properties of egg yolk and albumen range 20-400 MHz." Journal of the Acoustical Society of America **102**(6): 3774-3778.

Akimoto, S., M. Mitsumata, T. Sasaguri and Y. Yoshida (2000). "Laminar shear stress inhibits vascular endothelial cell proliferation by inducing cyclin-dependent kinase inhibitor p21(Sdi1/Cip1/Waf1)." Circ Res **86**(2): 185-190.

Aktories, K., U. Braun, S. Rosener, I. Just and A. Hall (1989). "The rho gene product expressed in E. coli is a substrate of botulinum ADP-ribosyltransferase C3." Biochem Biophys Res Commun **158**(1): 209-213.

Aktories, K. and A. Hall (1989). "Botulinum ADP-ribosyltransferase C3: a new tool to study low molecular weight GTP-binding proteins." Trends Pharmacol Sci **10**(10): 415-418.

Aktories, K., C. Mohr and G. Koch (1992). "Clostridium botulinum C3 ADP-ribosyltransferase." Curr Top Microbiol Immunol **175**: 115-131.

Aktories, K., U. Weller and G. S. Chhatwal (1987). "Clostridium botulinum type C produces a novel ADP-ribosyltransferase distinct from botulinum C2 toxin." FEBS Lett **212**(1): 109-113.

Aktories, K., C. Wilde and M. Vogelsang (2004). "Rho-modifying C3-like ADP-ribosyltransferases." Rev Physiol Biochem Pharmacol **152**: 1-22.

Al Akhrass, F., I. Al Wohoush, A. M. Chaftari, R. Reitzel, Y. Jiang, M. Ghannoum, J. Tarrand, R. Hachem and I. Raad (2012). "Rhodococcus Bacteremia in Cancer Patients Is Mostly Catheter Related and Associated with Biofilm Formation." Plos One **7**(3).

Alcaide, P., R. Martinelli, G. Newton, M. R. Williams, A. Adam, P. A. Vincent and F. W. Lusinskas (2012). "p120-Catenin prevents neutrophil transmigration independently of RhoA inhibition by impairing Src dependent VE-cadherin phosphorylation." American Journal of Cell Physiology **303**(4): C385-C395.

Ali, J., F. Liao, E. Martens and W. A. Muller (1997). "Vascular endothelial cadherin and role in (VE-cadherin): Cloning endothelial cell-cell adhesion." Microcirculation-London **4**(2): 267-277.

Allison, D. G. and P. Gilbert (1995). "Modification by surface association of antimicrobial susceptibility of bacterial-populations." Journal of Industrial Microbiology **15**(4): 311-317.

Allison, D. G., B. Ruiz, C. SanJose, A. Jaspe and P. Gilbert (1998). "Extracellular products as mediators of the formation and detachment of Pseudomonas fluorescens biofilms." Fems Microbiology Letters **167**(2): 179-184.

Anastasiadis, P. Z. and A. B. Reynolds (2000). "The p120 catenin family: complex roles in adhesion, signaling and cancer." J Cell Sci **113**(8): 1319-1334.

Anderson, C. R., X. Hu, H. Zhang, J. Tlaxca, A.-E. Decleves, R. Houghtaling, K. Sharma, M. Lawrence, K. W. Ferrara and J. J. Rychak (2011). "Ultrasound Molecular Imaging of Tumor Angiogenesis With an Integrin Targeted Microbubble Contrast Agent." Investigative Radiology **46**(4): 215-224.

Andriopoulou, P., P. Navarro, A. Zanetti, M. G. Lampugnani and E. Dejana (1999). "Histamine induces tyrosine phosphorylation of endothelial cell-to-cell adherens junctions." Arterioscler Thromb Vasc Biol **19**(10): 2286-2297.

Angst, B. D., C. Marozzi and A. I. Magee (2001). "The cadherin superfamily: diversity in form and function." J Cell Sci **114**(4): 629-641.

Angus, D. C., W. T. Linde-Zwirble, J. Lidicker, G. Clermont, J. Carcillo and M. R. Pinsky (2001). "Epidemiology of severe sepsis in the United States: analysis of incidence, outcome, and associated costs of care." Crit Care Med **29**(7): 1303-1310.

Angus, D. C., C. A. Pereira and E. Silva (2006). "Epidemiology of severe sepsis around the world." Endocr Metab Immune Disord Drug Targets **6**(2): 207-212.

Angus, D. C. and T. van der Poll (2013). "Severe sepsis and septic shock." N Engl J Med **369**(21): 2063.

Annecke, T., D. Chappell, C. Chen, M. Jacob, U. Welsch, C. P. Sommerhoff, M. Rehm, P. F. Conzen and B. F. Becker (2010). "Sevoflurane preserves the endothelial glycocalyx against ischaemia-reperfusion injury." Br J Anaesth **104**(4): 414-421.

Antonetti, D. A., A. J. Barber, L. A. Hollinger, E. B. Wolpert and T. W. Gardner (1999). "Vascular endothelial growth factor induces rapid phosphorylation of tight junction proteins occludin and zonula occluden 1. A potential mechanism for vascular permeability in diabetic retinopathy and tumors." J Biol Chem **274**(33): 23463-23467.

Antonetti, D. A., A. J. Barber, S. Khin, E. Lieth, J. M. Tarbell and T. W. Gardner (1998). "Vascular permeability in experimental diabetes is associated with reduced endothelial occludin content: vascular endothelial growth factor decreases occludin in retinal endothelial cells. Penn State Retina Research Group." Diabetes **47**(12): 1953-1959.

Antonny, B., D. Madden, S. Hamamoto, L. Orci and R. Schekman (2001). "Dynamics of the COPII coat with GTP and stable analogues." Nat Cell Biol **3**(6): 531-537.

Apolloni, S., P. Fabbri, C. Parisi, S. Amadio and C. Volonté (2014). "Clemastine Confers Neuroprotection and Induces an Anti-Inflammatory Phenotype in SOD1G93A Mouse Model of Amyotrophic Lateral Sclerosis." Molecular Neurobiology: 1-14.

Arap, W., M. G. Kolonin, M. Trepel, J. Lahdenranta, M. Cardo-Vila, R. J. Giordano, P. J. Mintz, P. U. Ardel, V. J. Yao, C. I. Vidal, L. Chen, A. Flamm, H. Valtanen, L. M. Weavind, M.

E. Hicks, R. E. Pollock, G. H. Botz, C. D. Bucana, E. Koivunen, D. Cahill, P. Troncoso, K. A. Baggerly, R. D. Pentz, K.-A. Do, C. J. Logothetis and R. Pasqualini (2002). "Steps toward mapping the human vasculature by phage display." Nature medicine **8**(2): 121-127.

Archibald, L. K. and R. P. Gaynes (1997). "Hospital-acquired infections in the United States. The importance of interhospital comparisons." Infect Dis Clin North Am **11**(2): 245-255.

Armstrong, L.-J., V. L. Heath, S. Sanderson, S. Kaur, J. F. J. Beesley, J. M. J. Herbert, J. A. Legg, R. Poulsom and R. Bicknell (2008). "ECM2, an endothelial specific filamin A binding protein that mediates chemotaxis." Arteriosclerosis, Thrombosis, and Vascular Biology **28**(9): 1640-1646.

Arnalich, F., E. Garcia-Palomero, J. Lopez, M. Jimenez, R. Madero, J. Renart, J. J. Vazquez and C. Montiel (2000). "Predictive value of nuclear factor kappaB activity and plasma cytokine levels in patients with sepsis." Infect Immun **68**(4): 1942-1945.

Asahara, T., H. Masuda, T. Takahashi, C. Kalka, C. Pastore, M. Silver, M. Kearne, M. Wagner and J. M. Isner (1999). "Bone marrow origin of endothelial progenitor cells responsible for postnatal vasculogenesis in physiological and pathological neovascularization." Circ Res **85**(3): 221-228.

Asahara, T., T. Murohara, A. Sullivan, M. Silver, R. van der Zee, T. Li, B. Witzenbichler, G. Schatteman and J. M. Isner (1997). "Isolation of putative progenitor endothelial cells for angiogenesis." Science **275**(5302): 964-967.

Atkins, G. B., M. K. Jain and A. Hamik (2011). "Endothelial differentiation: molecular mechanisms of specification and heterogeneity." Arterioscler Thromb Vasc Biol **31**(7): 1476-1484.

Aziz, M., A. Jacob, W.-L. Yang, A. Matsuda and P. Wang (2013). "Current trends in inflammatory and immunomodulatory mediators in sepsis." Journal of leukocyte biology **93**(3): 329-342.

Azzopardi, E. A., E. L. Ferguson and D. W. Thomas (2013). "The enhanced permeability retention effect: a new paradigm for drug targeting in infection." J Antimicrob Chemother **68**(2): 257-274.

Bacabac, R. G., T. H. Smit, S. C. Cowin, J. J. Van Loon, F. T. Nieuwstadt, R. Heethaar and J. Klein-Nulend (2005). "Dynamic shear stress in parallel-plate flow chambers." J Biomech **38**(1): 159-167.

Baddour, L. M., M. A. Bettmann, A. F. Bolger, A. E. Epstein, P. Ferrieri, M. A. Gerber, M. H. Gewitz, A. K. Jacobs, M. E. Levison, J. W. Newburger, T. J. Pallasch, W. R. Wilson, R. S. Baltimore, D. A. Falace, S. T. Shulman, L. Y. Tani and K. A. Taubert (2003). "Nonvalvular cardiovascular device-related infections." Circulation **108**(16): 2015-2031.

Baddour, L. M., W. R. Wilson, A. S. Bayer, V. G. J. Fowler, A. F. Bolger, M. E. Levison, P. Ferrieri, M. A. Gerber, L. Y. Tani, M. H. Gewitz, D. C. Tong, J. M. Steckelberg, R. S. Baltimore, S. T. Shulman, J. C. Burns, D. A. Falace, J. W. Newburger, T. J. Pallasch, M. T. Takahashi and K. A. Taubert (2005). "Infective endocarditis: Diagnosis, antimicrobial therapy, and management of complications." Circulation **112**(15): 2373.

Baddour, R. E., M. D. Sherar, J. W. Hunt, G. J. Czarnota and M. C. Kolios (2005). "High-frequency ultrasound scattering from microspheres and single cells." Journal of the Acoustical Society of America **117**(2): 934-943.

Bahlmann, F. H., K. De Groot, J. M. Spandau, A. L. Landry, B. Hertel, T. Duckert, S. M. Boehm, J. Menne, H. Haller and D. Fliser (2004). "Erythropoietin regulates endothelial progenitor cells." Blood **103**(3): 921-926.

Bahlmann, F. H., K. DeGroot, T. Duckert, E. Niemczyk, E. Bahlmann, S. M. Boehm, H. Haller and D. Fliser (2003). "Endothelial progenitor cell proliferation and differentiation is regulated by erythropoietin - Rapid communication." Kidney International **64**(5): 1648-1652.

Bajaj, M. S., M. N. Kuppuswamy, A. N. Manepalli and S. P. Bajaj (1999). "Transcriptional expression of tissue factor pathway inhibitor, thrombomodulin and von Willebrand factor in normal human tissues." Thrombosis and haemostasis **82**(3): 1047-1052.

Baldassarri, L., L. Montanaro, R. Creti and C. R. Arciola (2007). "Underestimated collateral effects of antibiotic therapy in prosthesis-associated bacterial infections." International Journal of Artificial Organs **30**: 786-791.

Baldwin, A. L. and G. Thurston (2001). "Mechanics of endothelial cell architecture and vascular permeability." Crit Rev Biomed Eng **29**(2): 247-278.

Ballermann, B. J., A. Dardik, E. Eng and A. Liu (1998). "Shear stress and the endothelium." Kidney Int Suppl **67**: S100-108.

Balyasnikova, I. V., R. Metzger, D. J. Visintine, V. Dimasius, Z. L. Sun, Y. V. Berestetskaya, T. D. McDonald, D. T. Curiel, R. D. Minshall and S. M. Danilov (2005). "Selective rat lung endothelial targeting with a new set of monoclonal antibodies to angiotensin I-converting enzyme." Pulm Pharmacol Ther **18**(4): 251-267.

Barbacid, M. (1987). "Ras genes." Annual Review of Biochemistry **56**(1): 779-827.

Bass-Zubek, A. E., L. M. Godsel, M. Delmar and K. J. Green (2009). "Plakophilins: multifunctional scaffolds for adhesion and signaling." Curr Opin Cell Biol **21**(5): 708-716.

Baumeister, U., R. Funke, K. Ebnet, H. Vorschmitt, S. Koch and D. Vestweber (2005). "Association of Csk to VE-cadherin and inhibition of cell proliferation." The EMBO Journal **24**(9): 1686-1695.

Baumer, Y., V. Spindler, R. C. Werthmann, M. Bunemann and J. Waschke (2009). "Role of Rac 1 and cAMP in Endothelial Barrier Stabilization and Thrombin-induced Barrier Breakdown." Journal of Cellular Physiology **220**(3): 716-726.

Bazzoni, G. (2006). "Endothelial tight junctions: permeable barriers of the vessel wall." Thromb Haemost **95**(1): 36-42.

Bazzoni, G. and E. Dejana (2004). "Endothelial cell-to-cell junctions: molecular organization and role in vascular homeostasis." Physiol Rev **84**(3): 869-901.

Bazzoni, G. and E. Dejana (2004). "Endothelial cell-to-cell junctions: molecular organization and role in vascular homeostasis." Physiological reviews **84**(3): 869-901.

Becker, B. F., D. Chappell and M. Jacob (2010). "Endothelial glycocalyx and coronary vascular permeability: the fringe benefit." Basic Res Cardiol **105**(6): 687-701.

Beckers, C. M., V. W. van Hinsbergh and G. P. van Nieuw Amerongen (2010). "Driving Rho GTPase activity in endothelial cells regulates barrier integrity." Thromb Haemost **103**(1): 40-55.

Bedolla, R. G., Y. Wang, A. Asuncion, K. Chamie, S. Siddiqui, M. M. Mudryj, T. J. Prihoda, J. Siddiqui, A. M. Chinnaiyan, R. Mehra, R. W. de Vere White and P. M. Ghosh (2009).

"Nuclear versus cytoplasmic localization of filamin A in prostate cancer: immunohistochemical correlation with metastases." Clin Cancer Res **15**(3): 788-796.

Bellanger, J. M., C. Astier, C. Sardet, Y. Ohta, T. P. Stossel and A. Debant (2000). "The Rac1- and RhoG-specific GEF domain of Trio targets filamin to remodel cytoskeletal actin." Nat Cell Biol **2**(12): 888-892.

Bendayan, M. (2002). "Morphological and cytochemical aspects of capillary permeability." Microsc Res Tech **57**(5): 327-349.

Berczi, I., L. Bertok and T. Bereznai (1966). "Comparative studies on the toxicity of Escherichia coli lipopolysaccharide endotoxin in various animal species." Can J Microbiol **12**(5): 1070-1071.

Berczi, I., L. Bertok and T. Bereznai (1966). "Comparative studies on the toxicity of Escherichia coli lipopolysaccharide endotoxin in various animal species." Canadian journal of microbiology **12**(5): 1070-1071.

Bevan, H. S., S. C. Slater, H. Clarke, P. A. Cahill, P. W. Mathieson, G. I. Welsh and S. C. Satchell (2011). "Acute laminar shear stress reversibly increases human glomerular endothelial cell permeability via activation of endothelial nitric oxide synthase." American Journal of Physiology - Renal Physiology **301**(4): F733-F742.

Bhullar, I. S., Y. S. Li, H. Miao, E. Zandi, M. Kim, J. Y. Shyy and S. Chien (1998). "Fluid shear stress activation of IkappaB kinase is integrin-dependent." J Biol Chem **273**(46): 30544-30549.

Bishop, A. L. and A. Hall (2000). "Rho GTPases and their effector proteins." Biochem J **348**(2): 241-255.

Blackwell, T. S. and J. W. Christman (1996). "Sepsis and cytokines: current status." British journal of anaesthesia **77**(1): 110-117.

Blum, M. S., E. Toninelli, J. M. Anderson, M. S. Balda, J. Zhou, L. O'Donnell, R. Pardi and J. R. Bender (1997). "Cytoskeletal rearrangement mediates human microvascular endothelial tight junction modulation by cytokines." Am J Physiol **273**(1): H286-294.

Boado, R. J., J. Y. Li, M. Nagaya, C. Zhang and W. M. Pardridge (1999). "Selective expression of the large neutral amino acid transporter at the blood-brain barrier." Proc Natl Acad Sci U S A **96**(21): 12079-12084.

Bogatcheva, N. V., M. A. Zemskova, Y. Kovalenkov, C. Poirier and A. D. Verin (2009). "Molecular mechanisms mediating protective effect of cAMP on lipopolysaccharide (LPS)-induced human lung microvascular endothelial cells (HLMVEC) hyperpermeability." J Cell Physiol **221**(3): 750-759.

Bognar, Z., V. Foldi, B. Rezman, L. Bogar and C. Csontos (2010). "Extravascular lung water index as a sign of developing sepsis in burns." Burns : journal of the International Society for Burn Injuries **36**(8): 1263-1270.

Bone, R. C., R. A. Balk, F. B. Cerra, R. P. Dellinger, A. M. Fein, W. A. Knaus, R. M. Schein and W. J. Sibbald (1992). "Definitions for sepsis and organ failure and guidelines for the use of innovative therapies in sepsis. The ACCP/SCCM Consensus Conference Committee. American College of Chest Physicians/Society of Critical Care Medicine." Chest **101**(6): 1644-1655.

Bonne, S., B. Gilbert, M. Hatzfeld, X. Chen, K. J. Green and F. van Roy (2003). "Defining desmosomal plakophilin-3 interactions." J Cell Biol **161**(2): 403-416.

Boo, Y. C., G. Sorescu, N. Boyd, I. Shiojima, K. Walsh, J. Du and H. Jo (2002). "Shear stress stimulates phosphorylation of endothelial nitric-oxide synthase at Ser1179 by Akt-independent mechanisms: role of protein kinase A." J Biol Chem **277**(5): 3388-3396.

Boriack-Sjodin, P. A., S. M. Margarit, D. Bar-Sagi and J. Kuriyan (1998). "The structural basis of the activation of Ras by SOS." Nature **394**(6691): 337-343.

Borrmann, C. M., C. Grund, C. Kuhn, I. Hofmann, S. Pieperhoff and W. W. Franke (2006). "The area composita of adhering junctions connecting heart muscle cells of vertebrates. II. Colocalizations of desmosomal and fascia adhaerens molecules in the intercalated disk." Eur J Cell Biol **85**(6): 469-485.

Bos, J. L. (1989). "Ras oncogenes in human cancer: a review." Cancer Res **49**(17): 4682-4689.

Bos, J. L. (1998). "All in the family? New insights and questions regarding interconnectivity of Ras, Rap1 and Ral." The EMBO Journal **17**(23): 6776-6782.

Bos, J. L., H. Rehmann and A. Wittinghofer (2007). "GEFs and GAPs: Critical Elements in the Control of Small G Proteins." Cell **129**(5): 865-877.

Brakebusch, C. and R. Fassler (2003). "The integrin-actin connection, an eternal love affair." The EMBO journal **22**(10): 2324-2333.

Brand, S., E. C. Weiss, R. M. Lemor and M. C. Kolios (2008). "High frequency ultrasound tissue characterization and acoustic microscopy of intracellular changes." Ultrasound in Medicine and Biology **34**(9): 1396-1407.

Brealey, D., S. Karyampudi, T. S. Jacques, M. Novelli, R. Stidwill, V. Taylor, R. T. Smolenski and M. Singer (2004). "Mitochondrial dysfunction in a long-term rodent model of sepsis and organ failure." Am J Physiol Regul Integr Comp Physiol **286**(3): R491-497.

Brealey, D. and M. Singer (2003). "Mitochondrial Dysfunction in Sepsis." Curr Infect Dis Rep **5**(5): 365-371.

Briggs, A., Ed. (1995). Advances in Acoustic Microscopy. New York, Plenum Press.

Briggs, A. and O. Kolosov (2010). Acoustic Microscopy. New York, Clarendon Press.

Briggs, G. A. D., J. Wang and R. Gundle (1993). "Quantitative acoustic microscopy of individual living human cells." Journal of Microscopy **172**(1): 3-12.

Brindle, N. P., P. Saharinen and K. Alitalo (2006). "Signaling and functions of angiopoietin-1 in vascular protection." Circ Res **98**(8): 1014-1023.

Broman, M. T., P. Kouklis, D. H. Jho, X. P. Gao and A. B. Malik (2002). "Expression of cytoplasmic domain of VE-cadherin in vivo induces cdc42-dependent increase in endothelial permeability." Faseb Journal **16**(4): A404-A404.

Brooks, P. C., R. A. Clark and D. A. Cheresh (1994). "Requirement of vascular integrin alpha v beta 3 for angiogenesis." Science **264**(5158): 569-571.

Brooks, P. C., A. M. Montgomery, M. Rosenfeld, R. A. Reisfeld, T. Hu, G. Klier and D. A. Cheresh (1994). "Integrin alpha v beta 3 antagonists promote tumor regression by inducing apoptosis of angiogenic blood vessels." Cell **79**(7): 1157-1164.

Brooks, P. C., S. Strömblad, R. Klemke, D. Visscher, F. H. Sarkar and D. A. Cheresh (1995). "Antiintegrin alpha v beta 3 blocks human breast cancer growth and angiogenesis in human skin." Journal of Clinical Investigation **96**(4): 1815-1822.

Brown, L. F., M. Detmar, K. Claffey, J. A. Nagy, D. Feng, A. M. Dvorak and H. F. Dvorak (1997). "Vascular permeability factor/vascular endothelial growth factor: a multifunctional angiogenic cytokine." Exs **79**: 233-269.

Brown, R. C. and T. P. Davis (2002). "Calcium modulation of adherens and tight junction function: a potential mechanism for blood-brain barrier disruption after stroke." Stroke **33**(6): 1706-1711.

Brown, R. C. and T. P. Davis (2005). "Hypoxia/aglycemia alters expression of occludin and actin in brain endothelial cells." Biochemical and Biophysical Research Communications **327**(4): 1114-1123.

Brummelkamp, T. R., R. Bernards and R. Agami (2002). "Stable suppression of tumorigenicity by virus-mediated RNA interference." Cancer Cell **2**(3): 243-247.

Bruns, R. R. and G. E. Palade (1968). "Studies on blood capillaries. I. General organization of blood capillaries in muscle." The Journal of cell biology **37**(2): 244-276.

Brutsaert, D. L., P. Fransen, L. J. Andries, G. W. De Keulenaer and S. U. Sys (1998). "Cardiac endothelium and myocardial function." Cardiovascular Research **38**(2): 281-290.

Burridge, K., L. Molony and T. Kelly (1987). "Adhesion plaques: sites of transmembrane interaction between the extracellular matrix and the actin cytoskeleton." J Cell Sci Suppl **8**: 211-229.

Buttenschoen, K., M. Kornmann, D. Berger, G. Leder, H. G. Beger and C. Vasilescu (2008). "Endotoxemia and endotoxin tolerance in patients with ARDS." Langenbecks Arch Surg **393**(4): 473-478.

Bystrevskaya, V. B., V. V. Lichkun, A. S. Antonov and N. A. Perov (1988). "An ultrastructural study of centriolar complexes in adult and embryonic human aortic endothelial cells." Tissue Cell **20**(4): 493-503.

Cai, B., E. A. Deitch and L. Ulloa (2010). "Novel insights for systemic inflammation in sepsis and hemorrhage." Mediators of inflammation **2010**.

Calderwood, D. A. (2004). "Integrin activation." J Cell Sci **117**(5): 657-666.

Caldwell, D. A. and D. Lovasik (2002). "Endocarditis in the Immunocompromised: A life-threatening condition that is challenging to recognize and treat." The American Journal of Nursing **102**: 32-36.

Calkins, C. C., B. L. Hoepner, C. M. Law, M. R. Novak, S. V. Setzer, M. Hatzfeld and A. P. Kowalczyk (2003). "The armadillo family protein p0071 is a VE-cadherin- and desmoplakin-binding protein." Journal of Biological Chemistry **278**(3): 1774-1783.

Castejon, O. J. (1980). "Electron microscopic study of capillary wall in human cerebral edema." J Neuropathol Exp Neurol **39**(3): 296-328.

Challier, J. C., G. Dubernard, M. Galtier, T. Bintein, C. Vervelle, D. Raison, M. J. Espie and S. Uzan (2005). "Junctions and adhesion molecules in first trimester and term human placentas." Cell Mol Biol **51**: 713-722.

Chappell, D., K. Hofmann-Kiefer, M. Jacob, M. Rehm, J. Briegel, U. Welsch, P. Conzen and B. F. Becker (2009). "TNF-alpha induced shedding of the endothelial glycocalyx is prevented by hydrocortisone and antithrombin." Basic Res Cardiol **104**(1): 78-89.

Chardin, P., P. Boquet, P. Madaule, M. R. Popoff, E. J. Rubin and D. M. Gill (1989). "The mammalian G protein rhoC is ADP-ribosylated by Clostridium botulinum exoenzyme C3 and affects actin microfilaments in Vero cells." EMBO J **8**(4): 1087-1092.

Chardin, P., J. H. Camonis, N. W. Gale, L. van Aelst, J. Schlessinger, M. H. Wigler and D. Bar-Sagi (1993). "Human Sos1: a guanine nucleotide exchange factor for Ras that binds to GRB2." Science **260**(5112): 1338-1343.

Chatzizisis, Y. S., A. U. Coskun, M. Jonas, E. R. Edelman, C. L. Feldman and P. H. Stone (2007). "Role of Endothelial Shear Stress in the Natural History of Coronary Atherosclerosis and Vascular Remodeling Molecular, Cellular, and Vascular Behavior." Journal of the American College of Cardiology **49**(25): 2379-2393.

Chelazzi, C., G. Villa, P. Mancinelli, A. R. De Gaudio and C. Adembri (2015). "Glycocalyx and sepsis-induced alterations in vascular permeability." Critical Care **19**(1): 26.

Chen, K. D., Y. S. Li, M. Kim, S. Li, S. Yuan, S. Chien and J. Y. Shyy (1999). "Mechanotransduction in response to shear stress. Roles of receptor tyrosine kinases, integrins, and Shc." J Biol Chem **274**(26): 18393-18400.

Chen, M. and A. Stracher (1989). "In situ phosphorylation of platelet actin-binding protein by cAMP-dependent protein kinase stabilizes it against proteolysis by calpain." J Biol Chem **264**(24): 14282-14289.

Chen, X., S. Bonne, M. Hatzfeld, F. van Roy and K. J. Green (2002). "Protein binding and functional characterization of plakophilin 2. Evidence for its diverse roles in desmosomes and beta -catenin signaling." J Biol Chem **277**(12): 10512-10522.

Cheresh, D. A. (1987). "Human endothelial cells synthesize and express an Arg-Gly-Asp-directed adhesion receptor involved in attachment to fibrinogen and von Willebrand factor." Proceedings of the National Academy of Sciences **84**(18): 6471-6475.

Chien, S. (2007). "Mechanotransduction and endothelial cell homeostasis: the wisdom of the cell." Am J Physiol Heart Circ Physiol **292**(3): H1209-1224.

Chien, S., S. Li and Y. J. Shyy (1998). "Effects of mechanical forces on signal transduction and gene expression in endothelial cells." Hypertension **31**(1): 162-169.

Chong, A. Y., G. J. Caine, B. Freestone, A. D. Blann and G. Y. Lip (2004). "Plasma angiopoietin-1, angiopoietin-2, and angiopoietin receptor tie-2 levels in congestive heart failure." J Am Coll Cardiol **43**(3): 423-428.

Christaki, E. and S. M. Opal (2008). "Is the mortality rate for septic shock really decreasing?" Curr Opin Crit Care **14**(5): 580-586.

Christensen, K. L. and M. J. Mulvany (2001). "Location of resistance arteries." J Vasc Res **38**(1): 1-12.

Christofidou-Solomidou, M., M. Bridges, G. F. Murphy, S. M. Albelda and H. M. DeLisser (1997). "Expression and function of endothelial cell alpha v integrin receptors in wound-induced human angiogenesis in human skin/SCID mice chimeras." Am J Pathol **151**(4): 975-983.

Cid, J., R. Aguinaco, R. Sanchez, G. Garcia-Pardo and A. Llorente (2010). "Neutrophil CD64 expression as marker of bacterial infection: a systematic review and meta-analysis." The Journal of infection **60**(5): 313-319.

Cines, D. B., E. S. Pollak, C. A. Buck, J. Loscalzo, G. A. Zimmerman, R. P. McEver, J. S. Pober, T. M. Wick, B. A. Konkle, B. S. Schwartz, E. S. Barnathan, K. R. McCrae, B. A. Hug, A. M. Schmidt and D. M. Stern (1998). "Endothelial cells in physiology and in the pathophysiology of vascular disorders." Blood **91**(10): 3527-3561.

Clark, I. A. (1982). "Correlation between susceptibility to malaria and babesia parasites and to endotoxicity." Transactions of the Royal Society of Tropical Medicine and Hygiene **76**(1): 4-7.

Clark, P. R., T. D. Manes, J. S. Pober and M. S. Kluger (2007). "Increased ICAM-1 expression causes endothelial cell leakiness, cytoskeletal reorganization and junctional alterations." J Invest Dermatol **127**(4): 762-774.

Clementi, F. and G. E. Palade (1969). "Intestinal capillaries. I. Permeability to peroxidase and ferritin." The Journal of cell biology **41**(1): 33-58.

Cobb, J. P., C. Natanson, Z. M. Quezado, W. D. Hoffman, C. A. Koev, S. Banks, R. Correa, R. Levi, R. J. Elin and J. M. Hosseini (1995). "Differential hemodynamic effects of L-NMMA in endotoxemic and normal dogs." The American journal of physiology **268**(4): H1634-1642.

Cohen, J. (2002). "The immunopathogenesis of sepsis." Nature **420**(6917): 885-891.

Coimbra, R., H. Melbostad, W. Loomis, R. D. Porcides, P. Wolf, M. Tobar and D. B. Hoyt (2006). "LPS-induced acute lung injury is attenuated by phosphodiesterase inhibition: effects on

proinflammatory mediators, metalloproteinases, NF-kappaB, and ICAM-1 expression." J Trauma **60**(1): 115-125.

Cole, A. L., G. Subbanagounder, S. Mukhopadhyay, J. A. Berliner and D. K. Vora (2003). "Oxidized phospholipid-induced endothelial cell/monocyte interaction is mediated by a cAMP-dependent R-Ras/PI3-kinase pathway." Arterioscler Thromb Vasc Biol **23**(8): 1384-1390.

Colgan, O. C., G. Ferguson, N. T. Collins, R. P. Murphy, G. Meade, P. A. Cahill and P. M. Cummins (2007). "Regulation of bovine brain microvascular endothelial tight junction assembly and barrier function by laminar shear stress." Am J Physiol Heart Circ Physiol **292**(6): H3190-3197.

Collins, C., C. Guilluy, C. Welch, E. T. O'Brien, K. Hahn, R. Superfine, K. Burrige and E. Tzima (2012). "Localized tensional forces on PECAM-1 elicit a global mechanotransduction response via the integrin-RhoA pathway." Curr Biol **22**(22): 2087-2094.

Conway, D. E. and M. A. Schwartz (2013). "Flow-dependent cellular mechanotransduction in atherosclerosis." J Cell Sci **126**(22): 5101-5109.

Cooke, J. P., E. Rossitch, Jr., N. A. Andon, J. Loscalzo and V. J. Dzau (1991). "Flow activates an endothelial potassium channel to release an endogenous nitrovasodilator." J Clin Invest **88**(5): 1663-1671.

Cooke, V. G., M. U. Naik and U. P. Naik (2006). "Fibroblast growth factor-2 failed to induce angiogenesis in junctional adhesion molecule-A-deficient mice." Arterioscler Thromb Vasc Biol **26**(9): 2005-2011.

Coomber, B. L. and P. A. Stewart (1986). "Three-dimensional reconstruction of vesicles in endothelium of blood-brain barrier versus highly permeable microvessels." Anat Rec **215**(3): 256-261.

Copeland, S., H. S. Warren, S. F. Lowry, S. E. Calvano, D. Remick, Inflammation and I. the Host Response to Injury (2005). "Acute inflammatory response to endotoxin in mice and humans." Clin Diagn Lab Immunol **12**(1): 60-67.

Costerton, J. W., P. S. Stewart and E. P. Greenberg (1999). "Bacterial biofilms: A common cause of persistent infections." Science **284**(5418): 1318-1322.

Cox, A. D. and C. J. Der (2010). "Ras history: The saga continues." Small GTPases **1**(1): 2-27.

Cox, A. D., S. W. Fesik, A. C. Kimmelman, J. Luo and C. J. Der (2014). "Drugging the undruggable RAS: Mission possible?" Nat Rev Drug Discov **13**(11): 828-851.

Critchley, D. R. (2000). "Focal adhesions - the cytoskeletal connection." Curr Opin Cell Biol **12**(1): 133-139.

Crone, C. (1984). "Lack of selectivity to small ions in paracellular pathways in cerebral and muscle capillaries of the frog." The Journal of physiology **353**: 317-337.

Crouser, E. D. (2004). "Mitochondrial dysfunction in septic shock and multiple organ dysfunction syndrome." Mitochondrion **4**(5-6): 729-741.

Crouser, E. D., M. W. Julian, D. V. Blaho and D. R. Pfeiffer (2002). "Endotoxin-induced mitochondrial damage correlates with impaired respiratory activity." Crit Care Med **30**(2): 276-284.

Curry, F. E. and R. H. Adamson (2012). "Endothelial glycocalyx: permeability barrier and mechanosensor." Ann Biomed Eng **40**(4): 828-839.

Dai, G., M. R. Kaazempur-Mofrad, S. Natarajan, Y. Zhang, S. Vaughn, B. R. Blackman, R. D. Kamm, G. Garcia-Cardena and M. A. Gimbrone, Jr. (2004). "Distinct endothelial phenotypes evoked by arterial waveforms derived from atherosclerosis-susceptible and -resistant regions of human vasculature." Proceedings of the National Academy of Sciences of the United States of America **101**(41): 14871-14876.

Dalby, M. J., N. Gadegaard, P. Herzyk, D. Sutherland, H. Agheli, C. D. Wilkinson and A. S. Curtis (2007). "Nanomechanotransduction and interphase nuclear organization influence on genomic control." J Cell Biochem **102**(5): 1234-1244.

Daniel, J. M. and A. B. Reynolds (1997). "Tyrosine phosphorylation and cadherin/catenin function." Bioessays **19**(10): 883-891.

Danner, R. L., C. Natanson, R. J. Elin, J. M. Hosseini, S. Banks, T. J. MacVittie and J. E. Parrillo (1990). "Pseudomonas aeruginosa compared with Escherichia coli produces less endotoxemia but more cardiovascular dysfunction and mortality in a canine model of septic shock." Chest **98**(6): 1480-1487.

Darling, H. (2002). "Health care cost drivers." Issue Brief (Inst Health Care Costs Solut) **1**(1): 1-6.

Davenport, J. R. and B. K. Yoder (2005). "An incredible decade for the primary cilium: a look at a once-forgotten organelle." Am J Physiol Renal Physiol **289**(6): F1159-1169.

Davey, M. E. and A. O'Toole G (2000). "Microbial biofilms: from ecology to molecular genetics." Microbiol Mol Biol Rev **64**(4): 847-867.

Davies, D. C. (2002). "Blood-brain barrier breakdown in septic encephalopathy and brain tumours." J Anat **200**(6): 639-646.

Davies, P. F. (1989). "How Do Vascular Endothelial Cells Respond to Flow?" Physiology **4**(1): 22-25.

Davies, P. F. (1995). "Flow-mediated endothelial mechanotransduction." Physiological reviews **75**(3): 519-560.

Davies, P. F. (1997). "Overview: temporal and spatial relationships in shear stress-mediated endothelial signalling." J Vasc Res **34**(3): 208-211.

Davies, P. F., K. A. Barbee, M. V. Volin, A. Robotewskyj, J. Chen, L. Joseph, M. L. Griem, M. N. Wernick, E. Jacobs, D. C. Polacek, N. dePaola and A. I. Barakat (1997). "Spatial relationships in early signaling events of flow-mediated endothelial mechanotransduction." Annual review of physiology **59**: 527-549.

Davies, P. F., C. F. Dewey, Jr., S. R. Bussolari, E. J. Gordon and M. A. Gimbrone, Jr. (1984). "Influence of hemodynamic forces on vascular endothelial function. In vitro studies of shear stress and pinocytosis in bovine aortic cells." J Clin Invest **73**(4): 1121-1129.

Davies, P. F., T. Mundel and K. A. Barbee (1995). "A mechanism for heterogeneous endothelial responses to flow in vivo and in vitro." J Biomech **28**(12): 1553-1560.

Davies, P. F., A. Robotewskyj and M. L. Griem (1994). "Quantitative studies of endothelial cell adhesion. Directional remodeling of focal adhesion sites in response to flow forces." J Clin Invest **93**(5): 2031-2038.

Davies, P. F. and S. C. Tripathi (1993). "Mechanical stress mechanisms and the cell. An endothelial paradigm." Circ Res **72**(2): 239-245.

de Wit, C., S. E. Wolfe and B. Hopfl (2006). "Connexin-dependent communication within the vascular wall: contribution to the control of arteriolar diameter." Advances in cardiology **42**: 268-283.

Debets, J. M., R. Kampmeijer, M. P. van der Linden, W. A. Buurman and C. J. van der Linden (1989). "Plasma tumor necrosis factor and mortality in critically ill septic patients." Crit Care Med **17**(6): 489-494.

DeDent, A. C., M. McAdow and O. Schneewind (2007). "Distribution of protein A on the surface of *Staphylococcus aureus*." J Bacteriol **189**(12): 4473-4484.

Deen, W. M., M. J. Lazzara and B. D. Myers (2001). "Structural determinants of glomerular permeability." American Journal of Physiology - Renal Physiology **281**(4): F579-F596.

Dejana, E. (2004). "Endothelial cell-cell junctions: Happy together." Nature Reviews Molecular Cell Biology **5**(4): 261-270.

Dejana, E., G. Bazzoni and M. G. Lampugnani (1999). "The role of endothelial cell-to-cell junctions in vascular morphogenesis." Thrombosis and haemostasis **82**(2): 755-761.

Dejana, E., M. Corada and M. G. Lampugnani (1995). "Endothelial cell-to-cell junctions." FASEB J **9**(10): 910-918.

Dejana, E., F. Orsenigo and M. G. Lampugnani (2008). "The role of adherens junctions and VE-cadherin in the control of vascular permeability." Journal of Cell Science **121**(13): 2115-2122.

Dejana, E., F. Orsenigo, C. Molendini, P. Baluk and D. M. McDonald (2009). "Organization and signaling of endothelial cell-to-cell junctions in various regions of the blood and lymphatic vascular trees." Cell Tissue Res **335**(1): 17-25.

Dejana, E., R. Spagnuolo and G. Bazzoni (2001). "Interendothelial junctions and their role in the control of angiogenesis, vascular permeability and leukocyte transmigration." Thromb Haemost **86**(1): 308-315.

Dejana, E., E. Tournier-Lasserre and B. M. Weinstein (2009). "The control of vascular integrity by endothelial cell junctions: molecular basis and pathological implications." Dev Cell **16**(2): 209-221.

Del Vecchio, P. J., A. Siflinger-Birnboim, P. N. Belloni, L. A. Holleran, H. Lum and A. B. Malik (1992). "Culture and characterization of pulmonary microvascular endothelial cells." In Vitro Cell Dev Biol **28A**(11-12): 711-715.

Dellinger, R. P., M. M. Levy, J. M. Carlet, J. Bion, M. M. Parker, R. Jaeschke, K. Reinhart, D. C. Angus, C. Brun-Buisson, R. Beale, T. Calandra, J. F. Dhainaut, H. Gerlach, M. Harvey, J. J. Marini, J. Marshall, M. Ranieri, G. Ramsay, J. Sevransky, B. T. Thompson, S. Townsend, J. S. Vender, J. L. Zimmerman, J. L. Vincent, C. International Surviving Sepsis Campaign Guidelines, N. American Association of Critical-Care, P. American College of Chest, P. American College of Emergency, S. Canadian Critical Care, M. European Society of Clinical, D. Infectious, M. European Society of Intensive Care, S. European Respiratory, F. International Sepsis, M. Japanese Association for Acute, M. Japanese Society of Intensive Care, M. Society of Critical Care, M. Society of Hospital, S. Surgical Infection, I. World Federation of Societies of and M. Critical Care (2008). "Surviving Sepsis Campaign: international guidelines for management of severe sepsis and septic shock: 2008." Crit Care Med **36**(1): 296-327.

Delva, E., D. K. Tucker and A. P. Kowalczyk (2009). "The desmosome." Cold Spring Harb Perspect Biol **1**(2): 2543.

DeMaio, L., Y. S. Chang, T. W. Gardner, J. M. Tarbell and D. A. Antonetti (2001). "Shear stress regulates occludin content and phosphorylation." Am J Physiol Heart Circ Physiol **281**(1): H105-113.

Demerath, E., B. Towne, J. Blangero and R. M. Siervogel (2001). "The relationship of soluble ICAM-1, VCAM-1, P-selectin and E-selectin to cardiovascular disease risk factors in healthy men and women." Ann Hum Biol **28**(6): 664-678.

DePaola, N., J. E. Phelps, L. Florez, C. R. Keese, F. L. Minnear, I. Giaever and P. Vincent (2001). "Electrical impedance of cultured endothelium under fluid flow." Ann Biomed Eng **29**(8): 648-656.

Devaraj, S., J. M. Yun, G. Adamson, J. Galvez and I. Jialal (2009). "C-reactive protein impairs the endothelial glycocalyx resulting in endothelial dysfunction." Cardiovasc Res **84**(3): 479-484.

Dimmeler, S., B. Assmus, C. Hermann, J. Haendeler and A. M. Zeiher (1998). "Fluid shear stress stimulates phosphorylation of Akt in human endothelial cells: involvement in suppression of apoptosis." Circ Res **83**(3): 334-341.

Dimmeler, S., I. Fleming, B. Fisslthaler, C. Hermann, R. Busse and A. M. Zeiher (1999). "Activation of nitric oxide synthase in endothelial cells by Akt-dependent phosphorylation." Nature **399**(6736): 601-605.

Dimmeler, S., J. Haendeler, V. Rippmann, M. Nehls and A. M. Zeiher (1996). "Shear stress inhibits apoptosis of human endothelial cells." FEBS Lett **399**(1-2): 71-74.

Discher, D. E., P. Janmey and Y. L. Wang (2005). "Tissue cells feel and respond to the stiffness of their substrate." Science **310**(5751): 1139-1143.

Doerschuk, C. M. (2001). "Mechanisms of leukocyte sequestration in inflamed lungs." Microcirculation **8**(2): 71-88.

Donlan, R. M. and J. W. Costerton (2002). "Biofilms: Survival mechanisms of clinically relevant microorganisms." Clinical Microbiology Reviews **15**(2): 167.

Donovan, S., K. M. Shannon and G. Bollag (2002). "GTPase activating proteins: critical regulators of intracellular signaling." Biochim Biophys Acta **1602**(1): 23-45.

Drake, J. M., J. K. Lee and O. N. Witte (2014). "Clinical targeting of mutated and wild-type protein tyrosine kinases in cancer." Mol Cell Biol **34**(10): 1722-1732.

Drake, T. A., J. Cheng, A. Chang and F. B. Taylor, Jr. (1993). "Expression of tissue factor, thrombomodulin, and E-selectin in baboons with lethal Escherichia coli sepsis." Am J Pathol **142**(5): 1458-1470.

Droge, W. (2002). "Free radicals in the physiological control of cell function." Physiological Reviews **82**(1): 47-95.

Dudek, S. M. and J. G. Garcia (2001). "Cytoskeletal regulation of pulmonary vascular permeability." J Appl Physiol (1985) **91**(4): 1487-1500.

Dudek, S. M., J. R. Jacobson, E. T. Chiang, K. G. Birukov, P. Wang, X. Zhan and J. G. Garcia (2004). "Pulmonary endothelial cell barrier enhancement by sphingosine 1-phosphate: roles for cortactin and myosin light chain kinase." J Biol Chem **279**(23): 24692-24700.

Durack, D. T., A. S. Lukes, D. K. Bright, M. J. Alberts, T. M. Bashore, G. R. Corey, J. M. Douglas, L. Gray, F. E. Harrell, J. K. Harrison, S. A. Heinle, A. Morris, J. A. Kisslo, L. M. Nicely, N. Oldham, L. M. Penning, D. J. Sexton, M. Towns and R. A. Waugh (1994). "New criteria for diagnosis of infective endocarditis - utilization of specific echocardiographic findings." American Journal of Medicine **96**(3): 200-209.

Durr, E., J. Yu, K. M. Krasinska, L. A. Carver, J. R. Yates, J. E. Testa, P. Oh and J. E. Schnitzer (2004). "Direct proteomic mapping of the lung microvascular endothelial cell surface in vivo and in cell culture." Nat Biotechnol **22**(8): 985-992.

Dvorak, A. M., S. Kohn, E. S. Morgan, P. Fox, J. A. Nagy and H. F. Dvorak (1996). "The vesiculo-vacuolar organelle (VVO): a distinct endothelial cell structure that provides a transcellular pathway for macromolecular extravasation." Journal of leukocyte biology **59**(1): 100-115.

Dvorak, H. F. (2010). "Vascular permeability to plasma, plasma proteins, and cells: an update." Curr Opin Hematol **17**(3): 225-229.

Dvorak, H. F., J. A. Nagy, D. Feng, L. F. Brown and A. M. Dvorak (1999). "Vascular permeability factor/vascular endothelial growth factor and the significance of microvascular hyperpermeability in angiogenesis." Current topics in microbiology and immunology **237**: 97-132.

Ebata, N., Y. Nodasaka, Y. Sawa, Y. Yamaoka, S. Makino, Y. Totsuka and S. Yoshida (2001). "Desmoplakin as a specific marker of lymphatic vessels." Microvascular Research **61**(1): 40-48.

Egan, S. E., B. W. Giddings, M. W. Brooks, L. Buday, A. M. Sizeland and R. A. Weinberg (1993). "Association of Sos Ras exchange protein with Grb2 is implicated in tyrosine kinase signal transduction and transformation." Nature **363**(6424): 45-51.

Ehrhardt, A., G. R. Ehrhardt, X. Guo and J. W. Schrader (2002). "Ras and relatives--job sharing and networking keep an old family together." Exp Hematol **30**(10): 1089-1106.

Ehrlicher, A. J., F. Nakamura, J. H. Hartwig, D. A. Weitz and T. P. Stossel (2011). "Mechanical strain in actin networks regulates FilGAP and integrin binding to filamin A." Nature **478**(7368): 260-263.

Eksioglu, Y. Z., I. E. Scheffer, P. Cardenas, J. Knoll, F. DiMario, G. Ramsby, M. Berg, K. Kamuro, S. F. Berkovic, G. M. Duyk, J. Parisi, P. R. Huttenlocher and C. A. Walsh (1996). "Periventricular heterotopia: an X-linked dominant epilepsy locus causing aberrant cerebral cortical development." Neuron **16**(1): 77-87.

Eliceiri, B. P., R. Paul, P. L. Schwartzberg, J. D. Hood, J. Leng and D. A. Cheresh (1999). "Selective requirement for Src kinases during VEGF-induced angiogenesis and vascular permeability." Mol Cell **4**(6): 915-924.

Eliceiri, B. P., X. S. Puente, J. D. Hood, D. G. Stupack, D. D. Schlaepfer, X. Z. Huang, D. Sheppard and D. A. Cheresh (2002). "Src-mediated coupling of focal adhesion kinase to integrin alpha(v)beta5 in vascular endothelial growth factor signaling." J Cell Biol **157**(1): 149-160.

Ellis, C. A., C. Tiruppathi, R. Sandoval, W. D. Niles and A. B. Malik (1999). "Time course of recovery of endothelial cell surface thrombin receptor (PAR-1) expression." Am J Physiol **276**(1): C38-45.

Ellis, C. G., J. Jagger and M. Sharpe (2005). "The microcirculation as a functional system." Critical care **9(4)**: S3-8.

Enerson, B. E. and L. R. Drewes (2006). "The rat blood-brain barrier transcriptome." J Cereb Blood Flow Metab **26(7)**: 959-973.

Eppihimer, M. J., B. Wolitzky, D. C. Anderson, M. A. Labow and D. N. Granger (1996). "Heterogeneity of expression of E- and P-selectins in vivo." Circ Res **79(3)**: 560-569.

Erickson, K. K., J. M. Sundstrom and D. A. Antonetti (2007). "Vascular permeability in ocular disease and the role of tight junctions." Angiogenesis **10(2)**: 103-117.

Ernst, F. R., W. N. Malatestinic and W. T. Linde-Zwirble (2006). "Evaluating the clinical and financial impact of severe sepsis with Medicare or other administrative hospital data." Am J Health Syst Pharm **63(6)**: 575-581.

Esser, S., M. G. Lampugnani, M. Corada, E. Dejana and W. Risau (1998). "Vascular endothelial growth factor induces VE-cadherin tyrosine phosphorylation in endothelial cells." J Cell Sci **111(13)**: 1853-1865.

Essler, M., J. M. Staddon, P. C. Weber and M. Aepfelbacher (2000). "Cyclic AMP blocks bacterial lipopolysaccharide-induced myosin light chain phosphorylation in endothelial cells through inhibition of rho/rho kinase signaling." The Journal of Immunology **164(12)**: 6543-6549.

Evans, T. J., D. Moyes, A. Carpenter, R. Martin, H. Loetscher, W. Lesslauer and J. Cohen (1994). "Protective effect of 55- but not 75-kD soluble tumor necrosis factor receptor-immunoglobulin G fusion proteins in an animal model of gram-negative sepsis." J Exp Med **180(6)**: 2173-2179.

Fanning, A. S. and J. M. Anderson (1996). "Protein-protein interactions: PDZ domain networks." Curr Biol **6**(11): 1385-1388.

Fanning, A. S. and J. M. Anderson (2009). "Zonula occludens-1 and -2 are cytosolic scaffolds that regulate the assembly of cellular junctions." Ann N Y Acad Sci **1165**: 113-120.

Fanning, A. S., B. J. Jameson, L. A. Jesaitis and J. M. Anderson (1998). "The tight junction protein ZO-1 establishes a link between the transmembrane protein occludin and the actin cytoskeleton." Journal of Biological Chemistry **273**(45): 29745-29753.

Fels, J., P. Jeggle, I. Liashkovich, W. Peters and H. Oberleithner (2014). "Nanomechanics of vascular endothelium." Cell Tissue Res **355**(3): 727-737.

Feng, D., J. A. Nagy, J. Hipp, H. F. Dvorak and A. M. Dvorak (1996). "Vesiculo-vacuolar organelles and the regulation of venule permeability to macromolecules by vascular permeability factor, histamine, and serotonin." J Exp Med **183**(5): 1981-1986.

Feng, D., J. A. Nagy, K. Pyne, I. Hammel, H. F. Dvorak and A. M. Dvorak (1999). "Pathways of macromolecular extravasation across microvascular endothelium in response to VPF/VEGF and other vasoactive mediators." Microcirculation **6**(1): 23-44.

Feng, Y., M. H. Chen, I. P. Moskowitz, A. M. Mendonza, L. Vidali, F. Nakamura, D. J. Kwiatkowski and C. A. Walsh (2006). "Filamin A (FLNA) is required for cell-cell contact in vascular development and cardiac morphogenesis." Proc Natl Acad Sci U S A **103**(52): 19836-19841.

Ferland, R. J., J. N. Gaitanis, K. Apse, U. Tantravahi, C. A. Walsh and V. L. Sheen (2006). "Periventricular nodular heterotopia and Williams syndrome." Am J Med Genet A **140**(12): 1305-1311.

Feuerhake, F., G. Fuchsl, R. Bals and U. Welsch (1998). "Expression of inducible cell adhesion molecules in the normal human lung: immunohistochemical study of their distribution in pulmonary blood vessels." Histochem Cell Biol **110**(4): 387-394.

Fiedler, U., M. Scharpfenecker, S. Koidl, A. Hegen, V. Grunow, J. M. Schmidt, W. Kriz, G. Thurston and H. G. Augustin (2004). "The Tie-2 ligand angiopoietin-2 is stored in and rapidly released upon stimulation from endothelial cell Weibel-Palade bodies." Blood **103**(11): 4150-4156.

Figuroa, X. F., D. L. Paul, A. M. Simon, D. A. Goodenough, K. H. Day, D. N. Damon and B. R. Duling (2003). "Central role of connexin40 in the propagation of electrically activated vasodilation in mouse cremasteric arterioles in vivo." Circulation research **92**(7): 793-800.

Fink, M. P. and H. S. Warren (2014). "Strategies to improve drug development for sepsis." Nat Rev Drug Discov **13**(10): 741-758.

Flaherty, J. T., J. E. Pierce, V. J. Ferrans, D. J. Patel, W. K. Tucker and D. L. Fry (1972). "Endothelial nuclear patterns in the canine arterial tree with particular reference to hemodynamic events." Circ Res **30**(1): 23-33.

Flanagan, L. A., J. Chou, H. Falet, R. Neujahr, J. H. Hartwig and T. P. Stossel (2001). "Filamin A, the Arp2/3 complex, and the morphology and function of cortical actin filaments in human melanoma cells." J Cell Biol **155**(4): 511-517.

Flemming, H. C. and J. Wingender (2010). "The biofilm matrix." Nat Rev Microbiol **8**(9): 623-633.

Flex, E., M. Jaiswal, F. Pantaleoni, S. Martinelli, M. Strullu, E. K. Fansa, A. Caye, A. De Luca, F. Lepri, R. Dvorsky, L. Pannone, S. Paolacci, S.-C. Zhang, V. Fodale, G. Bocchinfuso, C.

Rossi, E. M. M. Burkitt-Wright, A. Farrotti, E. Stellacci, S. Cecchetti, R. Ferese, L. Bottero, S. Castro, O. Fenneteau, B. Brethon, M. Sanchez, A. E. Roberts, H. G. Yntema, I. Van Der Burgt, P. Cianci, M.-L. Bondeson, M. Cristina Digilio, G. Zampino, B. Kerr, Y. Aoki, M. L. Loh, A. Palleschi, E. Di Schiavi, A. Care, A. Selicorni, B. Dallapiccola, I. C. Cirstea, L. Stella, M. Zenker, B. D. Gelb, H. Cave, M. R. Ahmadian and M. Tartaglia (2014). "Activating mutations in RAS underlie a phenotype within the RASopathy spectrum and contribute to leukaemogenesis." Human molecular genetics **23**(16): 4315-4327.

Florian, J. A., J. R. Kosky, K. Ainslie, Z. Y. Pang, R. O. Dull and J. M. Tarbell (2003). "Heparan sulfate proteoglycan is a mechanosensor on endothelial cells." Circulation Research **93**(10): E136-E142.

Forsyth, S. E., A. Hoger and J. H. Hoger (1997). "Molecular cloning and expression of a bovine endothelial inward rectifier potassium channel." FEBS Lett **409**(2): 277-282.

Fox, J. W., E. D. Lamperti, Y. Z. Eksioglu, S. E. Hong, Y. Feng, D. A. Graham, I. E. Scheffer, W. B. Dobyns, B. A. Hirsch, R. A. Radtke, S. F. Berkovic, P. R. Huttenlocher and C. A. Walsh (1998). "Mutations in filamin 1 prevent migration of cerebral cortical neurons in human periventricular heterotopia." Neuron **21**(6): 1315-1325.

Frame, M. C. (2002). "Src in cancer: deregulation and consequences for cell behaviour." Biochim Biophys Acta **1602**(2): 114-130.

Franke, W. W., C. M. Borrmann, C. Grund and S. Pieperhoff (2006). "The area composita of adhering junctions connecting heart muscle cells of vertebrates. I. Molecular definition in intercalated disks of cardiomyocytes by immunoelectron microscopy of desmosomal proteins." Eur J Cell Biol **85**(2): 69-82.

Franke, W. W., P. Cowin, C. Grund, C. Kuhn and H. P. Kapprell (1988). The endothelial junction: the plaque and its component. Endothelial Cell Biology in Health and Diseases. N. Simionescu and M. Simionescu. New York, Plenum Publishing Corporation: 147–166.

Freymann, D. M., R. J. Keenan, R. M. Stroud and P. Walter (1999). "Functional changes in the structure of the SRP GTPase on binding GDP and Mg²⁺+GDP." Nat Struct Biol **6**(8): 793-801.

Friedlander, M., P. C. Brooks, R. W. Shaffer, C. M. Kincaid, J. A. Varner and D. A. Cheresh (1995). "Definition of Two Angiogenic Pathways by Distinct α v Integrins." Science **270**(5241): 1500-1502.

Friedlander, M., C. L. Theesfeld, M. Sugita, M. Fruttiger, M. A. Thomas, S. Chang and D. A. Cheresh (1996). "Involvement of integrins alpha v beta 3 and alpha v beta 5 in ocular neovascular diseases." Proceedings of the National Academy of Sciences **93**(18): 9764-9769.

Fry, B. C., J. Lee, N. P. Smith and T. W. Secomb (2012). "Estimation of blood flow rates in large microvascular networks." Microcirculation **19**(6): 530-538.

Fujiwara, K., M. Masuda, M. Osawa, Y. Kano and K. Katoh (2001). "Is PECAM-1 a mechanoresponsive molecule?" Cell Struct Funct **26**(1): 11-17.

Furuse, M., T. Hirase, M. Itoh, A. Nagafuchi, S. Yonemura, S. Tsukita and S. Tsukita (1993). "Occludin: a novel integral membrane protein localizing at tight junctions." J Cell Biol **123**(6): 1777-1788.

Furuse, M., M. Itoh, T. Hirase, A. Nagafuchi, S. Yonemura, S. Tsukita and S. Tsukita (1994). "Direct association of occludin with ZO-1 and its possible involvement in the localization of occludin at tight junctions." J Cell Biol **127**(6): 1617-1626.

Furuse, M. and S. Tsukita (2006). "Claudins in occludin junctions of humans and flies." Trends in Cell Biology **16**(4): 181-188.

Furuya, E. Y. and F. D. Lowy (2003). "Antimicrobial strategies for the prevention and treatment of cardiovascular infections." Curr Opin Pharmacol **3**(5): 464-469.

Gabay, C., C. Lamacchia and G. Palmer (2010). "IL-1 pathways in inflammation and human diseases." Nat Rev Rheumatol **6**(4): 232-241.

Gabriels, J. E. and D. L. Paul (1998). "Connexin43 is highly localized to sites of disturbed flow in rat aortic endothelium but connexin37 and connexin40 are more uniformly distributed." Circulation research **83**(6): 636-643.

Galbraith, C. G., R. Skalak and S. Chien (1998). "Shear stress induces spatial reorganization of the endothelial cell cytoskeleton." Cell Motil Cytoskeleton **40**(4): 317-330.

Galbraith, C. G., K. M. Yamada and M. P. Sheetz (2002). "The relationship between force and focal complex development." The Journal of cell biology **159**(4): 695-705.

Galley, H. F. (2011). "Oxidative stress and mitochondrial dysfunction in sepsis." British journal of anaesthesia **107**(1): 57-64.

Gao, Q., W. Liu, J. Cai, M. Li, Y. Gao, W. Lin and Z. Li (2014). "EphB2 promotes cervical cancer progression by inducing epithelial-mesenchymal transition." Hum Pathol **45**(2): 372-381.

Garcia, J. G., A. Siflinger-Birnboim, R. Bizios, P. J. Del Vecchio, J. W. Fenton, 2nd and A. B. Malik (1986). "Thrombin-induced increase in albumin permeability across the endothelium." J Cell Physiol **128**(1): 96-104.

Gavard, J. (2009). "Breaking the VE-cadherin bonds." FEBS Lett **583**(1): 1-6.

Gavard, J. and J. S. Gutkind (2006). "VEGF controls endothelial-cell permeability by promoting the beta-arrestin-dependent endocytosis of VE-cadherin." Nat Cell Biol **8**(11): 1223-1234.

Gavard, J. and J. S. Gutkind (2008). "Protein Kinase C-related Kinase and ROCK Are Required for Thrombin-induced Endothelial Cell Permeability Downstream from G α 12/13 and G α 11/q." Journal of Biological Chemistry **283**(44): 29888-29896.

Gawecka, J. E., G. S. Griffiths, B. Ek-Rylander, J. W. Ramos and M. L. Matter (2010). "R-Ras Regulates Migration through an Interaction with Filamin A in Melanoma Cells." Plos One **5**(6).

Gebb, S. and T. Stevens (2004). "On lung endothelial cell heterogeneity." Microvasc Res **68**(1): 1-12.

Gehlsen, K. R., L. Dillner, E. Engvall and E. Ruoslahti (1988). "The human laminin receptor is a member of the integrin family of cell adhesion receptors." Science **241**(4870): 1228-1229.

Geiger, C., W. Nagel, T. Boehm, Y. van Kooyk, C. G. Figdor, E. Kremmer, N. Hogg, L. Zeitlmann, H. Dierks, K. S. Weber and W. Kolanus (2000). "Cytoshesin-1 regulates beta-2 integrin-mediated adhesion through both ARF-GEF function and interaction with LFA-1." The EMBO journal **19**(11): 2525-2536.

Geiger, R. V., B. C. Berk, R. W. Alexander and R. M. Nerem (1992). "Flow-induced calcium transients in single endothelial cells: spatial and temporal analysis." Am J Physiol **262**(6): C1411-1417.

Gellerich, F. N., S. Trumbeckaite, K. Hertel, S. Zierz, U. Muller-Werdan, K. Werdan, H. Redl and G. Schlag (1999). "Impaired energy metabolism in hearts of septic baboons: diminished activities of Complex I and Complex II of the mitochondrial respiratory chain." Shock **11**(5): 336-341.

Gellerich, F. N., S. Trumbeckaite, J. R. Opalka, J. F. Gellerich, Y. Chen, C. Neuhof, H. Redl, K. Werdan and S. Zierz (2002). "Mitochondrial dysfunction in sepsis: evidence from bacteraemic baboons and endotoxaemic rabbits." Biosci Rep **22**(1): 99-113.

Getsios, S., A. C. Huen and K. J. Green (2004). "Working out the strength and flexibility of desmosomes." Nat Rev Mol Cell Biol **5**(4): 271-281.

Ghosh, P. M., C. R. Keese and I. Giaever (1993). "Monitoring electropermeabilization in the plasma membrane of adherent mammalian cells." Biophys J **64**(5): 1602-1609.

Giaever, I. and C. R. Keese (1986). "Use of electric fields to monitor the dynamical aspect of cell behavior in tissue culture." IEEE Trans Biomed Eng **33**(2): 242-247.

Giaever, I. and C. R. Keese (1991). "Micromotion of mammalian-cells measured electrically." Proceedings of the National Academy of Sciences of the United States of America **88**(17): 7896-7900.

Giaever, I. and C. R. Keese (1991). "Micromotion of mammalian cells measured electrically." Proceedings of the National Academy of Sciences **88**(17): 7896-7900.

Giaever, I. and C. R. Keese (1993). "A morphological biosensor for mammalian-cells." Nature **366**(6455): 591-592.

Giancotti, F. G. and E. Ruoslahti (1999). "Integrin Signaling." Science **285**(5430): 1028-1033.

Gibbs, J. B., M. D. Schaber, W. J. Allard, I. S. Sigal and E. M. Scolnick (1988). "Purification of ras GTPase activating protein from bovine brain." Proceedings of the National Academy of Sciences of the United States of America **85**(14): 5026-5030.

Gilbert-McClain, L. I., A. D. Verin, S. Shi, R. P. Irwin and J. G. Garcia (1998). "Regulation of endothelial cell myosin light chain phosphorylation and permeability by vanadate." J Cell Biochem **70**(1): 141-155.

Giles, R. H., J. H. van Es and H. Clevers (2003). "Caught up in a Wnt storm: Wnt signaling in cancer." Biochim Biophys Acta **1653**(1): 1-24.

Gill, K. A. and N. P. J. Brindle (2005). "Angiopoietin-2 stimulates migration of endothelial progenitors and their interaction with endothelium." Biochemical and biophysical research communications **336**(2): 392-396.

Gilles, S., S. Zahler, U. Welsch, C. P. Sommerhoff and B. F. Becker (2003). "Release of TNF-alpha during myocardial reperfusion depends on oxidative stress and is prevented by mast cell stabilizers." Cardiovasc Res **60**(3): 608-616.

Gilman, A. G. (1987). "G proteins: transducers of receptor-generated signals." Annu Rev Biochem **56**: 615-649.

Girard, J. P. and T. A. Springer (1995). "High endothelial venules (HEVs): specialized endothelium for lymphocyte migration." Immunol Today **16**(9): 449-457.

Glode, L. M., S. E. Mergenhagen and D. L. Rosenstreich (1976). "Significant contribution of spleen cells in mediating the lethal effects of endotoxin in vivo." Infect Immun **14**(3): 626-630.

Glogauer, M., P. Arora, D. Chou, P. A. Janmey, G. P. Downey and C. A. McCulloch (1998). "The role of actin-binding protein 280 in integrin-dependent mechanoprotection." J Biol Chem **273**(3): 1689-1698.

Gloor, S. M., M. Wachtel, M. F. Bolliger, H. Ishihara, R. Landmann and K. Frei (2001). "Molecular and cellular permeability control at the blood-brain barrier." Brain research Brain research reviews **36**(2-3): 258-264.

Gloor, S. M., A. Weber, N. Adachi and K. Frei (1997). "Interleukin-1 modulates protein tyrosine phosphatase activity and permeability of brain endothelial cells." Biochem Biophys Res Commun **239**(3): 804-809.

Go, Y. M., H. Park, M. C. Maland, V. M. Darley-Usmar, B. Stoyanov, R. Wetzker and H. Jo (1998). "Phosphatidylinositol 3-kinase gamma mediates shear stress-dependent activation of JNK in endothelial cells." Am J Physiol **275**(5): H1898-1904.

Goertz, D. E., M. E. Frijlink, N. De Jong and A. Steen (2006). "Nonlinear intravascular ultrasound contrast imaging." Ultrasound in Medicine and Biology **32**(4): 491-502.

Goertz, D. E., M. E. Frijlink, D. Tempel, V. Bhagwandas, A. Gisolf, R. Krams, N. de Jong and A. F. W. van der Steen (2007). "Subharmonic contrast intravascular ultrasound for vasa vasorum imaging." Ultrasound in Medicine and Biology **33**(12): 1859-1872.

Goldfarb, R. D., W. Tambolini, S. M. Wiener and P. B. Weber (1983). "Canine left ventricular performance during LD50 endotoxemia." Am J Physiol **244**(3): H370-377.

Goldstein, I. J. and C. E. Hayes (1978). "The lectins: carbohydrate-binding proteins of plants and animals." Adv Carbohydr Chem Biochem **35**: 127-340.

Golenbock, D. T., J. A. Will, C. R. Raetz and R. A. Proctor (1987). "Lipid X ameliorates pulmonary hypertension and protects sheep from death due to endotoxin." Infection and immunity **55**(10): 2471-2476.

Gong, P., D. J. Angelini, S. Yang, G. Xia, A. S. Cross, D. Mann, D. D. Bannerman, S. N. Vogel and S. E. Goldblum (2008). "TLR4 signaling is coupled to SRC family kinase activation, tyrosine phosphorylation of zonula adherens proteins, and opening of the paracellular pathway in human lung microvascular endothelia." J Biol Chem **283**(19): 13437-13449.

Good, M. S., C. F. Wend, L. J. Bond, J. S. McLean, P. D. Panetta, S. Ahmed, S. L. Crawford and D. S. Daly (2006). "An estimate of biofilm properties using an acoustic microscope." IEEE Transactions on Ultrasonics, Ferroelectrics, and Frequency Control **53**(9): 1637-1646.

Goode, B. L., D. G. Drubin and G. Barnes (2000). "Functional cooperation between the microtubule and actin cytoskeletons." Current opinion in cell biology **12**(1): 63-71.

Goodenough, D. A. and D. L. Paul (2009). "Gap junctions." Cold Spring Harbor perspectives in biology **1**(1): 2576.

Goodwin, M. H., Jr. and T. K. Stapleton (1952). "The course of natural and induced infections of Plasmodium floridense Thompson and Huff in Sceloporus undulatus undulatus (Latreille)." Am J Trop Med Hyg **1**(5): 773-783.

Goody, R. S. (2003). "The significance of the free energy of hydrolysis of GTP for signal-transducing and regulatory GTPases." Biophys Chem **100**(1-3): 535-544.

Gorlin, J. B., R. Yamin, S. Egan, M. Stewart, T. P. Stossel, D. J. Kwiatkowski and J. H. Hartwig (1990). "Human endothelial actin-binding protein (ABP-280, nonmuscle filamin): a molecular leaf spring." J Cell Biol **111**(3): 1089-1105.

Gottlieb, A. B. (2007). "Tumor necrosis factor blockade: mechanism of action." J Investig Dermatol Symp Proc **12**(1): 1-4.

Gottlieb, A. I., B. L. Langille, M. K. Wong and D. W. Kim (1991). "Structure and function of the endothelial cytoskeleton." Laboratory investigation; a journal of technical methods and pathology **65**(2): 123-137.

Granger, D. N. and E. Senchenkova (2010). Inflammation and the microcirculation. Integrated systems physiology: from molecule to function. D. N. Granger and J. Granger, Morgan & Claypool Life Sciences.

Green, K. J. and C. L. Simpson (2007). "Desmosomes: New perspectives on a classic." Journal of Investigative Dermatology **127**(11): 2499-2515.

Greenspan, M. and C. E. Tschiegg (1959). "Tables of the Speed of Sound in Water." The Journal of the Acoustical Society of America **31**(1): 75-76.

Griffiths, G. S., M. Grundl, J. S. Allen and M. L. Matter (2011). "R-Ras interacts with Filamin A to maintain endothelial barrier function." Journal of Cellular Physiology **226**(9): 2287-2296.

Grisham, J. W., W. Nopanitaya, J. Compagno and A. E. Nagel (1975). "Scanning electron microscopy of normal rat liver: the surface structure of its cells and tissue components." The American journal of anatomy **144**(3): 295-321.

Gschwandtner, M., R. Purwar, M. Wittmann, W. Baumer, M. Kietzmann, T. Werfel and R. Gutzmer (2008). "Histamine upregulates keratinocyte MMP-9 production via the histamine H1 receptor." The Journal of investigative dermatology **128**(12): 2783-2791.

Gu, J. M., Y. Katsuura, G. L. Ferrell, P. Grammas and C. T. Esmon (2000). "Endotoxin and thrombin elevate rodent endothelial cell protein C receptor mRNA levels and increase receptor shedding in vivo." Blood **95**(5): 1687-1693.

Gudi, S., J. P. Nolan and J. A. Frangos (1998). "Modulation of GTPase activity of G proteins by fluid shear stress and phospholipid composition." Proceedings of the National Academy of Sciences of the United States of America **95**(5): 2515-2519.

Guerrini, R., D. Mei, S. Sisodiya, F. Sicca, B. Harding, Y. Takahashi, T. Dorn, A. Yoshida, J. Campistol, G. Kramer, F. Moro, W. B. Dobyns and E. Parrini (2004). "Germline and mosaic mutations of FLN1 in men with periventricular heterotopia." Neurology **63**(1): 51-56.

Gumbiner, B. M. (2000). "Regulation of cadherin adhesive activity." J Cell Biol **148**(3): 399-404.

Ha, C. H., A. M. Bennett and Z. G. Jin (2008). "A novel role of vascular endothelial cadherin in modulating c-Src activation and downstream signaling of vascular endothelial growth factor." J Biol Chem **283**(11): 7261-7270.

Hahn, C. and M. A. Schwartz (2009). "Mechanotransduction in vascular physiology and atherogenesis." Nat Rev Mol Cell Biol **10**(1): 53-62.

Hahne, M., U. Jager, S. Isenmann, R. Hallmann and D. Vestweber (1993). "Five tumor necrosis factor-inducible cell adhesion mechanisms on the surface of mouse endothelioma cells mediate the binding of leukocytes." J Cell Biol **121**(3): 655-664.

Hall-Stoodley, L., J. W. Costerton and P. Stoodley (2004). "Bacterial biofilms: From the natural environment to infectious diseases." Nature Reviews Microbiology **2**(2): 95-108.

Hammerling, B., C. Grund, J. Boda-Heggemann, R. Moll and W. W. Franke (2006). "The complexus adhaerens of mammalian lymphatic endothelia revisited: a junction even more complex than hitherto thought." Cell and Tissue Research **324**(1): 55-67.

Harhaj, N. S. and D. A. Antonetti (2004). "Regulation of tight junctions and loss of barrier function in pathophysiology." Int J Biochem Cell Biol **36**(7): 1206-1237.

Harhaj, N. S., E. A. Felinski, E. B. Wolpert, J. M. Sundstrom, T. W. Gardner and D. A. Antonetti (2006). "VEGF activation of protein kinase C stimulates occludin phosphorylation and contributes to endothelial permeability." Invest Ophthalmol Vis Sci **47**(11): 5106-5115.

Harper, S. and D. W. Speicher (2008). "Expression and purification of GST fusion proteins." Curr Protoc Protein Sci **6**: 66.

Harper, S. and D. W. Speicher (2011). "Purification of proteins fused to glutathione S-transferase." Methods Mol Biol **681**: 259-280.

Harris, L. G. and R. G. Richards (2006). "Staphylococci and implant surfaces: a review." Injury **37**: 3-14.

Hart, A. W., J. E. Morgan, J. Schneider, K. West, L. McKie, S. Bhattacharya, I. J. Jackson and S. H. Cross (2006). "Cardiac malformations and midline skeletal defects in mice lacking filamin A." Hum Mol Genet **15**(16): 2457-2467.

Hartwig, J. H. and T. P. Stossel (1975). "Isolation and properties of actin, myosin, and a new actinbinding protein in rabbit alveolar macrophages." J Biol Chem **250**(14): 5696-5705.

Haskins, J., L. Gu, E. S. Wittchen, J. Hibbard and B. R. Stevenson (1998). "ZO-3, a novel member of the MAGUK protein family found at the tight junction, interacts with ZO-1 and occludin." J Cell Biol **141**(1): 199-208.

Hastie, L. E., W. F. Patton, H. B. Hechtman and D. Shepro (1997). "H₂O₂-induced filamin redistribution in endothelial cells is modulated by the cyclic AMP-dependent protein kinase pathway." J Cell Physiol **172**(3): 373-381.

Hattori, K., S. Dias, B. Heissig, N. R. Hackett, D. Lyden, M. Tateno, D. J. Hicklin, Z. P. Zhu, L. Witte, R. G. Crystal, M. A. S. Moore and S. Rafii (2001). "Vascular endothelial growth factor and angiopoietin-1 stimulate postnatal hematopoiesis by recruitment of vasculogenic and hematopoietic stem cells." Journal of Experimental Medicine **193**(9): 1005-1014.

Hatzfeld, M. (1999). "The armadillo family of structural proteins." Int Rev Cytol **186**: 179-224.

Hatzfeld, M. (2007). "Plakophilins: Multifunctional proteins or just regulators of desmosomal adhesion?" Biochimica Et Biophysica Acta-Molecular Cell Research **1773**(1): 69-77.

Hatzfeld, M., K. J. Green and H. Sauter (2003). "Targeting of p0071 to desmosomes and adherens junctions is mediated by different protein domains." Journal of Cell Science **116**(7): 1219-1233.

Hawkins, B. T., T. J. Abbruscato, R. D. Egleton, R. C. Brown, J. D. Huber, C. R. Campos and T. P. Davis (2004). "Nicotine increases in vivo blood-brain barrier permeability and alters cerebral microvascular tight junction protein distribution." Brain Res **1027**(1-2): 48-58.

Hecht, A. and R. Kemler (2000). "Curbing the nuclear activities of beta-catenin. Control over Wnt target gene expression." EMBO Rep **1**(1): 24-28.

Heeschen, C., A. Aicher, R. Lehmann, S. Fichtischerer, M. Vasa, C. Urbich, C. Mildner-Rihm, H. Martin, A. M. Zeiher and S. Dimmeler (2003). "Erythropoietin is a potent physiologic stimulus for endothelial progenitor cell mobilization." Blood **102**(4): 1340-1346.

Heldin, C. H. and B. Westermark (1990). "Platelet-derived growth factor: mechanism of action and possible in vivo function." Cell Regul **1**(8): 555-566.

Hierck, B. P., K. Van der Heiden, F. E. Alkemade, S. Van de Pas, J. V. Van Thienen, B. C. Groenendijk, W. H. Bax, A. Van der Laarse, M. C. Deruiter, A. J. Horrevoets and R. E. Poelmann (2008). "Primary cilia sensitize endothelial cells for fluid shear stress." Dev Dyn **237**(3): 725-735.

Hildbrand, P., V. Cirulli, R. C. Prinsen, K. A. Smith, B. E. Torbett, D. R. Salomon and L. Crisa (2004). "The role of angiopoietins in the development of endothelial cells from cord blood CD34+ progenitors." Blood **104**(7): 2010-2019.

Hill, A. L., D. A. Lowes, N. R. Webster, C. C. Sheth, N. A. Gow and H. F. Galley (2009). "Regulation of pentraxin-3 by antioxidants." Br J Anaesth **103**(6): 833-839.

Hippenstiel, S., S. Soeth, B. Kellas, O. Fuhrmann, J. Seybold, M. Krüll, C. Eichel-Streiber, M. Goebeler, S. Ludwig and N. Suttrop (2000). "Rho proteins and the p38-MAPK pathway are important mediators for LPS-induced interleukin-8 expression in human endothelial cells." Blood **95**(10): 3044-3051.

Hirase, T., J. M. Staddon, M. Saitou, Y. Ando-Akatsuka, M. Itoh, M. Furuse, K. Fujimoto, S. Tsukita and L. L. Rubin (1997). "Occludin as a possible determinant of tight junction permeability in endothelial cells." J Cell Sci **110(14)**: 1603-1613.

Hirata, A., P. Baluk, T. Fujiwara and D. M. McDonald (1995). "Location of focal silver staining at endothelial gaps in inflamed venules examined by scanning electron microscopy." Am J Physiol **269(3)**: L403-418.

Hoesel, L. M., T. A. Neff, S. B. Neff, J. G. Younger, E. W. Olle, H. Gao, M. J. Pianko, K. D. Bernacki, J. V. Sarma and P. A. Ward (2005). "Harmful and protective roles of neutrophils in sepsis." Shock **24(1)**: 40-47.

Holmes, A. K., J. Laybourn-Parry, J. D. Parry, M. E. Unwin and R. E. Challis (2006). "Ultrasonic imaging of biofilms utilizing echoes from the biofilm/air interface." IEEE Trans Ultrason Ferroelectr Freq Control **53(1)**: 185-192.

Holmes, K., O. L. Roberts, A. M. Thomas and M. J. Cross (2007). "Vascular endothelial growth factor receptor-2: Structure, function, intracellular signalling and therapeutic inhibition." Cellular Signalling **19(10)**: 2003-2012.

Holthofer, B., R. Windoffer, S. Troyanovsky and R. E. Leube (2007). "Structure and function of desmosomes." Int Rev Cytol **264**: 65-163.

Honjo, T., Y. Nishizuka and O. Hayaishi (1968). "Diphtheria toxin-dependent adenosine diphosphate ribosylation of aminoacyl transferase II and inhibition of protein synthesis." J Biol Chem **243(12)**: 3553-3555.

Hop, C., A. Guilliatt, M. Daly, H. P. de Leeuw, H. J. Brinkman, I. R. Peake, J. A. van Mourik and H. Pannekoek (2000). "Assembly of multimeric von Willebrand factor directs sorting of P-selectin." Arterioscler Thromb Vasc Biol **20**(7): 1763-1768.

Hove, J. R., R. W. Koster, A. S. Forouhar, G. Acevedo-Bolton, S. E. Fraser and M. Gharib (2003). "Intracardiac fluid forces are an essential epigenetic factor for embryonic cardiogenesis." Nature **421**(6919): 172-177.

Hsieh, P. C., M. E. Davis, L. K. Lisowski and R. T. Lee (2006). "Endothelial-cardiomyocyte interactions in cardiac development and repair." Annu Rev Physiol **68**: 51-66.

Hsu, P. P., S. Li, Y. S. Li, S. Usami, A. Ratcliffe, X. Wang and S. Chien (2001). "Effects of flow patterns on endothelial cell migration into a zone of mechanical denudation." Biochem Biophys Res Commun **285**(3): 751-759.

Hu, G. C., Y. L. Wang, Y. Sun, A. B. Malik and R. D. Minshall (2010). "Endothelial p120 catenin inhibits LPS-induced lung inflammatory injury by suppression of MAPK and NF-kappa B activation." Faseb Journal **24**.

Huber, J. D., R. D. Egleton and T. P. Davis (2001). "Molecular physiology and pathophysiology of tight junctions in the blood-brain barrier." Trends Neurosci **24**(12): 719-725.

Hughes, P. E. and M. Pfaff (1998). "Integrin affinity modulation." Trends Cell Biol **8**(9): 359-364.

Hughes, P. E., M. W. Renshaw, M. Pfaff, J. Forsyth, V. M. Keivens, M. A. Schwartz and M. H. Ginsberg (1997). "Suppression of integrin activation: a novel function of a Ras/Raf-initiated MAP kinase pathway." Cell **88**(4): 521-530.

Huttunen, R., M. Hurme, J. Aittoniemi, H. Huhtala, R. Vuento, J. Laine, J. Jylhava and J. Syrjanen (2011). "High plasma level of long pentraxin 3 (PTX3) is associated with fatal disease in bacteremic patients: a prospective cohort study." PLoS One **6**(3): 17653.

Hynes, R. O. (1987). "Integrins: A family of cell surface receptors." Cell **48**(4): 549-554.

Hynes, R. O. (1992). "Integrins: versatility, modulation, and signaling in cell adhesion." Cell **69**(1): 11-25.

Hynes, R. O. (2002). "Integrins: bidirectional, allosteric signaling machines." Cell **110**(6): 673-687.

Iaizzo, P. A. (2009). General Features of the Cardiovascular System. Handbook of Cardiac Anatomy, Physiology, and Devices, Humana Press: 3-12.

Ingber, D. E. (2002). "Mechanical signaling and the cellular response to extracellular matrix in angiogenesis and cardiovascular physiology." Circ Res **91**(10): 877-887.

Inglis, T. J. (1993). "Evidence for dynamic phenomena in residual tracheal tube biofilm." Br J Anaesth **70**(1): 22-24.

Inglis, T. J. J., L. Titmenc, N. Mahlee, T. Eekoon and H. Kokpheng (1995). "Structural features of tracheal tube biofilm formed during prolonged mechanical ventilation." Chest **108**(4): 1049-1052.

Iomini, C., K. Tejada, W. Mo, H. Vaananen and G. Piperno (2004). "Primary cilia of human endothelial cells disassemble under laminar shear stress." J Cell Biol **164**(6): 811-817.

Ishii, H., H. H. Salem, C. E. Bell, E. A. Laposata and P. W. Majerus (1986). "Thrombomodulin, an endothelial anticoagulant protein, is absent from the human brain." Blood **67**(2): 362-365.

Itoh, M., K. Morita and S. Tsukita (1999). "Characterization of ZO-2 as a MAGUK family member associated with tight as well as adherens junctions with a binding affinity to occludin and alpha catenin." J Biol Chem **274**(9): 5981-5986.

Ivanov, D., M. Philippova, J. Antropova, F. Gubaeva, O. Iljinskaya, E. Tararak, V. Bochkov, P. Erne, T. Resink and V. Tkachuk (2001). "Expression of cell adhesion molecule T-cadherin in the human vasculature." Histochem Cell Biol **115**(3): 231-242.

Jacobs, E. R., C. Cheliakine, D. Gebremedhin, E. K. Birks, P. F. Davies and D. R. Harder (1995). "Shear activated channels in cell-attached patches of cultured bovine aortic endothelial cells." Pflugers Arch **431**(1): 129-131.

Jalali, S., Y. S. Li, M. Sotoudeh, S. Yuan, S. Li, S. Chien and J. Y. Shyy (1998). "Shear stress activates p60src-Ras-MAPK signaling pathways in vascular endothelial cells." Arterioscler Thromb Vasc Biol **18**(2): 227-234.

James, A. M. and M. P. Murphy (2002). "How mitochondrial damage affects cell function." Journal of biomedical science **9**(6): 475-487.

Janmey, P. A. and R. T. Miller (2011). "Mechanisms of mechanical signaling in development and disease." Journal of Cell Science **124**(1): 9-18.

Jay, D., E. J. Garcia, J. E. Lara, M. A. Medina and M. de la Luz Ibarra (2000). "Determination of a cAMP-dependent protein kinase phosphorylation site in the C-terminal region of human endothelial actin-binding protein." Arch Biochem Biophys **377**(1): 80-84.

Jeansson, M. and B. Haraldsson (2006). "Morphological and functional evidence for an important role of the endothelial cell glycocalyx in the glomerular barrier." American Journal of Physiology - Renal Physiology **290**(1): F111-F116.

Johansen, P., G. Senti, J. Maria Martinez Gomez and T. M. Kundig (2008). "Medication with antihistamines impairs allergen-specific immunotherapy in mice." Clin Exp Allergy **38**(3): 512-519.

Johansen, P., A. Weiss, A. Bunter, Y. Waeckerle-Men, A. Fettelschoss, B. Odermatt and T. M. Kundig (2011). "Clemastine causes immune suppression through inhibition of extracellular signal-regulated kinase-dependent proinflammatory cytokines." The Journal of allergy and clinical immunology **128**(6): 1286-1294.

Johnson, P. C. (1977). "Landis Award Lecture. The myogenic response and the microcirculation." Microvasc Res **13**(1): 1-18.

Johnson, P. C. (1989). "The myogenic response in the microcirculation and its interaction with other control systems." J Hypertens Suppl **7**(4): S33-39.

Johnson, P. C. (2008). Overview of the Microcirculation. Handbook of Physiology: Microcirculation. R. F. Tuma, N. W. Duran and K. Ley. San Diego, Academic Press.

Jones, N., K. Iljin, D. J. Dumont and K. Alitalo (2001). "Tie receptors: new modulators of angiogenic and lymphangiogenic responses." Nature reviews Molecular cell biology **2**(4): 257-267.

Josephs, M. D., F. R. Bahjat, K. Fukuzuka, R. Ksontini, C. C. Solorzano, C. K. Edwards, C. L. Tannahill, S. L. MacKay, E. M. Copeland and L. L. Moldawer (2000). "Lipopolysaccharide

and D-galactosamine-induced hepatic injury is mediated by TNF-alpha and not by Fas ligand." Am J Physiol Regul Integr Comp Physiol **278**(5): R1196-1201.

Just, I., F. Hofmann, H. Genth and R. Gerhard (2001). "Bacterial protein toxins inhibiting low-molecular-mass GTP-binding proteins." Int J Med Microbiol **291**(4): 243-250.

Just, I., C. Mohr, G. Schallehn, L. Menard, J. R. Didsbury, J. Vandekerckhove, J. van Damme and K. Aktories (1992). "Purification and characterization of an ADP-ribosyltransferase produced by *Clostridium limosum*." J Biol Chem **267**(15): 10274-10280.

Kainulainen, T., A. Pender, M. D'Addario, Y. Feng, P. Lekic and C. A. McCulloch (2002). "Cell death and mechanoprotection by filamin a in connective tissues after challenge by applied tensile forces." J Biol Chem **277**(24): 21998-22009.

Kakkar, P. and B. K. Singh (2007). "Mitochondria: a hub of redox activities and cellular distress control." Molecular and Cellular Biochemistry **305**(1-2): 235-253.

Kanner, S. B., A. B. Reynolds and J. T. Parsons (1991). "Tyrosine phosphorylation of a 120-kilodalton pp60src substrate upon epidermal growth factor and platelet-derived growth factor receptor stimulation and in polyomavirus middle-T-antigen-transformed cells." Mol Cell Biol **11**(2): 713-720.

Kaplan, J. B. (2005). "Methods for the treatment and opinion prevention of bacterial biofilms." Expert Opinion on Therapeutic Patents **15**(8): 955-965.

Kathuria, H., Y. X. Cao, M. I. Ramirez and M. C. Williams (2004). "Transcription of the caveolin-1 gene is differentially regulated in lung type I epithelial and endothelial cell lines. A role for ETS proteins in epithelial cell expression." The Journal of biological chemistry **279**(29): 30028-30036.

Kawamoto, S. and H. Hidaka (1984). "Ca²⁺-activated, phospholipid-dependent protein kinase catalyzes the phosphorylation of actin-binding proteins." Biochem Biophys Res Commun **118**(3): 736-742.

Keelan, E. T., S. T. Licence, A. M. Peters, R. M. Binns and D. O. Haskard (1994). "Characterization of E-selectin expression in vivo with use of a radiolabeled monoclonal antibody." The American journal of physiology **266**(1 Pt 2): H278-290.

Keely, P. J., E. V. Rusyn, A. D. Cox and L. V. Parise (1999). "R-Ras Signals through Specific Integrin α Cytoplasmic Domains to Promote Migration and Invasion of Breast Epithelial Cells." The Journal of Cell Biology **145**(5): 1077-1088.

Keese, C. R., K. Bhawe, J. Wegener and I. Giaever (2002). "Real-time impedance assay to follow the invasive activities of metastatic cells in culture." Biotechniques **33**(4): 842.

Keese, C. R. and I. Giaever (1990). "Electrical surveillance of mammalian-cells in culture." Biophysical Journal **57**(2): A378-A378.

Keese, C. R., J. Wegener, S. R. Walker and I. Giaever (2004). "Electrical wound-healing assay for cells in vitro." Proceedings of the National Academy of Sciences of the United States of America **101**(6): 1554-1559.

Keller, T. T., A. T. Mairuhu, M. D. de Kruif, S. K. Klein, V. E. Gerdes, H. ten Cate, D. P. Brandjes, M. Levi and E. C. van Gorp (2003). "Infections and endothelial cells." Cardiovasc Res **60**(1): 40-48.

Kelly, J. J., T. M. Moore, P. Babal, A. H. Diwan, T. Stevens and W. J. Thompson (1998). "Pulmonary microvascular and macrovascular endothelial cells: differential regulation of Ca²⁺ and permeability." Am J Physiol **274**(5): L810-819.

Kennedy, P., S. Brammah and E. Wills (2010). "Burns, biofilm and a new appraisal of burn wound sepsis." Burns **36**(1): 49-56.

Keon, B. H., S. Schafer, C. Kuhn, C. Grund and W. W. Franke (1996). "Symplekin, a novel type of tight junction plaque protein." J Cell Biol **134**(4): 1003-1018.

Khachigian, L. M., N. Resnick, M. A. Gimbrone, Jr. and T. Collins (1995). "Nuclear factor-kappa B interacts functionally with the platelet-derived growth factor B-chain shear-stress response element in vascular endothelial cells exposed to fluid shear stress." J Clin Invest **96**(2): 1169-1175.

Kim, H.-S., K. Y. Won, G. Y. Kim, S. C. Kim, Y.-K. Park and Y. W. Kim (2012). "Reduced expression of Raf-1 kinase inhibitory protein predicts regional lymph node metastasis and shorter survival in esophageal squamous cell carcinoma." Pathology - Research and Practice **208**(5): 292-299.

Kim, J. H., J. H. Kim, J. A. Park, S. W. Lee, W. J. Kim, Y. S. Yu and K. W. Kim (2006). "Blood-neural barrier: intercellular communication at glio-vascular interface." J Biochem Mol Biol **39**(4): 339-345.

Kim, K. L., I.-S. Shin, J.-M. Kim, J.-H. Choi, J. Byun, E.-S. Jeon, W. Suh and D.-K. Kim (2006). "Interaction between Tie receptors modulates angiogenic activity of angiopoietin2 in endothelial progenitor cells." Cardiovascular research **72**(3): 394-402.

Kim, M. P., S. I. Park, S. Kopetz and G. E. Gallick (2009). "Src family kinases as mediators of endothelial permeability: effects on inflammation and metastasis." Cell and Tissue Research **335**(1): 249-259.

Kim, S., L. Mi and L. Zhang (2012). "Specific elevation of DcR3 in sera of sepsis patients and its potential role as a clinically important biomarker of sepsis." Diagnostic microbiology and infectious disease **73**(4): 312-317.

Kim, Y. B. and D. W. Watson (1966). "Role of antibodies in reactions to gram-negative bacterial endotoxins." Ann N Y Acad Sci **133**(2): 727-745.

Kirman, I., R. L. Whelan and O. H. Nielsen (2004). "Infliximab: mechanism of action beyond TNF-alpha neutralization in inflammatory bowel disease." Eur J Gastroenterol Hepatol **16**(7): 639-641.

Kjoller, L. and A. Hall (1999). "Signaling to Rho GTPases." Exp Cell Res **253**(1): 166-179.

Klabunde, R. E. (2011). Cardiovascular physiology concepts, Lippincott Williams & Wilkins.

Klein, S., F. G. Giancotti, M. Presta, S. M. Albelda, C. A. Buck and D. B. Rifkin (1993). "Basic fibroblast growth factor modulates integrin expression in microvascular endothelial cells." Molecular Biology of the Cell **4**(10): 973-982.

Klibanov, A. L. (2006). "Microbubble contrast agents - Targeted ultrasound imaging and ultrasound-assisted drug-delivery applications." Investigative Radiology **41**(3): 354-362.

Klibanov, A. L. (2007). "Ultrasound molecular imaging with targeted microbubble contrast agents." Journal of Nuclear Cardiology **14**(6): 876-884.

Klibanov, A. L. (2009). "Preparation of targeted microbubbles: ultrasound contrast agents for molecular imaging." Medical & Biological Engineering & Computing **47**(8): 875-882.

Klibanov, A. L., M. S. Hughes, F. S. Villanueva, R. J. Jankowski, W. R. Wagner, J. K. Wojdyla, J. H. Wible and G. H. Brandenburger (1999). "Targeting and ultrasound imaging of microbubble-based contrast agents." Magnetic Resonance Materials in Biology, Physics, and Medicine **8**(3): 177-184.

Klymkowsky, M. W. (1999). "Weaving a tangled web: the interconnected cytoskeleton." Nature Cell Biology **1**(5): E121-E123.

Knspik, D. A., B. Starkoski, C. J. Pavlin and F. S. Foster (2000). "A 100-200 MHz ultrasound biomicroscope." IEEE Trans Ultrason Ferroelectr Freq Control **47**(6): 1540-1549.

Koga, S., S. Morris, S. Ogawa, H. Liao, J. P. Bilezikian, G. Chen, W. J. Thompson, T. Ashikaga, J. Brett, D. M. Stern and a. et (1995). "TNF modulates endothelial properties by decreasing cAMP." American Journal of Physiology **268**(5): C1104-C1113.

Koh, G. C., S. J. Peacock, T. van der Poll and W. J. Wiersinga (2012). "The impact of diabetes on the pathogenesis of sepsis." Eur J Clin Microbiol Infect Dis **31**(4): 379-388.

Kohn, S., J. A. Nagy, H. F. Dvorak and A. M. Dvorak (1992). "Pathways of macromolecular tracer transport across venules and small veins. Structural basis for the hyperpermeability of tumor blood vessels." Lab Invest **67**(5): 596-607.

Kolarova, H., B. Ambruzova, L. Svihalkova Sindlerova, A. Klinke and L. Kubala (2014). "Modulation of endothelial glycocalyx structure under inflammatory conditions." Mediators Inflamm **2014**: 694312.

Kolosova, I. A., T. Mirzapioiazova, L. Moreno-Vinasco, S. Sammani, J. G. Garcia and A. D. Verin (2008). "Protective effect of purinergic agonist ATPgammaS against acute lung injury." Am J Physiol Lung Cell Mol Physiol **294**(2): L319-324.

Komarova, Y. and A. B. Malik (2010). "Regulation of endothelial permeability via paracellular and transcellular transport pathways." Annu Rev Physiol **72**: 463-493.

Komatsu, M. and E. Ruoslahti (2005). "R-Ras is a global regulator of vascular regeneration that suppresses intimal hyperplasia and tumor angiogenesis." Nature medicine **11**(12): 1346-1350.

Kontos, C. D., E. H. Cha, J. D. York and K. G. Peters (2002). "The endothelial receptor tyrosine kinase Tie1 activates phosphatidylinositol 3-kinase and Akt to inhibit apoptosis." Mol Cell Biol **22**(6): 1704-1713.

Kowalczyk, A. P. and K. J. Green (2013). "Structure, function, and regulation of desmosomes." Prog Mol Biol Transl Sci **116**: 95-118.

Kozminski, K. G., K. A. Johnson, P. Forscher and J. L. Rosenbaum (1993). "A motility in the eukaryotic flagellum unrelated to flagellar beating." Proceedings of the National Academy of Sciences of the United States of America **90**(12): 5519-5523.

Krautkramer, E., S. Grouls, D. Hettwer, N. Rafat, B. Tonshoff and M. Zeier (2014). "Mobilization of circulating endothelial progenitor cells correlates with the clinical course of hantavirus disease." J Virol **88**(1): 483-489.

Kriegler, M., C. Perez, K. DeFay, I. Albert and S. D. Lu (1988). "A novel form of TNF/cachectin is a cell surface cytotoxic transmembrane protein: ramifications for the complex physiology of TNF." Cell **53**(1): 45-53.

Kruger, O., A. Plum, J. S. Kim, E. Winterhager, S. Maxeiner, G. Hallas, S. Kirchhoff, O. Traub, W. H. Lamers and K. Willecke (2000). "Defective vascular development in connexin 45-deficient mice." Development **127**(19): 4179-4193.

Kujundzic, E., A. C. Fonseca, E. A. Evans, M. Peterson, A. R. Greenberg and M. Hernandez (2007). "Ultrasonic monitoring of early-stage biofilm growth on polymeric surfaces." J Microbiol Methods **68**(3): 458-467.

Kustermann, S., T. Manigold, C. Ploix, M. Skubatz, T. Heckel, H. Hinton, T. Weiser, T. Singer, L. Suter and A. Roth (2014). "A real-time impedance-based screening assay for drug-induced vascular leakage." Toxicol Sci **138**(2): 333-343.

Kwon, R. Y., D. A. Hoey and C. R. Jacobs (2006). "Mechanobiology of primary cilia." Cellular and biomolecular mechanics and mechanobiology: 99-124.

Kyndt, F., J. P. Gueffet, V. Probst, P. Jaafar, A. Legendre, F. Le Bouffant, C. Toquet, E. Roy, L. McGregor, S. A. Lynch, R. Newbury-Ecob, V. Tran, I. Young, J. N. Trochu, H. Le Marec and J. J. Schott (2007). "Mutations in the gene encoding filamin A as a cause for familial cardiac valvular dystrophy." Circulation **115**(1): 40-49.

Lai, C. H. and K. H. Kuo (2005). "The critical component to establish in vitro BBB model: Pericyte." Brain Res Brain Res Rev **50**(2): 258-265.

Lakhani, S. A. and C. W. Bogue (2003). "Toll-like receptor signaling in sepsis." Current Opinion in Pediatrics **15**(3): 278-282.

Lamagna, C., K. M. Hodivala-Dilke, B. A. Imhof and M. Aurrand-Lions (2005). "Antibody against junctional adhesion molecule-C inhibits angiogenesis and tumor growth." Cancer Res **65**(13): 5703-5710.

Lambe, D. W., K. P. Ferguson, K. J. Mayberry-Carson, B. Tober-Meyer and J. W. Costerton (1991). "Foreign-Body-Associated Experimental Osteomyelitis Induced With Bacteroides

fragilis and Staphylococcus epidermidis in Rabbits." Clinical Orthopaedics and Related Research **266**: 285-294.

Lampugnani, M. G. (2012). "Endothelial cell-to-cell junctions: adhesion and signaling in physiology and pathology." Cold Spring Harb Perspect Med **2**(10): 6528.

Lampugnani, M. G., M. Corada, L. Caveda, F. Breviario, O. Ayalon, B. Geiger and E. Dejana (1995). "The molecular organization of endothelial cell to cell junctions: differential association of plakoglobin, beta-catenin, and alpha-catenin with vascular endothelial cadherin (VE-cadherin)." J Cell Biol **129**(1): 203-217.

Lampugnani, M. G. and E. Dejana (1997). "Interendothelial junctions: structure, signalling and functional roles." Curr Opin Cell Biol **9**(5): 674-682.

Lampugnani, M. G. and E. Dejana (2007). "Adherens junctions in endothelial cells regulate vessel maintenance and angiogenesis." Thromb Res **120**(2): S1-6.

Lampugnani, M. G., M. Resnati, M. Raiteri, R. Pigott, A. Pisacane, G. Houen, L. P. Ruco and E. Dejana (1992). "A novel endothelial-specific membrane protein is a marker of cell-cell contacts." The Journal of cell biology **118**(6): 1511-1522.

Langille, B. L. and F. O'Donnell (1986). "Reductions in arterial diameter produced by chronic decreases in blood flow are endothelium-dependent." Science **231**(4736): 405-407.

Langille, B. L., M. A. Reidy and R. L. Kline (1986). "Injury and repair of endothelium at sites of flow disturbances near abdominal aortic coarctations in rabbits." Arteriosclerosis **6**(2): 146-154.

Laszik, Z. G., X. J. Zhou, G. L. Ferrell, F. G. Silva and C. T. Esmon (2001). "Down-regulation of endothelial expression of endothelial cell protein C receptor and thrombomodulin in coronary atherosclerosis." The American journal of pathology **159**(3): 797-802.

Latour, S. and A. Veillette (2001). "Proximal protein tyrosine kinases in immunoreceptor signaling." Curr Opin Immunol **13**(3): 299-306.

Leckband, D. and S. Sivasankar (2000). "Mechanism of homophilic cadherin adhesion." Curr Opin Cell Biol **12**(5): 587-592.

Lee, H. J. and G. Y. Koh (2003). "Shear stress activates Tie2 receptor tyrosine kinase in human endothelial cells." Biochemical and biophysical research communications **304**(2): 399-404.

Lee, K. W., G. Y. Lip and A. D. Blann (2004). "Plasma angiopoietin-1, angiopoietin-2, angiopoietin receptor tie-2, and vascular endothelial growth factor levels in acute coronary syndromes." Circulation **110**(16): 2355-2360.

Levy, M., K. A. Krobert, K. Wittig, N. Voigt, M. Bermudez, G. Wolber, D. Dobrev, F. O. Levy and T. Wieland (2013). "NSC23766, a widely used inhibitor of Rac1 activation, additionally acts as a competitive antagonist at muscarinic acetylcholine receptors." J Pharmacol Exp Ther **347**(1): 69-79.

Lever, A. and I. Mackenzie (2007). "Sepsis: definition, epidemiology, and diagnosis." BMJ **335**(7625): 879-883.

Levesque, M. J. and R. M. Nerem (1985). "The elongation and orientation of cultured endothelial cells in response to shear stress." J Biomech Eng **107**(4): 341-347.

Levy, M. M., R. P. Dellinger, S. R. Townsend, W. T. Linde-Zwirble, J. C. Marshall, J. Bion, C. Schorr, A. Artigas, G. Ramsay, R. Beale, M. M. Parker, H. Gerlach, K. Reinhart, E. Silva, M. Harvey, S. Regan and D. C. Angus (2010). "The Surviving Sepsis Campaign: results of an international guideline-based performance improvement program targeting severe sepsis." Intensive Care Med **36**(2): 222-231.

Levy, M. M., M. P. Fink, J. C. Marshall, E. Abraham, D. Angus, D. Cook, J. Cohen, S. M. Opal, J. L. Vincent, G. Ramsay and C. International Sepsis Definitions (2003). "2001 SCCM/ESICM/ACCP/ATS/SIS International Sepsis Definitions Conference." Intensive Care Med **29**(4): 530-538.

Ley, K. (2003). "The role of selectins in inflammation and disease." Trends Mol Med **9**(6): 263-268.

Ley, K. (2008). The microcirculation in inflammation. Microcirculation. R. F. Tuma, N. W. Duran and K. Ley. San Diego, Academic Press: 387-448.

Li, G. and H. Qian (2002). "Kinetic Timing: A Novel Mechanism That Improves the Accuracy of GTPase Timers in Endosome Fusion and Other Biological Processes." Traffic **3**(4): 249-255.

Li, G. and X. C. Zhang (2004). "GTP hydrolysis mechanism of Ras-like GTPases." J Mol Biol **340**(5): 921-932.

Li, S., M. Kim, Y. L. Hu, S. Jalali, D. D. Schlaepfer, T. Hunter, S. Chien and J. Y. Shyy (1997). "Fluid shear stress activation of focal adhesion kinase. Linking to mitogen-activated protein kinases." J Biol Chem **272**(48): 30455-30462.

Li, Y. S., J. Y. Shyy, S. Li, J. Lee, B. Su, M. Karin and S. Chien (1996). "The Ras-JNK pathway is involved in shear-induced gene expression." Mol Cell Biol **16**(11): 5947-5954.

Li, Y. S. J., J. H. Haga and S. Chien (2005). "Molecular basis of the effects of shear stress on vascular endothelial cells." Journal of biomechanics **38**(10): 1949-1971.

Liang, H. D. and M. J. K. Blomley (2003). "The role of ultrasound in molecular imaging." Br J Radiol **76**(2): S140-150.

Liao, Z., H. Kato, M. Pandey, J. M. Cantor, A. J. Ablooglu, M. H. Ginsberg and S. J. Shattil (2015). "Interaction of kindlin-2 with integrin beta3 promotes outside-in signaling responses by the alphaVbeta3 vitronectin receptor." Blood **125**(12): 1995-2004.

Liaw, C. W., C. Cannon, M. D. Power, P. K. Kiboneka and L. L. Rubin (1990). "Identification and cloning of two species of cadherins in bovine endothelial cells." The EMBO journal **9**(9): 2701-2708.

Liebner, S., A. Fischmann, G. Rascher, F. Duffner, E. H. Grote, H. Kalbacher and H. Wolburg (2000). "Claudin-1 and claudin-5 expression and tight junction morphology are altered in blood vessels of human glioblastoma multiforme." Acta Neuropathol **100**(3): 323-331.

Lievano, S., L. Alarcon, B. Chavez-Munguia and L. Gonzalez-Mariscal (2006). "Endothelia of term human placentae display diminished expression of tight junction proteins during preeclampsia." Cell Tissue Res **324**(3): 433-448.

Lin, K., P.-P. Hsu, B. P. Chen, S. Yuan, S. Usami, J. Y. J. Shyy, Y.-S. Li and S. Chien (2000). "Molecular mechanism of endothelial growth arrest by laminar shear stress." Proceedings of the National Academy of Sciences of the United States of America **97**(17): 9385-9389.

Lin, M.-T., M.-L. Yen, C.-Y. Lin and M.-L. Kuo (2003). "Inhibition of Vascular Endothelial Growth Factor-Induced Angiogenesis by Resveratrol through Interruption of Src-Dependent Vascular Endothelial Cadherin Tyrosine Phosphorylation." Molecular Pharmacology **64**(5): 1029-1036.

Linnemann, T., C. Kiel, P. Herter and C. Herrmann (2002). "The activation of RalGDS can be achieved independently of its ras binding domain: Implications of an activation mechanism in ras effector specificity and signal distribution." Journal of Biological Chemistry **277**(10): 7831-7837.

Lipowsky, H. H., L. Gao and A. Lescanic (2011). "Shedding of the endothelial glycocalyx in arterioles, capillaries, and venules and its effect on capillary hemodynamics during inflammation." Am J Physiol Heart Circ Physiol **301**(6): H2235-2245.

Little, T. L., E. C. Beyer and B. R. Duling (1995). "Connexin-43 and Connexin-40 Gap Junctional Proteins Are Present in Arteriolar Smooth-Muscle and Endothelium in-Vivo." American Journal of Physiology-Heart and Circulatory Physiology **268**(2): H729-H739.

Liu, D., Y. L. Lau, Y. K. Chau and G. Pacepavicius (1994). "Simple technique for estimation of biofilm accumulation." Bull Environ Contam Toxicol **53**(6): 913-918.

Liu, M. and J. Yang (2009). "Electrokinetic effect of the endothelial glycocalyx layer on two-phase blood flow in small blood vessels." Microvasc Res **78**(1): 14-19.

Liu, S., D. A. Calderwood and M. H. Ginsberg (2000). "Integrin cytoplasmic domain-binding proteins." J Cell Sci **113**(20): 3563-3571.

Liu, Y., H. Miyoshi and M. Nakamura (2006). "Encapsulated ultrasound microbubbles: therapeutic application in drug/gene delivery." Journal of controlled release : official journal of the Controlled Release Society **114**(1): 89-99.

Lossinsky, A. S. and R. R. Shivers (2004). "Structural pathways for macromolecular and cellular transport across the blood-brain barrier during inflammatory conditions. Review." Histol Histopathol **19**(2): 535-564.

Lowe, D. G., D. J. Capon, E. Delwart, A. Y. Sakaguchi, S. L. Naylor and D. V. Goeddel (1987). "Structure of the human and murine R-ras genes, novel genes closely related to ras proto-oncogenes." Cell **48**(1): 137-146.

Lowe, D. G. and D. V. Goeddel (1987). "Heterologous expression and characterization of the human R-ras gene product." Mol Cell Biol **7**(8): 2845-2856.

Lu, T. T., M. Barreuther, S. Davis and J. A. Madri (1997). "Platelet endothelial cell adhesion molecule-1 is phosphorylatable by c-Src, binds Src-Src homology 2 domain, and exhibits immunoreceptor tyrosine-based activation motif-like properties." J Biol Chem **272**(22): 14442-14446.

Lum, H. and A. B. Malik (1994). "Regulation of vascular endothelial barrier function." Am J Physiol **267**(3): L223-241.

Lum, H. and A. B. Malik (1996). "Mechanisms of increased endothelial permeability." Can J Physiol Pharmacol **74**(7): 787-800.

Lundblad, C., P. Bentzer and P. O. Grande (2004). "The permeability-reducing effects of prostacyclin and inhibition of Rho kinase do not counteract endotoxin-induced increase in permeability in cat skeletal muscle." Microvasc Res **68**(3): 286-294.

Lupu, C., A. D. Westmuckett, G. Peer, L. Ivanciu, H. Zhu, F. B. Taylor, Jr. and F. Lupu (2005). "Tissue factor-dependent coagulation is preferentially up-regulated within arterial branching areas in a baboon model of Escherichia coli sepsis." The American journal of pathology **167**(4): 1161-1172.

Majcherczyk, P. A., H. Langen, D. Heumann, M. Fountoulakis, M. P. Glauser and P. Moreillon (1999). "Digestion of Streptococcus pneumoniae cell walls with its major peptidoglycan hydrolase releases branched stem peptides carrying proinflammatory activity." J Biol Chem **274**(18): 12537-12543.

Majno, G. and G. E. Palade (1961). "Studies on inflammation. 1. The effect of histamine and serotonin on vascular permeability: an electron microscopic study." The Journal of biophysical and biochemical cytology **11**: 571-605.

Malek, A. M. and S. Izumo (1996). "Mechanism of endothelial cell shape change and cytoskeletal remodeling in response to fluid shear stress." J Cell Sci **109**(4): 713-726.

Mammoto, A., S. Huang and D. E. Ingber (2007). "Filamin links cell shape and cytoskeletal structure to Rho regulation by controlling accumulation of p190RhoGAP in lipid rafts." J Cell Sci **120**(3): 456-467.

Maniotis, A. J., C. S. Chen and D. E. Ingber (1997). "Demonstration of mechanical connections between integrins, cytoskeletal filaments, and nucleoplasm that stabilize nuclear structure." Proceedings of the National Academy of Sciences of the United States of America **94**(3): 849-854.

Manning, G., D. B. Whyte, R. Martinez, T. Hunter and S. Sudarsanam (2002). "The protein kinase complement of the human genome." Science **298**(5600): 1912-1934.

Marshall, J. C., P. M. Walker, D. M. Foster, D. Harris, M. Ribeiro, J. Paice, A. D. Romaschin and A. N. Derzko (2002). "Measurement of endotoxin activity in critically ill patients using whole blood neutrophil dependent chemiluminescence." Crit Care **6**(4): 342-348.

Marte, B. M., P. Rodriguez-Viciano, S. Wennstrom, P. H. Warne and J. Downward (1997). "R-Ras can activate the phosphoinositide 3-kinase but not the MAP kinase arm of the Ras effector pathways." Curr Biol **7**(1): 63-70.

Marti, A., Z. Luo, C. Cunningham, Y. Ohta, J. Hartwig, T. P. Stossel, J. M. Kyriakis and J. Avruch (1997). "Actin-binding protein-280 binds the stress-activated protein kinase (SAPK) activator SEK-1 and is required for tumor necrosis factor-alpha activation of SAPK in melanoma cells." J Biol Chem **272**(5): 2620-2628.

Martich, G. D., R. L. Danner, M. Ceska and A. F. Suffredini (1991). "Detection of interleukin 8 and tumor necrosis factor in normal humans after intravenous endotoxin: the effect of antiinflammatory agents." The Journal of experimental medicine **173**(4): 1021-1024.

Martin, G. and E. T. Carroll (1959). "Tables of the Speed of Sound in Water." The Journal of the Acoustical Society of America **31**(1): 75-76.

Martin, M. U. and H. Wesche (2002). "Summary and comparison of the signaling mechanisms of the Toll/interleukin-1 receptor family." Biochim Biophys Acta **1592**(3): 265-280.

Mathison, J. C., E. Wolfson and R. J. Ulevitch (1988). "Participation of tumor necrosis factor in the mediation of gram negative bacterial lipopolysaccharide-induced injury in rabbits." J Clin Invest **81**(6): 1925-1937.

Matsudaira, P. (1994). "Actin crosslinking proteins at the leading edge." Semin Cell Biol **5**(3): 165-174.

Matsumoto, T., S. Bohman, J. Dixelius, T. Berge, A. Dimberg, P. Magnusson, L. Wang, C. Wikner, J. H. Qi, C. Wernstedt, J. Wu, S. Bruheim, H. Mugishima, D. Mukhopadhyay, A. Spurkland and L. Claesson-Welsh (2005). "VEGF receptor-2 Y951 signaling and a role for the adapter molecule TSA1 in tumor angiogenesis." EMBO J **24**(13): 2342-2353.

Matter, M. L. and E. Ruoslahti (2001). "A signaling pathway from the alpha5beta1 and alpha(v)beta3 integrins that elevates bcl-2 transcription." J Biol Chem **276**(30): 27757-27763.

Matter, M. L., Z. Zhang, C. Nordstedt and E. Ruoslahti (1998). "The alpha5beta1 integrin mediates elimination of amyloid-beta peptide and protects against apoptosis." J Cell Biol **141**(4): 1019-1030.

Mayr, F. B., S. Yende and D. C. Angus (2014). "Epidemiology of severe sepsis." Virulence **5**(1): 4-11.

McCann, J. A., S. D. Peterson, M. W. Plesniak, T. J. Webster and K. M. Haberstroh (2005). "Non-uniform flow behavior in a parallel plate flow chamber : alters endothelial cell responses." Ann Biomed Eng **33**(3): 328-336.

McCuskey, R. S., P. A. McCuskey, R. Urbaschek and B. Urbaschek (1984). "Species differences in Kupffer cells and endotoxin sensitivity." Infect Immun **45**(1): 278-280.

McEver, R. P., J. H. Beckstead, K. L. Moore, L. Marshall-Carlson and D. F. Bainton (1989). "GMP-140, a platelet alpha-granule membrane protein, is also synthesized by vascular endothelial cells and is localized in Weibel-Palade bodies." J Clin Invest **84**(1): 92-99.

McKenzie, J. A. and A. J. Ridley (2007). "Roles of Rho/ROCK and MLCK in TNF-alpha-induced changes in endothelial morphology and permeability." J Cell Physiol **213**(1): 221-228.

Medzhitov, R. (2001). "Toll-like receptors and innate immunity." Nat Rev Immunol **1**(2): 135-145.

Mehta, D. and A. B. Malik (2006). "Signaling mechanisms regulating endothelial permeability." Physiological reviews **86**(1): 279-367.

Mehta, D., A. Rahman and A. B. Malik (2001). "Protein Kinase C- α Signals Rho-Guanine Nucleotide Dissociation Inhibitor Phosphorylation and Rho Activation and Regulates the Endothelial Cell Barrier Function." Journal of Biological Chemistry **276**(25): 22614-22620.

Miao, H., E. Burnett, M. Kinch, E. Simon and B. Wang (2000). "Activation of EphA2 kinase suppresses integrin function and causes focal-adhesion-kinase dephosphorylation." Nat Cell Biol **2**(2): 62-69.

Michel, C. C. and C. R. Neal (1999). "Openings through endothelial cells associated with increased microvascular permeability." Microcirculation **6**(1): 45-54.

Mishra, V. (2007). "Oxidative stress and role of antioxidant supplementation in critical illness." Clin Lab **53**(3-4): 199-209.

Mitzner, W. and E. M. Wagner (2004). "Vascular remodeling in the circulations of the lung." Journal of Applied Physiology **97**(5): 1999-2004.

Miyasaka, M. and T. Tanaka (2004). "Lymphocyte trafficking across high endothelial venules: dogmas and enigmas." Nat Rev Immunol **4**(5): 360-370.

Mokart, D., M. Leone, A. Sannini, J. P. Brun, A. Tison, J. R. Delpero, G. Houvenaeghel, J. L. Blache and C. Martin (2005). "Predictive perioperative factors for developing severe sepsis after major surgery." Br J Anaesth **95**(6): 776-781.

Moore, M. A. S., K. Hattori, B. Heissig, J. H. Shieh, S. Dias, R. G. Crystal and S. Rafii (2001). "Mobilization of endothelial and hematopoietic stem and progenitor cells by adenovector-mediated elevation of serum levels of SDF-1, VEGF, and angiopoietin-1." Hematopoietic Stem Cells 2000 Basic and Clinical Sciences **938**: 36-47.

Mora, N., R. Rosales and C. Rosales (2007). "R-Ras promotes metastasis of cervical cancer epithelial cells." Cancer Immunol Immunother **56**(4): 535-544.

Moran, C. M., R. J. Watson, K. A. A. Fox and W. N. McDicken (2002). "In vitro acoustic characterisation of four intravenous ultrasonic contrast agents at 30 MHz." Ultrasound in Medicine & Biology **28**(6): 785-791.

Morath, S., A. Geyer and T. Hartung (2001). "Structure-function relationship of cytokine induction by lipoteichoic acid from *Staphylococcus aureus*." J Exp Med **193**(3): 393-397.

Morita, K., H. Sasaki, K. Furuse, M. Furuse, S. Tsukita and Y. Miyachi (2003). "Expression of claudin-5 in dermal vascular endothelia." Exp Dermatol **12**(3): 289-295.

Moro, F., R. Carrozzo, P. Veggiotti, G. Tortorella, D. Toniolo, A. Volzone and R. Guerrini (2002). "Familial periventricular heterotopia: missense and distal truncating mutations of the FLN1 gene." Neurology **58**(6): 916-921.

Moyon, D., L. Pardanaud, L. Yuan, C. Breant and A. Eichmann (2001). "Plasticity of endothelial cells during arterial-venous differentiation in the avian embryo." Development (Cambridge, England) **128**(17): 3359-3370.

Muller, L. M., K. J. Gorter, E. Hak, W. L. Goudzwaard, F. G. Schellevis, A. I. Hoepelman and G. E. Rutten (2005). "Increased risk of common infections in patients with type 1 and type 2 diabetes mellitus." Clin Infect Dis **41**(3): 281-288.

Muller, S. L., M. Portwich, A. Schmidt, D. I. Utepbergenov, O. Huber, I. E. Blasig and G. Krause (2005). "The tight junction protein occludin and the adherens junction protein alpha-catenin share a common interaction mechanism with ZO-1." Journal of Biological Chemistry **280**(5): 3747-3756.

Murray, C. K. (2008). "Epidemiology of infections associated with combat-related injuries in Iraq and Afghanistan." J Trauma **64**(3): S232-238.

Nakamura, F., T. M. Osborn, C. A. Hartemink, J. H. Hartwig and T. P. Stossel (2007). "Structural basis of filamin A functions." The Journal of Cell Biology **179**(5): 1011-1025.

Nakamura, F., T. P. Stossel and J. H. Hartwig (2011). "The filamins: organizers of cell structure and function." Cell Adh Migr **5**(2): 160-169.

Naruse, K. and M. Sokabe (1993). "Involvement of stretch-activated ion channels in Ca²⁺ mobilization to mechanical stretch in endothelial cells." Am J Physiol **264**(4): C1037-1044.

Natanson, C., R. L. Danner, R. J. Elin, J. M. Hosseini, K. W. Peart, S. M. Banks, T. J. MacVittie, R. I. Walker and J. E. Parrillo (1989). "Role of endotoxemia in cardiovascular dysfunction and mortality. Escherichia coli and Staphylococcus aureus challenges in a canine model of human septic shock." J Clin Invest **83**(1): 243-251.

Nduka, O. O. and J. E. Parrillo (2011). "The pathophysiology of septic shock." Critical care nursing clinics of North America **23**(1): 41-66.

Nickel, J. C., J. B. Wright, I. Ruseska, T. J. Marrie, C. Whitfield and J. W. Costerton (1985). "Antibiotic-resistance of pseudomonas-aeruginosa colonizing a urinary catheter *in vitro*." European Journal of Clinical Microbiology & Infectious Diseases **4**(2): 213-218.

Nieuwdorp, M., M. C. Meuwese, H. L. Mooij, C. Ince, L. N. Broekhuizen, J. J. Kastelein, E. S. Stroes and H. Vink (2008). "Measuring endothelial glycocalyx dimensions in humans: a potential novel tool to monitor vascular vulnerability." J Appl Physiol (1985) **104**(3): 845-852.

Nieuwdorp, M., T. W. van Haften, M. C. Gouverneur, H. L. Mooij, M. H. van Lieshout, M. Levi, J. C. Meijers, F. Holleman, J. B. Hoekstra, H. Vink, J. J. Kastelein and E. S. Stroes (2006). "Loss of endothelial glycocalyx during acute hyperglycemia coincides with endothelial dysfunction and coagulation activation in vivo." Diabetes **55**(2): 480-486.

Nishigaki, M., K. Aoyagi, I. Danjoh, M. Fukaya, K. Yanagihara, H. Sakamoto, T. Yoshida and H. Sasaki (2005). "Discovery of aberrant expression of R-RAS by cancer-linked DNA hypomethylation in gastric cancer using microarrays." Cancer Res **65**(6): 2115-2124.

Nitta, T., M. Hata, S. Gotoh, Y. Seo, H. Sasaki, N. Hashimoto, M. Furuse and S. Tsukita (2003). "Size-selective loosening of the blood-brain barrier in claudin-5-deficient mice." J Cell Biol **161**(3): 653-660.

Nollert, M. U. and L. V. McIntire (1992). "Convective mass transfer effects on the intracellular calcium response of endothelial cells." J Biomech Eng **114**(3): 321-326.

Noria, S., D. B. Cowan, A. I. Gotlieb and B. L. Langille (1999). "Transient and steady-state effects of shear stress on endothelial cell adherens junctions." Circ Res **85**(6): 504-514.

Noria, S., F. Xu, S. McCue, M. Jones, A. I. Gotlieb and B. L. Langille (2004). "Assembly and reorientation of stress fibers drives morphological changes to endothelial cells exposed to shear stress." Am J Pathol **164**(4): 1211-1223.

Norvell, S. M., M. Alvarez, J. P. Bidwell and F. M. Pavalko (2004). "Fluid shear stress induces beta-catenin signaling in osteoblasts." Calcif Tissue Int **75**(5): 396-404.

Oda, M., H. Yokomori and J. Y. Han (2003). "Regulatory mechanisms of hepatic microcirculation." Clin Hemorheol Microcirc **29**(3-4): 167-182.

Oelze, M. L. and W. D. O'Brien (2004). "Improved scatterer property estimates from ultrasound backscatter for small gate lengths using a gate-edge correction factor." Journal of the Acoustical Society of America **116**(5): 3212-3223.

Ohta, Y. and J. H. Hartwig (1996). "Phosphorylation of actin-binding protein 280 by growth factors is mediated by p90 ribosomal protein S6 kinase." J Biol Chem **271**(20): 11858-11864.

Ohta, Y., N. Suzuki, S. Nakamura, J. H. Hartwig and T. P. Stossel (1999). "The small GTPase RalA targets filamin to induce filopodia." Proc Natl Acad Sci U S A **96**(5): 2122-2128.

Okamoto, T., M. Akiyama, M. Takeda, E. C. Gabazza, T. Hayashi and K. Suzuki (2009). "Connexin32 is expressed in vascular endothelial cells and participates in gap-junction intercellular communication." Biochemical and biophysical research communications **382**(2): 264-268.

Olesen, S. P., D. E. Clapham and P. F. Davies (1988). "Haemodynamic shear stress activates a K⁺ current in vascular endothelial cells." Nature **331**(6152): 168-170.

Opal, S. M. and C. E. Huber (2002). "Bench-to-bedside review: Toll-like receptors and their role in septic shock." Critical care (London, England) **6**(2): 125-136.

Orsenigo, F., C. Giampietro, A. Ferrari, M. Corada, A. Galaup, S. Sigismund, G. Ristagno, L. Maddaluno, G. Y. Koh, D. Franco, V. Kurtcuoglu, D. Poulikakos, P. Baluk, D. McDonald, M. Grazia Lampugnani and E. Dejana (2012). "Phosphorylation of VE-cadherin is modulated by haemodynamic forces and contributes to the regulation of vascular permeability in vivo." Nature communications **3**: 1208.

Osterud, B., M. S. Bajaj and S. P. Bajaj (1995). "Sites of tissue factor pathway inhibitor (TFPI) and tissue factor expression under physiologic and pathologic conditions. On behalf of the Subcommittee on Tissue factor Pathway Inhibitor (TFPI) of the Scientific and Standardization Committee of the ISTH." Thrombosis and haemostasis **73**(5): 873-875.

Othman-Hassan, K., K. Patel, M. Papoutsis, M. Rodriguez-Niedenfuhr, B. Christ and J. Wilting (2001). "Arterial identity of endothelial cells is controlled by local cues." Developmental biology **237**(2): 398-409.

Ozawa, T. (1999). "Mitochondrial genome mutation in cell death and aging." Journal of bioenergetics and biomembranes **31**(4): 377-390.

Palladino, M. A., F. R. Bahjat, E. A. Theodorakis and L. L. Moldawer (2003). "Anti-TNF-[alpha] therapies: the next generation." Nat Rev Drug Discov **2**(9): 736-746.

Pappenheimer, J. R., E. M. Renkin and L. M. Borrero (1951). "Filtration, diffusion and molecular sieving through peripheral capillary membranes; a contribution to the pore theory of capillary permeability." The American journal of physiology **167**(1): 13-46.

Parker, M. M., J. H. Shelhamer, C. Natanson, D. W. Alling and J. E. Parrillo (1987). "Serial cardiovascular variables in survivors and nonsurvivors of human septic shock: heart rate as an early predictor of prognosis." Crit Care Med **15**(10): 923-929.

Parsek, M. R. and P. K. Singh (2003). "Bacterial biofilms: An emerging link to disease pathogenesis." Annual Review of Microbiology **57**: 677-701.

Partanen, J., E. Armstrong, T. P. Makela, J. Korhonen, M. Sandberg, R. Renkonen, S. Knuutila, K. Huebner and K. Alitalo (1992). "A novel endothelial cell surface receptor tyrosine

kinase with extracellular epidermal growth factor homology domains." Mol Cell Biol **12**(4): 1698-1707.

Pasqualini, R. and W. Arap (2002). "Profiling the molecular diversity of blood vessels." Cold Spring Harbor symposia on quantitative biology **67**: 223-225.

Passerini, A. G., D. C. Polacek, C. Shi, N. M. Francesco, E. Manduchi, G. R. Grant, W. F. Pritchard, S. Powell, G. Y. Chang, C. J. Stoeckert, Jr. and P. F. Davies (2004). "Coexisting proinflammatory and antioxidative endothelial transcription profiles in a disturbed flow region of the adult porcine aorta." Proceedings of the National Academy of Sciences of the United States of America **101**(8): 2482-2487.

Pastores, S. M., D. P. Katz and V. Kvetan (1996). "Splanchnic ischemia and gut mucosal injury in sepsis and the multiple organ dysfunction syndrome." The American journal of gastroenterology **91**(9): 1697-1710.

Paterson, H. E., A. J. Self, M. D. Garrett, I. Just, K. Aktories and H. Hall (1990). "Microinjection of recombinant p21rho induces rapid changes in cell morphology." The Journal of Cell Biology **111**(3): 1001-1007.

Paterson, R. L., H. F. Galley, J. K. Dhillon and N. R. Webster (2000). "Increased nuclear factor kappa B activation in critically ill patients who die." Crit Care Med **28**(4): 1047-1051.

Patschan, S. A., D. Patschan, J. Temme, P. Korsten, J. T. Wessels, M. Koziolk, E. Henze and G. A. Muller (2011). "Endothelial progenitor cells (EPC) in sepsis with acute renal dysfunction (ARD)." Crit Care **15**(2): R94.

Paulus, W. J. (1994). "Endothelial control of vascular and myocardial function in heart failure." Cardiovasc Drugs Ther **8**(3): 437-446.

Peddibhotla, S. S., B. F. Brinkmann, D. Kummer, H. Tuncay, M. Nakayama, R. H. Adams, V. Gerke and K. Ebnet (2013). "Tetraspanin CD9 links junctional adhesion molecule-A to alpha(v)beta3 integrin to mediate basic fibroblast growth factor-specific angiogenic signaling." Mol Biol Cell **24**(7): 933-944.

Peng, X., P. M. Hassoun, S. Sammani, B. J. McVerry, M. J. Burne, H. Rabb, D. Pearse, R. M. Tuder and J. G. Garcia (2004). "Protective effects of sphingosine 1-phosphate in murine endotoxin-induced inflammatory lung injury." Am J Respir Crit Care Med **169**(11): 1245-1251.

Peters, W., V. Druppel, K. Kusche-Vihrog, C. Schubert and H. Oberleithner (2012). "Nanomechanics and sodium permeability of endothelial surface layer modulated by hawthorn extract WS 1442." PLoS One **7**(1): 29972.

Petrache, I., A. Birukova, S. I. Ramirez, J. G. Garcia and A. D. Verin (2003). "The role of the microtubules in tumor necrosis factor-alpha-induced endothelial cell permeability." Am J Respir Cell Mol Biol **28**(5): 574-581.

Petti, C. A. and V. G. Fowler, Jr. (2003). "Staphylococcus aureus bacteremia and endocarditis." Cardiol Clin **21**(2): 219-233.

Petzelbauer, P., J. R. Bender, J. Wilson and J. S. Pober (1993). "Heterogeneity of dermal microvascular endothelial cell antigen expression and cytokine responsiveness in situ and in cell culture." J Immunol **151**(9): 5062-5072.

Phelps, J. E. and N. DePaola (2000). "Spatial variations in endothelial barrier function in disturbed flows in vitro." Am J Physiol Heart Circ Physiol **278**(2): H469-476.

Phillips, L. C., A. L. Klibanov, B. R. Wamhoff and J. A. Hossack (2012). "Intravascular ultrasound detection and delivery of molecularly targeted microbubbles for gene delivery." IEEE Transactions on Ultrasonics, Ferroelectrics, and Frequency Control **59**(7): 1596-1601.

Pitchford, S. C., R. C. Furze, C. P. Jones, A. M. Wengner and S. M. Rankin (2009). "Differential Mobilization of Subsets of Progenitor Cells from the Bone Marrow." Cell Stem Cell **4**(1): 62-72.

Pober, J. S. (2008). Physiology and Pathobiology of Microvascular Endothelium. Handbook of Physiology: Microcirculation (Second Edition). R. F. Tuma, N. W. Duran and K. Ley. San Diego, Academic Press: 37-55.

Pober, J. S., L. A. Lapierre, A. H. Stolpen, T. A. Brock, T. A. Springer, W. Fiers, M. P. Bevilacqua, D. L. Mendrick and M. A. Gimbrone, Jr. (1987). "Activation of cultured human endothelial cells by recombinant lymphotoxin: comparison with tumor necrosis factor and interleukin 1 species." J Immunol **138**(10): 3319-3324.

Pober, J. S., W. Min and J. R. Bradley (2009). "Mechanisms of endothelial dysfunction, injury, and death." Annu Rev Pathol **4**: 71-95.

Pober, J. S. and W. C. Sessa (2007). "Evolving functions of endothelial cells in inflammation." Nat Rev Immunol **7**(10): 803-815.

Poiseuille, J. L. M. (1830). "Research on the causes of blood movement through the veins [Recherches sur les causes du mouvement du sang dans les veines]." J. Physiol. Exp. Pathol **10**: 277-295.

Potente, M., H. Gerhardt and P. Carmeliet (2011). "Basic and therapeutic aspects of angiogenesis." Cell **146**(6): 873-887.

Potter, D. R. and E. R. Damiano (2008). "The hydrodynamically relevant endothelial cell glycocalyx observed in vivo is absent in vitro." Circ Res **102**(7): 770-776.

Potter, M. D., S. Barbero and D. A. Cheresh (2005). "Tyrosine phosphorylation of VE-cadherin prevents binding of p120- and beta-catenin and maintains the cellular mesenchymal state." J Biol Chem **280**(36): 31906-31912.

Prasad, A. R., S. A. Logan, R. M. Nerem, C. J. Schwartz and E. A. Sprague (1993). "Flow-related responses of intracellular inositol phosphate levels in cultured aortic endothelial cells." Circ Res **72**(4): 827-836.

Preston, G. M. and P. Agre (1991). "Isolation of the cDNA for erythrocyte integral membrane protein of 28 kilodaltons: member of an ancient channel family." Proc Natl Acad Sci U S A **88**(24): 11110-11114.

Pries, A. R., T. W. Secomb and P. Gaehtgens (1996). "Biophysical aspects of blood flow in the microvasculature." Cardiovascular research **32**(4): 654-667.

Pries, A. R., T. W. Secomb and P. Gaehtgens (2000). "The endothelial surface layer." Pflugers Arch **440**(5): 653-666.

Pusztaszeri, M. P., W. Seelentag and F. T. Bosman (2006). "Immunohistochemical expression of endothelial markers CD31, CD34, von Willebrand factor, and Fli-1 in normal human tissues." J Histochem Cytochem **54**(4): 385-395.

Pylyayeva-Gupta, Y., E. Grabocka and D. Bar-Sagi (2011). "RAS oncogenes: weaving a tumorigenic web." Nat Rev Cancer **11**(11): 761-774.

Raberg, L., D. Sim and A. F. Read (2007). "Disentangling genetic variation for resistance and tolerance to infectious diseases in animals." Science **318**(5851): 812-814.

Rabiet, M. J., J. L. Plantier, Y. Rival, Y. Genoux, M. G. Lampugnani and E. Dejana (1996). "Thrombin-induced increase in endothelial permeability is associated with changes in cell-to-cell junction organization." Arterioscler Thromb Vasc Biol **16**(3): 488-496.

Rafat, N., C. Hanusch, P. T. Brinkkoetter, J. Schulte, J. Brade, J. G. Zijlstra, F. J. van der Woude, K. van Ackern, B. A. Yard and G. Beck (2007). "Increased circulating endothelial progenitor cells in septic patients: correlation with survival." Crit Care Med **35**(7): 1677-1684.

Ranieri, V. M., G. D. Rubenfeld, B. T. Thompson, N. D. Ferguson, E. Caldwell, E. Fan, L. Camporota and A. S. Slutsky (2012). "Acute respiratory distress syndrome: the Berlin Definition." JAMA **307**(23): 2526-2533.

Ravid, D., D. Chuderland, L. Landsman, Y. Lavie, R. Reich and M. Liscovitch (2008). "Filamin A is a novel caveolin-1-dependent target in IGF-I-stimulated cancer cell migration." Experimental Cell Research **314**(15): 2762-2773.

Raza, A. (2000). "Anti-TNF therapies in rheumatoid arthritis, Crohn's disease, sepsis, and myelodysplastic syndromes." Microsc Res Tech **50**(3): 229-235.

Reddin, J. L., B. Starzecki and W. W. Spink (1966). "Comparative hemodynamic and humoral responses of puppies and adult dogs to endotoxin." Am J Physiol **210**(3): 540-544.

Reddy, L., H.-S. Wang, C. R. Keese, I. Giaever and T. J. Smith (1998). "Assessment of Rapid Morphological Changes Associated with Elevated cAMP Levels in Human Orbital Fibroblasts." Experimental Cell Research **245**(2): 360-367.

Reil, J. C., S. Gilles, S. Zahler, A. Brandl, H. Drexler, L. Hultner, L. M. Matrisian, U. Welsch and B. F. Becker (2007). "Insights from knock-out models concerning postischemic release of TNFalpha from isolated mouse hearts." J Mol Cell Cardiol **42**(1): 133-141.

Reitsma, S., D. W. Slaaf, H. Vink, M. A. van Zandvoort and M. G. oude Egbrink (2007). "The endothelial glycocalyx: composition, functions, and visualization." Pflugers Arch **454**(3): 345-359.

Resnick, N., H. Yahav, A. Shay-Salit, M. Shushy, S. Schubert, L. C. M. Zilberman and E. Wofovitz (2003). "Fluid shear stress and the vascular endothelium: for better and for worse." Progress in biophysics and molecular biology **81**(3): 177-199.

Reuther, G. W. and C. J. Der (2000). "The Ras branch of small GTPases: Ras family members don't fall far from the tree." Curr Opin Cell Biol **12**(2): 157-165.

Reynolds, A. B. and R. H. Carnahan (2004). "Regulation of cadherin stability and turnover by p120ctn: implications in disease and cancer." Semin Cell Dev Biol **15**(6): 657-663.

Reynolds, K., B. Novosad, A. Hoffhines, J. Gipson, J. Johnson, J. Peters, F. Gonzalez, J. Gimble and M. Hill (2002). "Pretreatment with troglitazone decreases lethality during endotoxemia in mice." J Endotoxin Res **8**(4): 307-314.

Rhodin, J. A. (1968). "Ultrastructure of mammalian venous capillaries, venules, and small collecting veins." J Ultrastruct Res **25**(5): 452-500.

Rincon-Arano, H., R. Rosales, N. Mora, A. Rodriguez-Castaneda and C. Rosales (2003). "R-Ras promotes tumor growth of cervical epithelial cells." Cancer **97**(3): 575-585.

Robertson, S. P. (2005). "Filamin A: phenotypic diversity." Curr Opin Genet Dev **15**(3): 301-307.

Robertson, S. P., S. R. Twigg, A. J. Sutherland-Smith, V. Biancalana, R. J. Gorlin, D. Horn, S. J. Kenwright, C. A. Kim, E. Morava, R. Newbury-Ecob, K. H. Orstavik, O. W. Quarrell, C. E. Schwartz, D. J. Shears, M. Suri, J. Kendrick-Jones and A. O. Wilkie (2003). "Localized mutations in the gene encoding the cytoskeletal protein filamin A cause diverse malformations in humans." Nat Genet **33**(4): 487-491.

Romer, L. H., K. Burridge and C. E. Turner (1992). "Signaling between the extracellular matrix and the cytoskeleton: tyrosine phosphorylation and focal adhesion assembly." Cold Spring Harbor symposia on quantitative biology **57**: 193-202.

Rosenbaum, J. L. and G. B. Witman (2002). "Intraflagellar transport." Nat Rev Mol Cell Biol **3**(11): 813-825.

Ruoslahti, E., N. A. Noble, S. Kagami and W. A. Border (1994). "Integrins." Kidney Int Suppl **44**: S17-22.

Ruoslahti, E. and M. D. Pierschbacher (1987). "New perspectives in cell adhesion: RGD and integrins." Science **238**(4826): 491-497.

Rybin, V., O. Ullrich, M. Rubino, K. Alexandrov, I. Simon, M. C. Seabra, R. Goody and M. Zerial (1996). "GTPase activity of Rab5 acts as a timer for endocytic membrane fusion." Nature **383**(6597): 266-269.

Saijo, Y., T. Miyakawa, H. Sasaki, M. Tanaka and S. I. Nitta (2004). "Acoustic properties of aortic aneurysm obtained with scanning acoustic microscopy." Ultrasonics **42**(1-9): 695-698.

Saijo, Y., E. Santos, H. Sasaki, T. Yambe, M. Tanaka, N. Hozumi, K. Kobayashi and N. Okada (2007). "Ultrasonic tissue characterization of atherosclerosis by a speed-of-sound microscanning system." IEEE Transactions On Ultrasonics Ferroelectrics and Frequency Control **54**(8): 1571-1577.

Saijo, Y., H. Sasaki, S. Nitta, M. Tanaka, C. S. Jorgensen and E. Falk (2000). "Collagen characterization by polarized and acoustic microscopy." Ultrasound in Medicine and Biology **26**(2).

Saijo, Y., H. Sasaki, H. Okawai, S. Nitta and M. Tanaka (1998). "Acoustic properties of atherosclerosis of human aorta obtained with high-frequency ultrasound." Ultrasound in Medicine and Biology **24**(7): 1061-1064.

Saijo, Y., M. Tanaka, H. Okawai, H. Sasaki, S. I. Nitta and F. Dunn (1997). "Ultrasonic tissue characterization of infarcted myocardium by scanning acoustic microscopy." Ultrasound in Medicine and Biology **23**(1): 77-85.

Saito, M., D. K. Tucker, D. Kohlhorst, C. M. Niessen and A. P. Kowalczyk (2012). "Classical and desmosomal cadherins at a glance." Journal of Cell Science **125**(11): 2547-2552.

Sands, K. E., D. W. Bates, P. N. Lanken, P. S. Graman, P. L. Hibberd, K. L. Kahn, J. Parsonnet, R. Panzer, E. J. Orav, D. R. Snyderman, E. Black, J. S. Schwartz, R. Moore, B. L. Johnson, Jr., R. Platt and G. Academic Medical Center Consortium Sepsis Project Working (1997). "Epidemiology of sepsis syndrome in 8 academic medical centers." JAMA **278**(3): 234-240.

Sauter, C. and C. Wolfensberger (1980). "Interferon in human serum after injection of endotoxin." Lancet **2**(8199): 852-853.

Sawada, J. and M. Komatsu (2012). "Normalization of tumor vasculature by R-Ras." Cell Cycle **11**(23): 4285-4286.

Sawada, J., F. Li and M. Komatsu (2015). "R-Ras protein inhibits autophosphorylation of vascular endothelial growth factor receptor 2 in endothelial cells and suppresses receptor activation in tumor vasculature." J Biol Chem **290**(13): 8133-8145.

Sawada, N., M. Murata, K. Kikuchi, M. Osanai, H. Tobioka, T. Kojima and H. Chiba (2003). "Tight junctions and human diseases." Med Electron Microsc **36**(3): 147-156.

Sawamiphak, S., S. Seidel, C. L. Essmann, G. A. Wilkinson, M. E. Pitulescu, T. Acker and A. Acker-Palmer (2010). "Ephrin-B2 regulates VEGFR2 function in developmental and tumour angiogenesis." Nature **465**(7297): 487.

Sbeity, F., S. Menigot, J. Charara and J. M. Girault (2013). "Contrast improvement in sub- and ultraharmonic ultrasound contrast imaging by combining several hammerstein models." Int J Biomed Imaging **2013**: 270523.

Schaedler, R. W. and R. J. Dubos (1961). "The susceptibility of mice to bacterial endotoxins." J Exp Med **113**: 559-570.

Schiffer, E. R. C., G. Reber, P. De Moerloose and D. R. Morel (2002). "Evaluation of unfractionated heparin and recombinant hirudin on survival in a sustained ovine endotoxin shock model." Critical care medicine **30**(12): 2689-2699.

Schlegel, N., Y. Baumer, D. Drenckhahn and J. Waschke (2009). "Lipopolysaccharide-induced endothelial barrier breakdown is cyclic adenosine monophosphate dependent in vivo and in vitro." Crit Care Med **37**(5): 1735-1743.

Schlegel, N. and J. Waschke (2009). "Impaired cAMP and Rac 1 Signaling Contribute to TNF--induced Endothelial Barrier Breakdown in Microvascular Endothelium." Microcirculation **16**(6): 521-533.

Schmelz, M. and W. W. Franke (1993). "Complexus adhaerentes, a new group of desmoplakin-containing junctions in endothelial cells: the syndesmos connecting retothelial cells of lymph nodes." Eur J Cell Biol **61**(2): 274-289.

Schmid-Schonbein, G. W. and H. Murakami (1985). "Blood flow in contracting arterioles." Int J Microcirc Clin Exp **4**(4): 311-328.

Schmid-Schönbein, G. W., T. C. Skalak, E. T. Engelson and B. W. Zweifach (1986). The microvasculature in skeletal muscle. Microvascular Networks: Experimental and Theoretical Studies. A. S. Popel and P. C. Johnson, Karger.

Schneewind, O., A. Fowler and K. F. Faull (1995). "Structure of the cell wall anchor of surface proteins in Staphylococcus aureus." Science **268**(5207): 103-106.

Schneider, C. A., W. S. Rasband and K. W. Eliceiri (2012). "NIH Image to ImageJ: 25 years of image analysis." Nature Methods **9**(7): 671-675.

Schneider, D. S. and J. S. Ayres (2008). "Two ways to survive infection: what resistance and tolerance can teach us about treating infectious diseases." Nature reviews Immunology **8**(11): 889-895.

Schnitzer, J. E., P. Oh, E. Pinney and J. Allard (1994). "Filipin-sensitive caveolae-mediated transport in endothelium: reduced transcytosis, scavenger endocytosis, and capillary permeability of select macromolecules." J Cell Biol **127**(5): 1217-1232.

Schnitzer, J. E., A. Siflinger-Birnboim, P. J. Del Vecchio and A. B. Malik (1994). "Segmental differentiation of permeability, protein glycosylation, and morphology of cultured bovine lung vascular endothelium." Biochem Biophys Res Commun **199**(1): 11-19.

Schulte, W., J. Bernhagen and R. Bucala (2013). "Cytokines in sepsis: potent immunoregulators and potential therapeutic targets--an updated view." Mediators of inflammation **2013**: 165974.

Secomb, T. W., R. Hsu and A. R. Pries (1998). "A model for red blood cell motion in glycocalyx-lined capillaries." Am J Physiol **274**(3): H1016-1022.

Sehr, P., G. Joseph, H. Genth, I. Just, E. Pick and K. Aktories (1998). "Glucosylation and ADP ribosylation of rho proteins: effects on nucleotide binding, GTPase activity, and effector coupling." Biochemistry **37**(15): 5296-5304.

Sethi, T., M. H. Ginsberg, J. Downward and P. E. Hughes (1999). "The Small GTP-binding Protein R-Ras Can Influence Integrin Activation by Antagonizing a Ras/Raf-initiated Integrin Suppression Pathway." Molecular Biology of the Cell **10**(6): 1799-1809.

Severson, E. A., W. Y. Lee, C. T. Capaldo, A. Nusrat and C. A. Parkos (2009). "Junctional adhesion molecule A interacts with Afadin and PDZ-GEF2 to activate Rap1A, regulate beta1 integrin levels, and enhance cell migration." Mol Biol Cell **20**(7): 1916-1925.

Seybold, J., D. Thomas, M. Witzernath, S. Boral, A. C. Hocke, A. Bürger, A. Hatzelmann, H. Tenor, C. Schudt, M. Krüll, H. Schütte, S. Hippenstiel and N. Suttorp (2005). "Tumor necrosis factor- α -dependent expression of phosphodiesterase 2: role in endothelial hyperpermeability." Blood **105**(9): 3569-3576.

Shah, B. R. and J. E. Hux (2003). "Quantifying the risk of infectious diseases for people with diabetes." Diabetes Care **26**(2): 510-513.

Shao, H., J. Li, Y. Zhou, Z. Ge, J. Fan, Z. Shao and Y. Zeng (2008). "Dose-dependent protective effect of propofol against mitochondrial dysfunction in ischaemic/reperfused rat heart: role of cardiolipin." Br J Pharmacol **153**(8): 1641-1649.

Shao, H. W., Y. H. Tan, D. Eton, Z. Yang, M. G. Uberti, S. Li, A. Schulick and H. Yu (2008). "Statin and stromal cell-derived factor-1 additively promote angiogenesis by enhancement of progenitor cells incorporation into new vessels." Stem Cells **26**(5): 1376-1384.

Sheagren, J. N., S. M. Wolff and N. R. Shulman (1967). "Febrile and hematologic responses of rhesus monkeys to bacterial endotoxin." The American journal of physiology **212**(4): 884-890.

Shemesh, H., D. E. Goertz, L. W. van der Sluis, N. de Jong, M. K. Wu and P. R. Wesselink (2007). "High frequency ultrasound imaging of a single-species biofilm." J Dent **35**(8): 673-678.

Shen, J., R. G. Ham and S. Karmiol (1995). "Expression of adhesion molecules in cultured human pulmonary microvascular endothelial cells." Microvasc Res **50**(3): 360-372.

Shi, S., A. D. Verin, K. L. Schaphorst, L. I. Gilbert-McClain, C. E. Patterson, R. P. Irwin, V. Natarajan and J. G. Garcia (1998). "Role of tyrosine phosphorylation in thrombin-induced endothelial cell contraction and barrier function." Endothelium **6**(2): 153-171.

Shimizu, Y. and G. N. Garcia (2013). The endothelial cytoskeleton: multifunctional role of the endothelial actomyosin cytoskelton. Endothelial cytoskeleton. J. A. Rosado and P. C. Redondo, CRC Press.

Shimokawa, T., K. Yamamoto, T. Kojima and H. Saito (2000). "Down-regulation of murine tissue factor pathway inhibitor mRNA by endotoxin and tumor necrosis factor-alpha in vitro and in vivo." Thromb Res **100**(3): 211-221.

Short, S. M., G. A. Talbott and R. L. Juliano (1998). "Integrin-mediated signaling events in human endothelial cells." Mol Biol Cell **9**(8): 1969-1980.

Shyu, K.-G. (2006). "Enhancement of new vessel formation by angiopoietin-2/Tie2 signaling in endothelial progenitor cells: a new hope for future therapy?" Cardiovascular research **72**(3): 359-360.

Shyu, K. G., Y. J. Liang, H. Chang, B. W. Wang, J. G. Leu and P. Kuan (2004). "Enhanced expression of angiopoietin-2 and the Tie2 receptor but not angiopoietin-1 or the Tie1 receptor in a rat model of myocardial infarction." J Biomed Sci **11**(2): 163-171.

Shyy, J. Y. and S. Chien (2002). "Role of integrins in endothelial mechanosensing of shear stress." Circ Res **91**(9): 769-775.

Sill, H. W., Y. S. Chang, J. R. Artman, J. A. Frangos, T. M. Hollis and J. M. Tarbell (1995). "Shear stress increases hydraulic conductivity of cultured endothelial monolayers." Am J Physiol **268**(2): H535-543.

Silverman, R. H. (2009). "High-resolution ultrasound imaging of the eye - a review." Clin Experiment Ophthalmol **37**(1): 54-67.

Silverman, R. H., J. Cannata, K. K. Shung, O. Gal, M. Patel, H. O. Lloyd, E. J. Feleppa and D. J. Coleman (2006). "75 MHz ultrasound biomicroscopy of anterior segment of eye." Ultrasonic Imaging **28**(3): 179-188.

Simionescu, M. (2000). Structural biochemical and functional differentiation of the vascular endothelium. Morphogenesis of Endothelium. W. Risau and G. M. Rubanyi, Harwood Academic: 1–21.

Simionescu, M., A. Gafencu and F. Antohe (2002). "Transcytosis of plasma macromolecules in endothelial cells: a cell biological survey." Microsc Res Tech **57**(5): 269-288.

Simionescu, M., N. Simionescu and G. E. Palade (1974). "Morphometric data on the endothelium of blood capillaries." The Journal of cell biology **60**(1): 128-152.

Smith, D. B. and L. M. Corcoran (2001). "Expression and purification of glutathione-S-transferase fusion proteins." Curr Protoc Mol Biol **Chapter 16**.

Smyth, S. S., C. C. Joneckis and L. V. Parise (1993). "Regulation of vascular integrins." Blood **81**(11): 2827-2843.

Song, J., B. Zheng, X. Bu, Y. Fei and S. Shi (2014). "Negative association of R-Ras activation and breast cancer development." Oncol Rep **31**(6): 2776-2784.

Spaargaren, M., G. A. Martin, F. McCormick, M. J. Fernandez-Sarabia and J. R. Bischoff (1994). "The Ras-related protein R-ras interacts directly with Raf-1 in a GTP-dependent manner." Biochem J **300**(2): 303-307.

Srinivasan, S. and N. G. Avadhani (2012). "Cytochrome c oxidase dysfunction in oxidative stress." Free radical biology & medicine **53**(6): 1252-1263.

Staddon, J. M., K. Herrenknecht, C. Smales and L. L. Rubin (1995). "Evidence that tyrosine phosphorylation may increase tight junction permeability." J Cell Sci **108**(2): 609-619.

Stamatovic, S. M., R. F. Keep and A. V. Andjelkovic (2008). "Brain Endothelial Cell-Cell Junctions: How to "Open" the Blood Brain Barrier." Current Neuropharmacology **6**(3): 179-192.

Stan, R. V., M. Kubitza and G. E. Palade (1999). "PV-1 is a component of the fenestral and stomatal diaphragms in fenestrated endothelia." Proceedings of the National Academy of Sciences of the United States of America **96**(23): 13203-13207.

Stephen, A. G., D. Esposito, R. K. Bagni and F. McCormick (2014). "Dragging ras back in the ring." Cancer Cell **25**(3): 272-281.

Stevens, A. P., V. Hlady and R. O. Dull (2007). "Fluorescence correlation spectroscopy can probe albumin dynamics inside lung endothelial glycocalyx." Am J Physiol Lung Cell Mol Physiol **293**(2): L328-335.

Stewart, P. S. and J. W. Costerton (2001). "Antibiotic resistance of bacteria in biofilms." Lancet **358**(9276): 135-138.

Stidwill, R. P., D. M. Rosser and M. Singer (1998). "Cardiorespiratory, tissue oxygen and hepatic NADH responses to graded hypoxia." Intensive care medicine **24**(11): 1209-1216.

Stief, T. W., O. Ijagha, B. Weiste, I. Herzum, H. Renz and M. Max (2007). "Analysis of hemostasis alterations in sepsis." Blood Coagul Fibrinolysis **18**(2): 179-186.

Stossel, T. P., J. Condeelis, L. Cooley, J. H. Hartwig, A. Noegel, M. Schleicher and S. S. Shapiro (2001). "Filamins as integrators of cell mechanics and signalling." Nat Rev Mol Cell Biol **2**(2): 138-145.

Strathmann, M., J. Wingender and H. C. Flemming (2002). "Application of fluorescently labelled lectins for the visualization and biochemical characterization of polysaccharides in biofilms of *Pseudomonas aeruginosa*." J Microbiol Methods **50**(3): 237-248.

Strohm, E. M., G. J. Czarnota and M. C. Kolios (2010). "Quantitative Measurements of Apoptotic Cell Properties Using Acoustic Microscopy." IEEE Transactions On Ultrasonics Ferroelectrics and Frequency Control **57**(10): 2293-2304.

Stromblad, S., J. C. Becker, M. Yebra, P. C. Brooks and D. A. Cheresh (1996). "Suppression of p53 activity and p21WAF1/CIP1 expression by vascular cell integrin alpha(v)beta3 during angiogenesis." J Clin Invest **98**(2): 426-433.

Suffredini, A. F., R. E. Fromm, M. M. Parker, M. Brenner, J. A. Kovacs, R. A. Wesley and J. E. Parrillo (1989). "The cardiovascular response of normal humans to the administration of endotoxin." N Engl J Med **321**(5): 280-287.

Suffredini, A. F., P. C. Harpel and J. E. Parrillo (1989). "Promotion and subsequent inhibition of plasminogen activation after administration of intravenous endotoxin to normal subjects." N Engl J Med **320**(18): 1165-1172.

Sullam, P. M., T. A. Drake and M. A. Sande (1985). "Pathogenesis of endocarditis." Am J Med **78**(6B): 110-115.

Sun, H. R., J. W. Breslin, J. Zhu, S. Y. Yuan and M. H. Wu (2006). "Rho and ROCK signaling in VEGF-induced microvascular endothelial hyperpermeability." Microcirculation **13**(3): 237-247.

Surbatovic, M., N. Filipovic, S. Radakovic, N. Stankovic and Z. Slavkovic (2007). "Immune cytokine response in combat casualties: blast or explosive trauma with or without secondary sepsis." Mil Med **172**(2): 190-195.

Suter, E. R. and G. Majno (1964). "Ultrastructure of the joint capsule in the rat: Presence of two kinds of capillaries." Nature **202**: 920-921.

Takahashi, M., T. Ishida, O. Traub, M. A. Corson and B. C. Berk (1997). "Mechanotransduction in endothelial cells: temporal signaling events in response to shear stress." J Vasc Res **34**(3): 212-219.

Takahashi, T., S. Yamaguchi, K. Chida and M. Shibuya (2001). "A single autophosphorylation site on KDR/Flk-1 is essential for VEGF-A-dependent activation of PLC-gamma and DNA synthesis in vascular endothelial cells." EMBO J **20**(11): 2768-2778.

Takai, Y., T. Sasaki and T. Matozaki (2001). "Small GTP-binding proteins." Physiol Rev **81**(1): 153-208.

Takaya, A., T. Kamio, M. Masuda, N. Mochizuki, H. Sawa, M. Sato, K. Nagashima, A. Mizutani, A. Matsuno, E. Kiyokawa and M. Matsuda (2007). "R-Ras Regulates Exocytosis by Rgl2/Rlf-mediated Activation of RalA on Endosomes." Molecular Biology of the Cell **18**(5): 1850-1860.

Tardy, Y., N. Resnick, T. Nagel, M. A. Gimbrone, Jr. and C. F. Dewey, Jr. (1997). "Shear stress gradients remodel endothelial monolayers in vitro via a cell proliferation-migration-loss cycle." Arterioscler Thromb Vasc Biol **17**(11): 3102-3106.

Tasaka, S., H. Koh, W. Yamada, M. Shimizu, Y. Ogawa, N. Hasegawa, K. Yamaguchi, Y. Ishii, S. E. Richer, C. M. Doerschuk and A. Ishizaka (2005). "Attenuation of endotoxin-induced

acute lung injury by the Rho-associated kinase inhibitor, Y-27632." Am J Respir Cell Mol Biol **32**(6): 504-510.

Taveira da Silva, A. M., H. C. Kaulbach, F. S. Chuidian, D. R. Lambert, A. F. Suffredini and R. L. Danner (1993). "Brief report: shock and multiple-organ dysfunction after self-administration of Salmonella endotoxin." The New England journal of medicine **328**(20): 1457-1460.

Thomason, H. A., A. Scothern, S. McHarg and D. R. Garrod (2010). "Desmosomes: adhesive strength and signalling in health and disease." Biochemical Journal **429**: 419-433.

Thompson, H. (2013). "US National Cancer Institute's new Ras project targets an old foe." Nat Med **19**(8): 949-950.

Tiruppathi, C., A. B. Malik, P. J. Del Vecchio, C. R. Keese and I. Giaever (1992). "Electrical method for detection of endothelial cell shape change in real time: assessment of endothelial barrier function." Proceedings of the National Academy of Sciences **89**(17): 7919-7923.

Tiruppathi, C., J. Shimizu, K. Miyawaki-Shimizu, S. M. Vogel, A. M. Bair, R. D. Minshall, D. Predescu and A. B. Malik (2008). "Role of NF-kappaB-dependent caveolin-1 expression in the mechanism of increased endothelial permeability induced by lipopolysaccharide." J Biol Chem **283**(7): 4210-4218.

Tojkander, S., G. Gateva and P. Lappalainen (2012). "Actin stress fibers--assembly, dynamics and biological roles." J Cell Sci **125**(8): 1855-1864.

Tornavaca, O., M. Chia, N. Dufton, L. O. Almagro, D. E. Conway, A. M. Randi, M. A. Schwartz, K. Matter and M. S. Balda (2015). "ZO-1 controls endothelial adherens junctions, cell-cell tension, angiogenesis, and barrier formation." J Cell Biol **208**(6): 821-838.

Tracey, D., L. Klareskog, E. H. Sasso, J. G. Salfeld and P. P. Tak (2008). "Tumor necrosis factor antagonist mechanisms of action: a comprehensive review." Pharmacol Ther **117**(2): 244-279.

Tracey, M. D. K. J. and P. D. A. Cerami (1994). "Tumor necrosis factor: A pleiotropic cytokine and therapeutic target." Annual Review of Medicine **45**(1): 491-503.

Trahey, M. and F. McCormick (1987). "A cytoplasmic protein stimulates normal N-ras p21 GTPase, but does not affect oncogenic mutants." Science **238**(4826): 542-545.

Traub, O. and B. C. Berk (1998). "Laminar shear stress: mechanisms by which endothelial cells transduce an atheroprotective force." Arterioscler Thromb Vasc Biol **18**(5): 677-685.

Traut, T. W. (1994). "Physiological concentrations of purines and pyrimidines." Mol Cell Biochem **140**(1): 1-22.

Tseng, H., T. E. Peterson and B. C. Berk (1995). "Fluid shear stress stimulates mitogen-activated protein kinase in endothelial cells." Circ Res **77**(5): 869-878.

Turowski, P., R. Martinelli, R. Crawford, D. Wateridge, A. P. Papageorgiou, M. G. Lampugnani, A. C. Gamp, D. Vestweber, P. Adamson, E. Dejana and J. Greenwood (2008). "Phosphorylation of vascular endothelial cadherin controls lymphocyte emigration." J Cell Sci **121**(1): 29-37.

Turrens, J. F. (2003). "Mitochondrial formation of reactive oxygen species." Journal of Physiology-London **552**(2): 335-344.

Tzima, E. (2006). "Role of small GTPases in endothelial cytoskeletal dynamics and the shear stress response." Circulation research **98**(2): 176-185.

Tzima, E., M. A. Del Pozo, W. B. Kiosses, S. A. Mohamed, S. Li, S. Chien and M. A. Schwartz (2002). "Activation of Rac1 by shear stress in endothelial cells mediates both cytoskeletal reorganization and effects on gene expression." EMBO J **21**(24): 6791-6800.

Tzima, E., M. A. del Pozo, S. J. Shattil, S. Chien and M. A. Schwartz (2001). "Activation of integrins in endothelial cells by fluid shear stress mediates Rho-dependent cytoskeletal alignment." EMBO J **20**(17): 4639-4647.

Tzima, E., M. Irani-Tehrani, W. Kiosses, E. Dejana, D. Schultz, B. Engelhardt, G. Y. Cao, H. DeLisser and M. A. Schwartz (2006). "A mechanosensory complex that mediates the endothelial cell response to fluid shear stress." Faseb Journal **20**(5): A1378-A1378.

Tzima, E., M. Irani-Tehrani, W. B. Kiosses, E. Dejana, D. A. Schultz, B. Engelhardt, G. Cao, H. DeLisser and M. A. Schwartz (2005). "A mechanosensory complex that mediates the endothelial cell response to fluid shear stress." Nature **437**(7057): 426-431.

Tzima, E., W. B. Kiosses, M. A. del Pozo and M. A. Schwartz (2003). "Localized cdc42 activation, detected using a novel assay, mediates microtubule organizing center positioning in endothelial cells in response to fluid shear stress." J Biol Chem **278**(33): 31020-31023.

Ueda, M., C. Oho, H. Takisawa and S. Ogihara (1992). "Interaction of the low-molecular-mass, guanine-nucleotide-binding protein with the actin-binding protein and its modulation by the cAMP-dependent protein kinase in bovine platelets." Eur J Biochem **203**(3): 347-352.

Ukropec, J. A., M. K. Hollinger, S. M. Salva and M. J. Woolkalis (2000). "SHP2 association with VE-cadherin complexes in human endothelial cells is regulated by thrombin." J Biol Chem **275**(8): 5983-5986.

Ullrich, A. and J. Schlessinger (1990). "Signal transduction by receptors with tyrosine kinase activity." Cell **61**(2): 203-212.

Unnikrishnan, S. and A. L. Klibanov (2012). "Microbubbles as Ultrasound Contrast Agents for Molecular Imaging: Preparation and Application." American Journal of Roentgenology **199**(2): 292-299.

Uusitalo-Seppala, R., R. Huttunen, J. Aittoniemi, P. Koskinen, A. Leino, T. Vahlberg and E. M. Rintala (2013). "Pentraxin 3 (PTX3) is associated with severe sepsis and fatal disease in emergency room patients with suspected infection: a prospective cohort study." PloS one **8**(1): e53661.

Uzarski, J. S., E. W. Scott and P. S. McFetridge (2013). "Adaptation of endothelial cells to physiologically-modeled, variable shear stress." PloS one **8**(2): e57004.

Vaidya, K., R. Osgood, D. Ren, M. E. Pichichero and M. Helguera (2014). "Ultrasound Imaging and Characterization of Biofilms Based on Wavelet De-noised Radiofrequency Data." Ultrasound Med Biol **40**(3): 583-595.

Vaidyanathan, H., J. Opoku-Ansah, S. Pastorino, H. Renganathan, M. L. Matter and J. W. Ramos (2007). "ERK MAP kinase is targeted to RSK2 by the phosphoprotein PEA-15." Proc Natl Acad Sci U S A **104**(50): 19837-19842.

Vajkoczy, P. and M. D. Menger (2000). "Vascular microenvironment in gliomas." J Neurooncol **50**(1-2): 99-108.

van den Berg, B. M., H. Vink and J. A. Spaan (2003). "The endothelial glycocalyx protects against myocardial edema." Circ Res **92**(6): 592-594.

van der Poll, T., H. R. Buller, H. ten Cate, C. H. Wortel, K. A. Bauer, S. J. van Deventer, C. E. Hack, H. P. Sauerwein, R. D. Rosenberg and J. W. ten Cate (1990). "Activation of coagulation after administration of tumor necrosis factor to normal subjects." N Engl J Med **322**(23): 1622-1627.

van Deventer, S. J., H. R. Buller, J. W. ten Cate, L. A. Aarden, C. E. Hack and A. Sturk (1990). "Experimental endotoxemia in humans: analysis of cytokine release and coagulation, fibrinolytic, and complement pathways." Blood **76**(12): 2520-2526.

van Haaren, P. M., E. VanBavel, H. Vink and J. A. Spaan (2003). "Localization of the permeability barrier to solutes in isolated arteries by confocal microscopy." Am J Physiol Heart Circ Physiol **285**(6): H2848-2856.

Van Itallie, C. M., A. S. Fanning, A. Bridges and J. M. Anderson (2009). "ZO-1 Stabilizes the Tight Junction Solute Barrier through Coupling to the Perijunctional Cytoskeleton." Molecular Biology of the Cell **20**(17): 3930-3940.

van Kempen, M. J. A. and H. J. Jongsma (1999). "Distribution of connexin37, connexin40 and connexin43 in the aorta and coronary artery of several mammals." Histochemistry and Cell Biology **112**(6): 479-486.

van Nieuw Amerongen, G. P., R. Draijer, M. A. Vermeer and V. W. van Hinsbergh (1998). "Transient and prolonged increase in endothelial permeability induced by histamine and thrombin: role of protein kinases, calcium, and RhoA." Circ Res **83**(11): 1115-1123.

Van Remmen, H. and A. Richardson (2001). "Oxidative damage to mitochondria and aging." Experimental gerontology **36**(7): 957-968.

Van Teeffelen, J. W., J. Brands, E. S. Stroes and H. Vink (2007). "Endothelial glycocalyx: sweet shield of blood vessels." Trends Cardiovasc Med **17**(3): 101-105.

Vandenbroucke, E., D. Mehta, R. Minshall and A. B. Malik (2008). "Regulation of Endothelial Junctional Permeability." **1123**(1): 145.

Venkiteswaran, K., K. Xiao, S. Summers, C. C. Calkins, P. A. Vincent, K. Pumiglia and A. P. Kowalczyk (2002). "Regulation of endothelial barrier function and growth by VE-cadherin, plakoglobin, and beta-catenin." American journal of physiology Cell physiology **283**(3): C811-821.

Verkman, A. S. (1998). "Role of aquaporin water channels in kidney and lung." Am J Med Sci **316**(5): 310-320.

Vetter, I. R. (2014). The structure of the G domain of the Ras superfamily. Ras superfamily small G proteins: Biology and mechanisms. A. Wittinghofer, Springer.

Vetter, I. R. and A. Wittinghofer (2001). "The guanine nucleotide-binding switch in three dimensions." Science **294**(5545): 1299-1304.

Victor, V. M., J. V. Espulgues, A. Hernandez-Mijares and M. Rocha (2009). "Oxidative stress and mitochondrial dysfunction in sepsis: a potential therapy with mitochondria-targeted antioxidants." Infect Disord Drug Targets **9**(4): 376-389.

Vincent, J. L., S. M. Opal, J. C. Marshall and K. J. Tracey (2013). "Sepsis definitions: time for change." Lancet **381**(9868): 774-775.

Vink, H., P. A. Wieringa and J. A. Spaan (1995). "Evidence that cell surface charge reduction modifies capillary red cell velocity-flux relationships in hamster cremaster muscle." J Physiol **489 (Pt 1)**: 193-201.

Vogelstein, B., N. Papadopoulos, V. E. Velculescu, S. Zhou, L. A. Diaz, Jr. and K. W. Kinzler (2013). "Cancer genome landscapes." Science **339(6127)**: 1546-1558.

Vojtek, A. B. and C. J. Der (1998). "Increasing Complexity of the Ras Signaling Pathway." Journal of Biological Chemistry **273(32)**: 19925-19928.

Wagner, D. D. (1993). "The Weibel-Palade body: the storage granule for von Willebrand factor and P-selectin." Thromb Haemost **70(1)**: 105-110.

Wallach, D., P. J. Davies and I. Pastan (1978). "Cyclic AMP-dependent phosphorylation of filamin in mammalian smooth muscle." J Biol Chem **253(13)**: 4739-4745.

Wallez, Y., F. Cand, F. Cruzalegui, C. Wernstedt, S. Souchelnytskyi, I. Vilgrain and P. Huber (2007). "Src kinase phosphorylates vascular endothelial-cadherin in response to vascular endothelial growth factor: identification of tyrosine 685 as the unique target site." Oncogene **26(7)**: 1067-1077.

Wallez, Y. and P. Huber (2008). "Endothelial adherens and tight junctions in vascular homeostasis, inflammation and angiogenesis." Biochim Biophys Acta **1778(3)**: 794-809.

Wang, B., J. X. Zou, B. Ek-Rylander and E. Ruoslahti (2000). "R-Ras contains a proline-rich site that binds to SH3 domains and is required for integrin activation by R-Ras." J Biol Chem **275(7)**: 5222-5227.

Wang, J. E., P. F. Jorgensen, M. Almlof, C. Thiemermann, S. J. Foster, A. O. Aasen and R. Solberg (2000). "Peptidoglycan and lipoteichoic acid from *Staphylococcus aureus* induce tumor necrosis factor alpha, interleukin 6 (IL-6), and IL-10 production in both T cells and monocytes in a human whole blood model." Infect Immun **68**(7): 3965-3970.

Wang, K., J. F. Ash and S. J. Singer (1975). "Filamin, a new high-molecular-weight protein found in smooth muscle and non-muscle cells." Proc Natl Acad Sci U S A **72**(11): 4483-4486.

Wang, N., J. D. Tytell and D. E. Ingber (2009). "Mechanotransduction at a distance: mechanically coupling the extracellular matrix with the nucleus." Nat Rev Mol Cell Biol **10**(1): 75-82.

Wang, Q., W. F. Patton, H. B. Hechtman and D. Shepro (1997). "A novel anti-inflammatory peptide inhibits endothelial cell cytoskeletal rearrangement, nitric oxide synthase translocation, and paracellular permeability increases." J Cell Physiol **172**(2): 171-182.

Warren, H. S., C. Fitting, E. Hoff, M. Adib-Conquy, L. Beasley-Topliffe, B. Tesini, X. Liang, C. Valentine, J. Hellman, D. Hayden and J.-M. Cavaillon (2010). "Resilience to bacterial infection: difference between species could be due to proteins in serum." The Journal of infectious diseases **201**(2): 223-232.

Waschke, J., D. Drenckhahn, R. H. Adamson and F. E. Curry (2004). Role of adhesion and contraction in Rac 1-regulated endothelial barrier function in vivo and in vitro.

Watanabe, H., R. Takahashi, X. X. Zhang, Y. Goto, H. Hayashi, J. Ando, M. Isshiki, M. Seto, H. Hidaka, I. Niki and R. Ohno (1998). "An essential role of myosin light-chain kinase in the regulation of agonist- and fluid flow-stimulated Ca²⁺ influx in endothelial cells." FASEB J **12**(3): 341-348.

Wegener, J., C. R. Keese and I. Giaever (2000). "Electric cell-substrate impedance sensing (ECIS) as a noninvasive means to monitor the kinetics of cell spreading to artificial surfaces." Experimental Cell Research **259**(1): 158-166.

Wegener, J., S. Zink, P. Rosen and H. Galla (1999). "Use of electrochemical impedance measurements to monitor beta-adrenergic stimulation of bovine aortic endothelial cells." Pflugers Arch **437**(6): 925-934.

Weihing, R. R. (1988). "Actin-binding and dimerization domains of HeLa cell filamin." Biochemistry **27**(6): 1865-1869.

Weinbaum, S., J. M. Tarbell and E. R. Damiano (2007). "The structure and function of the endothelial glycocalyx layer." Annu Rev Biomed Eng **9**: 121-167.

Weis, S., S. Shintani, A. Weber, R. Kirchmair, M. Wood, A. Cravens, H. McSharry, A. Iwakura, Y. S. Yoon, N. Himes, D. Burstein, J. Doukas, R. Soll, D. Losordo and D. Cheresh (2004). "Src blockade stabilizes a Flk/cadherin complex, reducing edema and tissue injury following myocardial infarction." J Clin Invest **113**(6): 885-894.

Weis, S. M. and D. A. Cheresh (2005). "Pathophysiological consequences of VEGF-induced vascular permeability." Nature **437**(7058): 497-504.

Weis, W. I. and W. J. Nelson (2006). "Resolving the cadherin-catenin-actin conundrum." Journal of Biological Chemistry **281**(47): 35593-35597.

Weiss, E. C., P. Anastasiadis, G. Pilarczyk, R. M. Lerner and P. V. Zinin (2007). "Mechanical properties of single cells by high-frequency time-resolved acoustic microscopy." Ultrasonics, Ferroelectrics and Frequency Control, IEEE Transactions on **54**(11): 2257-2271.

Weiss, E. C., R. M. Lemor, G. Pilarczyk, P. Anastasiadis and P. V. Zinin (2007). "Imaging of Focal Contacts of Chicken Heart Muscle Cells by High-Frequency Acoustic Microscopy." Ultrasound in Medicine and Biology **33**(8): 1320-1326.

Weller, A., S. Isenmann and D. Vestweber (1992). "Cloning of the mouse endothelial selectins. Expression of both E- and P-selectin is inducible by tumor necrosis factor alpha." The Journal of biological chemistry **267**(21): 15176-15183.

Welsh, D. G. and S. S. Segal (1998). "Endothelial and smooth muscle cell conduction in arterioles controlling blood flow." The American journal of physiology **274**(1 Pt 2): H178-186.

Wiegers, W., I. Just, H. Muller, A. Hellwig, P. Traub and K. Aktories (1991). "Alteration of the cytoskeleton of mammalian cells cultured in vitro by Clostridium botulinum C2 toxin and C3 ADP-ribosyltransferase." Eur J Cell Biol **54**(2): 237-245.

Wiesinger, A., W. Peters, D. Chappell, D. Kentrup, S. Reuter, H. Pavenstadt, H. Oberleithner and P. Kumpers (2013). "Nanomechanics of the endothelial glycocalyx in experimental sepsis." PLoS One **8**(11): e80905.

Williams, M. D., L. A. Braun, L. M. Cooper, J. Johnston, R. V. Weiss, R. L. Qualy and W. Linde-Zwirble (2004). "Hospitalized cancer patients with severe sepsis: analysis of incidence, mortality, and associated costs of care." Critical Care **8**(5): R291-R298.

Williams, M. J., P. E. Hughes, T. E. O'Toole and M. H. Ginsberg (1994). "The inner world of cell adhesion: integrin cytoplasmic domains." Trends in Cell Biology **4**(4): 109-112.

Wingender, J., T. R. Neu and H. C. Flemming (1999). What are bacterial extracellular substances? Microbial Extracellular Polymeric Substances: Characterization, Structure and Function. J. Wingender, T. R. Neu and H. C. Flemming. Berlin, Springer: 1 - 19.

Witkin, A. J., D. H. Fischer, C. L. Shields, D. Reichstein and J. A. Shields (2012). "Enhanced depth imaging spectral-domain optical coherence tomography of a subtle choroidal metastasis." Eye **26**(12): 1598-1599.

Wittchen, E. S., J. Haskins and B. R. Stevenson (1999). "Protein interactions at the tight junction. Actin has multiple binding partners, and ZO-1 forms independent complexes with ZO-2 and ZO-3." J Biol Chem **274**(49): 35179-35185.

Wittinghofer, A. and N. Nassar (1996). "How Ras-related proteins talk to their effectors." Trends Biochem Sci **21**(12): 488-491.

Wojciak-Stothard, B., S. Potempa, T. Eichholtz and A. J. Ridley (2001). "9Rgr and Rac but not Cdc42 regulate endothelial cell permeability." Journal of Cell Science **114**(7): 1343-1355.

Wolburg, H., K. Wolburg-Buchholz, J. Kraus, G. Rascher-Eggstein, S. Liebner, S. Hamm, F. Duffner, E. H. Grote, W. Risau and B. Engelhardt (2003). "Localization of claudin-3 in tight junctions of the blood-brain barrier is selectively lost during experimental autoimmune encephalomyelitis and human glioblastoma multiforme." Acta Neuropathol **105**(6): 586-592.

Wolff, S. M., J. H. Mulholland and S. B. Ward (1965). "Quantitative Aspects of the Pyrogenic Response of Rabbits to Endotoxin." J Lab Clin Med **65**: 268-275.

Wong, H. R., C. J. Lindsell, P. Lahni, K. W. Hart and S. Gibot (2013). "Interleukin 27 as a sepsis diagnostic biomarker in critically ill adults." Shock (Augusta, Ga) **40**(5): 382-386.

Wong, H. R., K. D. Liu, K. N. Kangelaris, P. Lahni and C. S. Calfee (2014). "Performance of interleukin-27 as a sepsis diagnostic biomarker in critically ill adults." Journal of critical care **29**(5): 718-722.

Woodcock, T. E. and T. M. Woodcock (2012). "Revised Starling equation and the glycocalyx model of transvascular fluid exchange: an improved paradigm for prescribing intravenous fluid therapy." Br J Anaesth **108**(3): 384-394.

Wright, T. J., L. Leach, P. E. Shaw and P. Jones (2002). "Dynamics of vascular endothelial-cadherin and beta-catenin localization by vascular endothelial growth factor-induced angiogenesis in human umbilical vein cells." Experimental Cell Research **280**(2): 159-168.

Xiao, K., D. F. Allison, K. M. Buckley, M. D. Kottke, P. A. Vincent, V. Faundez and A. P. Kowalczyk (2003). "Cellular levels of p120 catenin function as a set point for cadherin expression levels in microvascular endothelial cells." J Cell Biol **163**(3): 535-545.

Yabkowitz, R., S. Meyer, T. Black, G. Elliott, L. A. Merewether and H. K. Yamane (1999). "Inflammatory cytokines and vascular endothelial growth factor stimulate the release of soluble tie receptor from human endothelial cells via metalloprotease activation." Blood **93**(6): 1969-1979.

Yabkowitz, R., S. Meyer, D. Yanagihara, D. Brankow, T. Staley, G. Elliott, S. Hu and B. Ratzkin (1997). "Regulation of tie receptor expression on human endothelial cells by protein kinase C-mediated release of soluble tie." Blood **90**(2): 706-715.

Yada, Y., Y. Okano and Y. Nozawa (1990). "Enhancement of GTP gamma S-binding activity by cAMP-dependent phosphorylation of a filamin-like 250 kDa membrane protein in human platelets." Biochem Biophys Res Commun **172**(1): 256-261.

Yagi, T. and M. Takeichi (2000). "Cadherin superfamily genes: functions, genomic organization, and neurologic diversity." Genes Dev **14**(10): 1169-1180.

Yamashita, S., N. Mochizuki, Y. Ohba, M. Tobiume, Y. Okada, H. Sawa, K. Nagashima and M. Matsuda (2000). "CalDAG-GEFIII Activation of Ras, R-Ras, and Rap1." Journal of Biological Chemistry **275**(33): 25488-25493.

Yamazaki, Y., K. Umeda, M. Wada, S. Nada, M. Okada, S. Tsukita and S. Tsukita (2008). "ZO-1- and ZO-2-dependent integration of myosin-2 to epithelial zonula adherens." Mol Biol Cell **19**(9): 3801-3811.

Yang, Z., W. H. Xia, Y. Y. Zhang, S. Y. Xu, X. Liu, X. Y. Zhang, B. B. Yu, Y. X. Qiu and J. Tao (2012). "Shear stress-induced activation of Tie2-dependent signaling pathway enhances reendothelialization capacity of early endothelial progenitor cells." J Mol Cell Cardiol **52**(5): 1155-1163.

Yano, K., P. C. Liaw, J. M. Mullington, S.-C. Shih, H. Okada, N. Bodyak, P. M. Kang, L. Toltl, B. Belikoff, J. Buras, B. T. Simms, J. P. Mizgerd, P. Carmeliet, S. A. Karumanchi and W. C. Aird (2006). "Vascular endothelial growth factor is an important determinant of sepsis morbidity and mortality." The Journal of experimental medicine **203**(6): 1447-1458.

Yoder, B. K. (2007). "Role of primary cilia in the pathogenesis of polycystic kidney disease." J Am Soc Nephrol **18**(5): 1381-1388.

Yoshikawa, N., H. Ariyoshi, M. Ikeda, M. Sakon, T. Kawasaki and M. Monden (1997). "Shear-stress causes polarized change in cytoplasmic calcium concentration in human umbilical vein endothelial cells (HUVECs)." Cell Calcium **22**(3): 189-194.

Zhang, C. (2008). "The role of inflammatory cytokines in endothelial dysfunction." Basic Res Cardiol **103**(5): 398-406.

Zhang, H., S. W. Sunnarborg, K. K. McNaughton, T. G. Johns, D. C. Lee and J. E. Faber (2008). "Heparin-binding epidermal growth factor-like growth factor signaling in flow-induced arterial remodeling." Circ Res **102**(10): 1275-1285.

Zhang, R. Y., Y. Y. Liu, L. Li, W. Cui, K. J. Zhao, W. C. Huang, X. W. Gu, W. Liu, J. Wu, D. Min, E. Q. Mao and Y. Q. Tang (2010). "Increased levels of soluble vascular endothelial cadherin are associated with poor outcome in severe sepsis." J Int Med Res **38**(4): 1497-1506.

Zhang, Z., K. Vuori, H. Wang, J. C. Reed and E. Ruoslahti (1996). "Integrin activation by R-ras." Cell **85**(1): 61-69.

Zinin, P. V., J. S. Allen, 3rd and V. M. Levin (2005). "Mechanical resonances of bacteria cells." Phys Rev E Stat Nonlin Soft Matter Phys **72**(6 Pt 1): 061907.

Zinin, P. V. and J. S. Allen, III (2009). "Deformation of biological cells in the acoustic field of an oscillating bubble." Physical Review E **79**(2).

Zou, J. X., Y. Liu, E. B. Pasquale and E. Ruoslahti (2002). "Activated SRC oncogene phosphorylates R-ras and suppresses integrin activity." J Biol Chem **277**(3): 1824-1827.

Zou, J. X., B. Wang, M. S. Kalo, A. H. Zisch, E. B. Pasquale and E. Ruoslahti (1999). "An Eph receptor regulates integrin activity through R-Ras." Proc Natl Acad Sci U S A **96**(24): 13813-13818.